Searches for Higgs boson pair production with the ATLAS experiment at the LHC

Alessandra Betti

Seminar INFN Roma 1
06/06/2022

Why are searches for di-Higgs production interesting?

The Higgs potential and the Higgs self-coupling

$$V(\Phi) = \mu^2\Phi^2 + \lambda\Phi^4$$

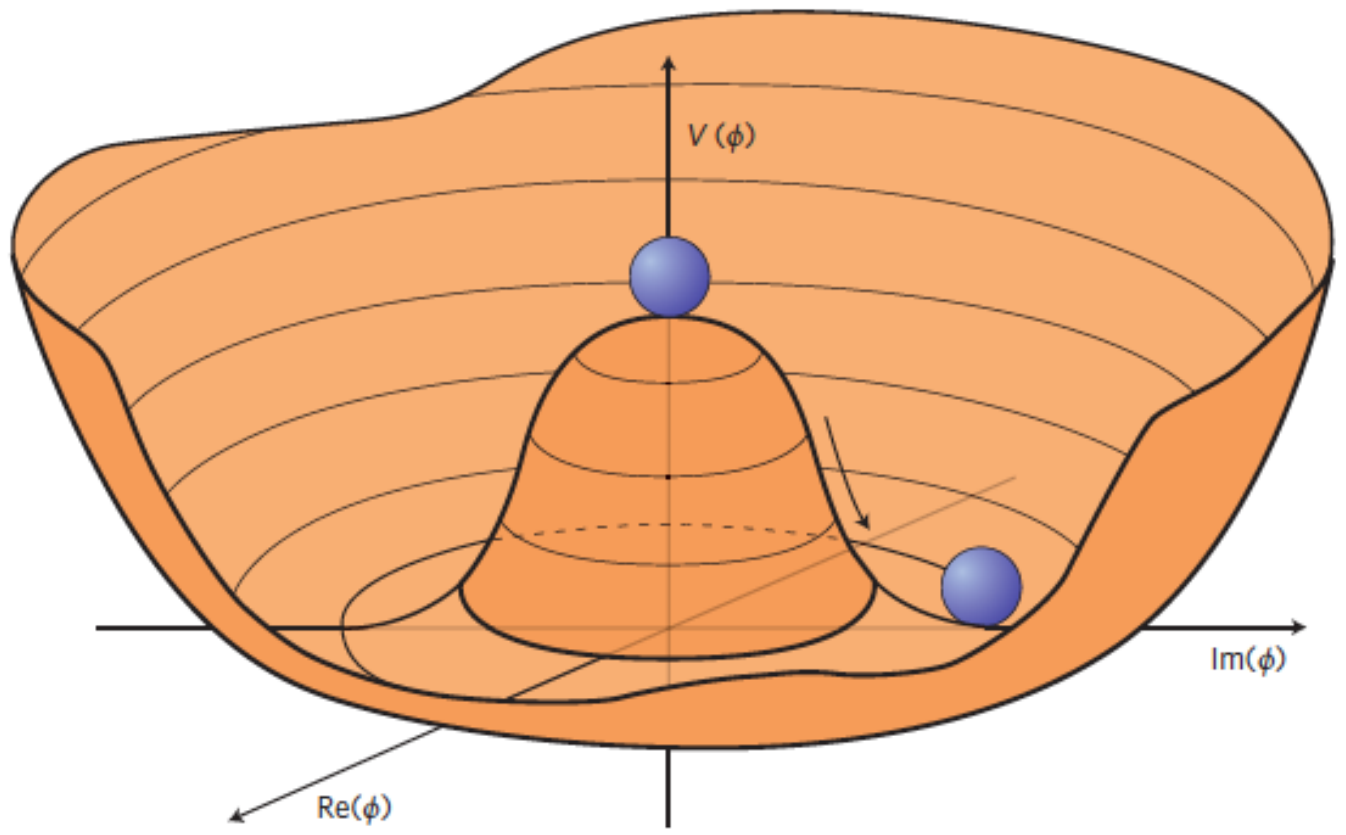

Expanding around the minimum, $\Phi = v + h$:

$$V(h) = \lambda v^2 h^2 + \lambda v h^3 + \frac{1}{4}\lambda h^4 = \frac{1}{2}m_h^2 h^2 + \lambda_3 h^3 + \lambda_4 h^4$$

Mass term

$$m_h = \sqrt{2\lambda v}$$

triple Higgs coupling

$$\lambda_3 = \lambda v = \frac{m_h^2}{2v}$$

quartic Higgs coupling

$$\lambda_4 = \frac{\lambda}{4} = \frac{m_h^2}{8v^2}$$

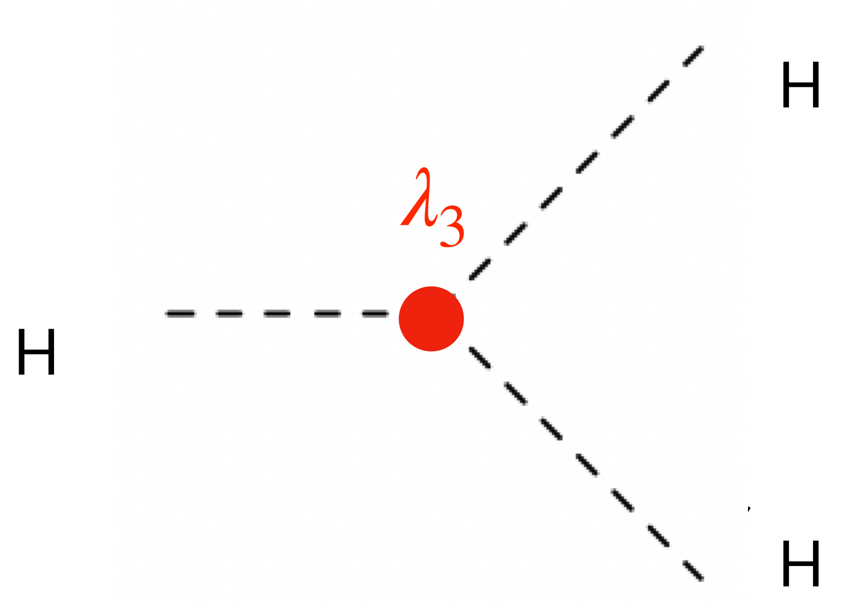

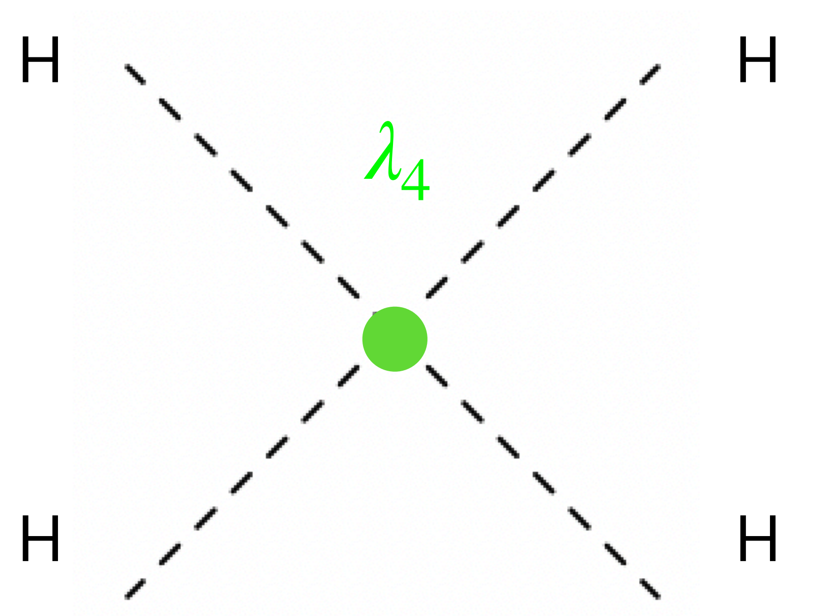

- λ_3 and λ_4 determine the shape of the Higgs potential and in the Standard Model they have defined values once the Higgs mass and the vacuum expectation value are known from experimental measurements
- Still largely unconstrained by direct experimental measurements, measuring these couplings probes the validity of the Higgs mechanism and of the Standard Model itself (λ_4 out of reach at the LHC but λ_3 accessible at the LHC through HH production)

Measuring the Higgs self-coupling at the LHC

di-Higgs production provides a direct probe of the triple Higgs coupling ($\kappa_\lambda = \frac{\lambda_3}{\lambda_3^{SM}}, \kappa_\lambda^{SM} = 1, \kappa_\lambda \neq 1 \rightarrow$ hint of BSM physics!)

At the LHC, the leading HH production mode is gluon-gluon Fusion (ggF): $\sigma_{ggF}^{SM} = 31.05$ fb

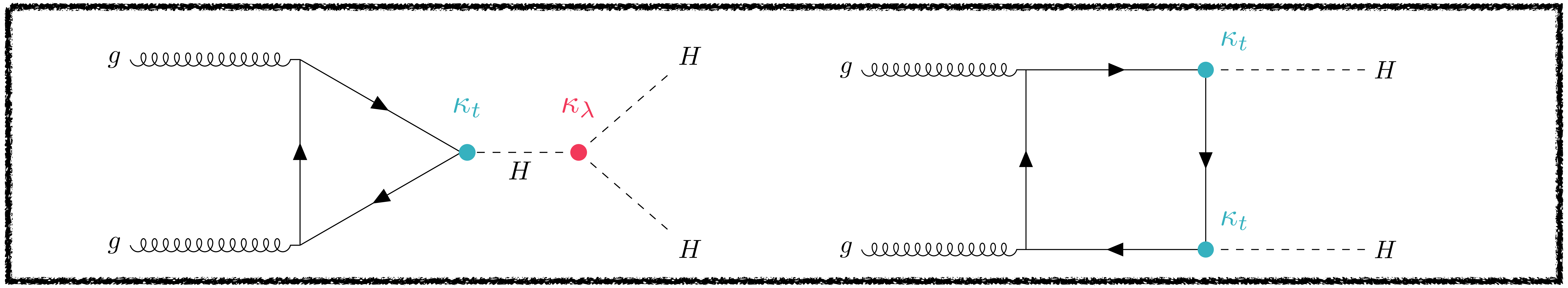

Second leading HH production mode is vector-boson-fusion (VBF): $\sigma_{VBF}^{SM} = 1.73$ fb

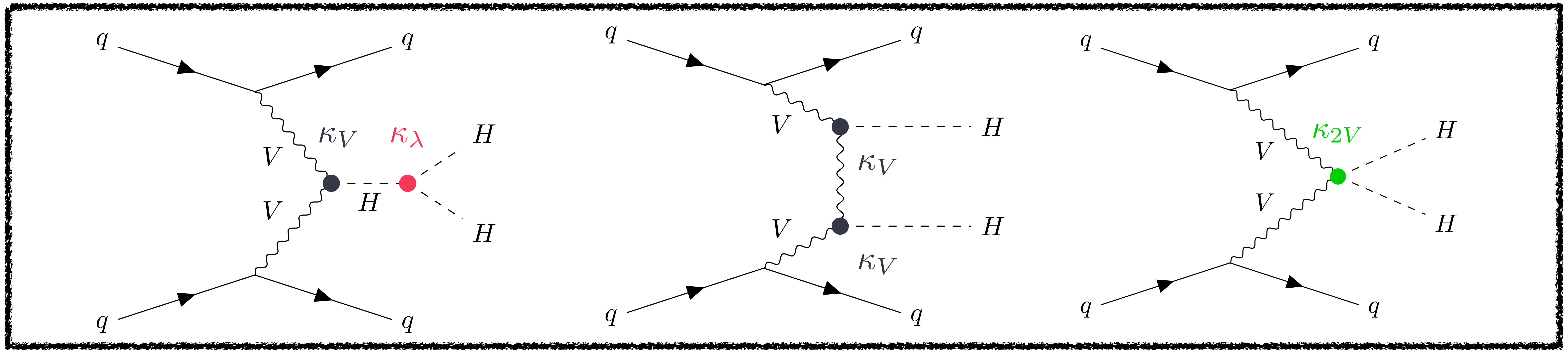

Beyond Standard Model physics in di-Higgs production

SM HH production cross section very small (more than 1000 times smaller than single-Higgs production!)

→ Needs very high statistics to be observed but still very interesting to study now as beyond the SM physics could lead to modified Higgs Boson self-coupling resulting in enhanced HH production rate and modified kinematics of the process

JHEP04 (2013) 151

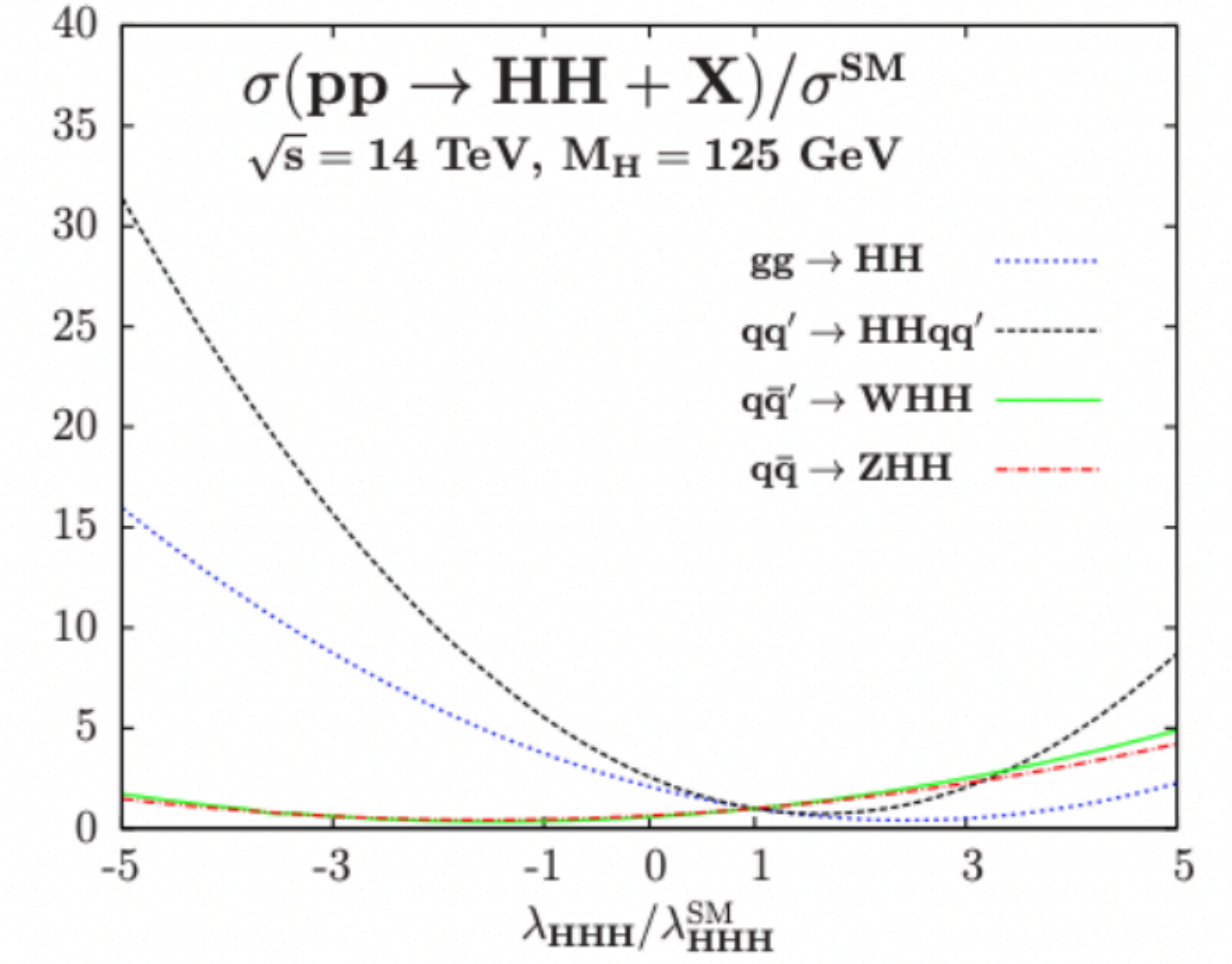

Large variations of non-resonant cross section with modifications of κ_λ for ggF and VBF:

- More than a factor of 2 increase at $\kappa_\lambda = 0$
- More than a factor of 4 increase at $\kappa_\lambda = -1$

Modifications of the kinematics of the process with variations of κ_λ due to different contributions and interference of the Feynman diagrams

Rev. Phys. 5, 100045 (2020)

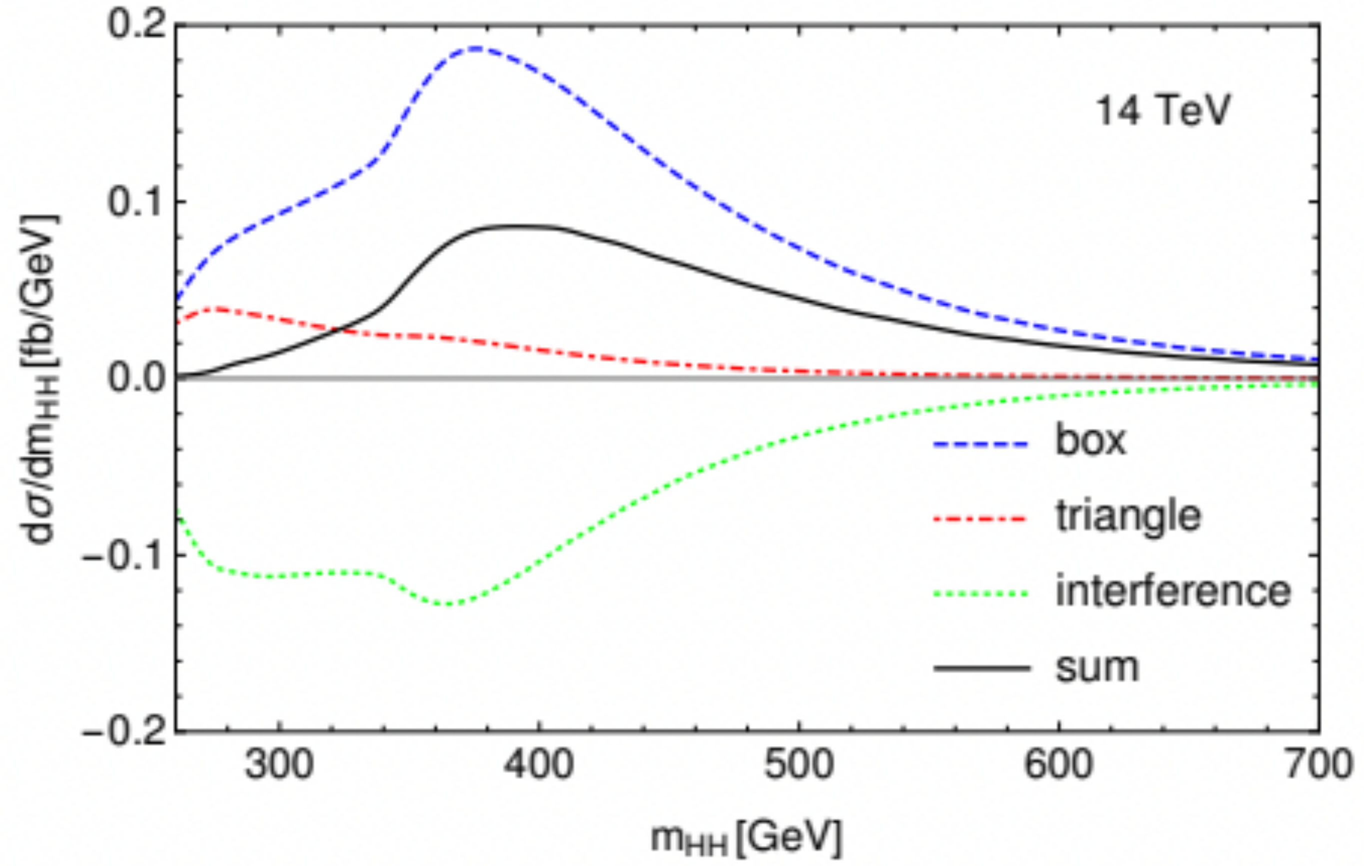

Phys. Lett. B 800 (2020) 135103

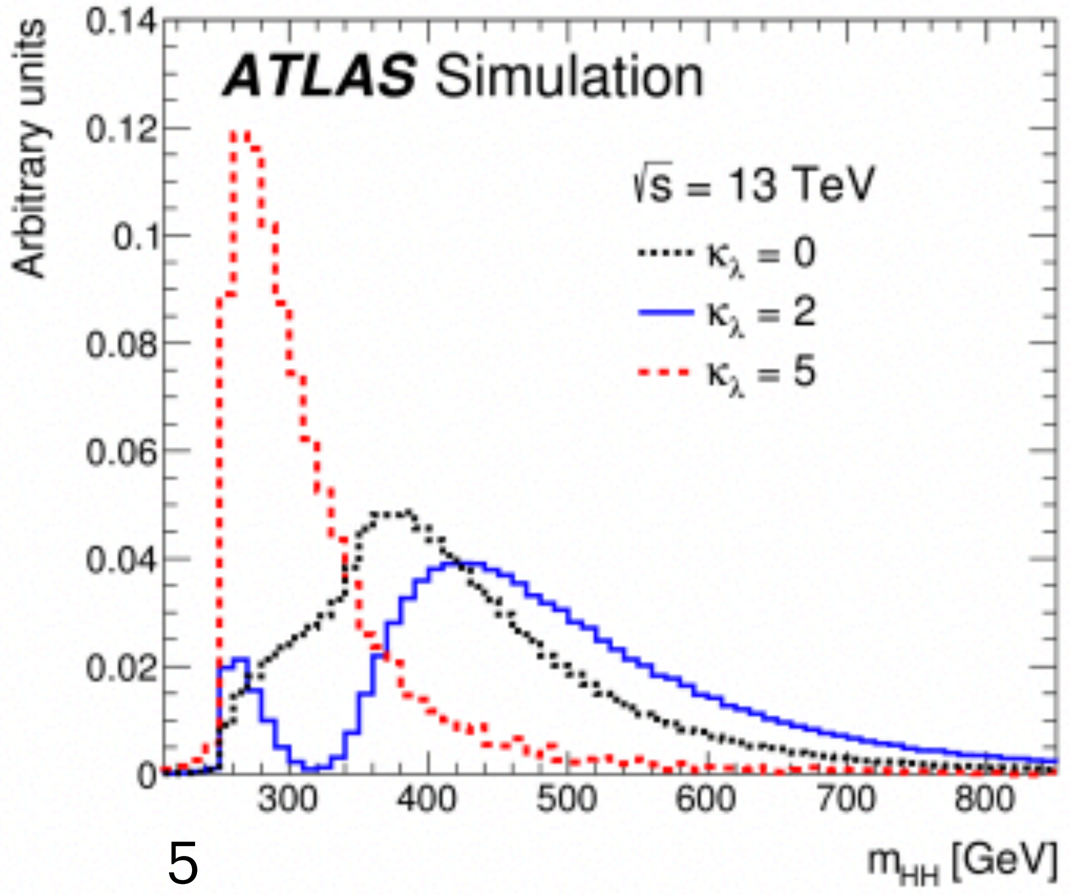

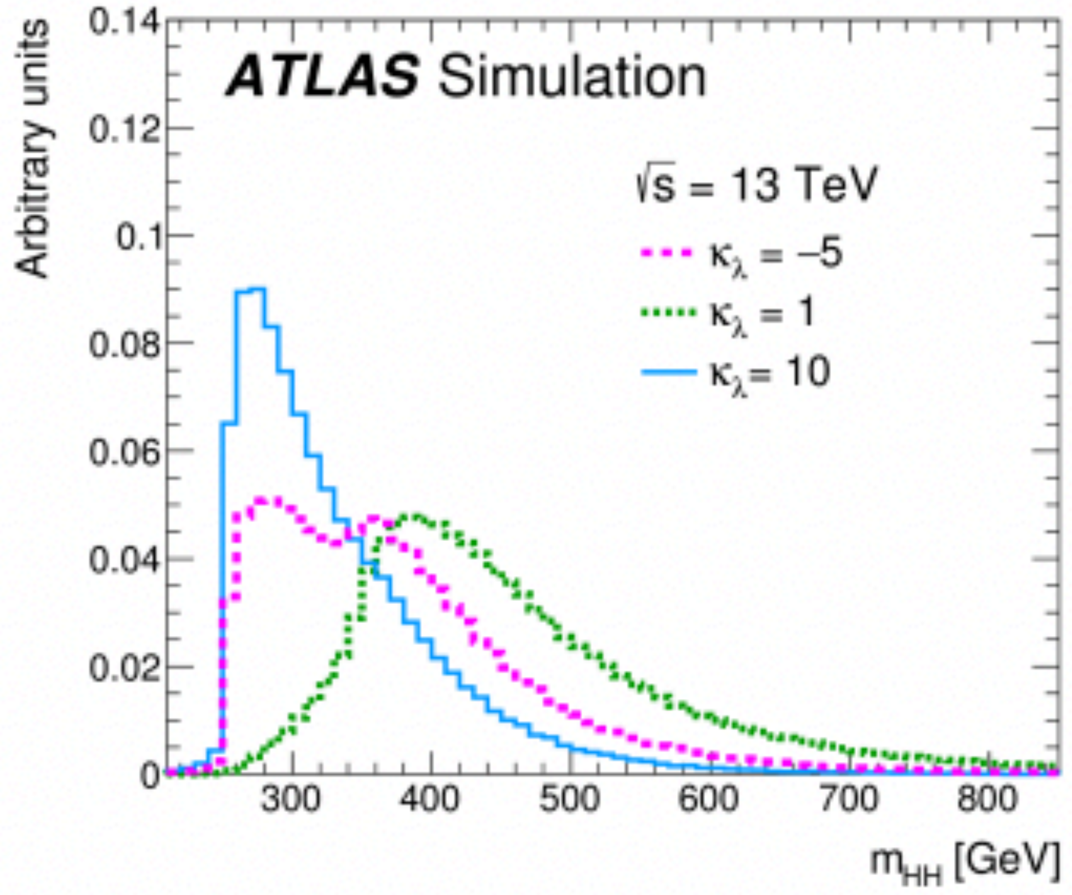

Beyond Standard Model resonances in di-Higgs production

Production of BSM resonances X decaying to HH
enhancing the production rate and modifying the kinematics

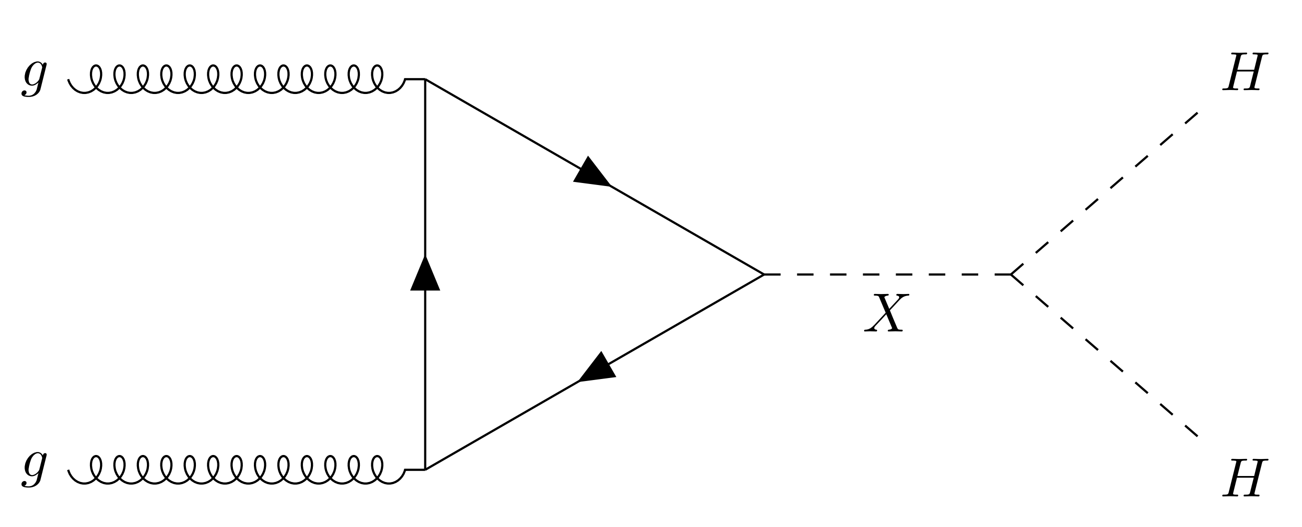

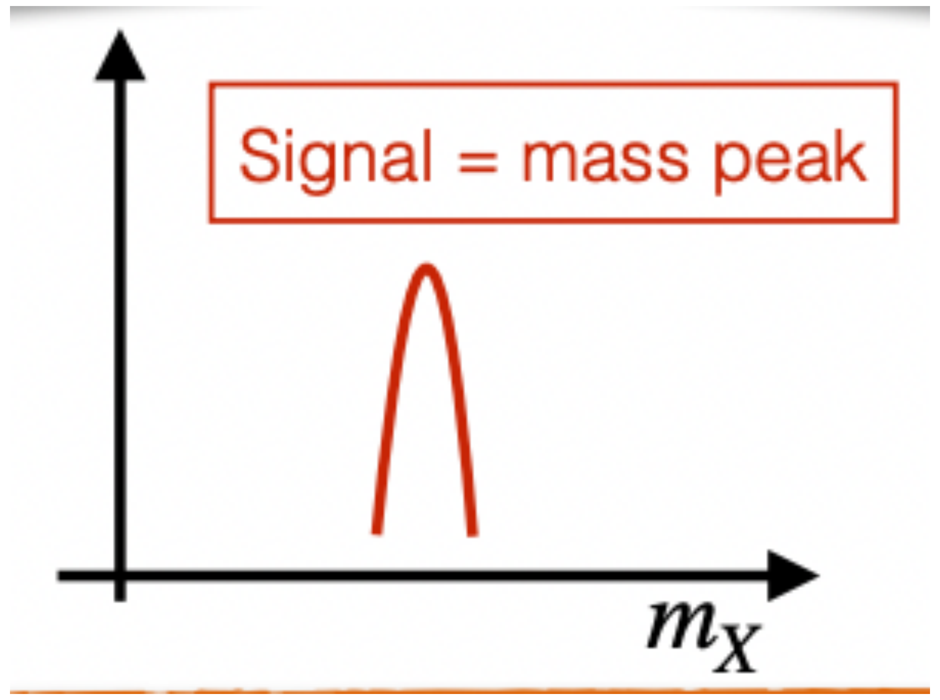

Several BSM models predict new heavy resonances,
decay BRs of the new resonances are very model dependent …
some models predict high BRs of X to HH in some X mass ranges

→ searches for resonances in the HH channel
can be competitive with other channels
to set constraints on several BSM models

2HDM type-I (fermiophobic) $\tan\beta = 1.5$

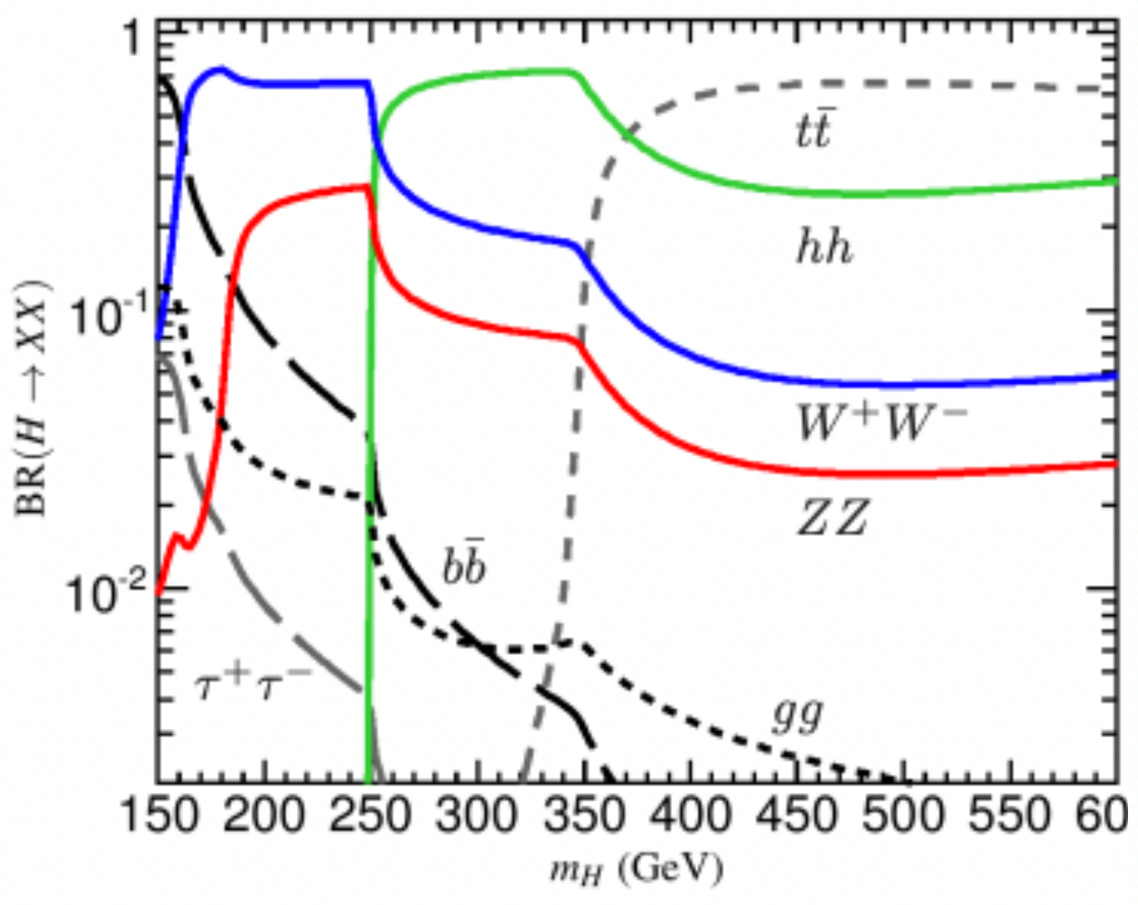

2HDM type-II (MSSM-like) $\tan\beta = 1.5$

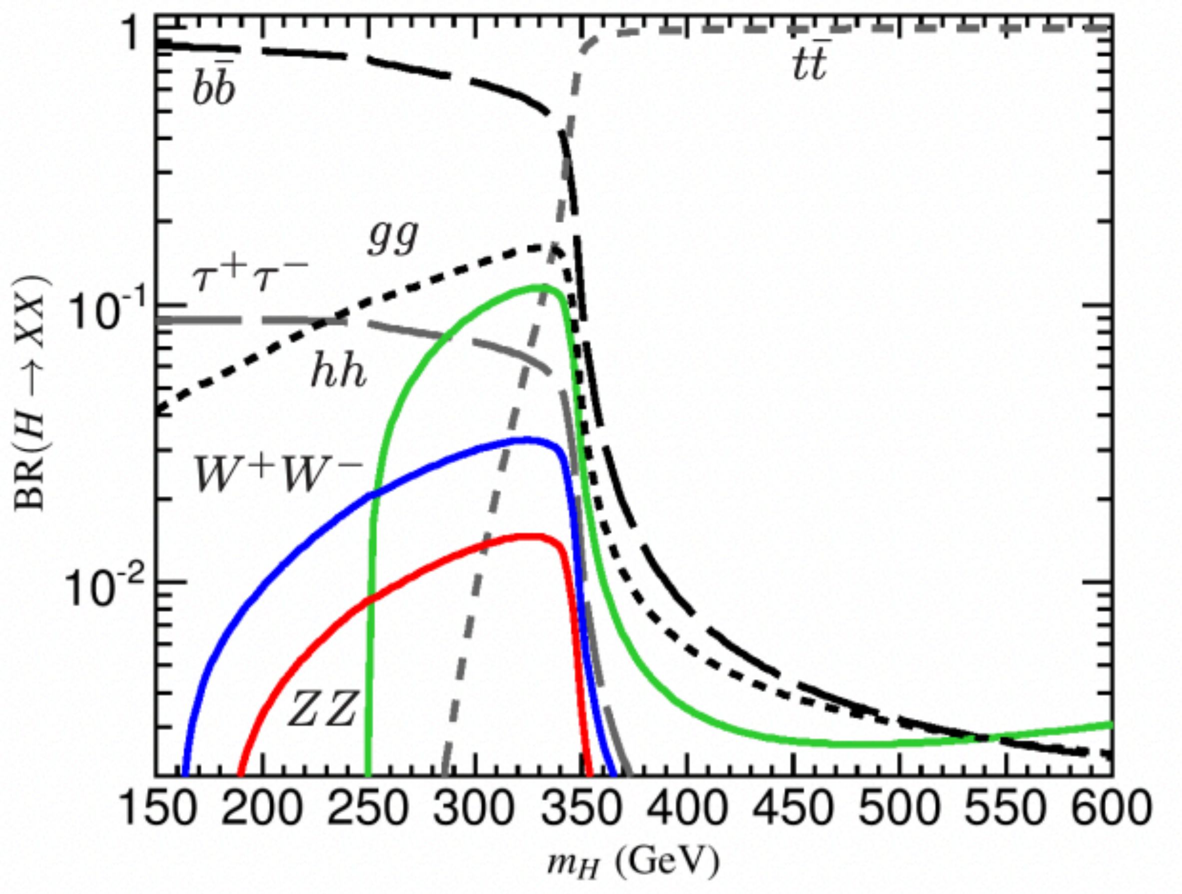

https://arxiv.org/pdf/1507.04281.pdf

Graviton

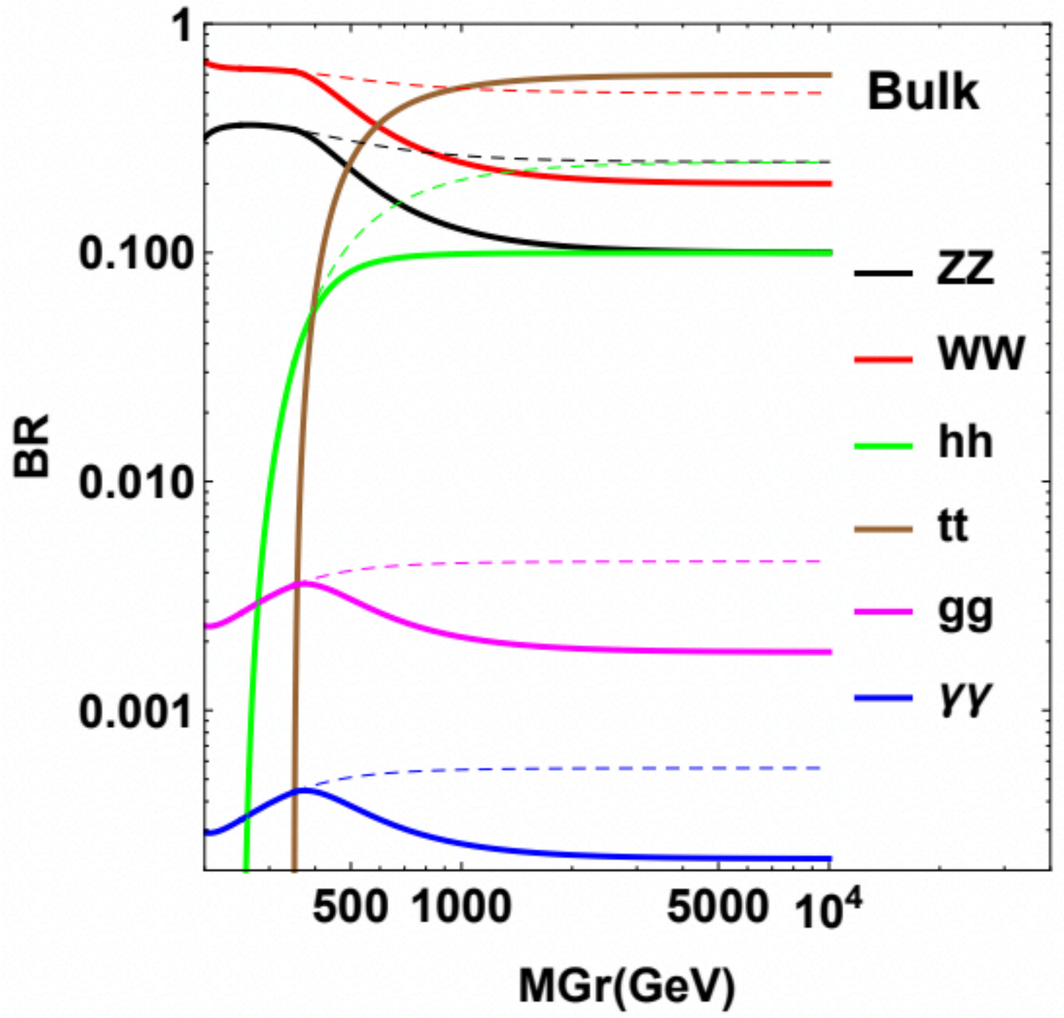

Radion

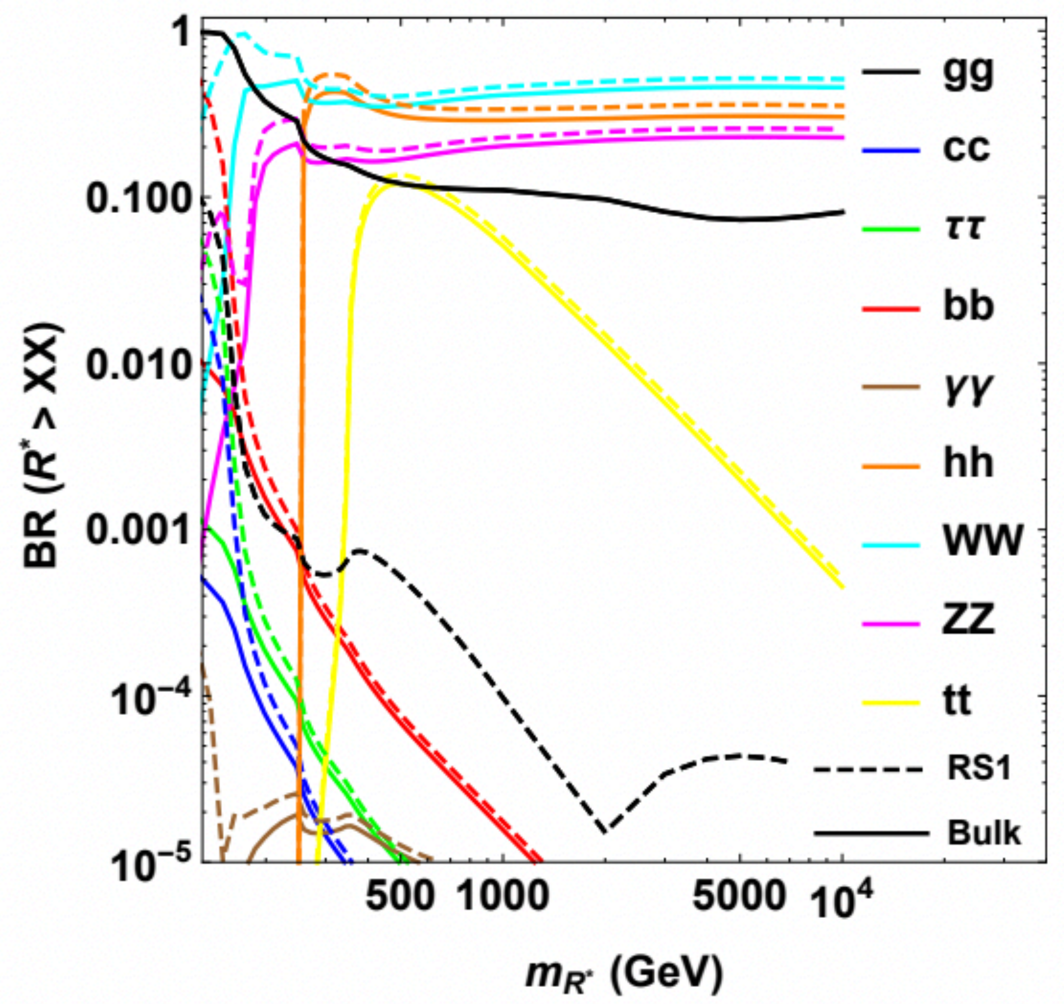

https://arxiv.org/pdf/1404.0102.pdf

How do we search for di-Higgs production in ATLAS?

Higgs boson decay

Searching for events with 2 Higgs bosons ...

How do we identify the Higgs boson?

The Higgs boson has a very short lifetime, decays almost immediately (lifetime of $\tau = 1.56 \times 10^{-22}$ s)

→ we can only detect it indirectly by reconstructing its decay products

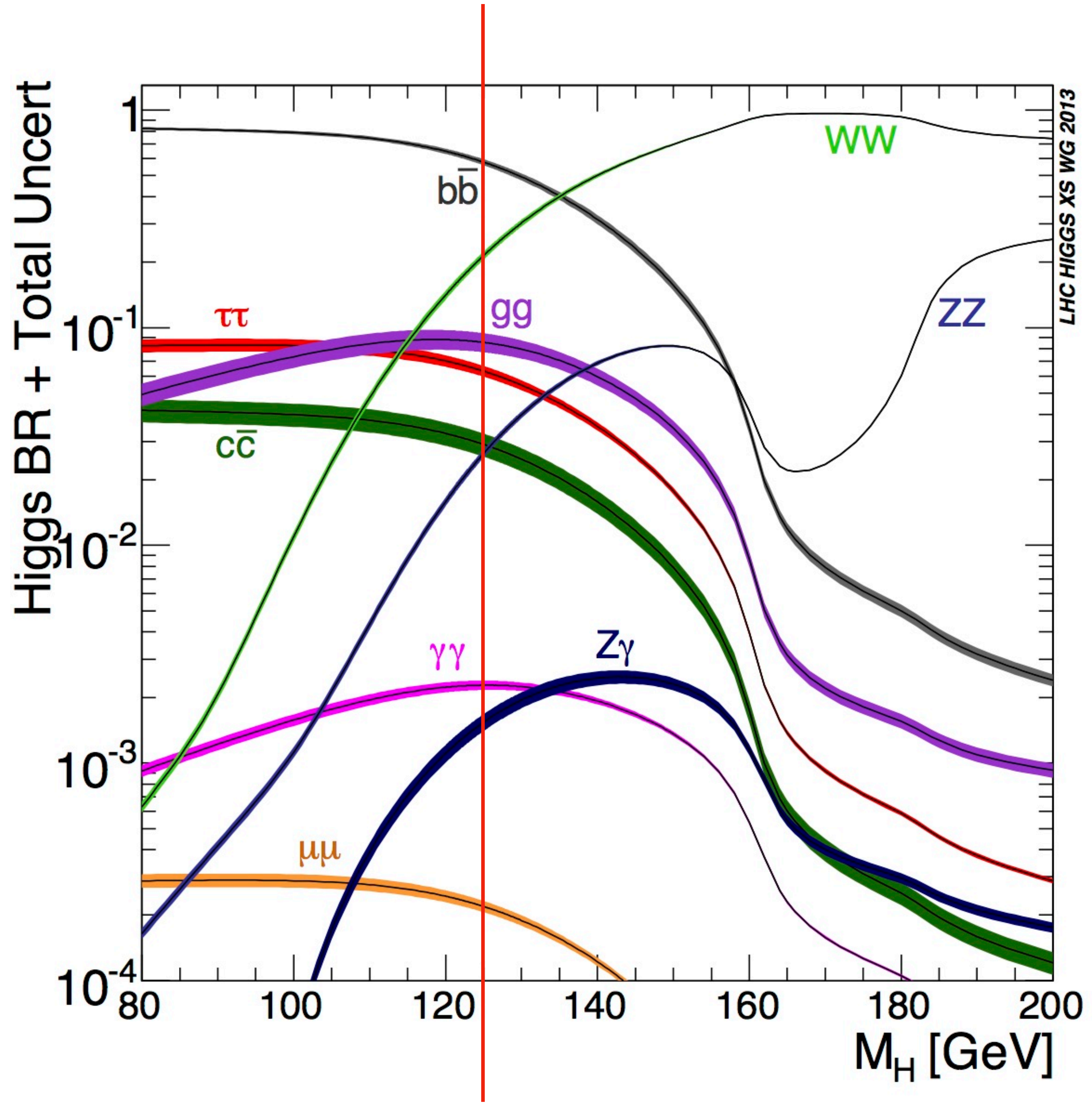

125 GeV

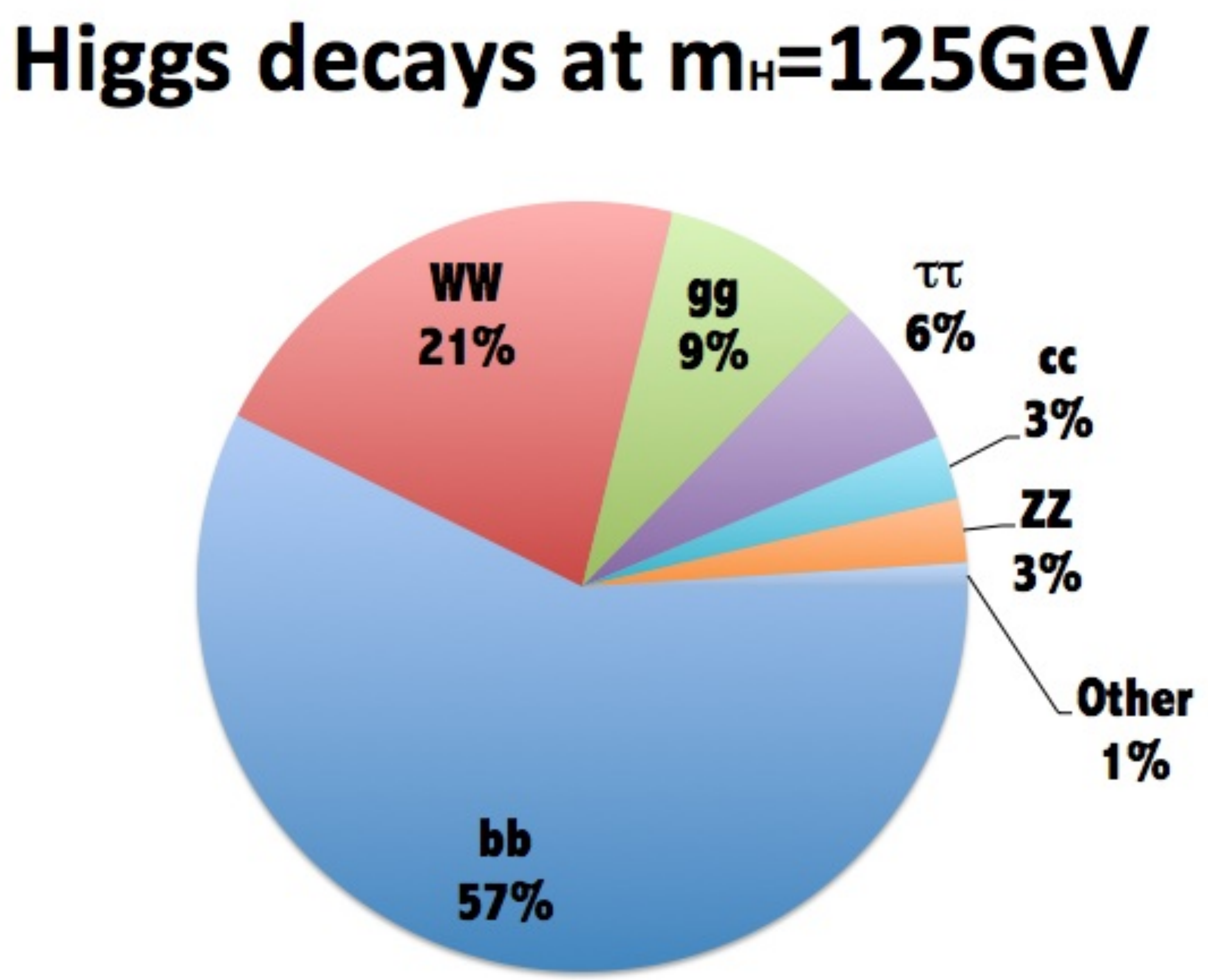

Higgs boson candidates:
final state objects from the Higgs decays with invariant mass around $m_H = 125$ GeV

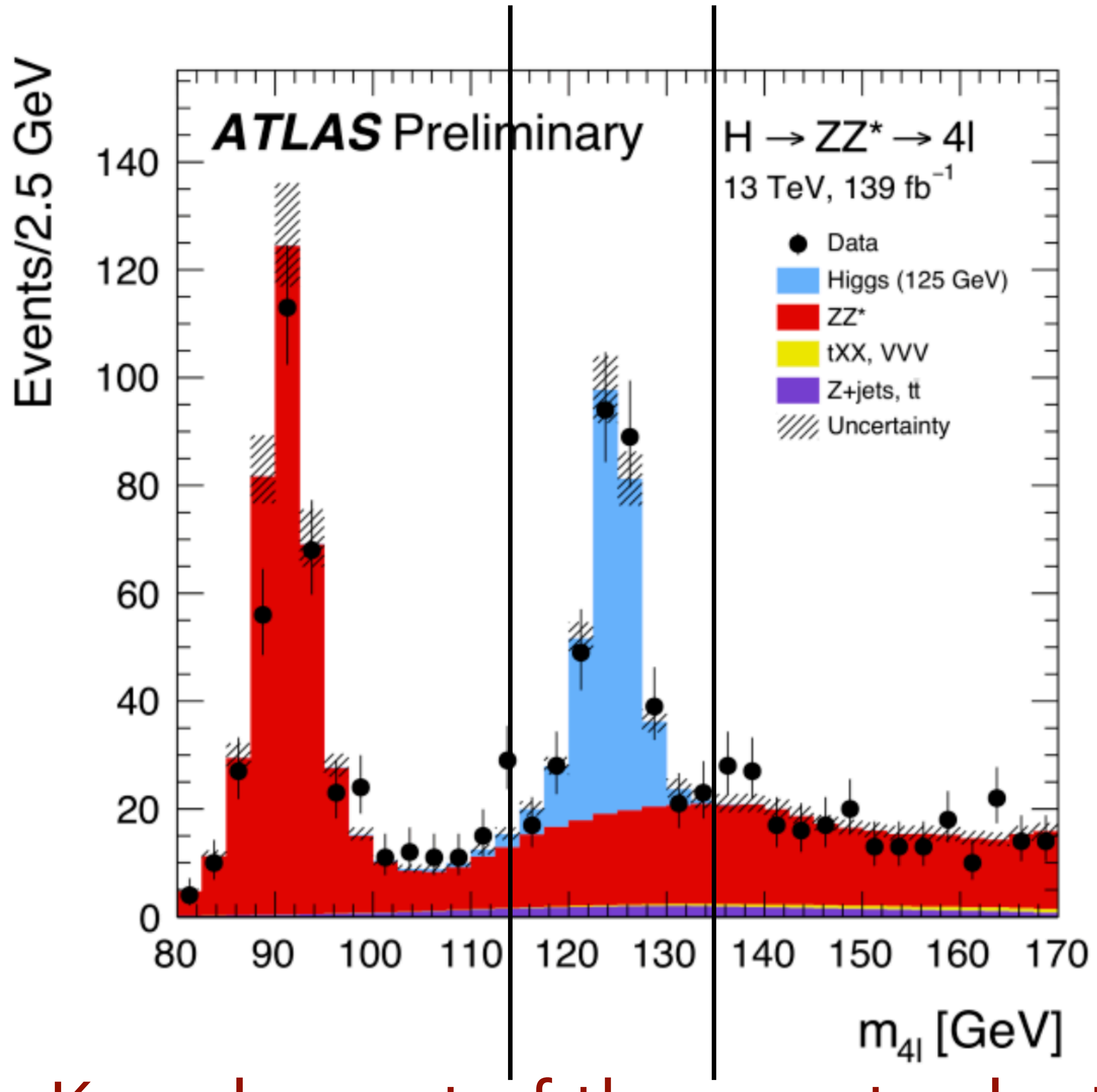

→ Key element of the event selection common to all HH searches

di-Higgs decay channels and ATLAS di-Higgs searches

Many different final states in the Higgs pair decay given by all possible combinations of Higgs Boson decays

ATLAS di-Higgs searches covering large part of possible decays with results on partial ($36\ fb^{-1}$) and full ($139\ fb^{-1}$) LHC Run 2 datasets

	bb	WW	ττ	ZZ	γγ
bb	34%				
WW	25%	4.6%			
ττ	7.3%	2.7%	0.39%		
ZZ	3.1%	1.1%	0.33%	0.069%	
γγ	0.26%	0.10%	0.028%	0.012%	0.0005%

Most HH searches exploit decay channels with one H→bb for the high BR

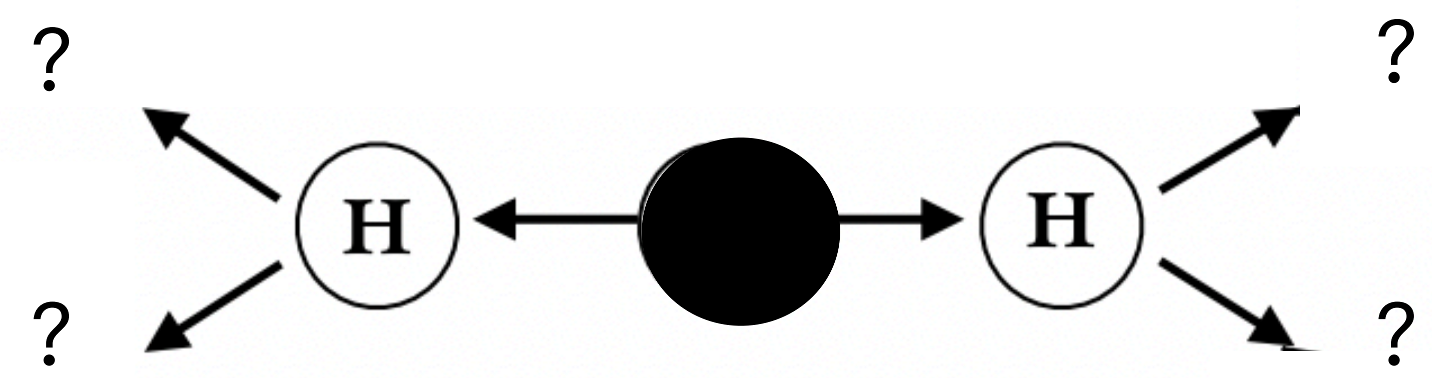

Analyses in different decay channels have very different characteristics given the different signal decay BRs, different objects in the final state and different backgrounds

→ Presenting here the latest ATLAS HH analyses and results in the bbbb, bbττ and bbγγ channels using full Run 2 LHC dataset and published between 2021 and 2022

ATLAS detector

ATLAS is one of the two multi-purpose experiments that detect the products of the LHC pp collisions

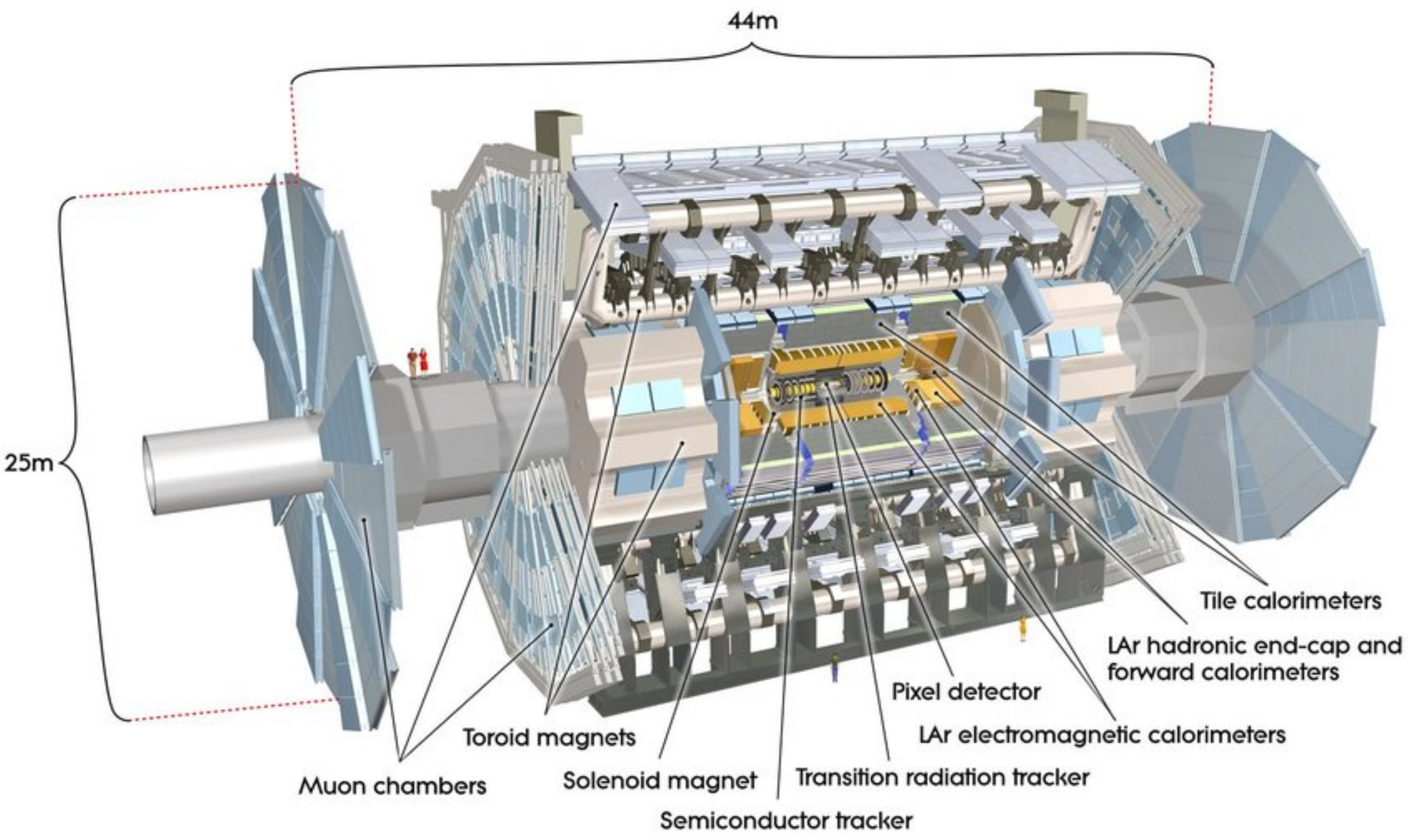

Detector with cylindrical shape around the pp interaction point with several sub-detectors:

- Inner detector for tracking of charged particles
- Electromagnetic calorimeter for measuring energies of electrons and photons
- Hadronic calorimeter for measuring energies of hadrons
- Muon spectrometer for tracking and measuring the momentum of muons

ATLAS event selection for di-Higgs searches

The LHC delivered 139 fb^{-1} of data in Run 2, number of HH events expected in the dataset:

$$N_{HH}^{SM} = \sigma_{HH} \times L = 33 \text{ fb} \times 139 \text{ fb}^{-1} \simeq 4600$$

Looking at the bbbb, bbττ, bbγγ decay channels:

$$N_{HH}^{SM} = \sigma_{HH} \times BR \times L = 33 \text{ fb} \times (0.33 + 0.073 \times (0.46 + 0.42) + 0.0026) \times 139 \text{ fb}^{-1} \simeq 1800$$

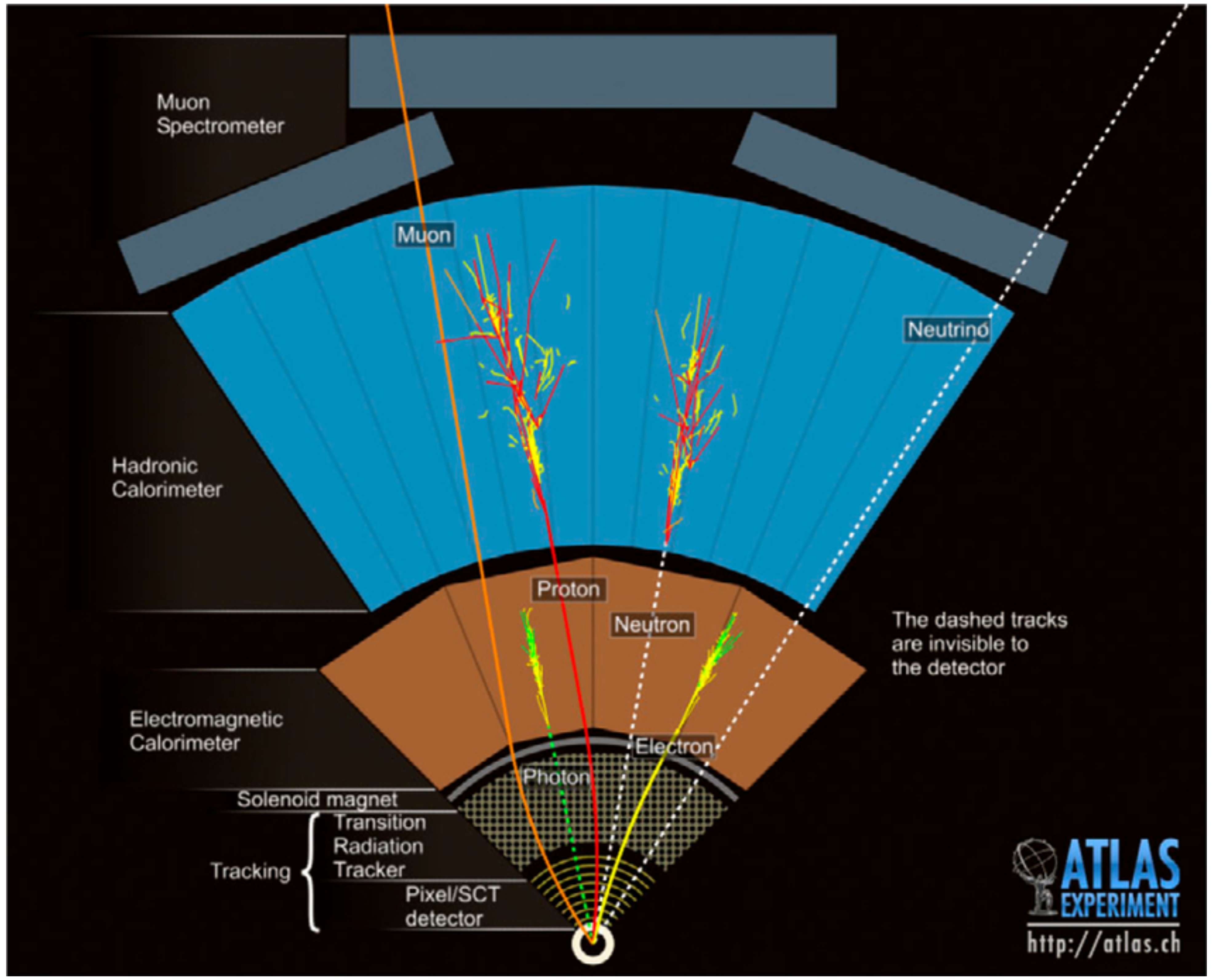

All parts of the detector important for the HH searches in these 3 channels to reconstruct, identify and select events with b-jets, hadronically decaying τ-leptons, leptonically decaying τ-leptons and photons

Particles reconstructed and identified thanks to the different signatures in the different sub-detectors

Dedicated object-identification algorithms combine information from the subdetectors in likelihood based and neural network based discriminants to be used for online (trigger) and offline event selection

ATLAS event selection for di-Higgs searches

Trigger selection:

- Events selected online using b-jet triggers, τ-lepton triggers, light-lepton triggers and photon triggers

→ Trigger selection signal efficiencies between 25% and 80% for the SM HH signal

Physics objects reconstruction and identification:

- Light-leptons and photon identification: >95% per-object efficiency
- b-jet-tagging and τ-lepton identification: 80% per-object efficiency

Analysis-level event selections to reject background

→ Total signal acceptance x efficiency between 5% and 10% for the SM HH signal

→ Signal acceptance x efficiency depends on κ_λ

ATLAS-CONF-2021-052

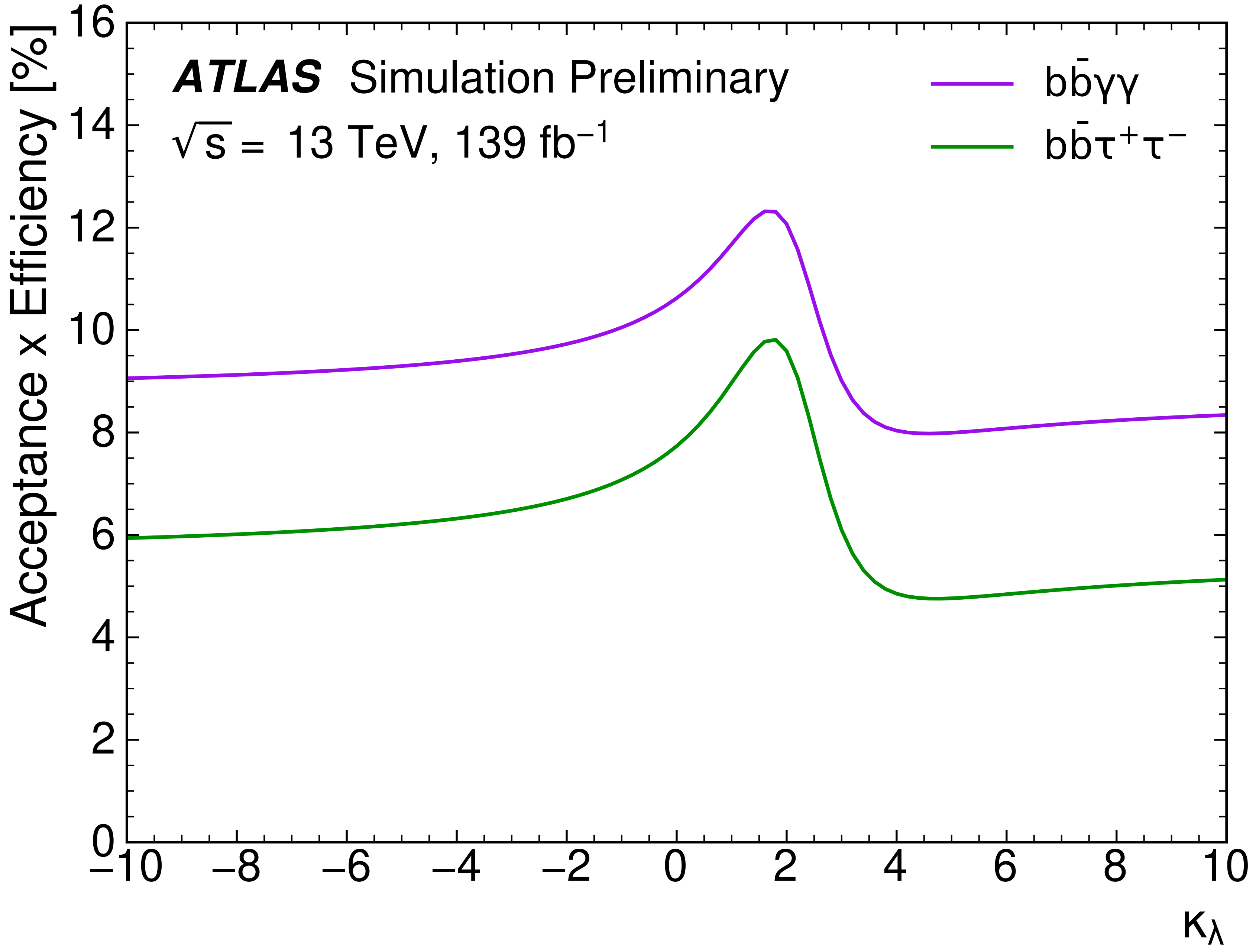

→ Signal acceptance x efficiency lower for BSM signals with variations of κ_λ, mainly due to lower trigger selection efficiency because of the softer m_{HH} spectrum giving lower p_T objects not passing the trigger thresholds

Number of selected SM HH events: $N_{HH}^{SM} = \sigma_{HH} \times BR \times L \times A \times \epsilon < 100$

Not only small cross section, but also very difficult to reconstruct, identify and select these events!

Selection of ATLAS HH analyses and results with full Run 2 LHC dataset ($bbbb$, $bb\tau\tau$, $bb\gamma\gamma$)

Searches for non-resonant HH production

Non-resonant HH→bbbb with full Run 2 data

bbbb decay channel has the largest BR (34%), but large QCD multi-jet events background difficult to model and challenging combinatorial problem for building the Higgs candidates

- Search for SM and BSM non-resonant HH production
- ggF and VBF HH production
- HH→bbbb
- At least 4 b-tagged central jets

- Targeting ggF and VBF production modes with dedicated categories
  - Events at least two additional jets with large pseudo-rapidity separation and large invariant mass classified as VBF
  - Rest of the events classified as ggF

- b-tagged jets paired to form the 2 Higgs candidates based on minimum dR requirement

- Signal regions defined by selections in the 2D m_{H1}-m_{H2} plane

$$X_{HH} = \sqrt{\left(\frac{m_{H1} - 124\ \mathrm{GeV}}{0.1\ m_{H1}}\right)^2 + \left(\frac{m_{H2} - 117\ \mathrm{GeV}}{0.1\ m_{H2}}\right)^2}$$

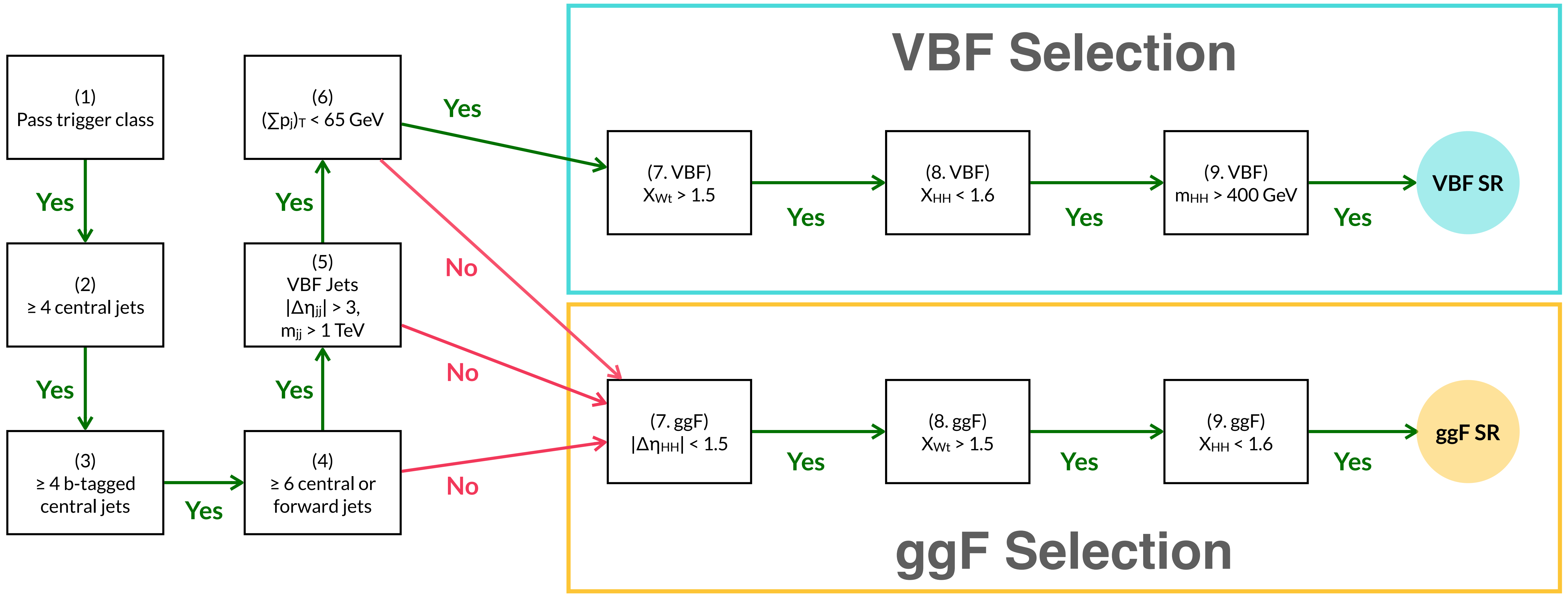

ATLAS-CONF-2022-035

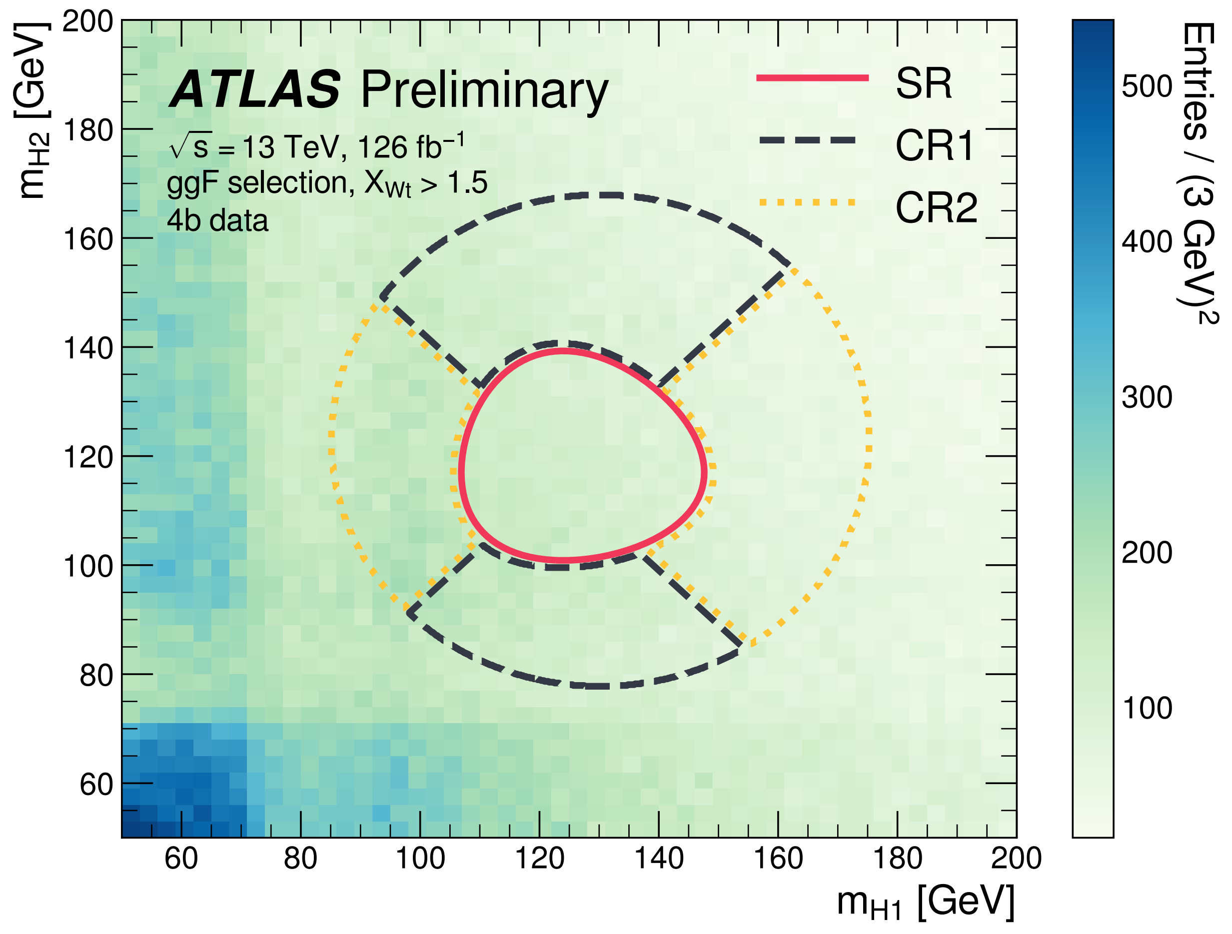

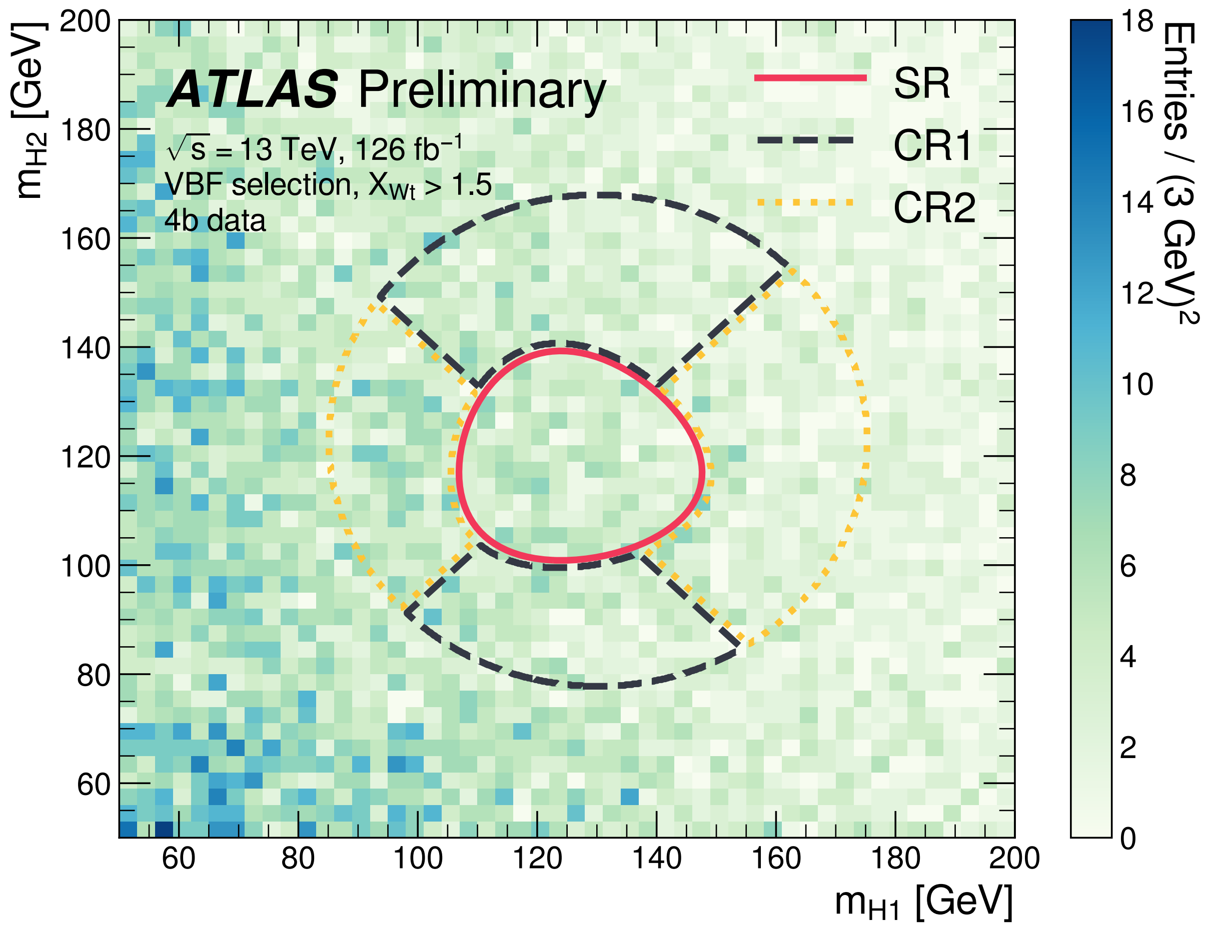

Non-resonant HH→bbbb with full Run 2 data

Main background: QCD multi-jet background

Data-driven estimation for the total background: using a neural network re-weighting with the neural network trained in control regions to reweight 2b data to look like 4b data, then applied to 2b data in the signal region to model 4b data in the signal region

ATLAS-CONF-2022-035

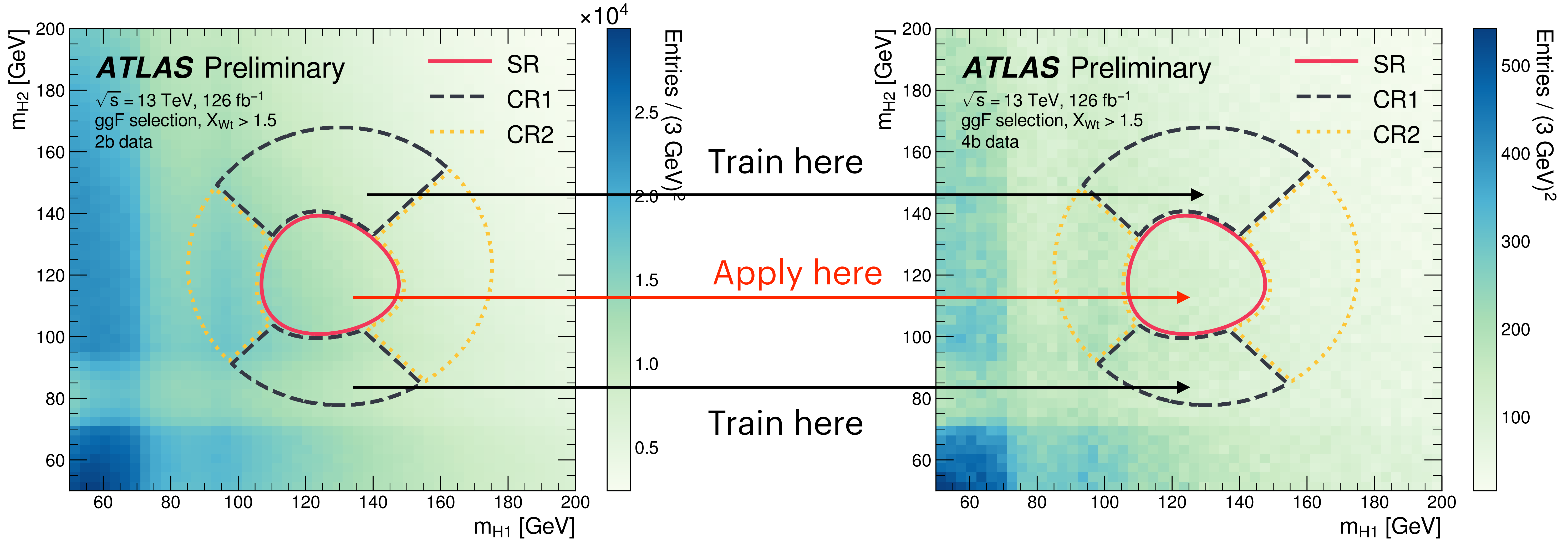

Before re-weighting

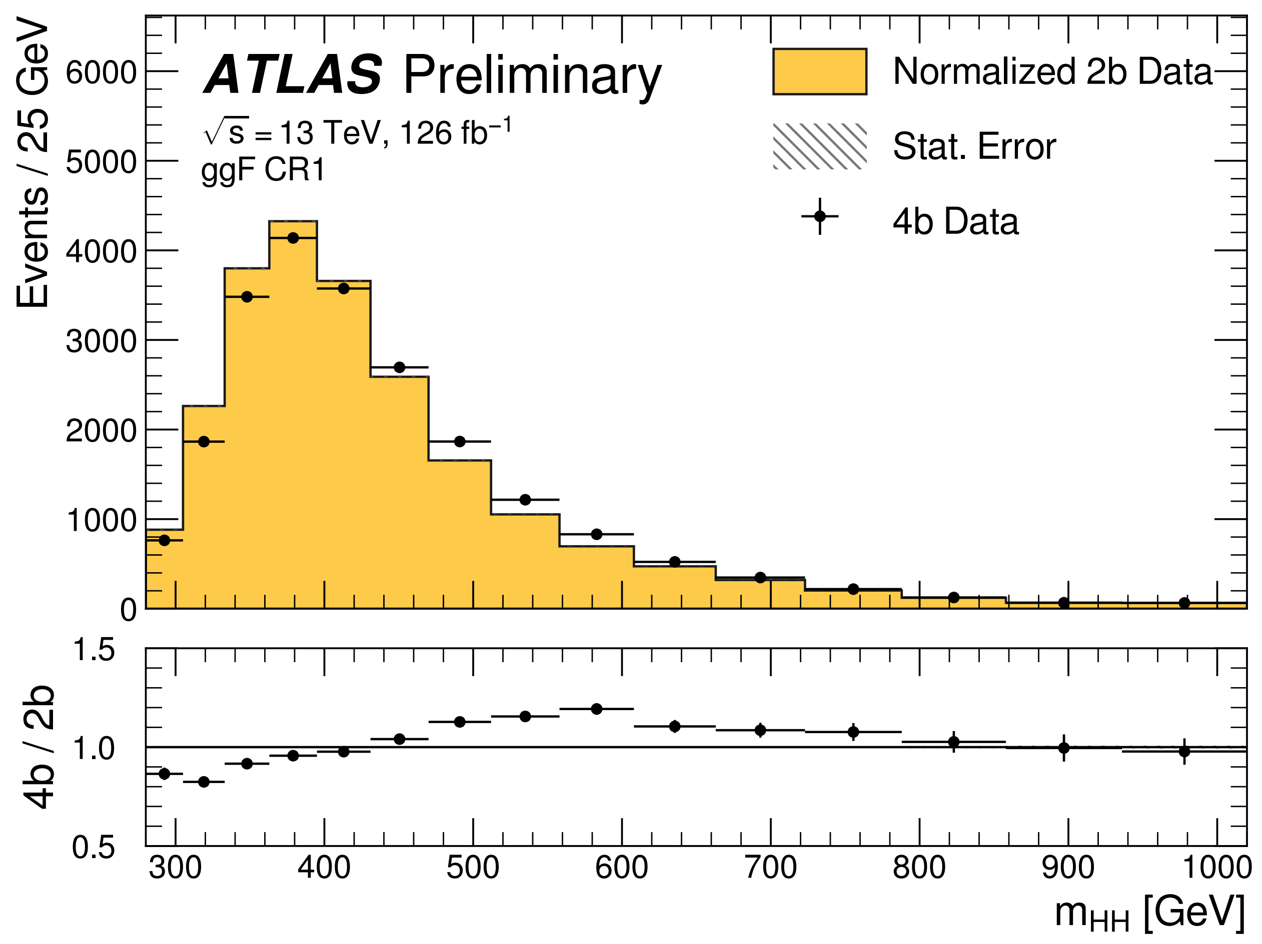

After re-weighting

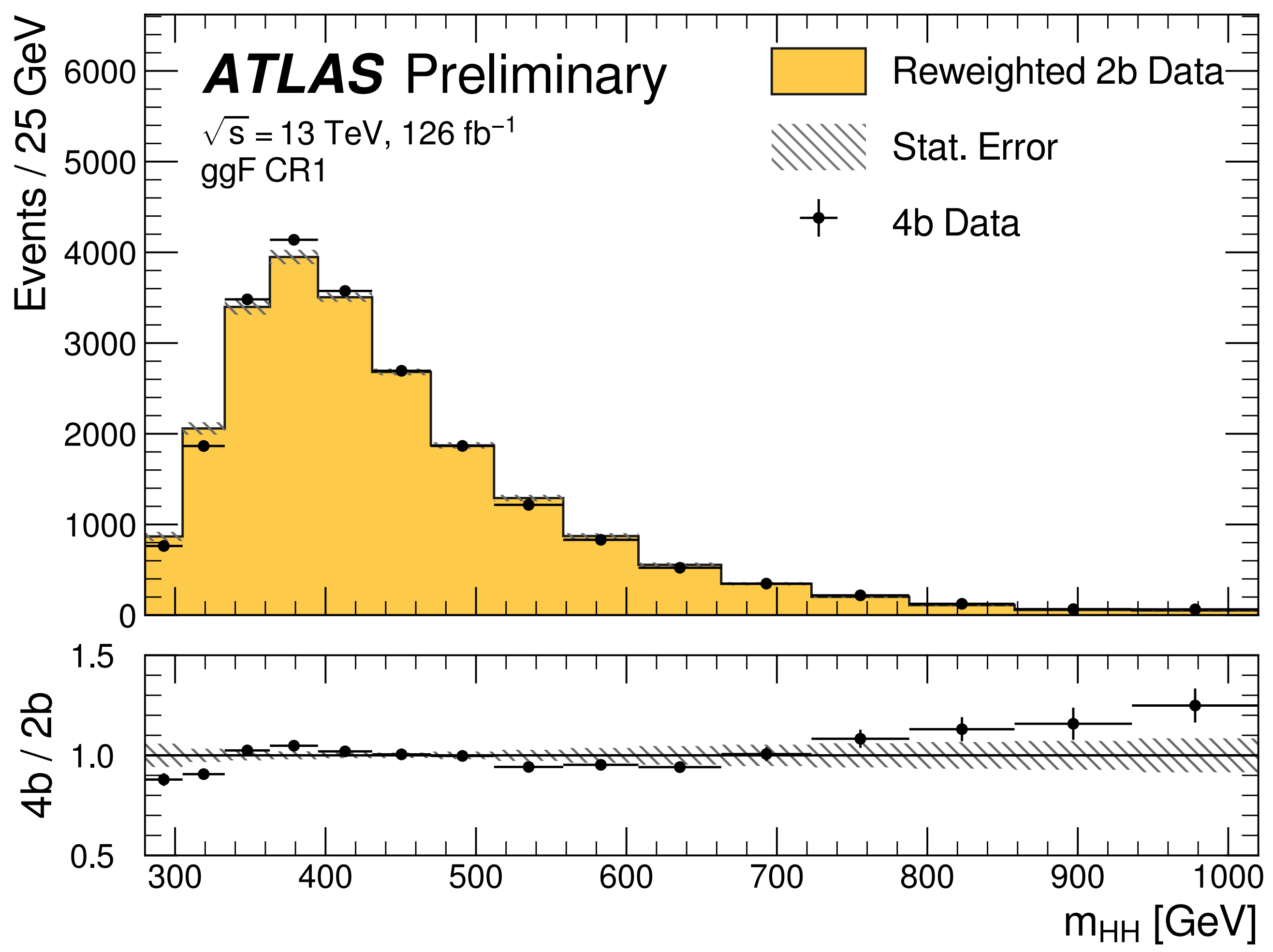

Non-resonant HH→bbbb with full Run 2 data

ggF and VBF categories further split to enhance sensitivity to SM signal and to signals with BSM couplings

- ggF categories:
  3x2 categories in bins of
  $|\Delta\eta_{HH}| \times X_{HH}$

- VBF categories:
  2 categories in bins of
  $|\Delta\eta_{HH}|$

m_{HH} used as final discriminant variable in the 8 signal regions, searching for an excess of events in the di-Higgs mass spectrum

ATLAS-CONF-2022-035

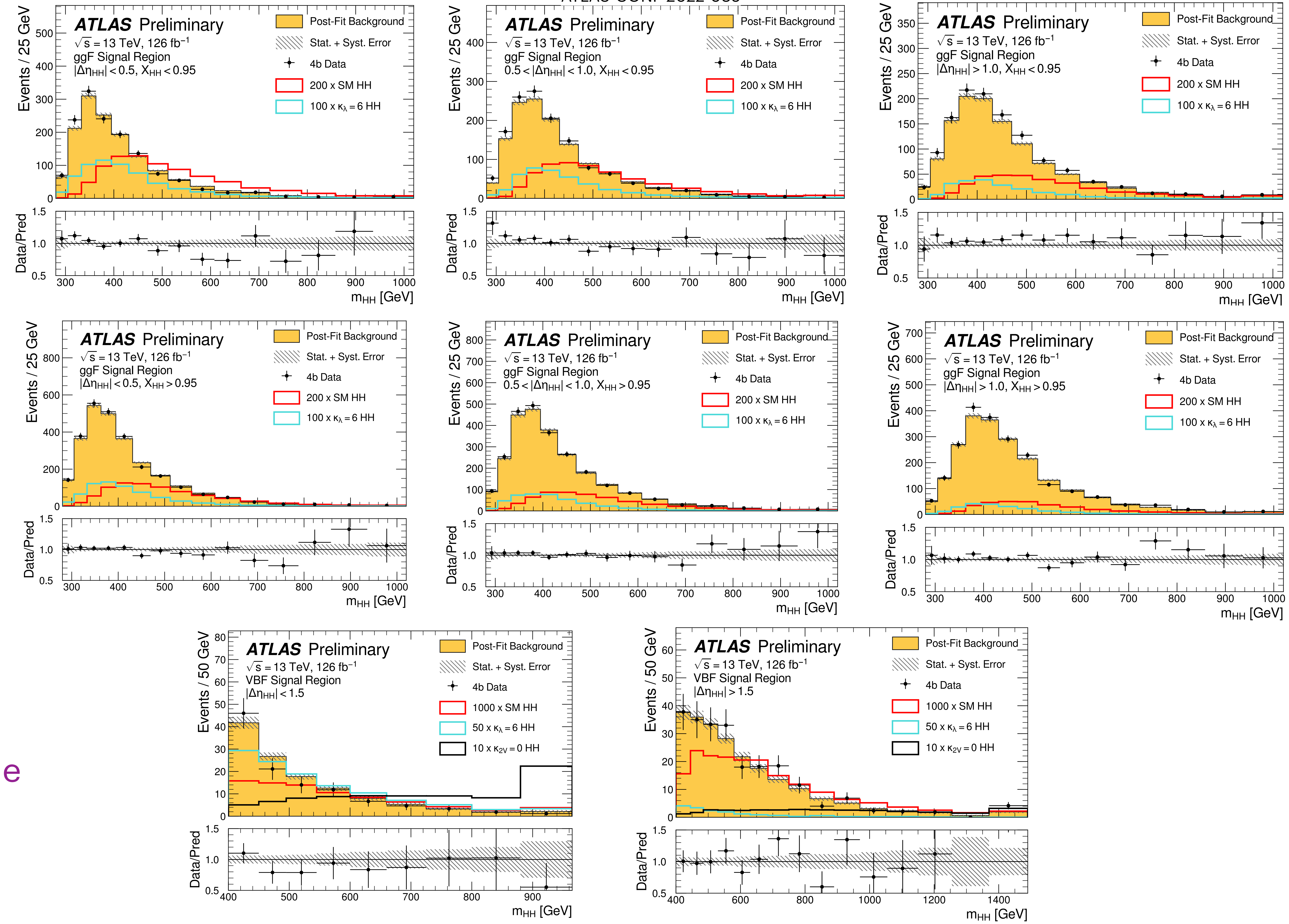

Non-resonant HH→bbbb with full Run 2 data

ATLAS-CONF-2022-035

	Observed Limit	-2σ	-1σ	Expected Limit	$+1\sigma$	$+2\sigma$
$\sigma_{\mathrm{ggF}}/\sigma_{\mathrm{ggF}}^{\mathrm{SM}}$	5.5	4.4	5.9	8.2	12.4	19.6
$\sigma_{\mathrm{VBF}}/\sigma_{\mathrm{VBF}}^{\mathrm{SM}}$	130.5	71.6	96.1	133.4	192.9	279.3
$\sigma_{\mathrm{ggF+VBF}}/\sigma_{\mathrm{ggF+VBF}}^{\mathrm{SM}}$	5.4	4.3	5.8	8.1	12.2	19.1

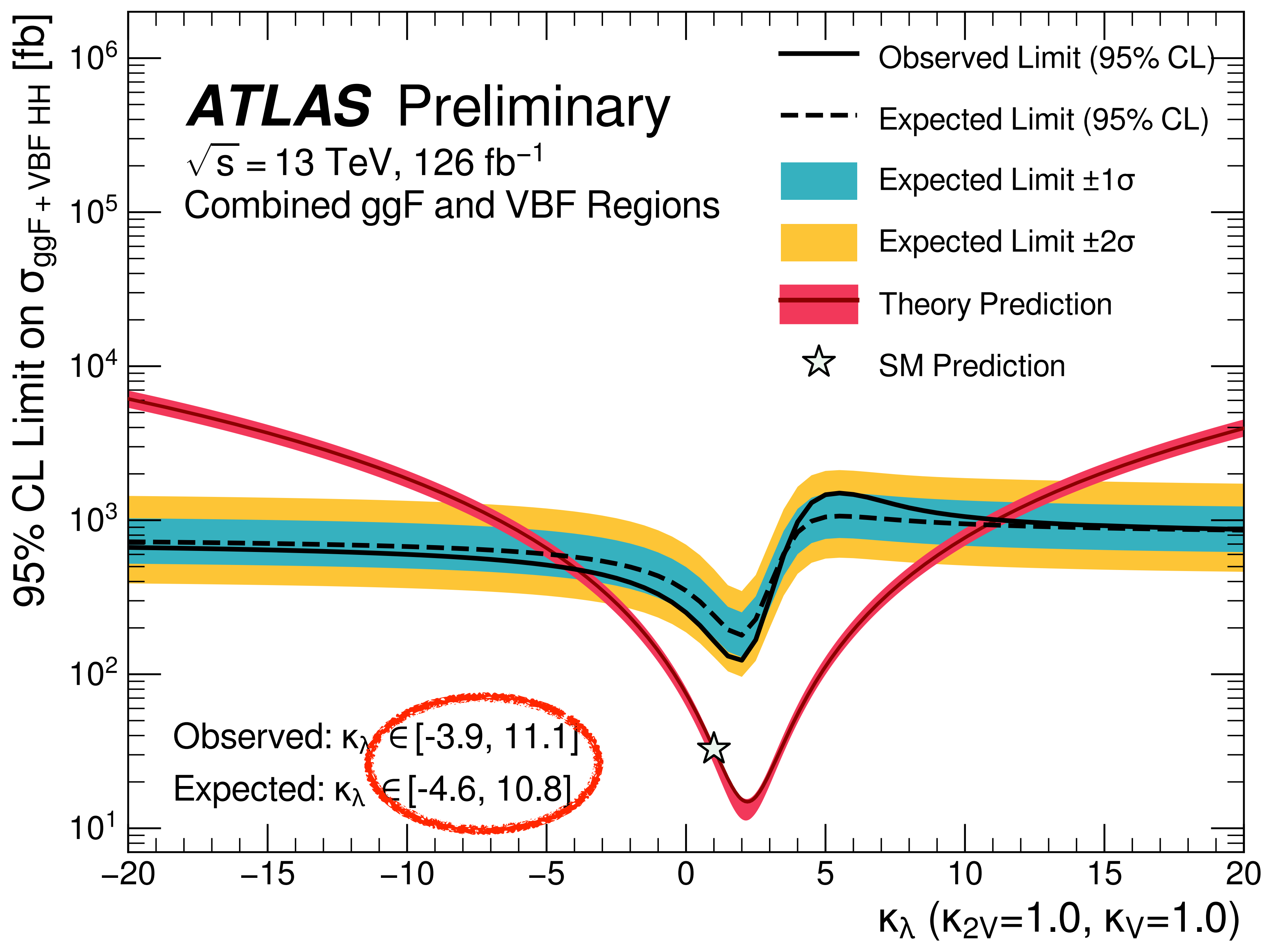

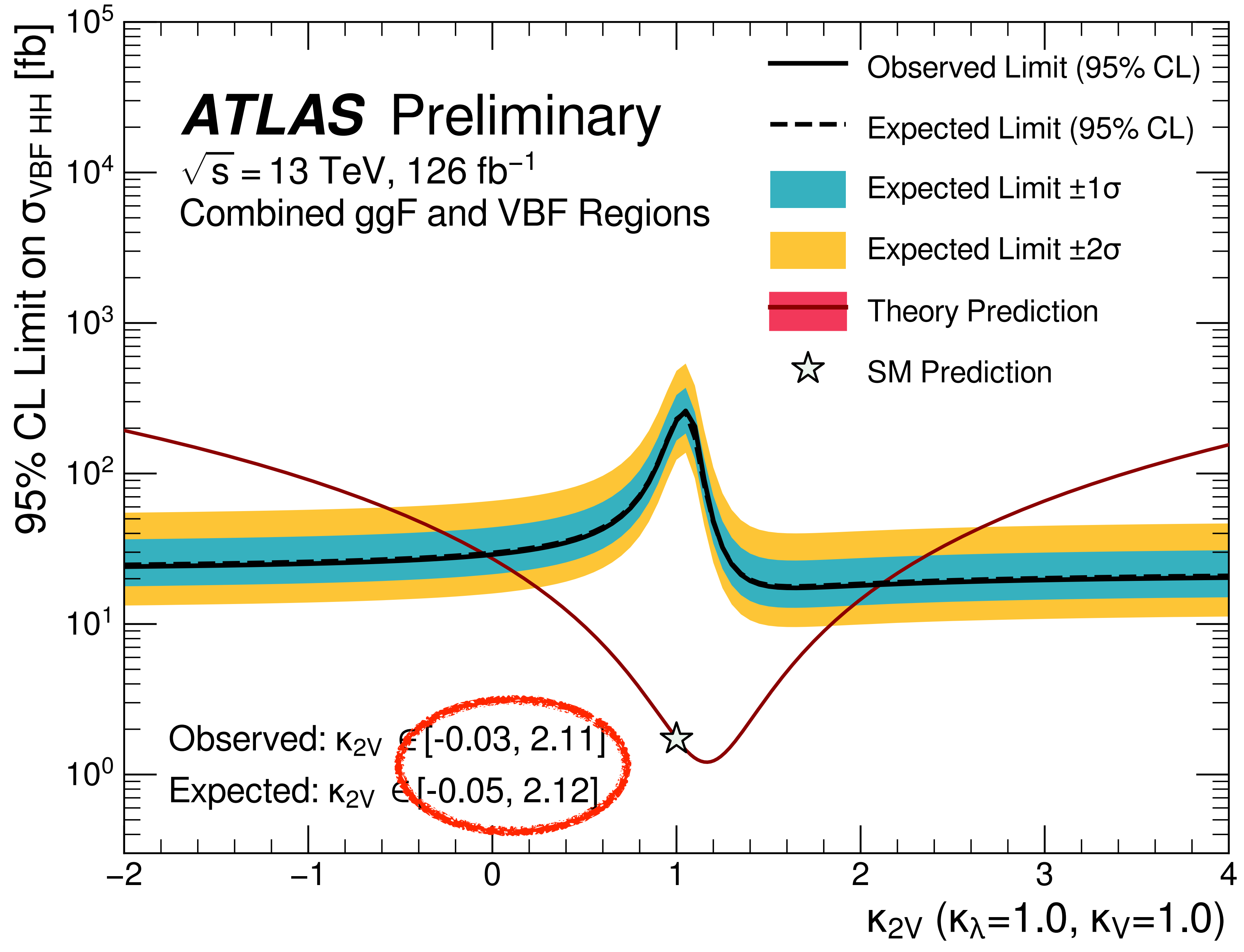

Factor 3 improvement compared to previous partial Run 2 dataset bbbb results:
factor 2 from luminosity increase, rest from improvements in objects reconstruction and identification (b-tagging) and event selection and categorization

Non-resonant HH→bbbb with full Run 2 data

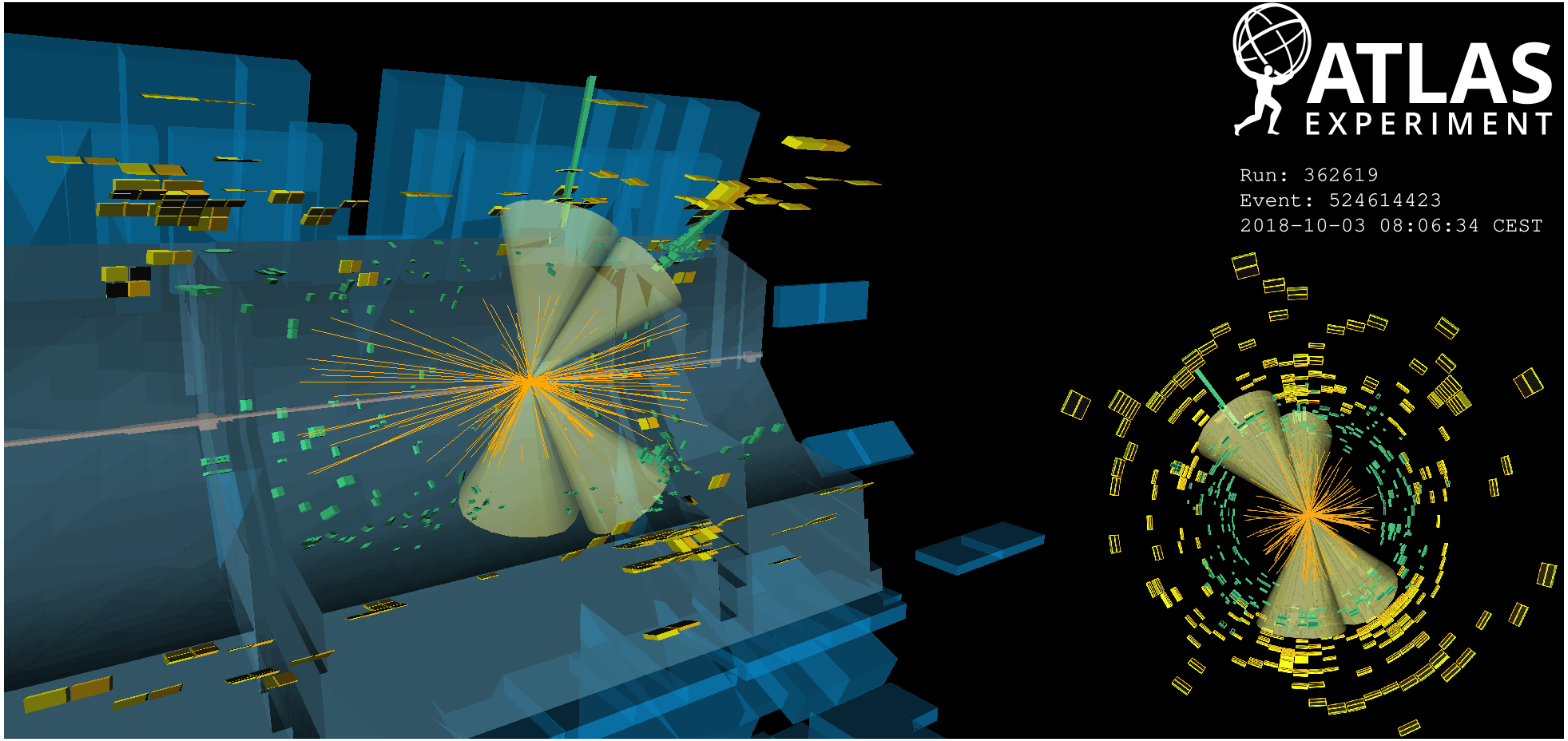

Data event in the ggF category

$m_{HH} = 588$ GeV, $m_{bb} = 126$ GeV and $m_{bb} = 114$ GeV

Non-resonant HH→bbττ with full Run 2 data

bbττ decay channel has relatively high BR (7.3%) and relatively clean signature,
but background with jets faking hadronically decaying τ-leptons difficult to model

- Search for SM and BSM non-resonant HH production
- ggF and VBF HH production
- H→bb and H→ττ
- Semi-leptonic (LepHad) and fully hadronic (HadHad) decays of the di-τ system
- 1 lepton (e/mu) and 1 τ in LepHad, 2 τ in HadHad
- 2 b-tagged jets
- 3 signal regions defined depending on the di-τ system decay mode and trigger decision

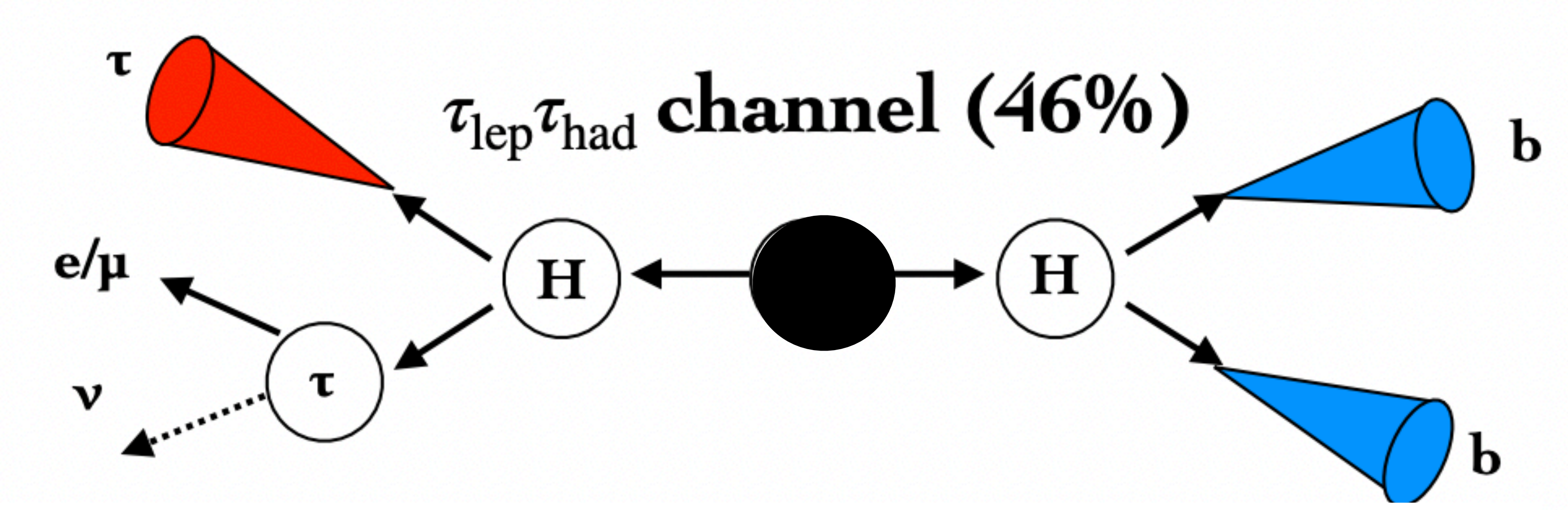

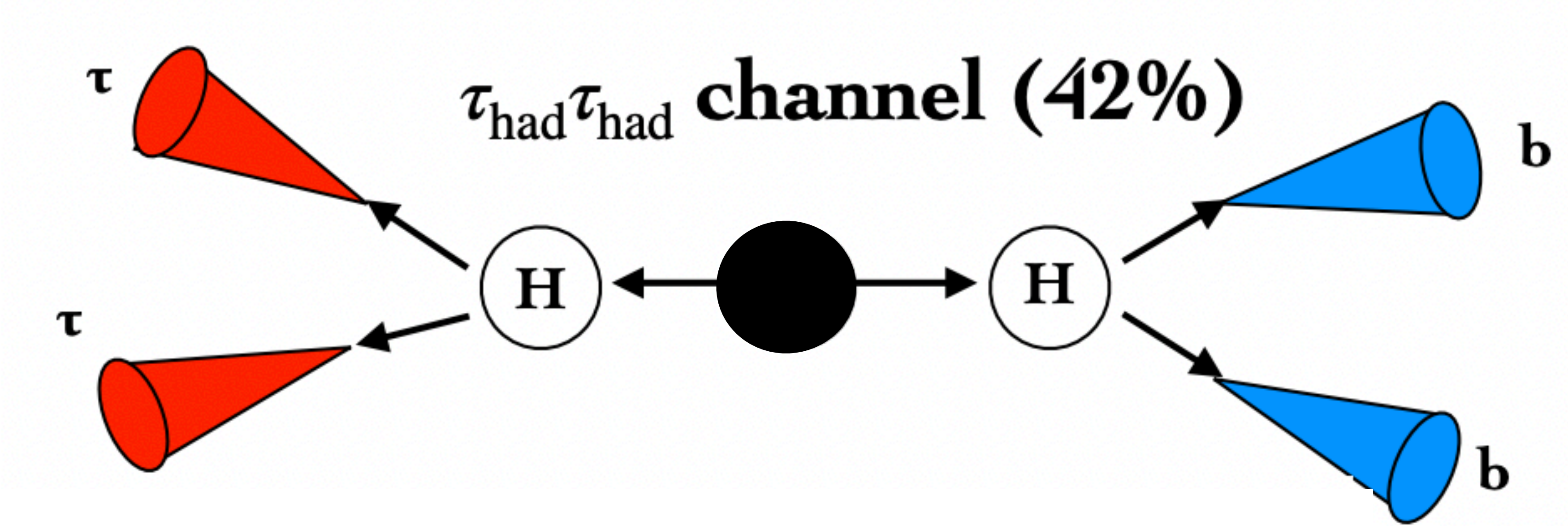

Main backgrounds:

- ttbar and Z+heavy flavour jets (with real τ), modelled with Monte Carlo simulations, with normalisation from fit to data in control regions
- Events with jets faking hadronically decaying τ-leptons from ttbar and QCD multi-jet (data-driven methods)

HadHad

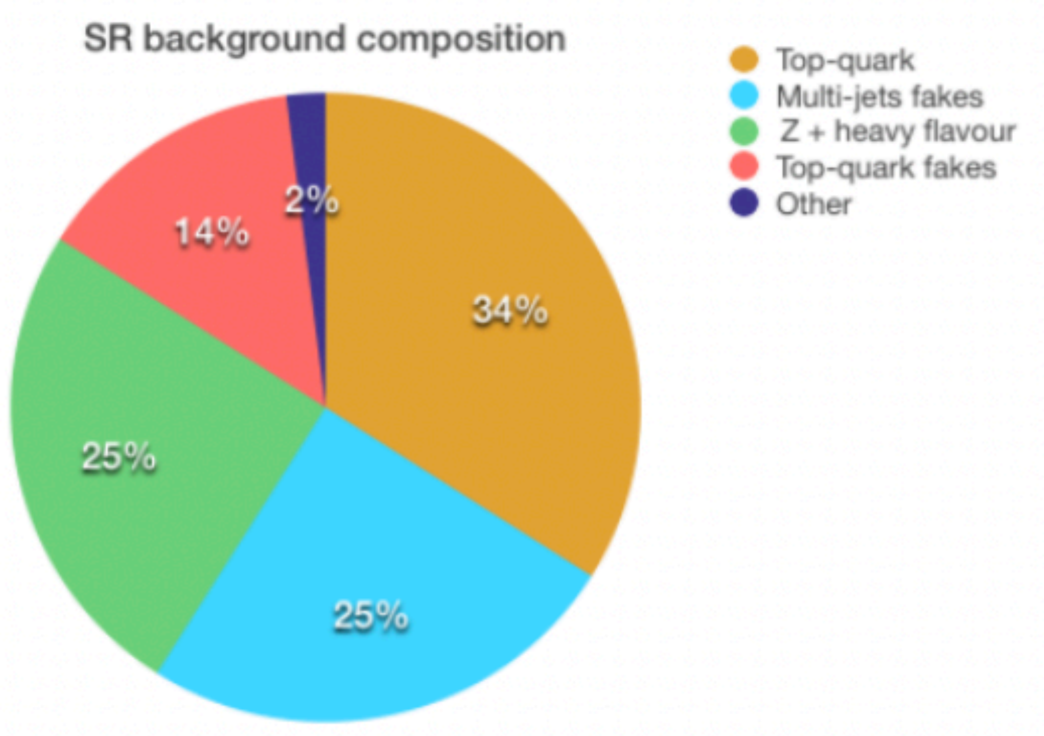

LepHad

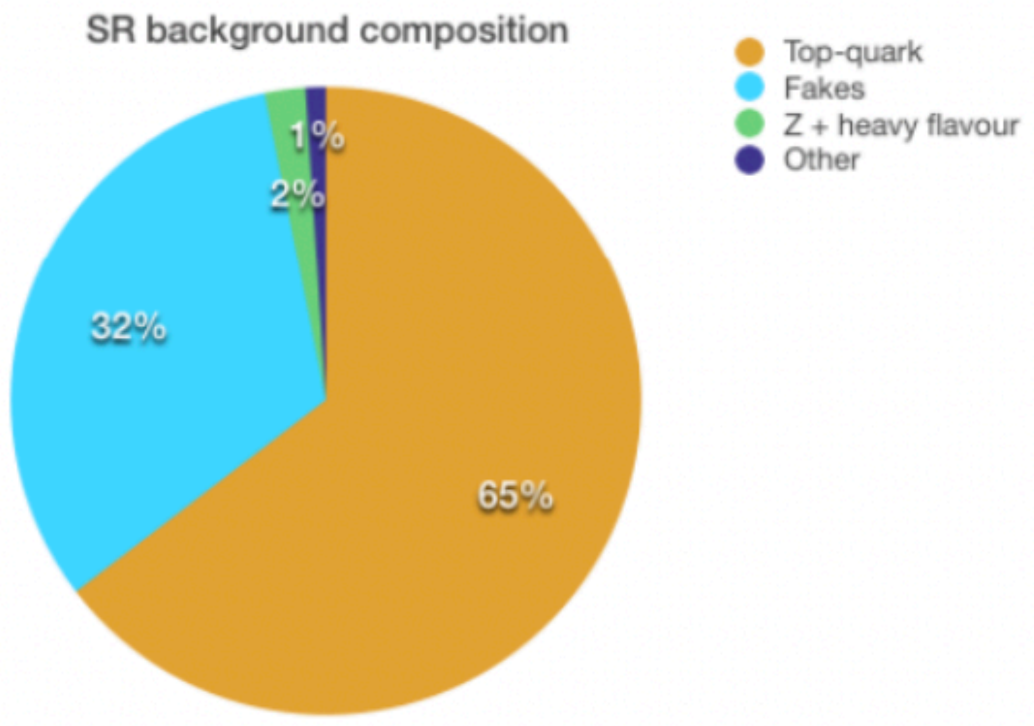

Non-resonant HH→bbττ with full Run 2 data

Different data-driven methods used in the HadHad and LepHad channels to estimate the contribution from events with jets faking hadronically decaying τ-leptons

HadHad channel:

- QCD multi-jet: fake-factor method with fake-factors derived from data in 2 control regions and applied to data in a 3rd control region to obtain the signal region template
- ttbar fakes: scale-factor method with scale-factors derived from data in a control region using MC template fits and applied to the MC in the signal region to obtained the corrected template

LepHad channel:

- Combined fake-factor method for fakes from QCD and ttbar with separate fake-factors derived in dedicated control regions then combined and applied to data in another control region to obtain the signal region template

HadHad QCD fake-factors method

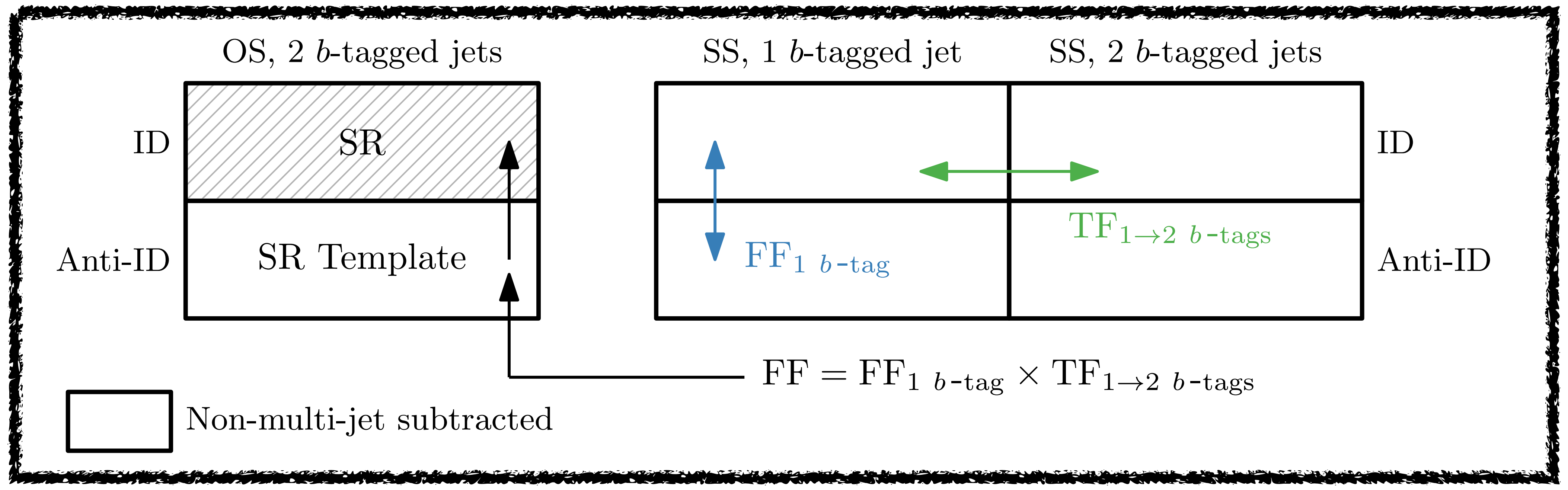

HadHad ttbar scale-factor method

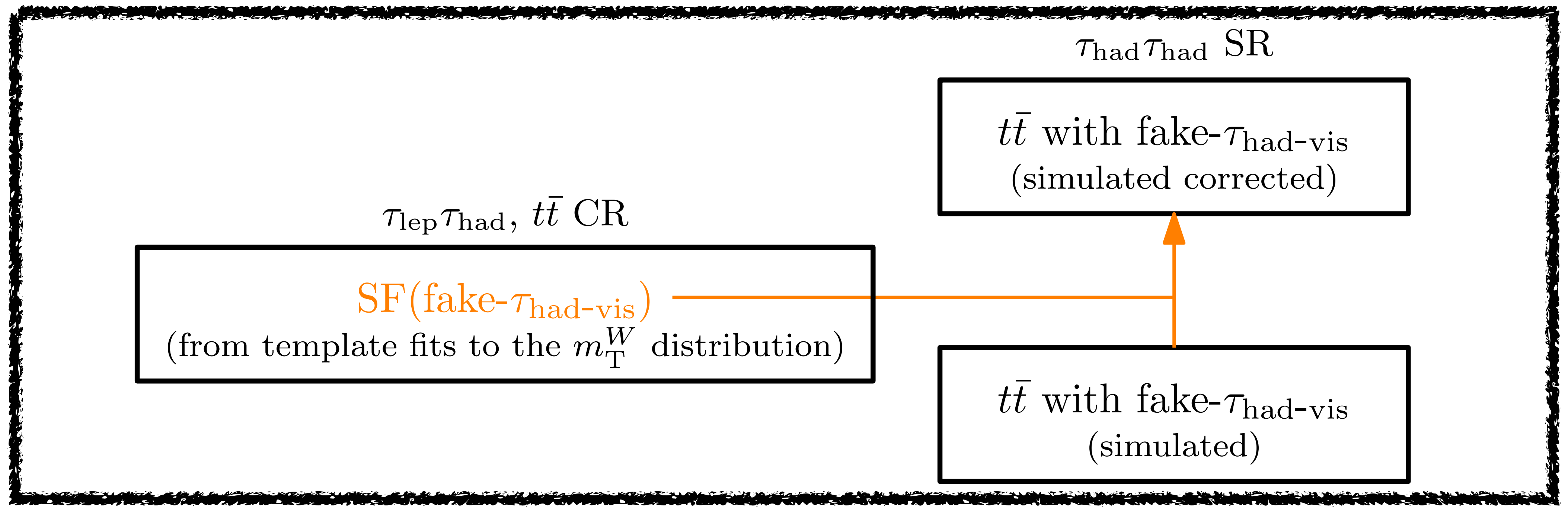

LepHad combined fake-factor method

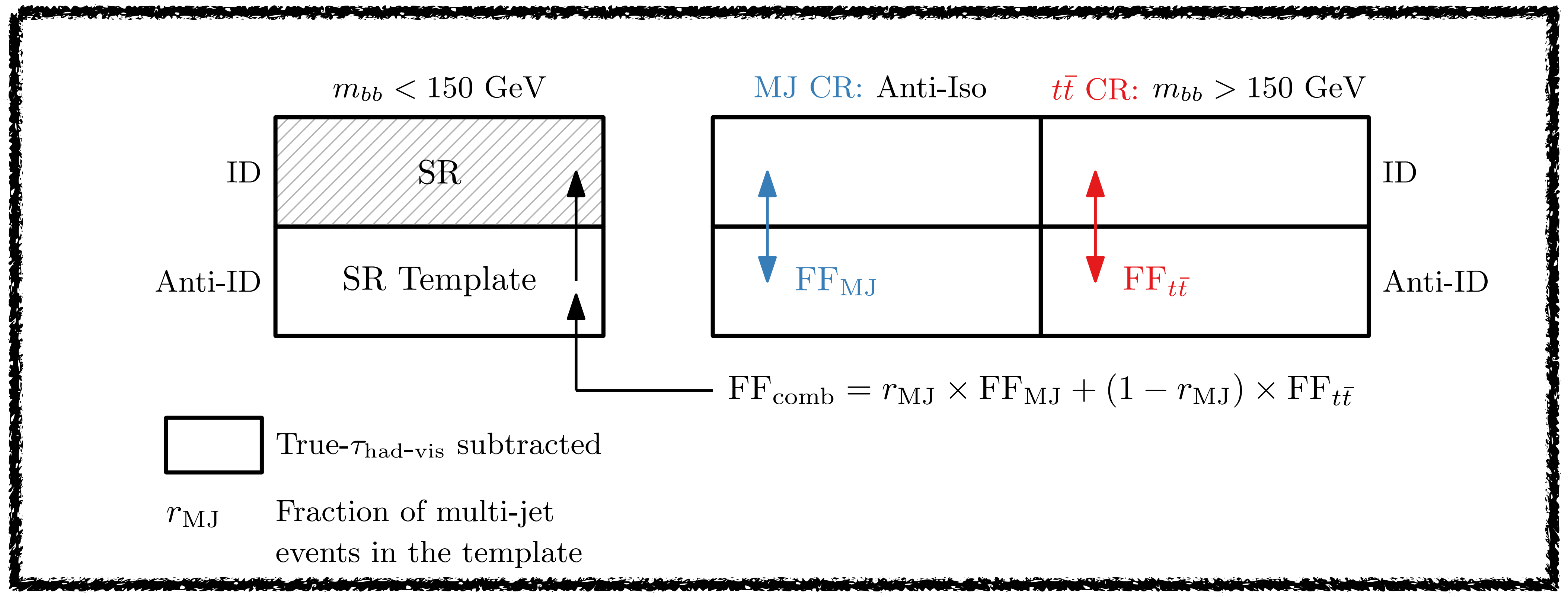

Non-resonant HH→bbττ with full Run 2 data

- Multi-variate analysis (MVA) discriminants (Boosted Decision Trees and Neural Networks) used to separate signal from background

- Important input variables: reconstructed di-Higgs invariant mass m_{HH}, reconstructed invariant masses of the two Higgs boson candidates m_{bb} and $m_{\tau\tau}$

- MVA outputs used as final discriminants searching for an excess of events in the most signal-like bins of the MVAs

ATLAS-CONF-2021-030

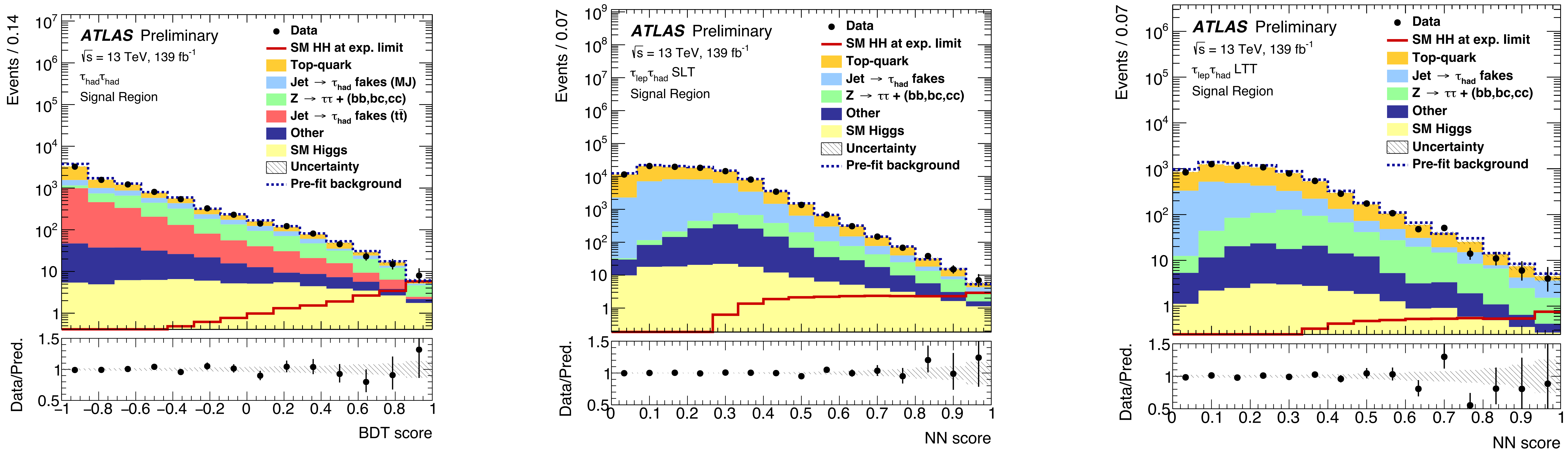

Non-resonant HH→bbττ with full Run 2 data

ATLAS-CONF-2021-030

		Observed	−2 σ	−1 σ	Expected	+1 σ	+2 σ
$\tau_{had}\tau_{had}$	$\sigma_{ggF+VBF}$ [fb]	145	70.5	94.6	131	183	245
	$\sigma_{ggF+VBF}/\sigma^{SM}_{ggF+VBF}$	4.95	2.38	3.19	4.43	6.17	8.27
$\tau_{lep}\tau_{had}$	$\sigma_{ggF+VBF}$ [fb]	265	124	167	231	322	432
	$\sigma_{ggF+VBF}/\sigma^{SM}_{ggF+VBF}$	9.16	4.22	5.66	7.86	10.9	14.7
Combined	$\sigma_{ggF+VBF}$ [fb]	135	61.3	82.3	114	159	213
	$\sigma_{ggF+VBF}/\sigma^{SM}_{ggF+VBF}$	4.65	2.08	2.79	3.87	5.39	7.22

Best (expected) upper limit on non-resonant HH production from a single HH decay channel with full Run 2 dataset

ATLAS-CONF-2021-052

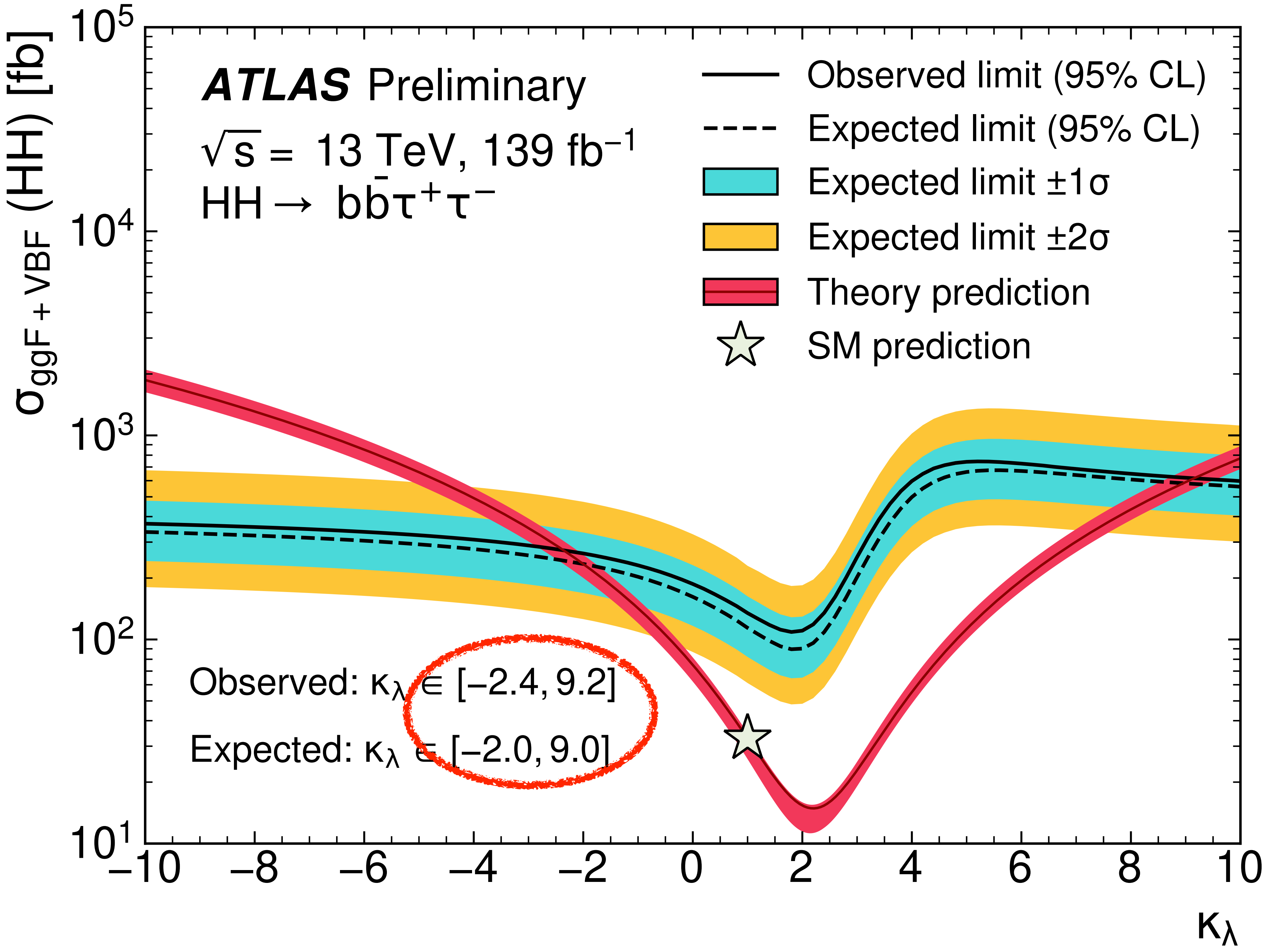

Factor 4 improvement compared to previous partial Run 2 dataset bbττ results:

factor 2 from luminosity increase and factor 2 from improvements in objects reconstruction and event selection (b-tagging and τ-identification)

Non-resonant HH→bbττ with full Run 2 data

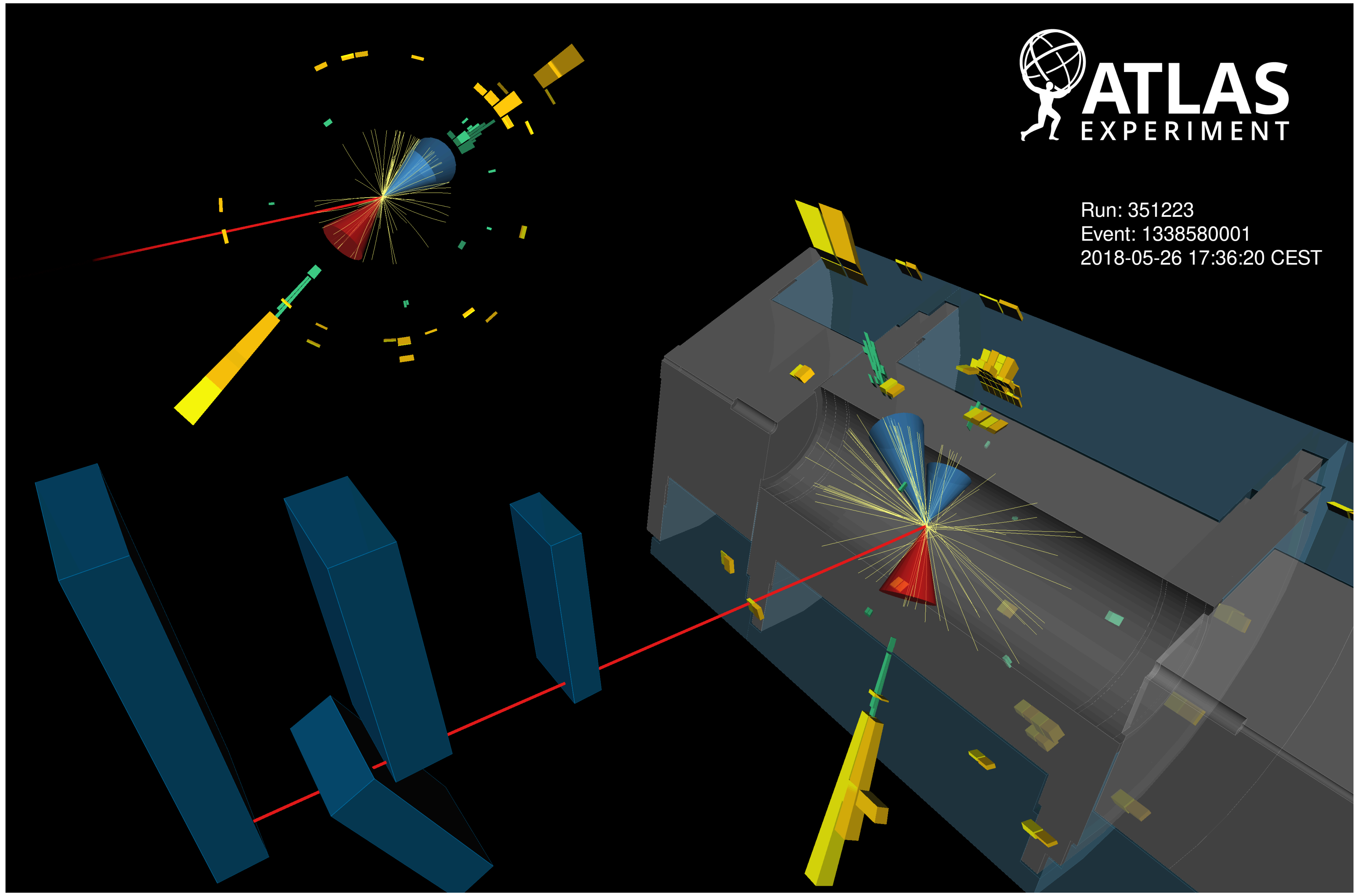

Data event in the $\tau_{lep}\tau_{had}$ channel signal region

$m_{HH} = 680$ GeV, $m_{bb} = 120$ GeV and $m_{\tau\tau}^{MMC} = 120$ GeV

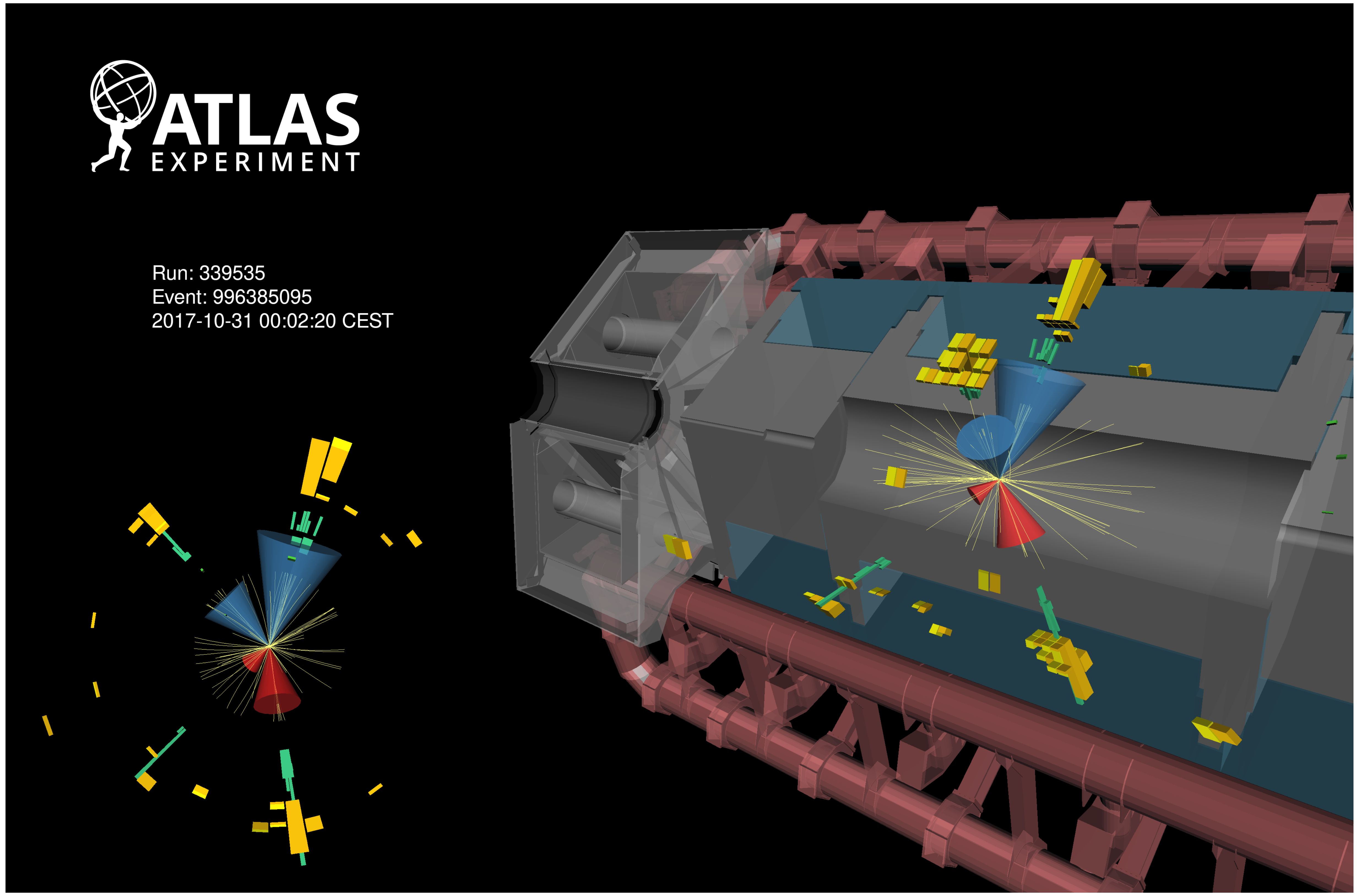

Data event in the $\tau_{had}\tau_{had}$ channel signal region

$m_{HH} = 510$ GeV, $m_{bb} = 130$ GeV and $m_{\tau\tau}^{MMC} = 130$ GeV

Non-resonant HH→bbγγ with full Run 2 data

bbγγ decay channel has very small BR (0.26%) but very clean signature from the photons and clean smoothly falling di-photon background

- Search for SM and BSM non-resonant HH production
- ggF and VBF HH production

- H→bb and H→γγ
- 2 photons and 2 b-tagged jets
- $105\ \text{GeV} < m_{\gamma\gamma} < 160\ \text{GeV}$

arXiv:2112.11876

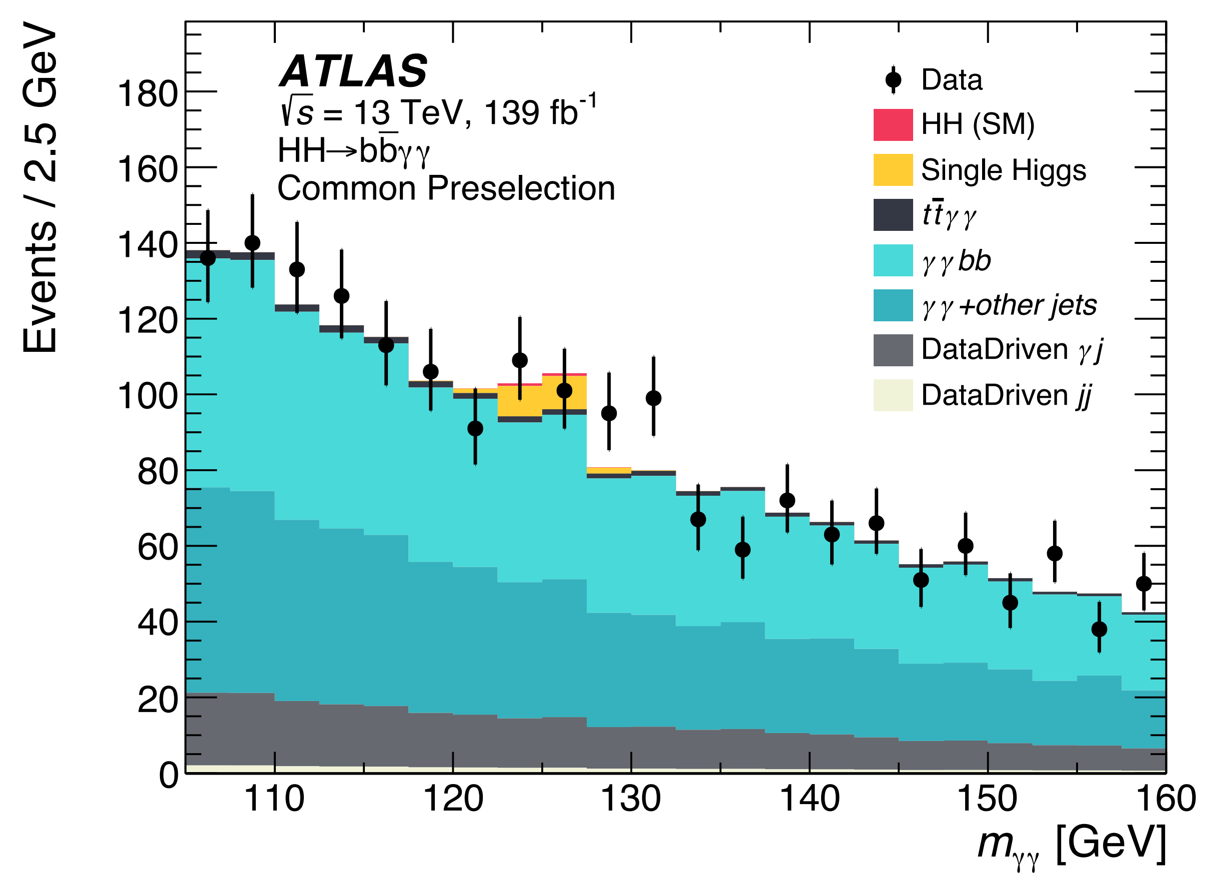

- Major backgrounds: γγ+jets modelled with exponential function derived from data in CRs and single-Higgs modelled with double-sided Crystal-Ball function derived from Monte Carlo simulations

- Signal shape also modelled with double-sided Crystal-ball function derived from Monte Carlo simulations

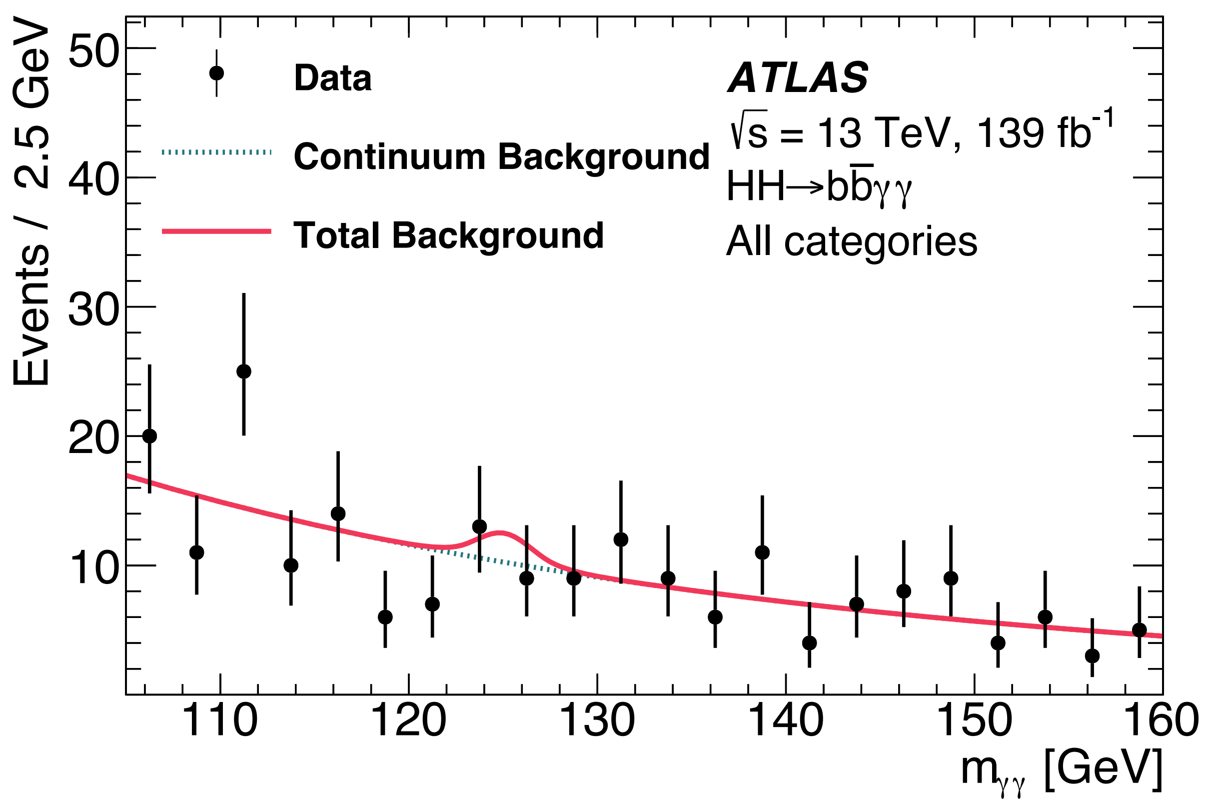

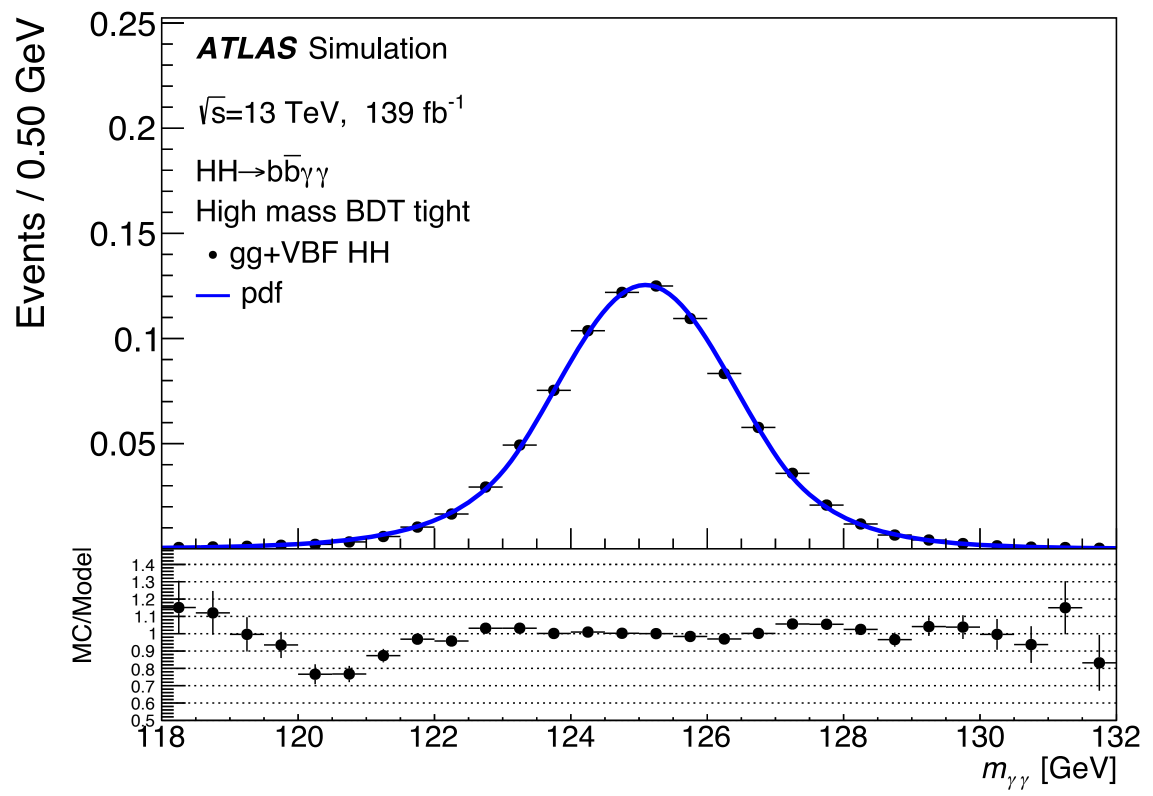

- Boosted Decision Trees used to discriminate signal and background
- Important input variable: reconstructed invariant mass of the Higgs boson candidate m_{bb}

Non-resonant HH→bbγγ with full Run 2 data

4 signal region categories

defined by selections on $m_{bb\gamma\gamma}$ and on BDT outputs,
targeting the SM HH signal and BSM signals with varied κ_λ

- Two HH mass categories:
  low mass $m_{bb\gamma\gamma} < 350$ GeV and high mass
  $m_{bb\gamma\gamma} > 350$ GeV

- One BDT trained in each mass region,
on BSM signal with $\kappa_\lambda = 10$ for low mass
and on SM signal with $\kappa_\lambda = 1$ for high mass

- Two BDT categories:
  BDT-tight and BDT-loose, in each of the two mass categories

→ total of 4 signal region categories

arXiv:2112.11876

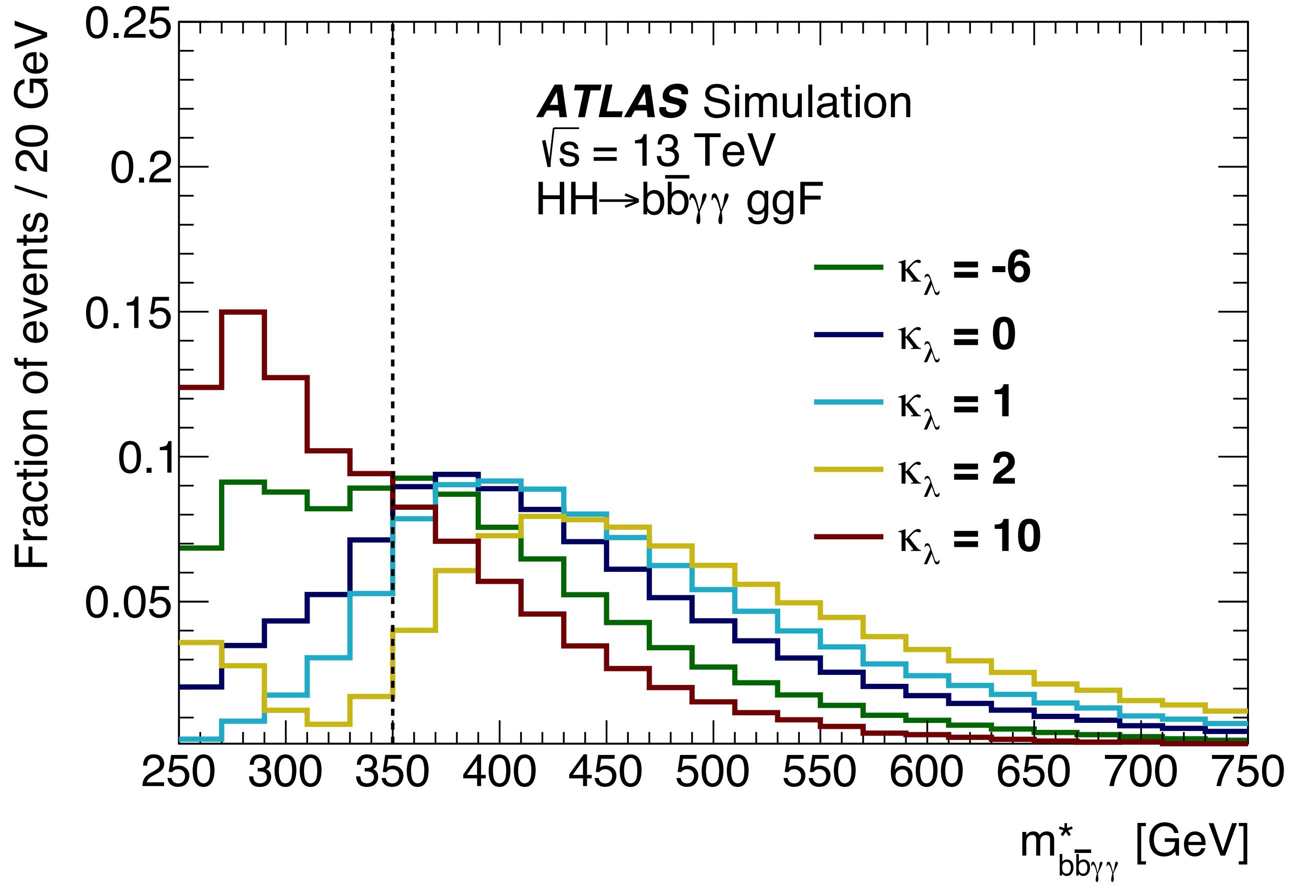

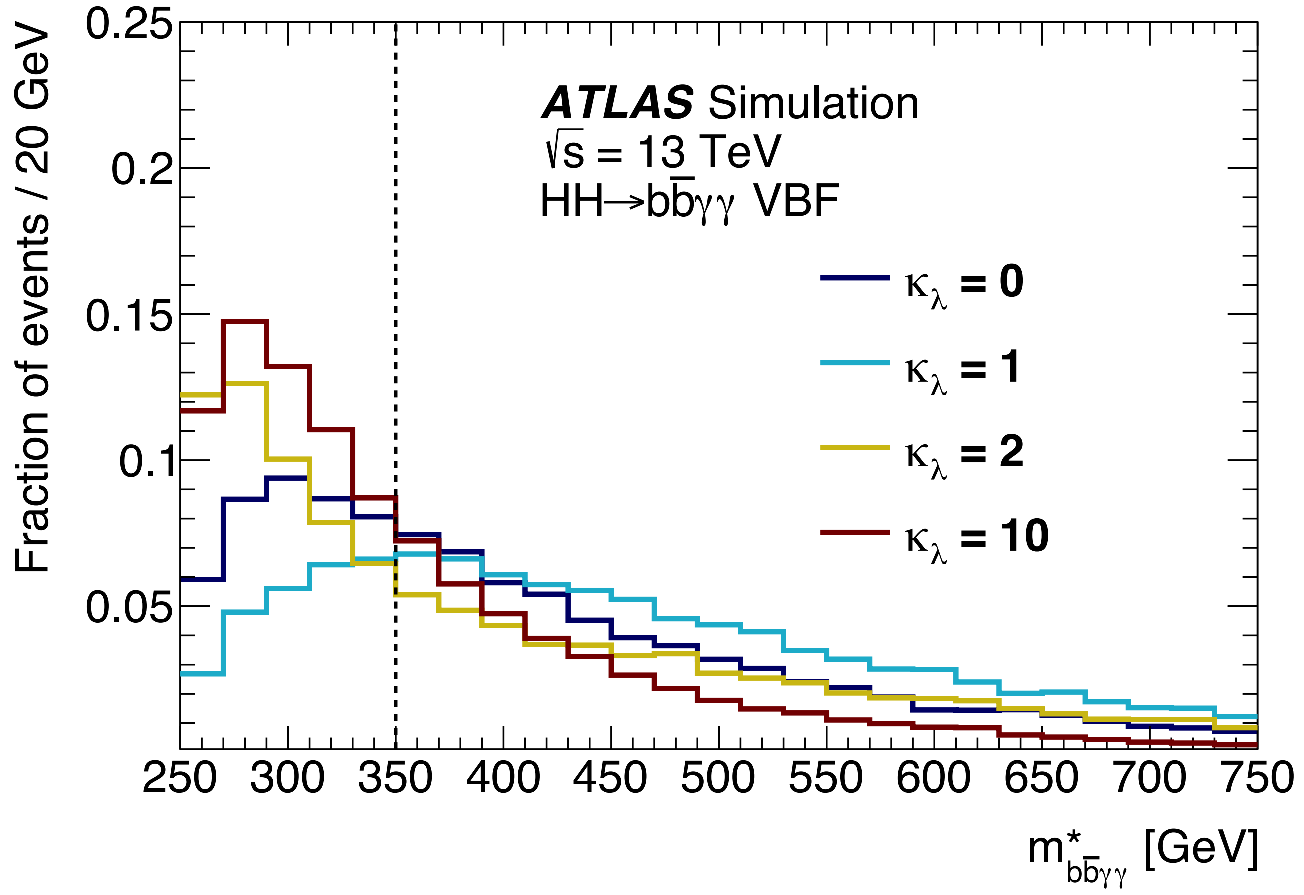

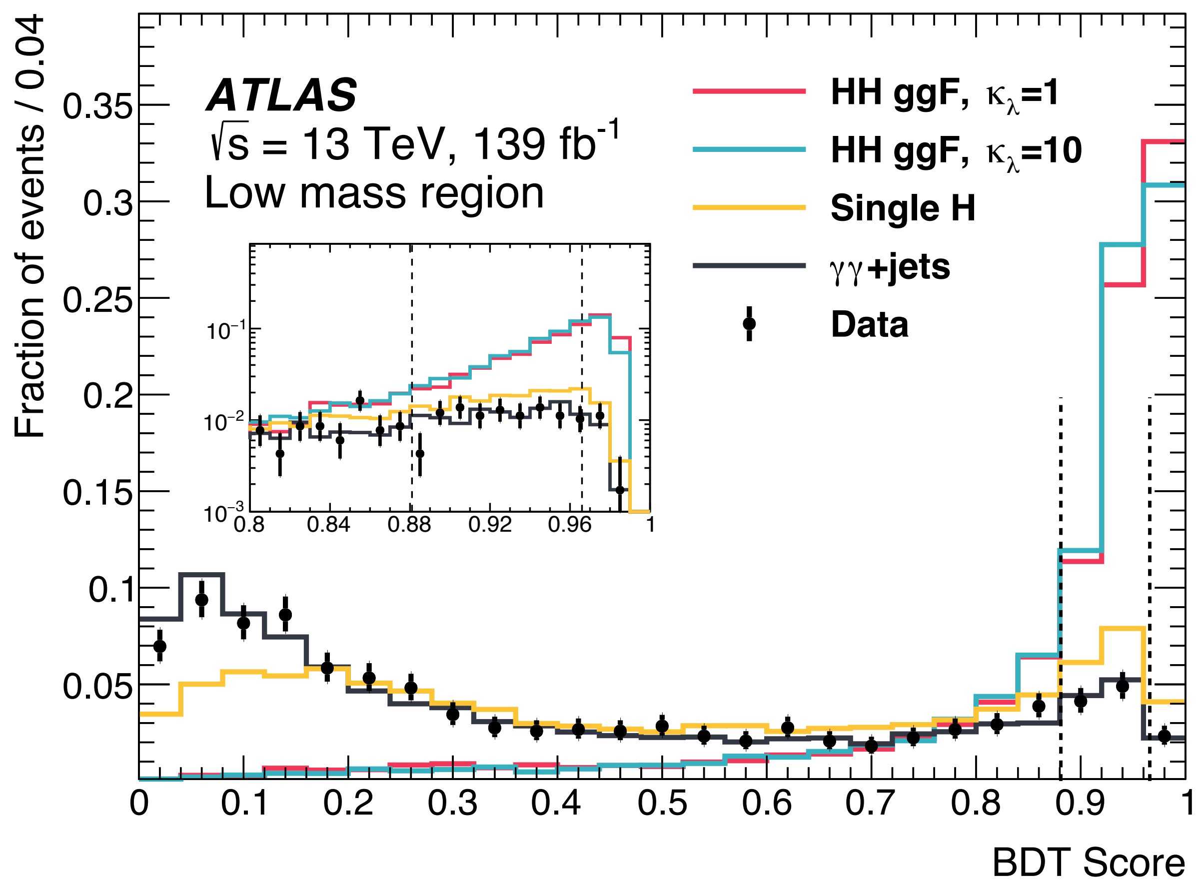

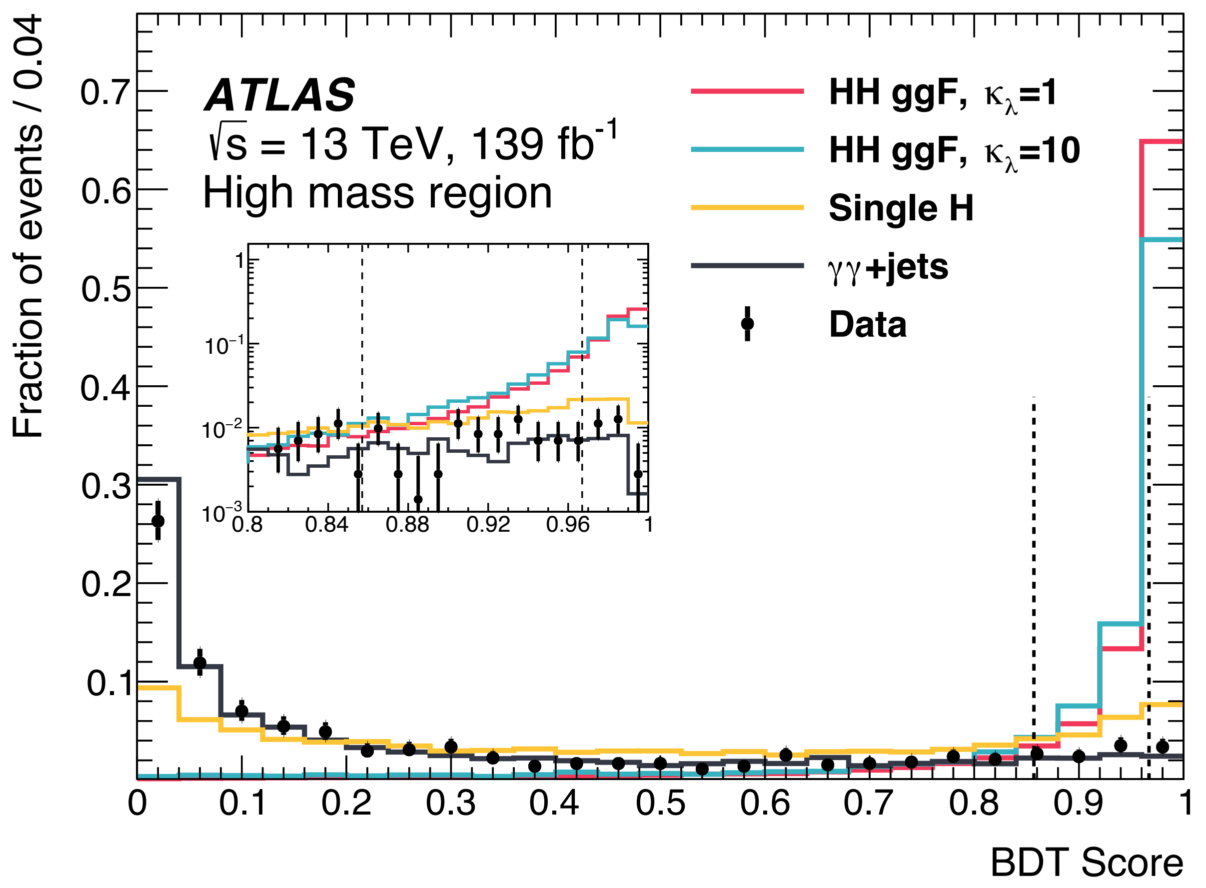

Non-resonant HH→bbγγ with full Run 2 data

arXiv:2112.11876

$m_{\gamma\gamma}$ used as final discriminant variable in the 4 signal regions, searching for an excess of events in the Higgs mass peak

Upper limit on the non-resonant ggF+VBF HH cross section of 4.2 x SM observed (5.7 x SM expected)

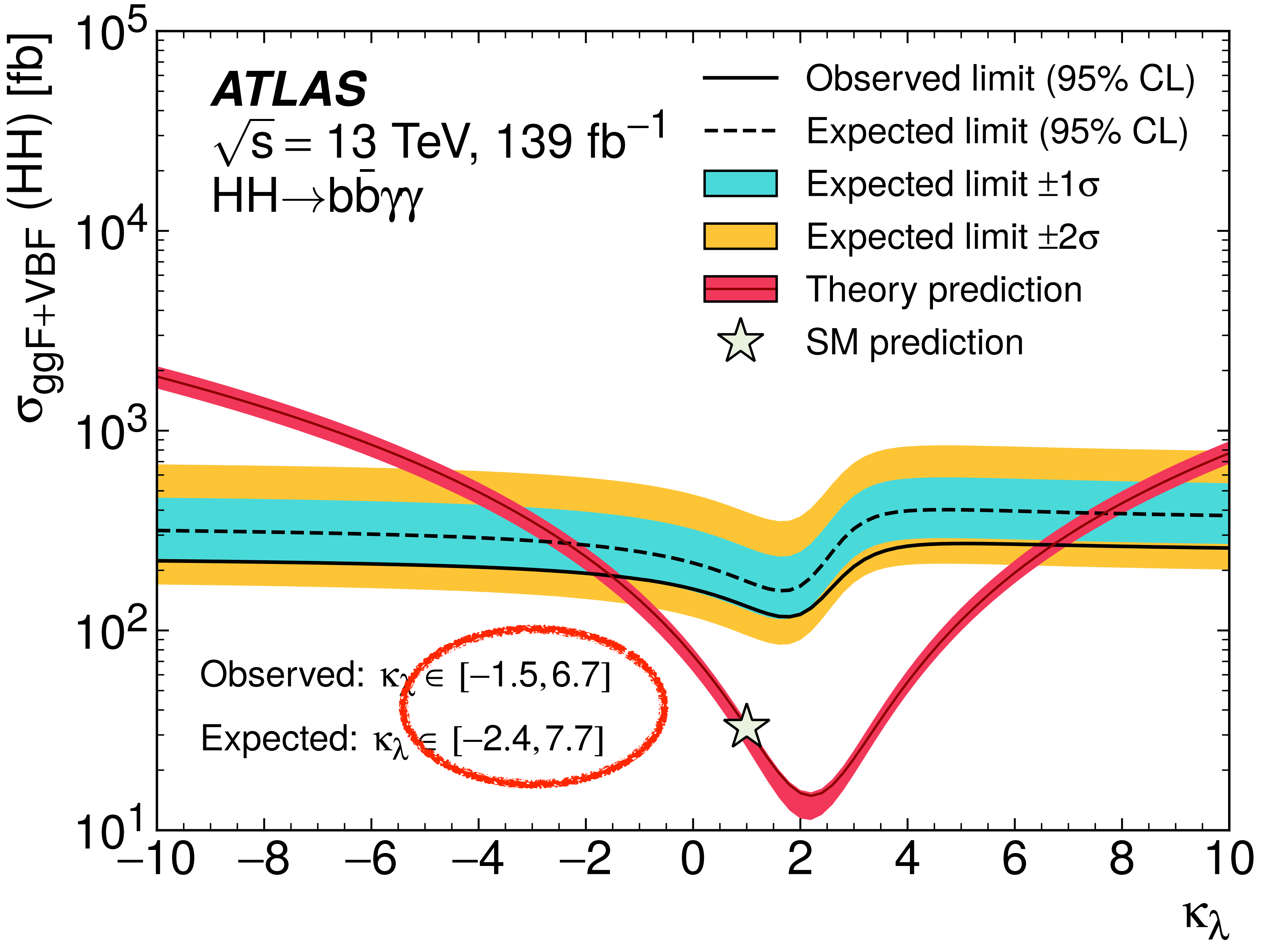

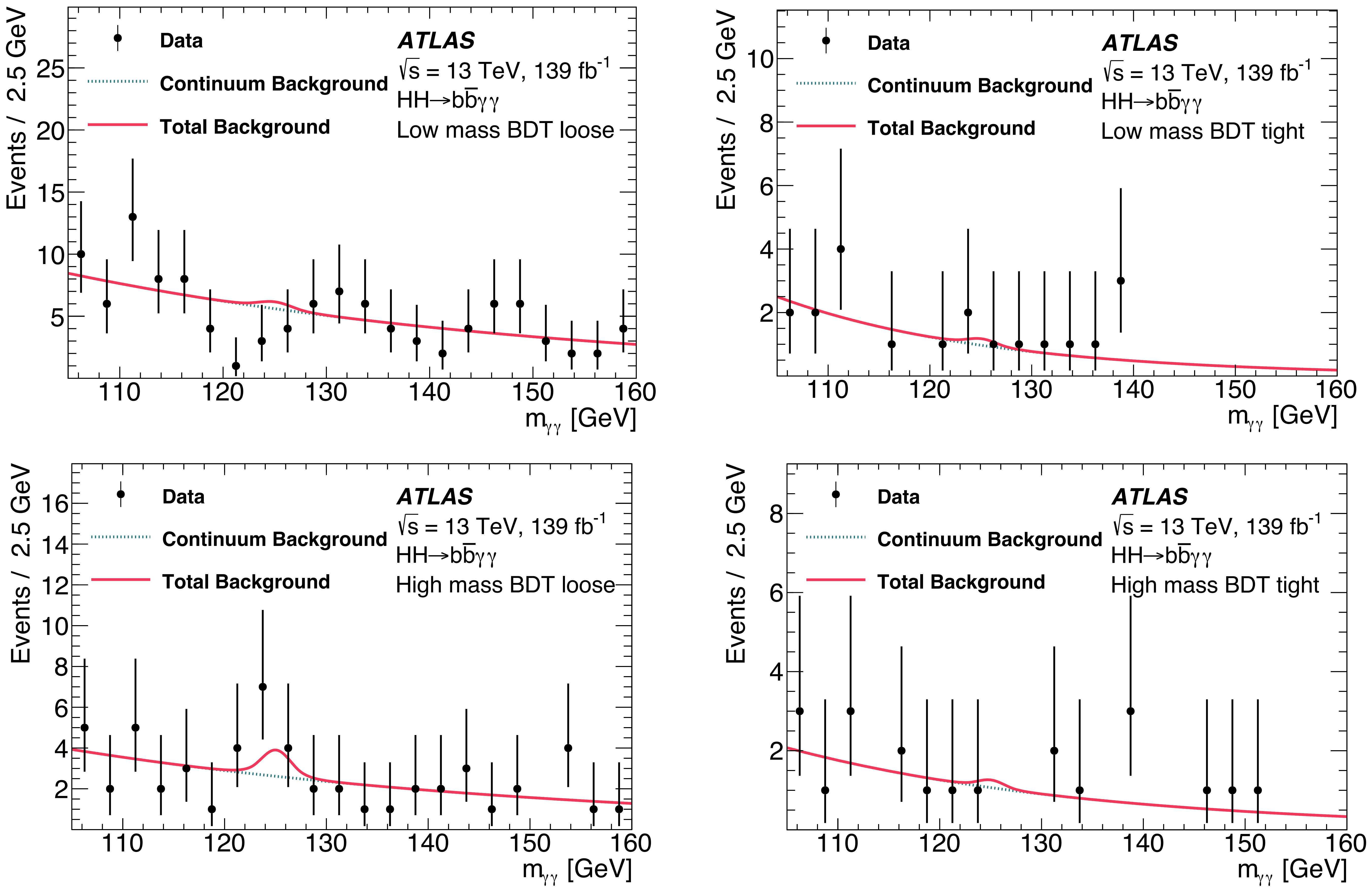

Factor 5 improvement compared to previous partial Run 2 dataset bbγγ results:

factor 2 from luminosity increase, rest from improvements in objects reconstruction and identification (b-tagging) and event categorisation in m_{HH} and BDT bins

Non-resonant HH→bbγγ with full Run 2 data

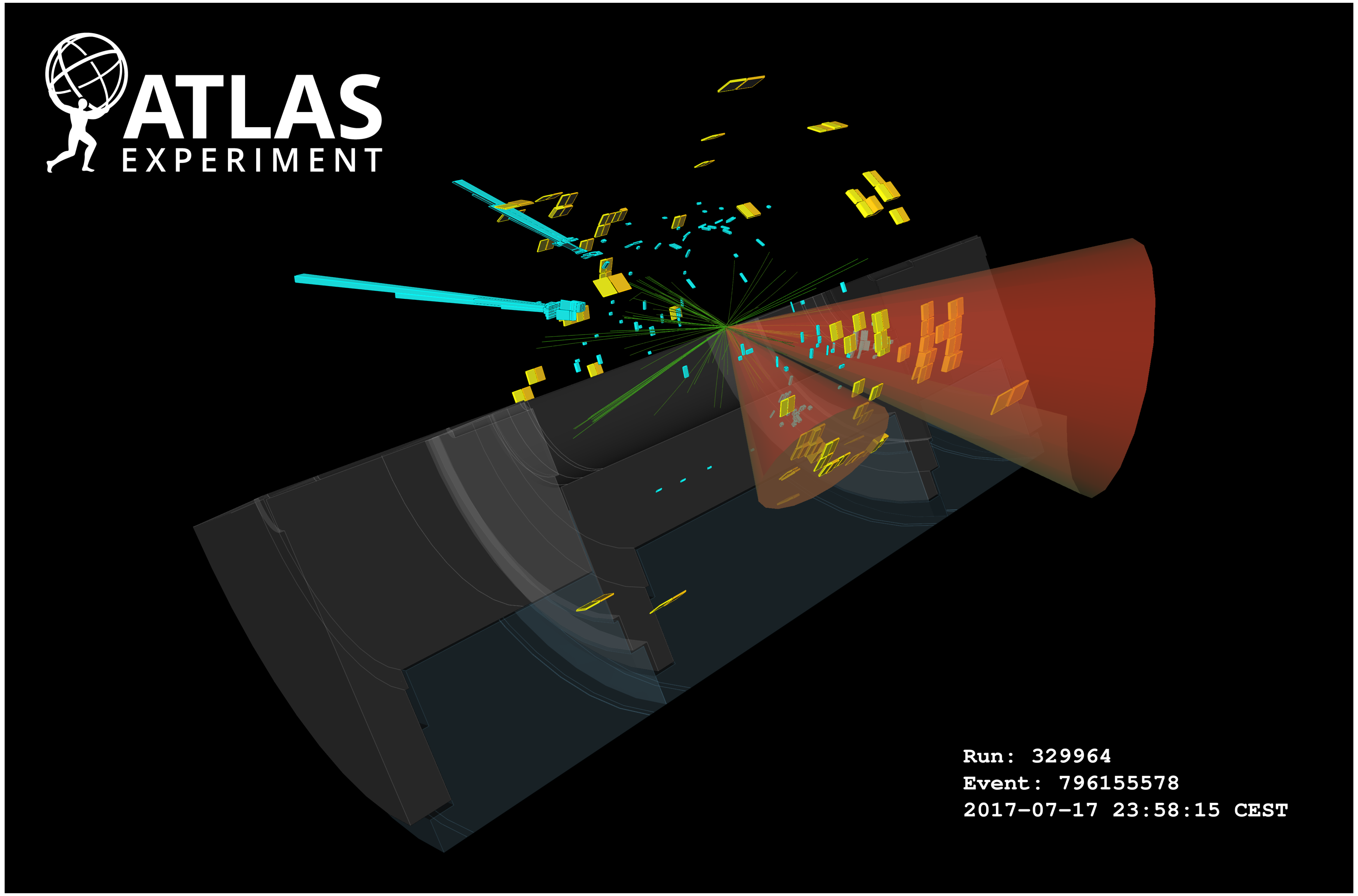

Data event of the non-resonant high mass BDT tight signal region

$m_{HH} = 625$ GeV, $m_{bb} = 113$ GeV and $m_{\gamma\gamma} = 123$ GeV

Non-resonant HH combination with full Run 2 data

Combination of HH analyses performed in 2 decay channels using full Run 2 LHC data corresponding to $139\ \mathrm{fb}^{-1}$:

- bbττ and bbγγ channels for the search of non-resonant HH production (results in the bbbb channel very new so not included in this combination)

ATLAS-CONF-2021-052

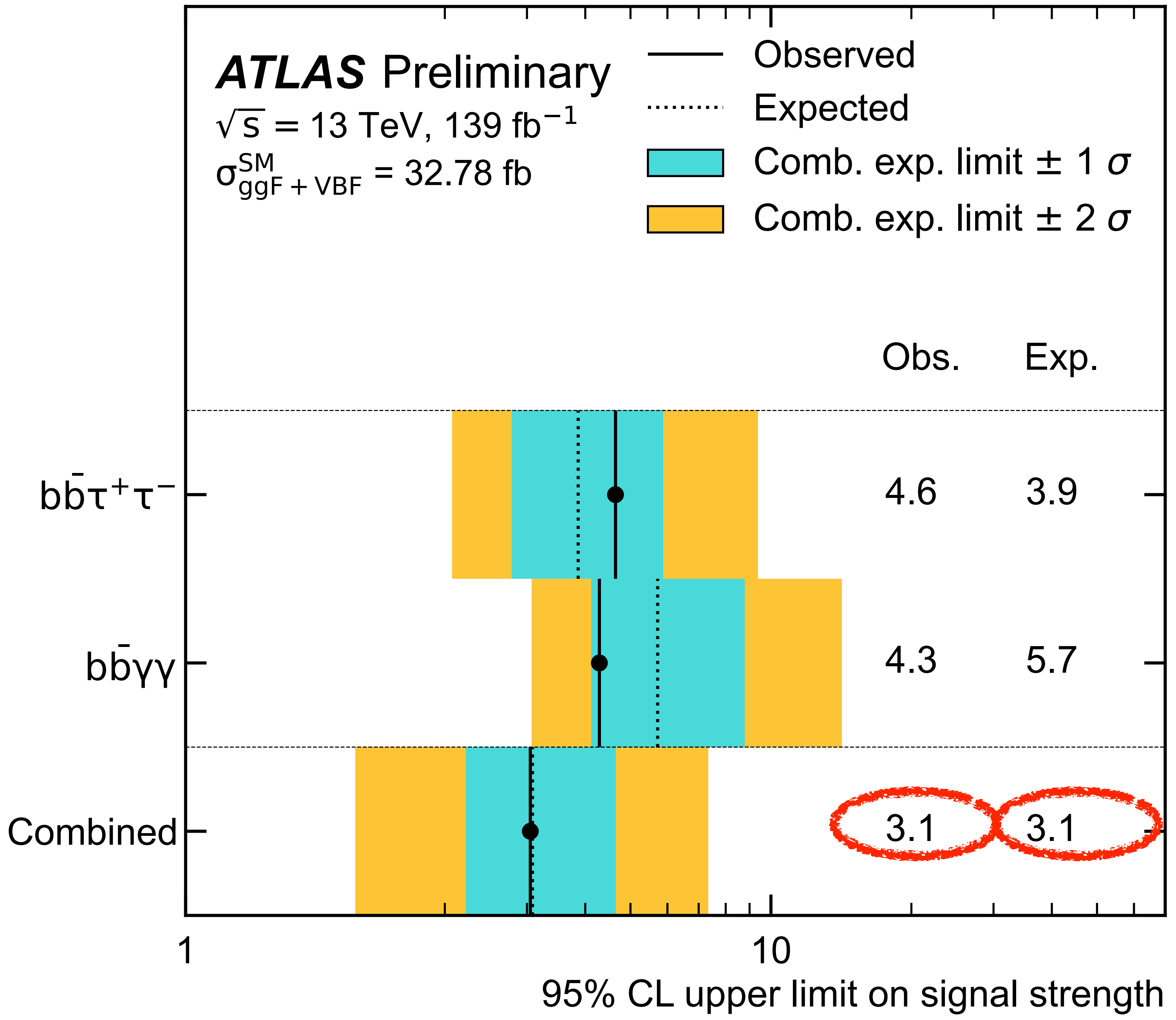

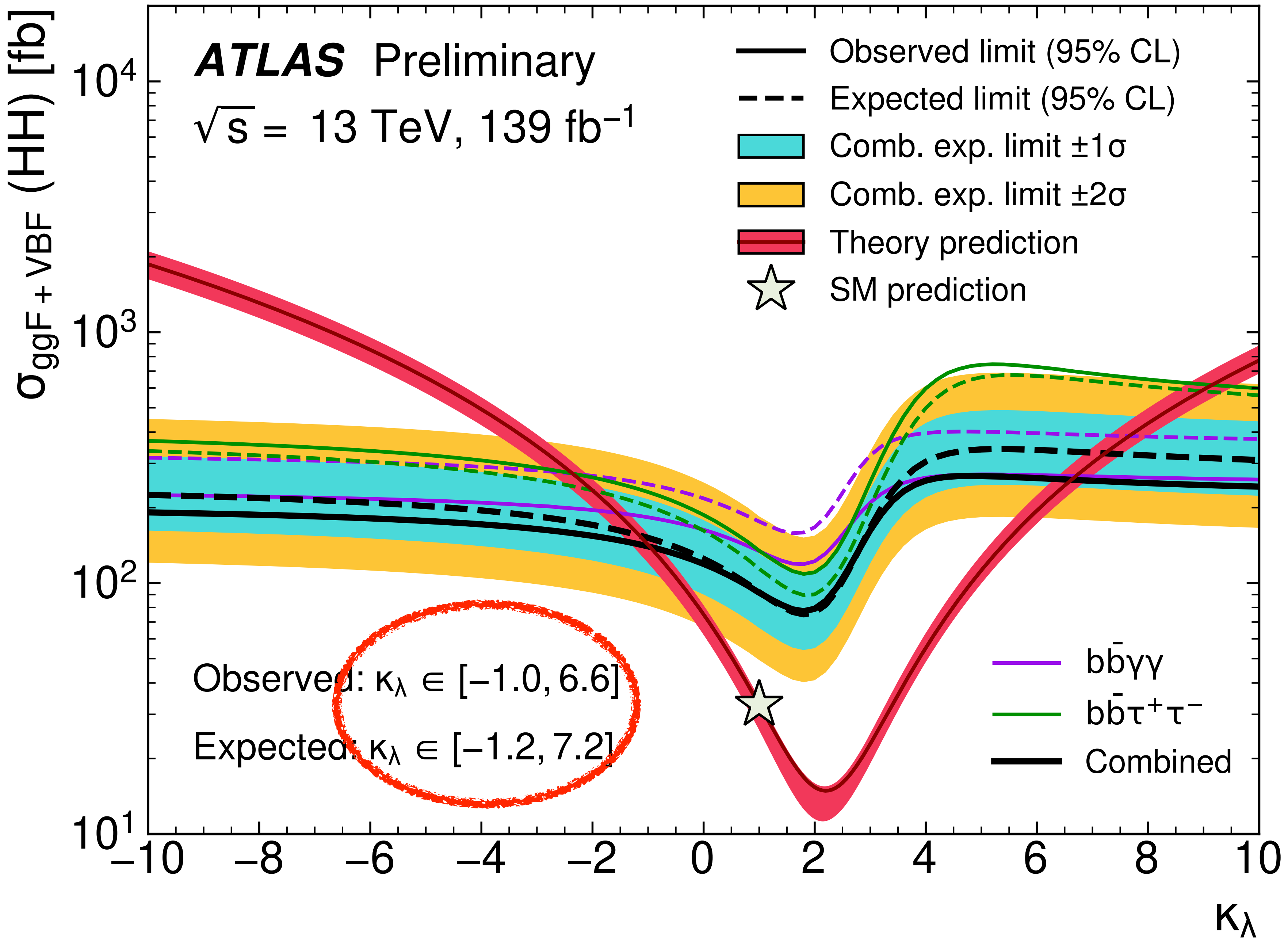

	Obs.	Exp.
$b\bar{b}\gamma\gamma$	$[-1.6, 6.7]$	$[-2.4, 7.7]$
$b\bar{b}\tau^+\tau^-$	$[-2.4, 9.2]$	$[-2.0, 9.0]$
Combined	$[-1.0, 6.6]$	$[-1.2, 7.2]$

- bbγγ most sensitive for very high and very low κ_λ
- bbττ most sensitive to κ_λ values closer to SM

Improvement of more than a factor 3 compared to partial Run 2 dataset combination (even including less decay channels)

World's best upper limit on non-resonant HH production and constraints on κ_λ up to now!

Effective field theory interpretations of the di-Higgs searches

Effective Field Theory (EFT) interpretations

In addition to the interpretations of the results in the κ-framework, where the effect of the BSM physics is modelled simply through Higgs Boson coupling modifiers $\kappa = \frac{c}{c^{SM}}$

→ Interpretations in the Effective Field Theory (EFT) framework, where the effect of BSM physics is parameterised through the addition of higher orders operators in the Lagrangian with effective couplings at the low-energy scale

Higgs Effective Field Theory (HEFT):

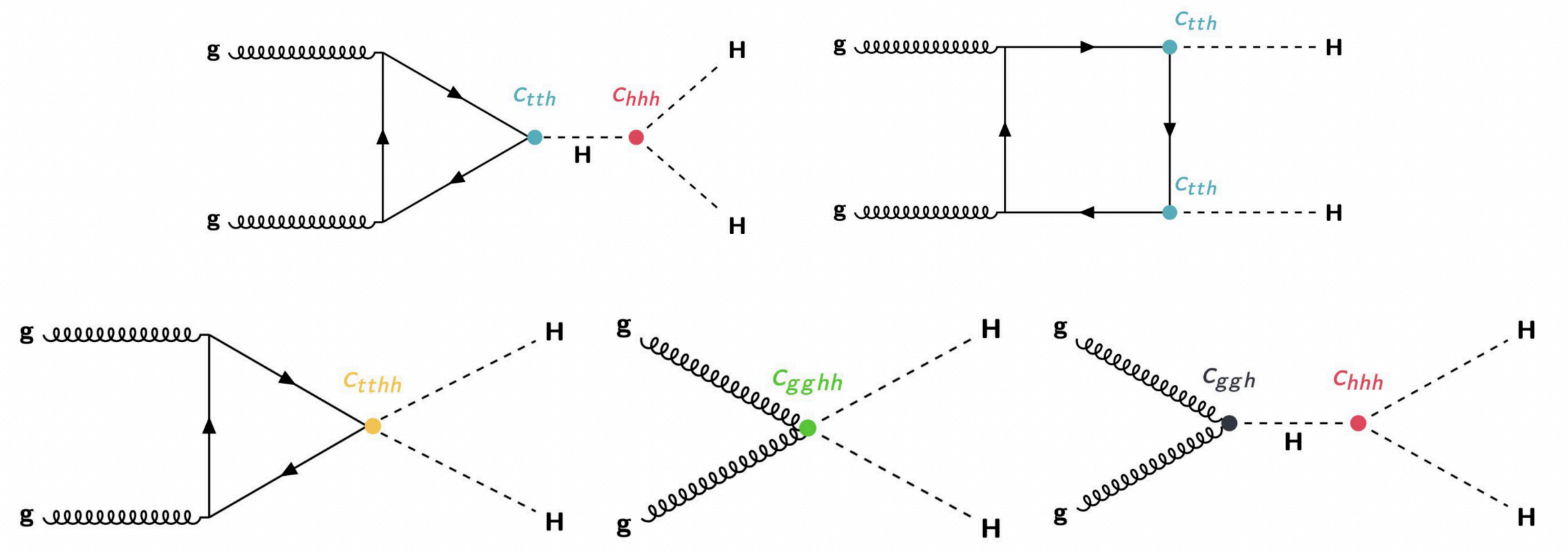

In HEFT for ggF HH production at LO there are 5 operators and their corresponding Wilson coefficients representing the Higgs Boson coupling modifiers affecting ggF HH production

→ HH production has unique access to c_{hhh}, c_{tthh} and c_{gghh}

Effective Field Theory (EFT) interpretations

7 HEFT m_{HH} shape benchmarks identified using a cluster analysis on the modified m_{HH} shape with different values of the HEFT Higgs coupling parameters

JHEP03(2020)091

Benchmark model	c_{hhh}	c_{tth}	c_{ggh}	c_{gghh}	c_{tthh}
SM	1	1	0	0	0
BM 1	3.94	0.94	1/2	1/3	−1/3
BM 2	6.84	0.61	0.0	−1/3	1/3
BM 3	2.21	1.05	1/2	1/2	−1/3
BM 4	2.79	0.61	−1/2	1/6	1/3
BM 5	3.95	1.17	1/6	−1/2	−1/3
BM 6	5.68	0.83	−1/2	1/3	1/3
BM 7	−0.10	0.94	1/6	−1/6	1

ATL-PHYS-PUB-2022-019

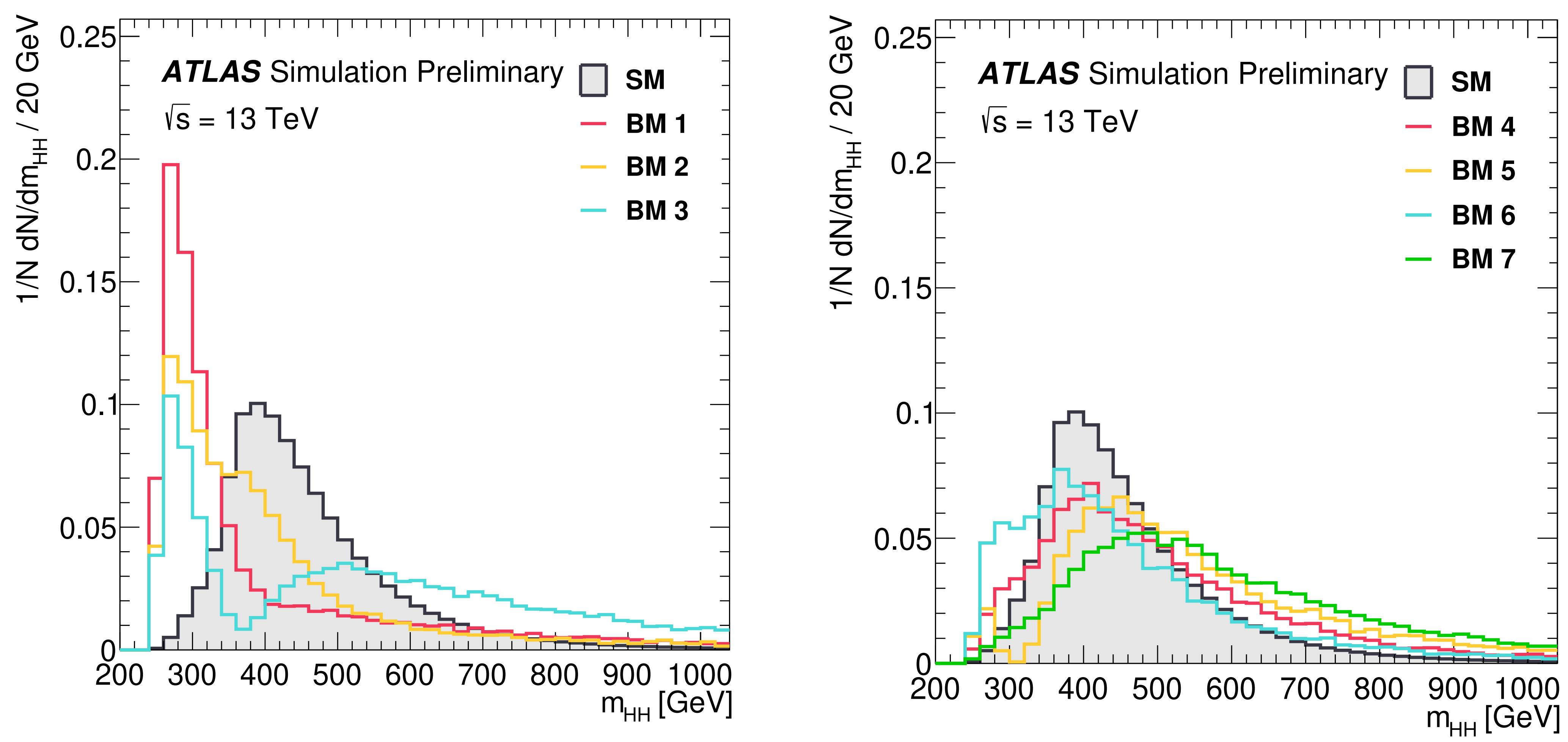

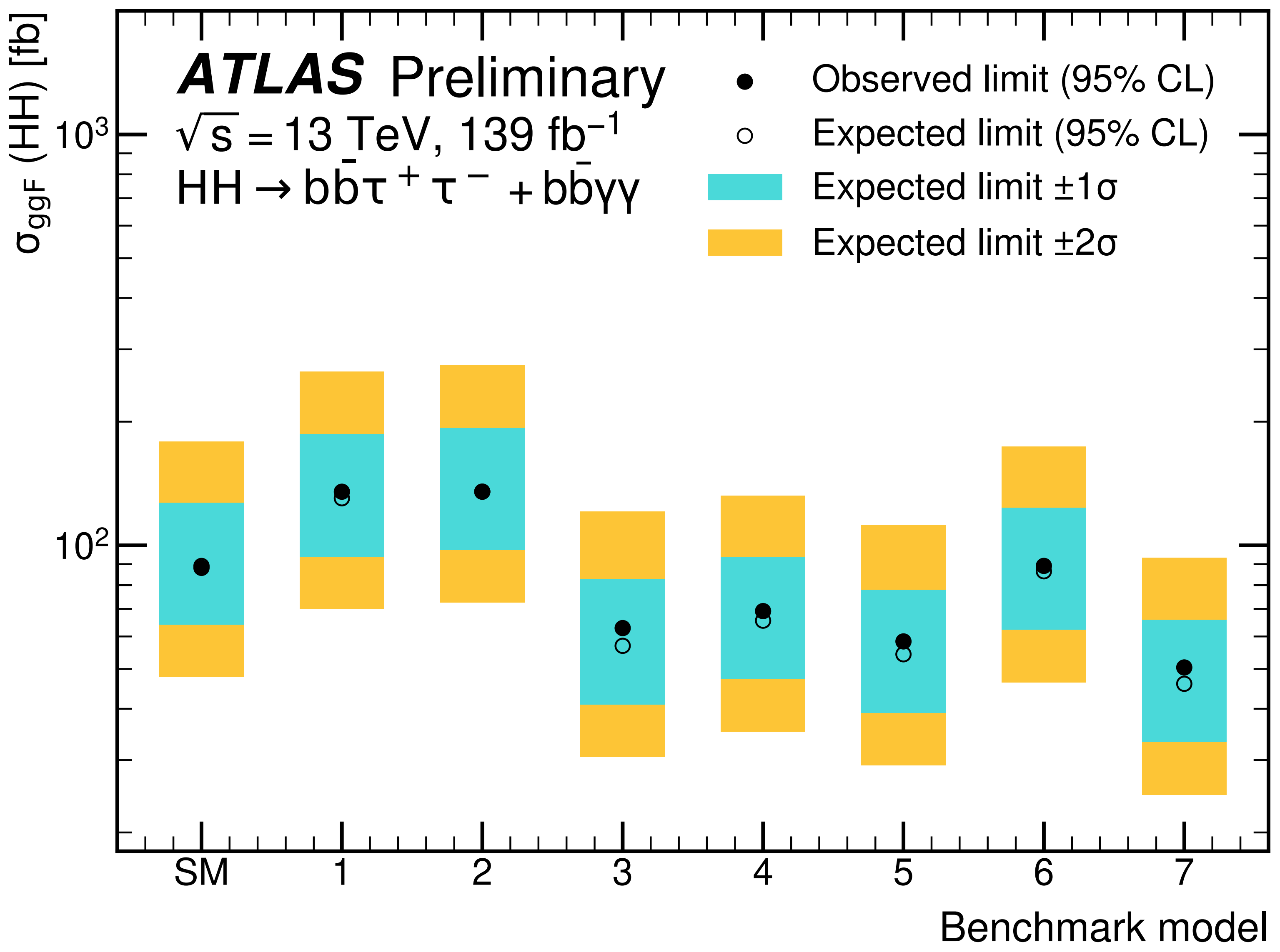

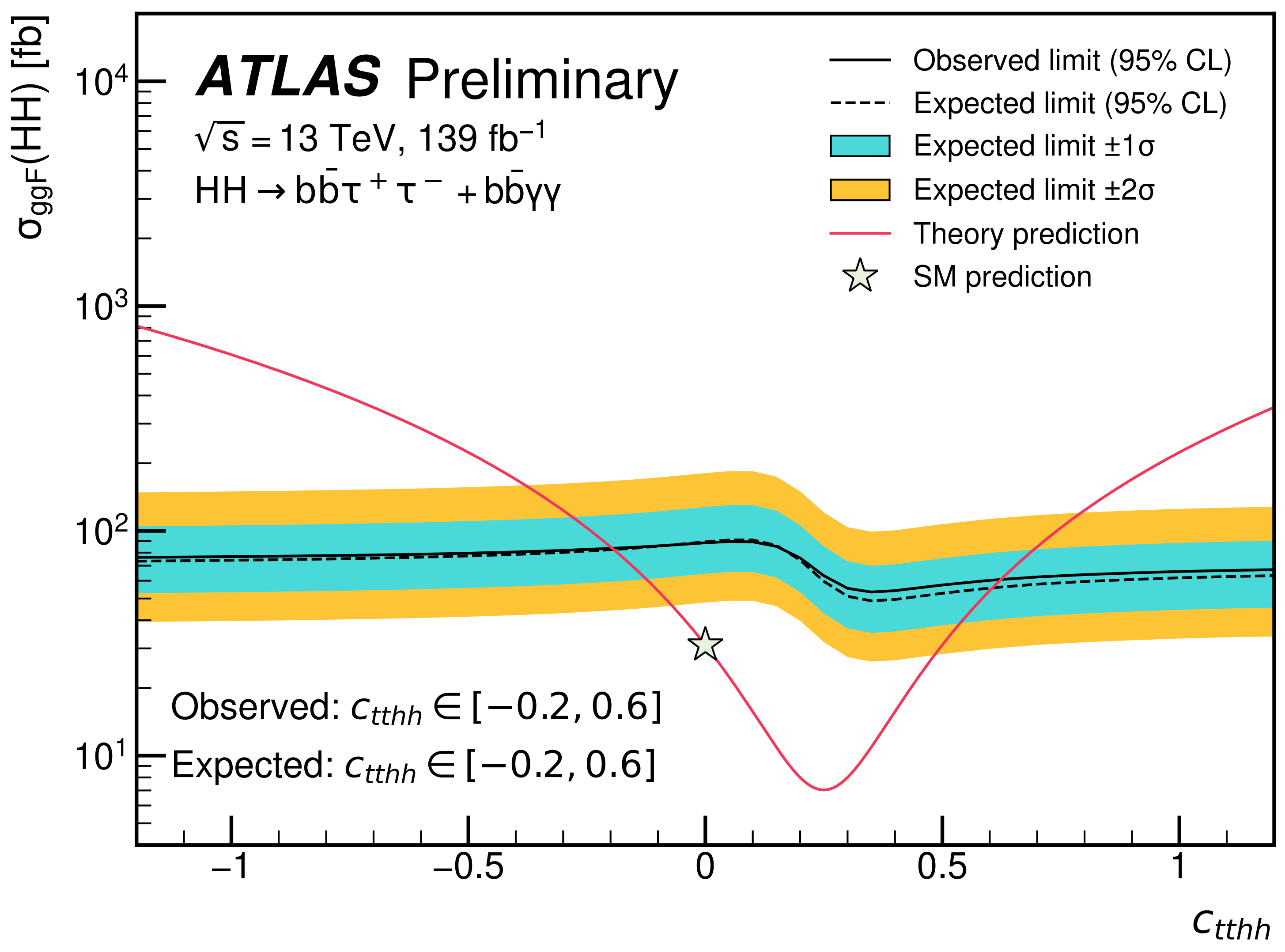

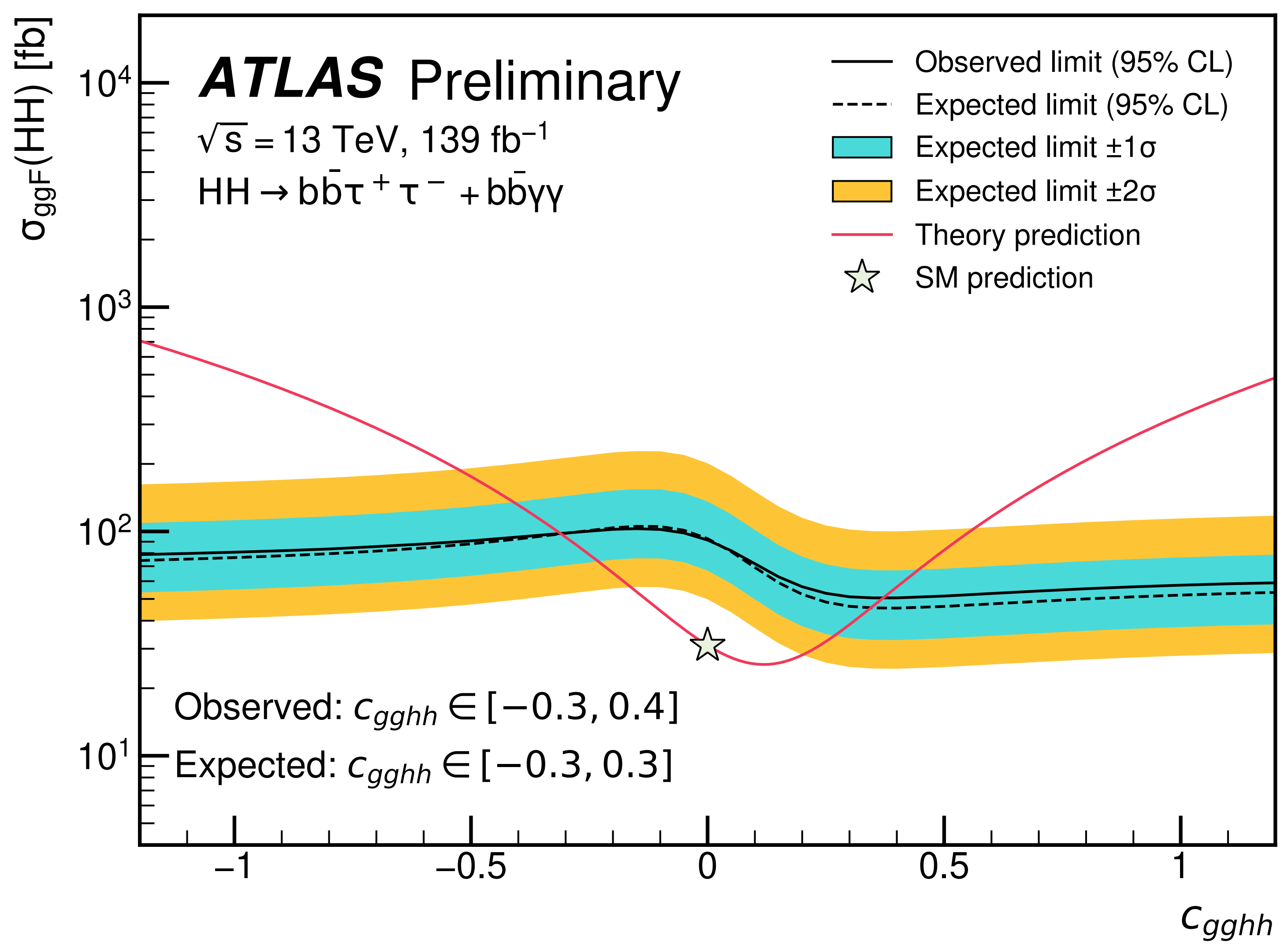

Prospects for di-Higgs searches at the HL-LHC

LHC schedule

The LHC has a program of operation with different running periods and periods of shutdown for upgrades in between them

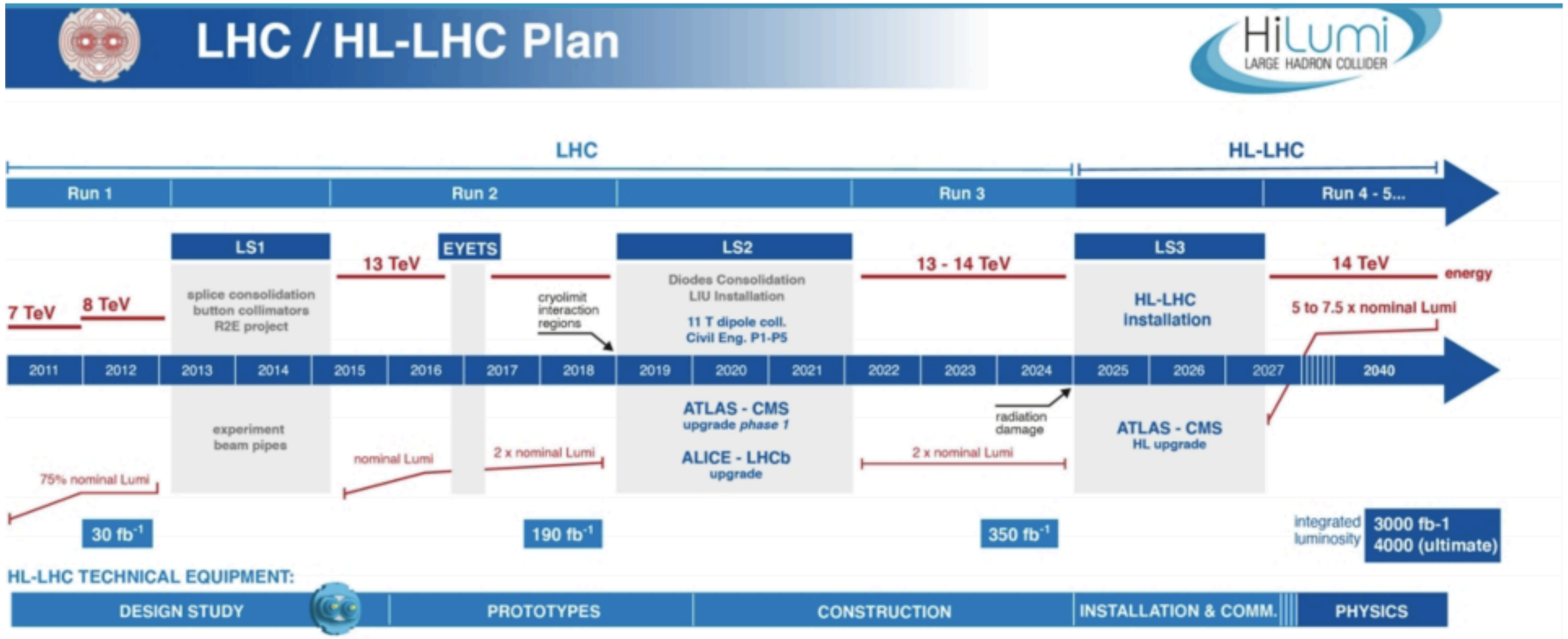

- Successful Run 2 ended in 2018

- Run 3 is starting now and will continue until 2024: instantaneous luminosity of about x1.5 the Run 2 value (3×10^{34} cm^{-2}s^{-1}) and average pile-up that will reach about x2 the Run 2 value (80)

- HL-LHC will start in 2027: very challenging operation environment with instantaneous luminosity of about x3 the Run 2 value ($5 - 7 \times 10^{34}$ cm^{-2}s^{-1}) and average pile-up that will reach about x5 the Run 2 value (200)
  $\rightarrow$ 3000 fb^{-1} expected at the end of the HL-LHC
  $\rightarrow$ about 100000 SM HH events expected in this dataset!

Prospects for di-Higgs searches at the HL-LHC

Extrapolations of ATLAS full Run 2 non-resonant HH searches in the bbττ and bbγγ channels to HL-LHC with $3000\ \mathrm{fb}^{-1}$

Extrapolations performed with different assumptions on the systematic uncertainties:

- Run 2 systematics: both the theoretical and experimental systematic uncertainties are assumed to keep their Run 2 values
- Theoretical systematic uncertainties halved: theoretical systematic uncertainties are reduced by a factor of 2, while experimental systematic uncertainties are assumed to keep their Run 2 values
- Baseline: both theoretical and experimental systematic uncertainties reduced
- No systematic uncertainties

Baseline scenario:

- Theoretical systematic uncertainties reduced by a factor of two
- Experimental systematic uncertainties are reduced taking into account the reduction of their statistical component
- MC statistical uncertainties neglected (dominant systematic uncertainty for bbττ)
- Spurious signal uncertainty neglected (dominant systematic uncertainty for bbγγ)

ATL-PHYS-PUB-2022-005

Source	Scale factor	$b\bar{b}\gamma\gamma$	$b\bar{b}\tau^+\tau^-$
Experimental Uncertainties			
Luminosity	0.6	*	*
b-jet tagging efficiency	0.5	*	*
c-jet tagging efficiency	0.5	*	*
Light-jet tagging efficiency	1.0	*	*
Jet energy scale and resolution, $E_{\mathrm{T}}^{\mathrm{miss}}$	1.0	*	*
κ_λ reweighting	0.0	*	*
Photon efficiency (ID, trigger, isolation efficiency)	0.8	*	
Photon energy scale and resolution	1.0	*	
Spurious signal	0.0	*	
Value of m_H	0.08	*	
τ_{had} efficiency (statistical)	0.0		*
τ_{had} efficiency (systematic)	1.0		*
τ_{had} energy scale	1.0		*
Fake-τ_{had} estimation	1.0		*
MC statistical uncertainties	0.0		*
Theoretical Uncertainties	0.5	*	*

Detector performance assumed to be the same as Run 2 in the more challenging HL-LHC detector operation environment thanks to the program of upgrades of the detector, trigger and data acquisition systems

Prospects for di-Higgs searches at the HL-LHC

Systematic uncertainties will become important for HH searches at the HL-LHC

ATL-PHYS-PUB-2022-005

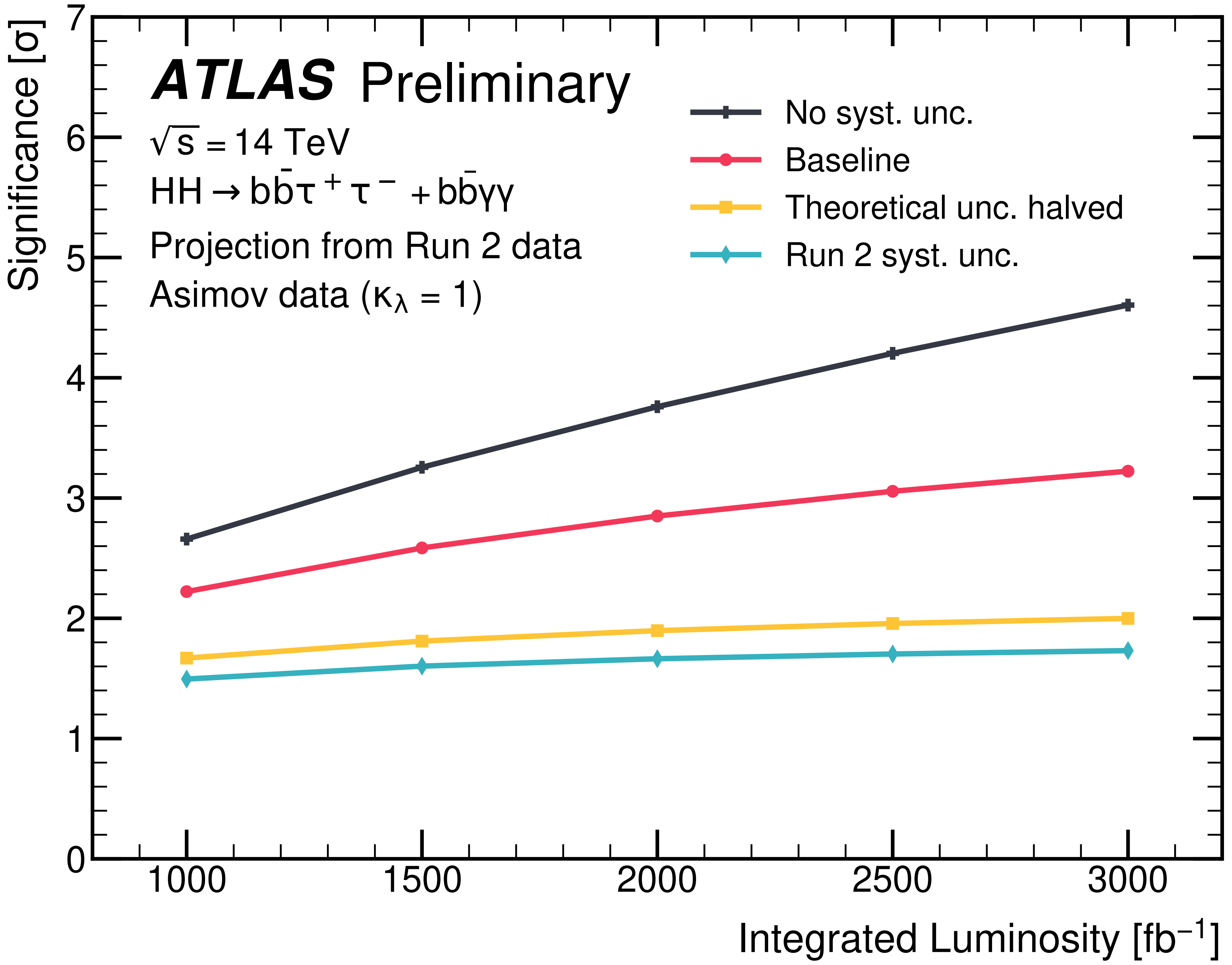

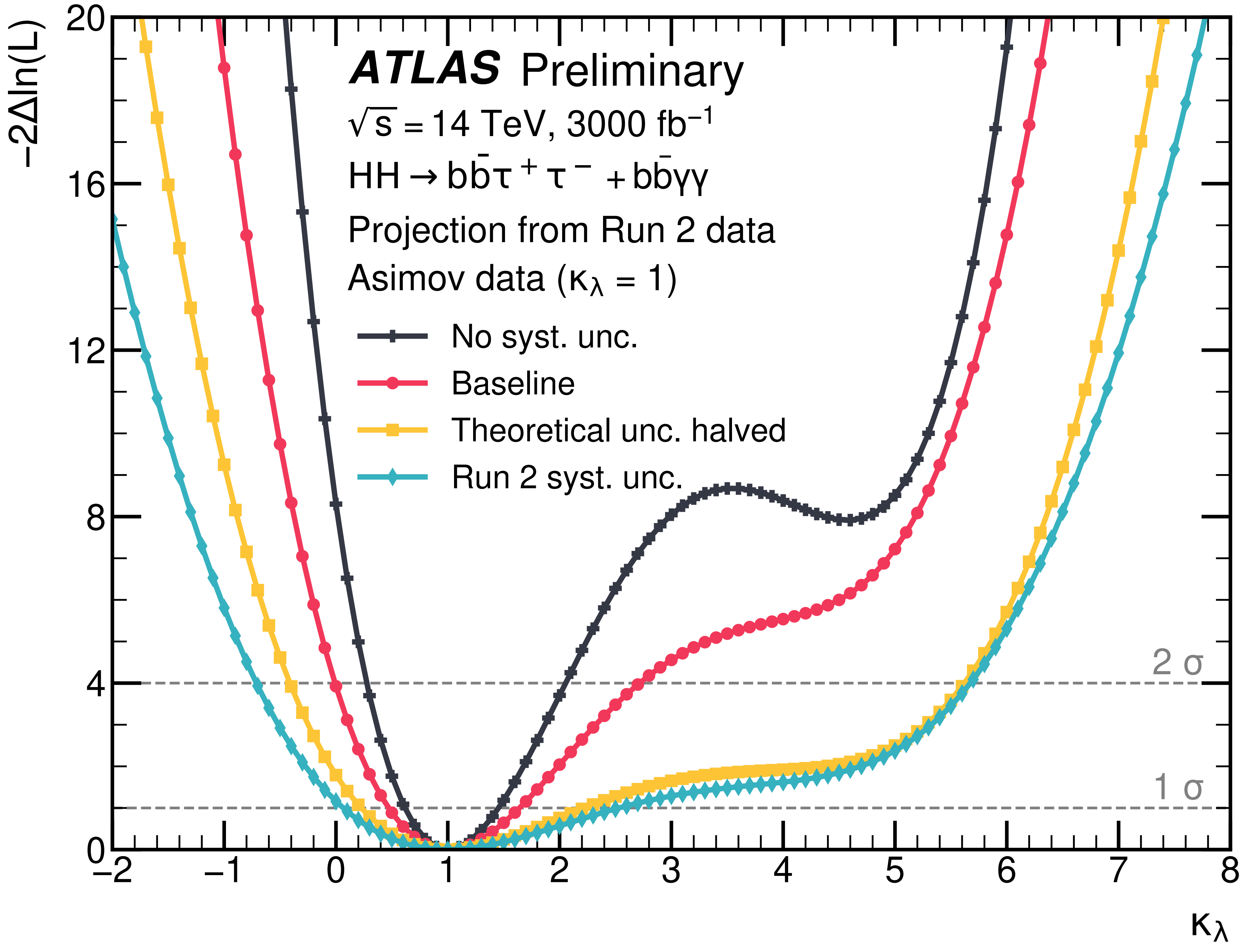

Uncertainty scenario	Significance [σ] $b\bar{b}\gamma\gamma$	$b\bar{b}\tau^+\tau^-$	Combination	Combined signal strength precision [%]
No syst. unc.	2.3	4.0	4.6	$-23/+23$
Baseline	2.2	2.8	3.2	$-31/+34$
Theoretical unc. halved	1.1	1.7	2.0	$-49/+51$
Run 2 syst. unc.	1.1	1.5	1.7	$-57/+68$

Uncertainty scenario	Likelihood scan 1 σ CI	Likelihood scan 2 σ CI
No syst. unc.	$[0.6, 1.5]$	$[0.3, 2.1]$
Baseline	$[0.5, 1.6]$	$[0.0, 2.7]$
Theoretical unc. halved	$[0.2, 2.2]$	$[-0.4, 5.6]$
Run 2 syst. unc.	$[0.1, 2.5]$	$[-0.7, 5.7]$

Baseline scenario: Expected significance of 3.2σ and 30% uncertainty on the signal strength for SM HH signal

Baseline scenario: 50% uncertainty on κ_λ for SM HH signal

Summary of searches for resonant HH production

Resonant HH combination with full Run 2 data

- Searches for BSM resonant HH production: resonances with masses between 250 GeV and 5 TeV
- $X \to HH \to bbbb, bb\tau\tau, bb\gamma\gamma$
- Similar baseline event selections and background estimations to the non-resonant searches in the same final states
- Optimised signal region selections and discriminants specifically for the resonant signals

ATLAS-CONF-2021-052

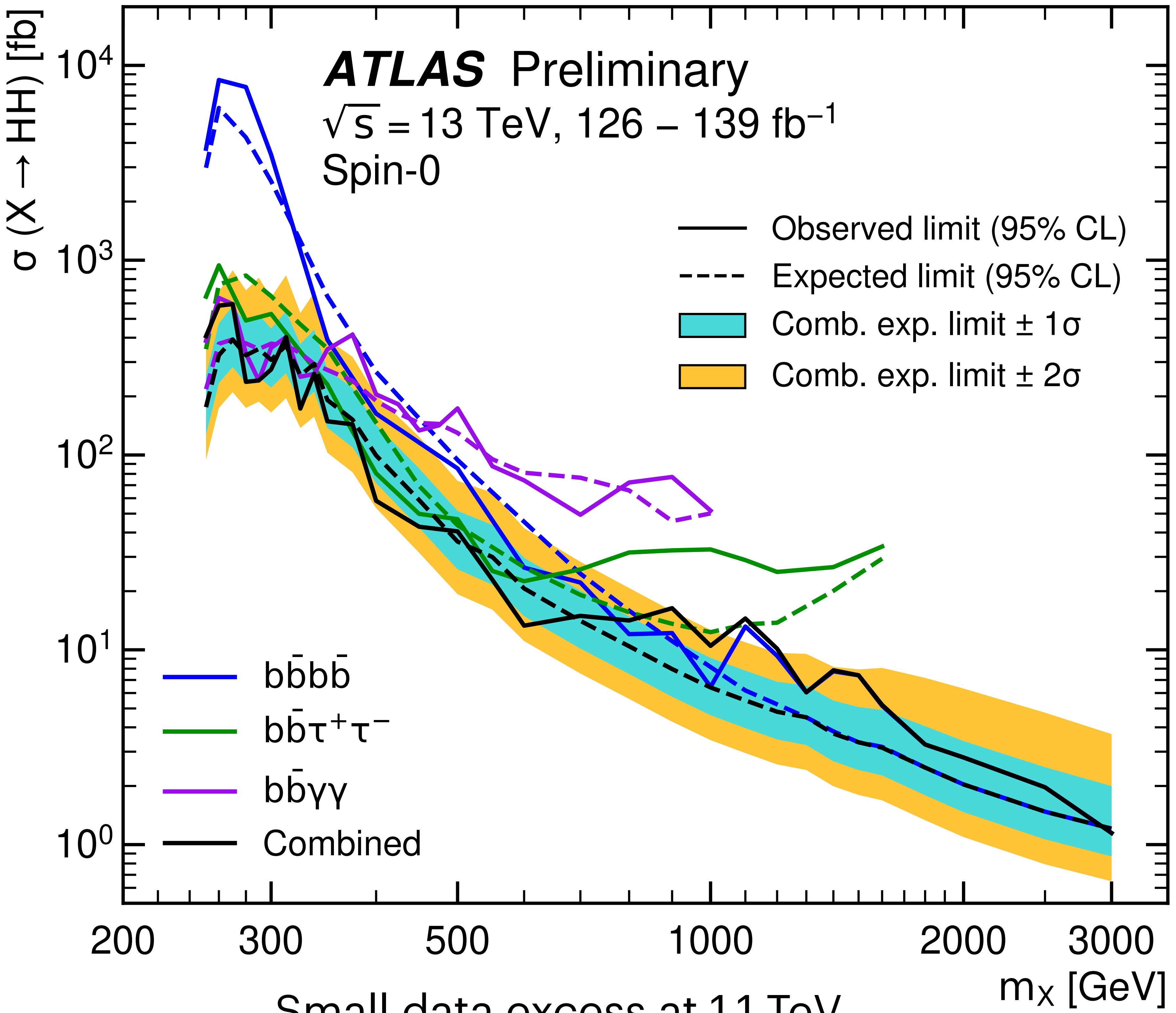

Small data excess at 1.1 TeV, significance 3.2σ (2.1σ) local (global)

Combination of HH analyses performed in 3 decay channels using full Run 2 LHC data corresponding to $139\ \mathrm{fb}^{-1}$:

- $bbbb$, $bb\tau\tau$ and $bb\gamma\gamma$ channels for the searches for resonant HH production

Complementarity of searches in different decay channels:
- $bb\gamma\gamma$ best sensitivity at low mass
- $bb\tau\tau$ best sensitivity in medium mass range
- $bbbb$ best sensitivity at high mass

Summary and outlook

di-Higgs searches allow to directly probe the triple Higgs boson coupling, which controls the shape of the Higgs potential

Latest ATLAS di-Higgs searches with full Run 2 LHC dataset
have significantly improved the results beyond luminosity increase
compared to previous partial Run 2 dataset results

New HL-LHC extrapolations based on latest results improved
compared to the ones based on the partial Run 2 analyses:
Expected 3.2σ evidence and 50% uncertainty on κ_λ for SM HH from ATLAS,
5σ observation expected to be possible from ATLAS+CMS combination of HH searches!

Finalising now ATLAS HH analyses with full Run 2 dataset:
Covering more HH decay channels and more interpretations of the results

Preparing for the Run 3 HH analyses program:
Run 2 + Run 3 dataset of $300 - 400\ \mathrm{fb}^{-1}$, with possible further analysis improvements,
will allow large improvement in constraining κ_λ and learning more about the Higgs potential

Summary and outlook

Higgs Pairs Workshop last week in Dubrovnik (Croatia): https://indico.cern.ch/event/1001391/timetable/

Very constructive discussions between ATLAS, CMS, theory and future colliders communities studying di-Higgs for developing future searches (and measurements) and interpretations!

Thank you for your attention!

Back-up slides

ATLAS b-tagging and τ-identification

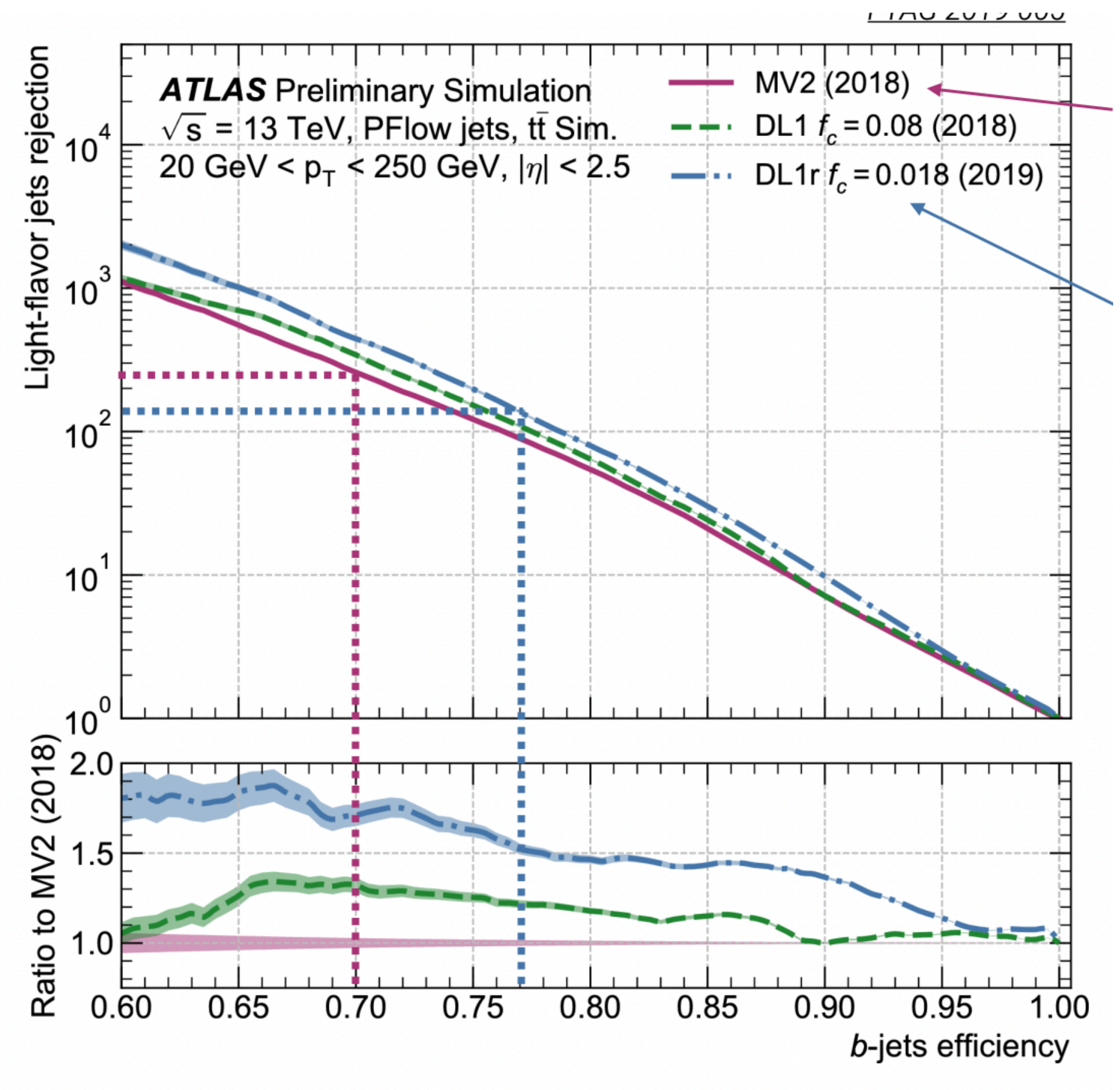

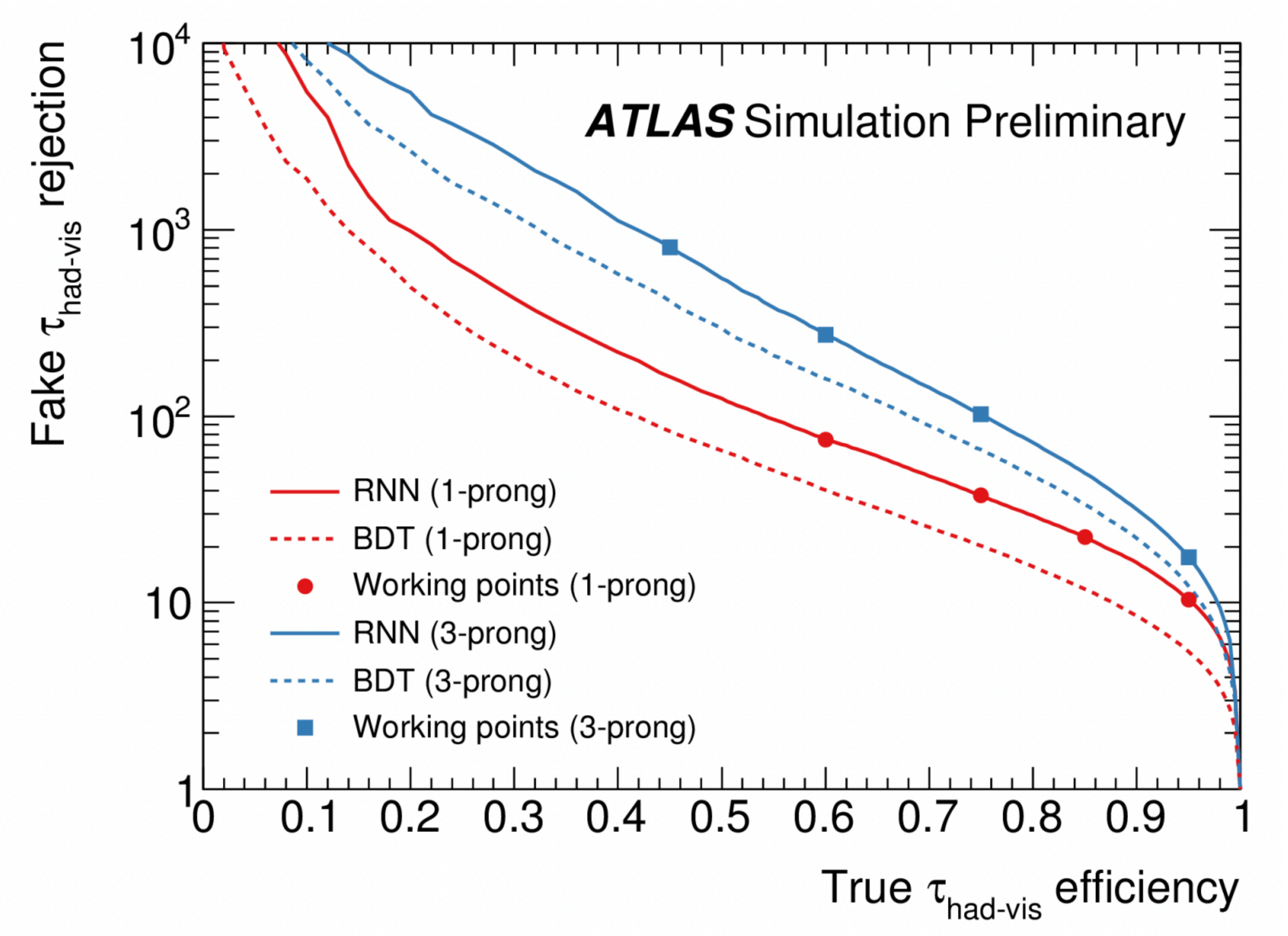

Higgs Boson self-coupling in BSM

Several BSM models predict deviations of the Higgs self-coupling

Phys. Rev. D 88, 055024

Model	$\Delta g_{hhh}/g_{hhh}^{SM}$
Mixed-in Singlet	$-18\,\%$
Composite Higgs	tens of %
Minimal Supersymmetry	$-2\,\%^{a}$ $\quad -15\,\%^{b}$
NMSSM	$-25\,\%$

- Mixed-in Singlet Model: a theory with an extra singlet where the singlet mixes with the SM Higgs through a renormalisable operator
- Composite Higgs Model: composite Higgs models are speculative extensions of the SM where the Higgs Boson is about state of new strong interactions
- Minimal Supersymmetry Model: the Minimal Supersymmetric Standard Model (MSSM) exhibits an extended High sector with two Higgs Boson doublets
- NMSSM: extension of the MSSM adding a mass term in a way similar to the generation of quark and lepton masses in the SM

Effective Field Theory (EFT) interpretations

Several challenges/considerations with using Effective Field Theories (EFTs)

Can construct more than one EFT with different constraints/relations on operators

HEFT:

Higgs boson field $h(x)$ is $\mathrm{SU}(2)_L \times \mathrm{U}(1)_Y$ singlet

Expand in loop orders $\sim 1/(16\pi^2)$

$$\mathscr{L}_{\mathrm{HEFT}} = \mathscr{L}_2 + \sum_{L=1}^{\infty} \sum_i \left(\frac{1}{16\pi^2}\right)^L C_i^{(L)} O_i^{(L)}$$

A priori no relation between c_{ggh} & c_{gghh}

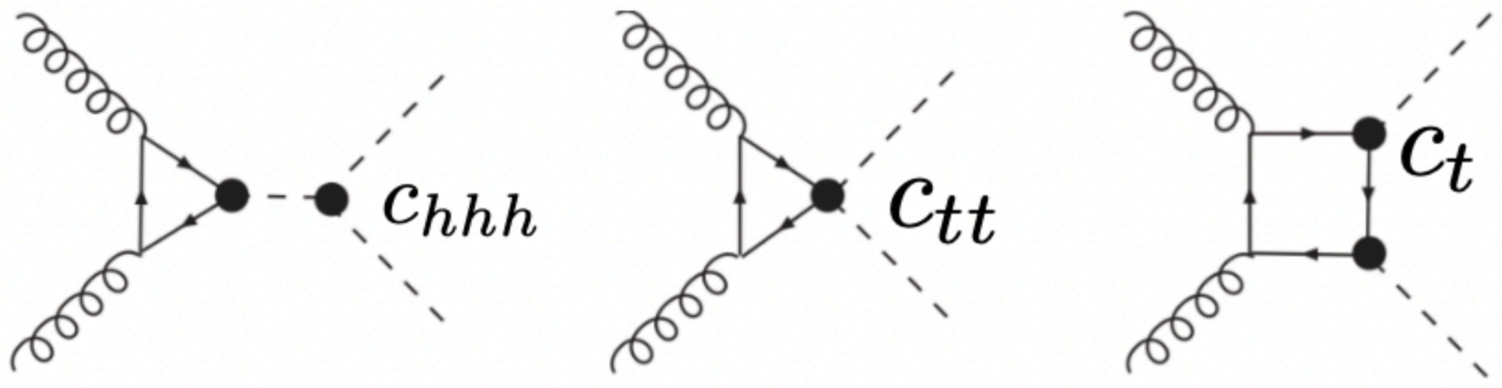

SMEFT ⊂ HEFT:

Higgs field complex doublet

Expand in canonical dimension $\sim 1/\Lambda^2$

$$\mathscr{L}_{\mathrm{SMEFT}} = \mathscr{L}_{\mathrm{SM}} + \sum_i \frac{C_i^{(6)}}{\Lambda^2} O_i^{(6)} + \mathcal{O}\left(\frac{1}{\Lambda^3}\right)$$

Relation $c_{ggh} \sim c_{gghh}$

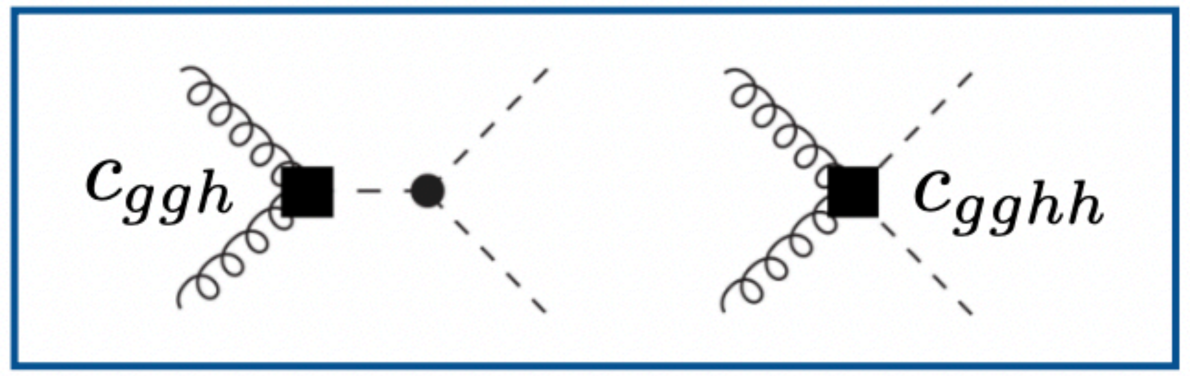

Related in SMEFT

https://indico.cern.ch/event/1001391/contributions/4818269/

Effective Field Theory (EFT) interpretations

- SMEFT:

$$\Delta\mathcal{L}_{\text{SMEFT}}^{(\text{Warsaw})} = \frac{C_{H,\Box}}{\Lambda^2}(\phi^\dagger\phi)\Box(\phi^\dagger\phi) + \frac{C_{HD}}{\Lambda^2}(\phi^\dagger D_\mu\phi)^*(\phi^\dagger D^\mu\phi)$$
$$+ \frac{C_H}{\Lambda^2}(\phi^\dagger\phi)^3 + \left(\frac{C_{uH}}{\Lambda^2}\phi^\dagger\phi\bar{q}_L\phi^c t_R + h.c.\right) + \frac{C_{HG}}{\Lambda^2}\phi^\dagger\phi G^a_{\mu\nu}G^{\mu\nu,a}$$

- HEFT:

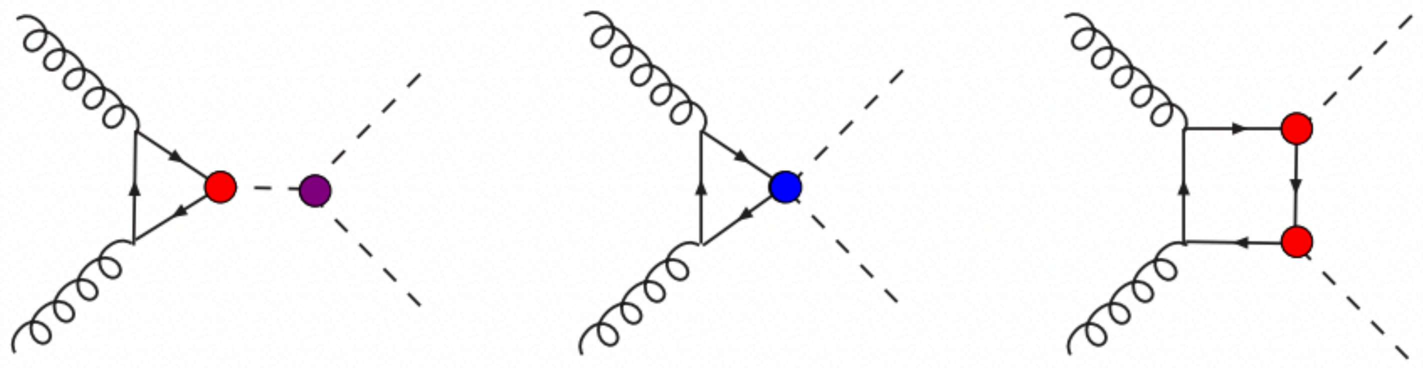

$$\Delta\mathcal{L}_{\text{HEFT}} = -\,c_{hhh}\frac{m_h^2}{2v}h^3$$
$$-\,m_t\left(c_t\frac{h}{v} + c_{tt}\frac{h^2}{v^2}\right)\bar{t}\,t$$
$$+\,\frac{\alpha_s}{8\pi}\left(c_{ggh}\frac{h}{v} + c_{gghh}\frac{h^2}{v^2}\right)G^a_{\mu\nu}G^{a,\mu\nu}$$

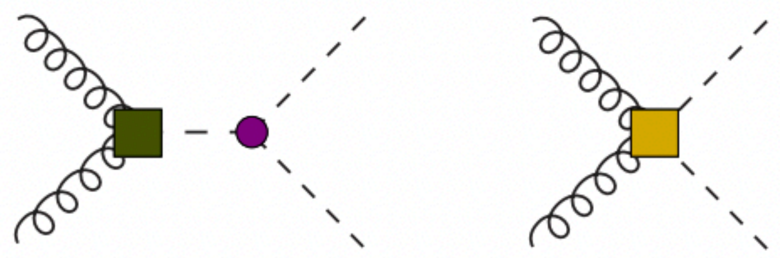

https://indico.cern.ch/event/1001391/contributions/4827320/

Effective Field Theory (EFT) interpretations

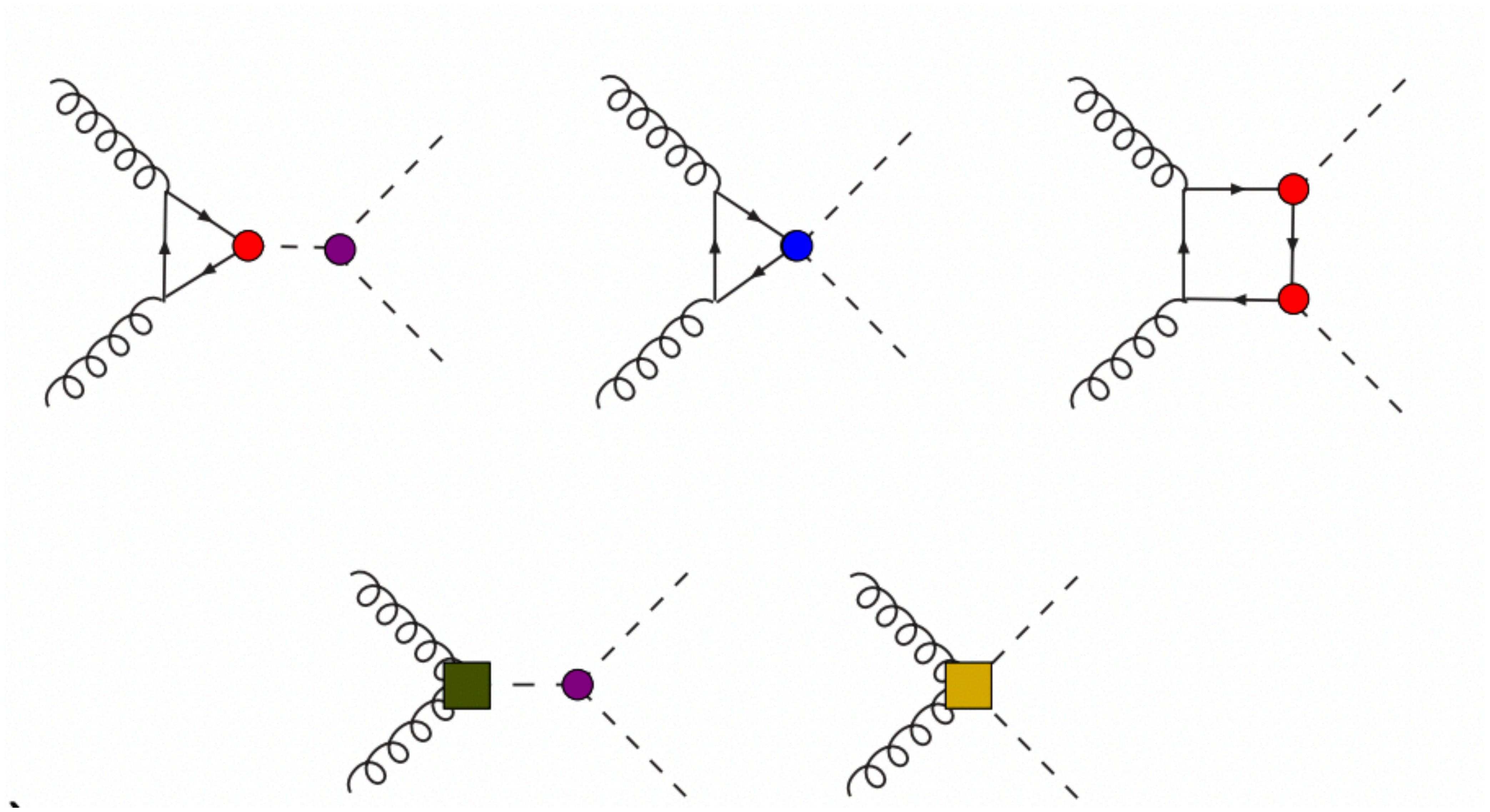

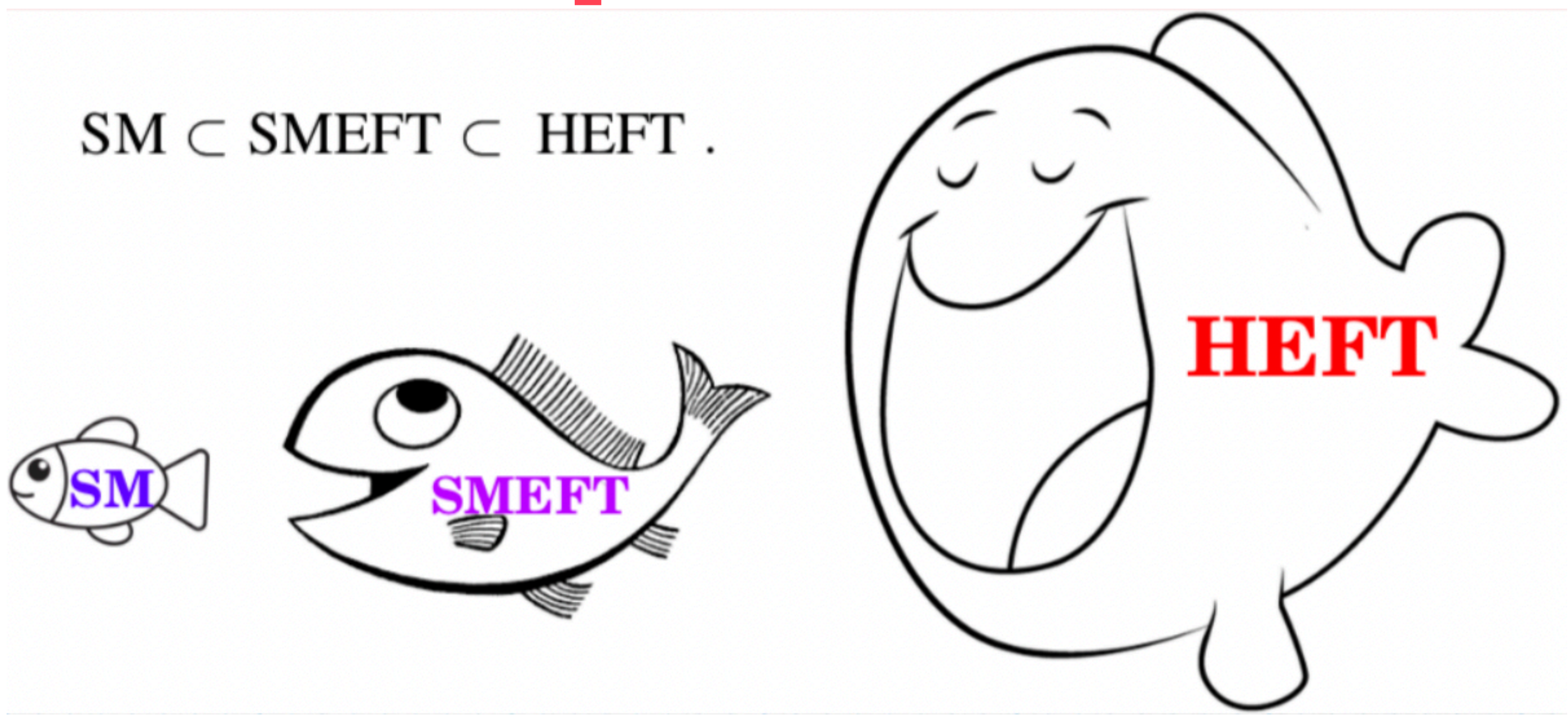

HEFT vs SMEFT translation

HEFT	SILH	Warsaw
c_{hhh}	$1+\bar{c}_6-\frac{3}{2}\bar{c}_H$	$1-2\frac{v^4}{m_h^2}C_H+3c_{H,kin}$
c_t	$1-\frac{\bar{c}_H}{2}-\bar{c}_u$	$1+c_{H,kin}-C_{uH}\frac{v^3}{\sqrt{2}m_t}$
c_{tt}	$-\left(\frac{3}{2}\bar{c}_u+\frac{\bar{c}_H}{2}\right)$	$-C_{uH}\frac{3v^3}{2\sqrt{2}m_t}+c_{H,kin}$
c_{ggh}	$\frac{128\pi^2}{g_2^2}\bar{c}_g$	$\frac{8\pi}{\alpha_s}v^2C_{HG}$
c_{gghh}	$\frac{64\pi^2}{g_2^2}\bar{c}_g$	$\frac{4\pi}{\alpha_s}v^2C_{HG}$

HEFT chosen for first set of HH EFT interpretations because:

- More generic model
- First EFT framework implemented in MC generators for di-Higgs and several theory papers available HEFT in di-Higgs
- Easier interpretations in HH alone (without including single-Higgs constraints) some couplings are constrainable only in HH, ctthh and cgghh

Effective Field Theory (EFT) interpretations

ATL-PHYS-PUB-2022-019

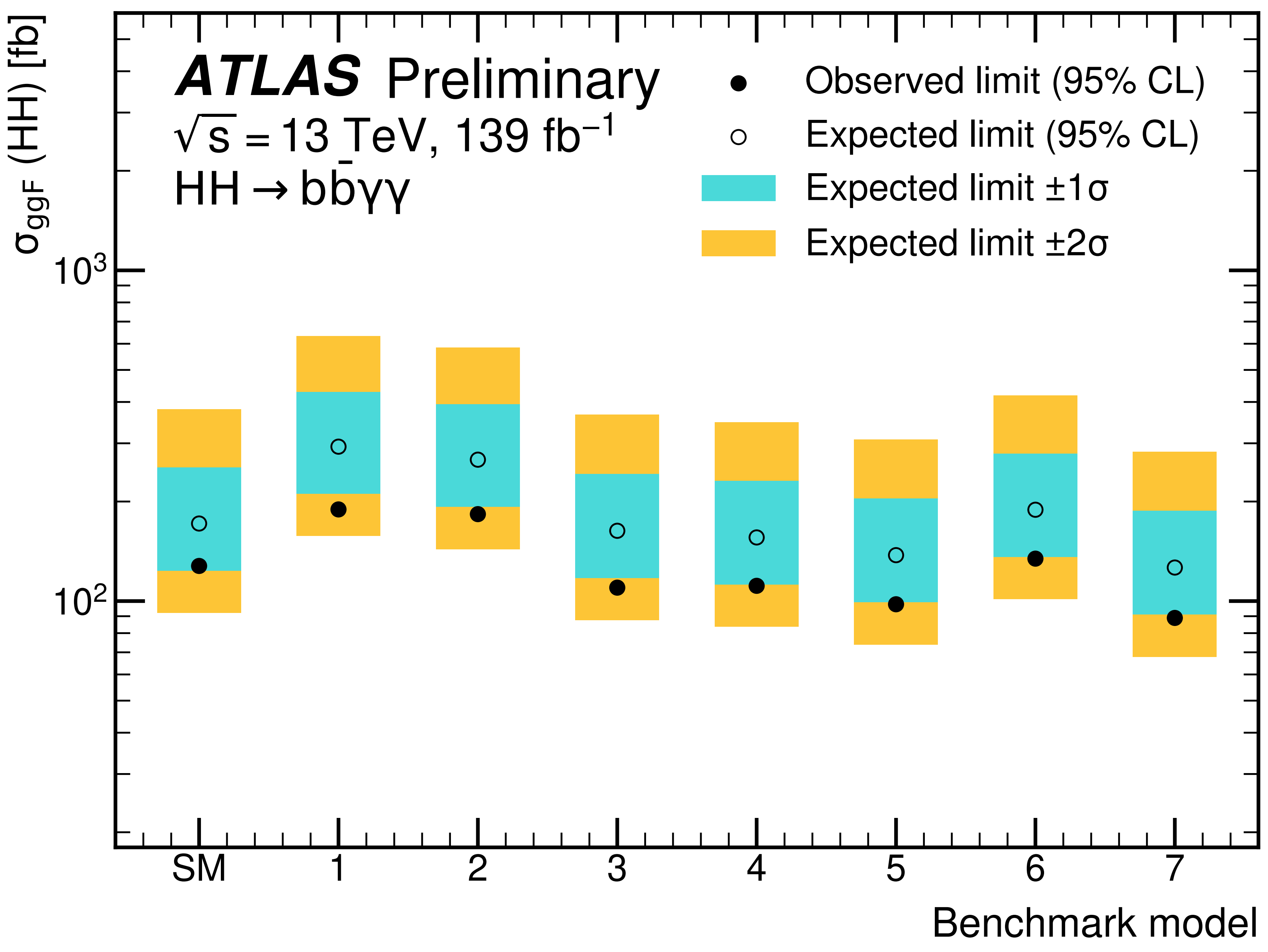

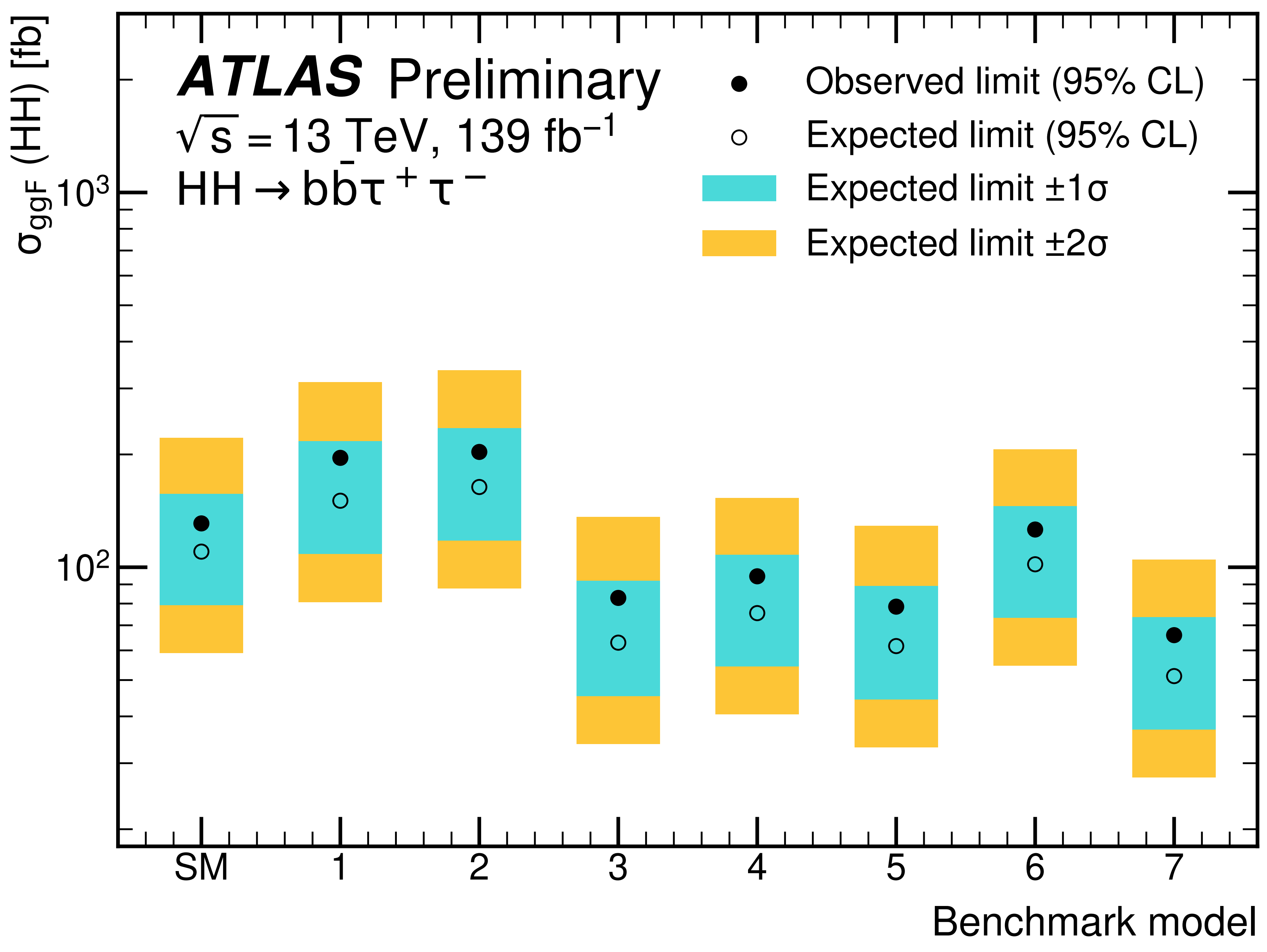

Effective Field Theory (EFT) interpretations

ATL-PHYS-PUB-2022-019

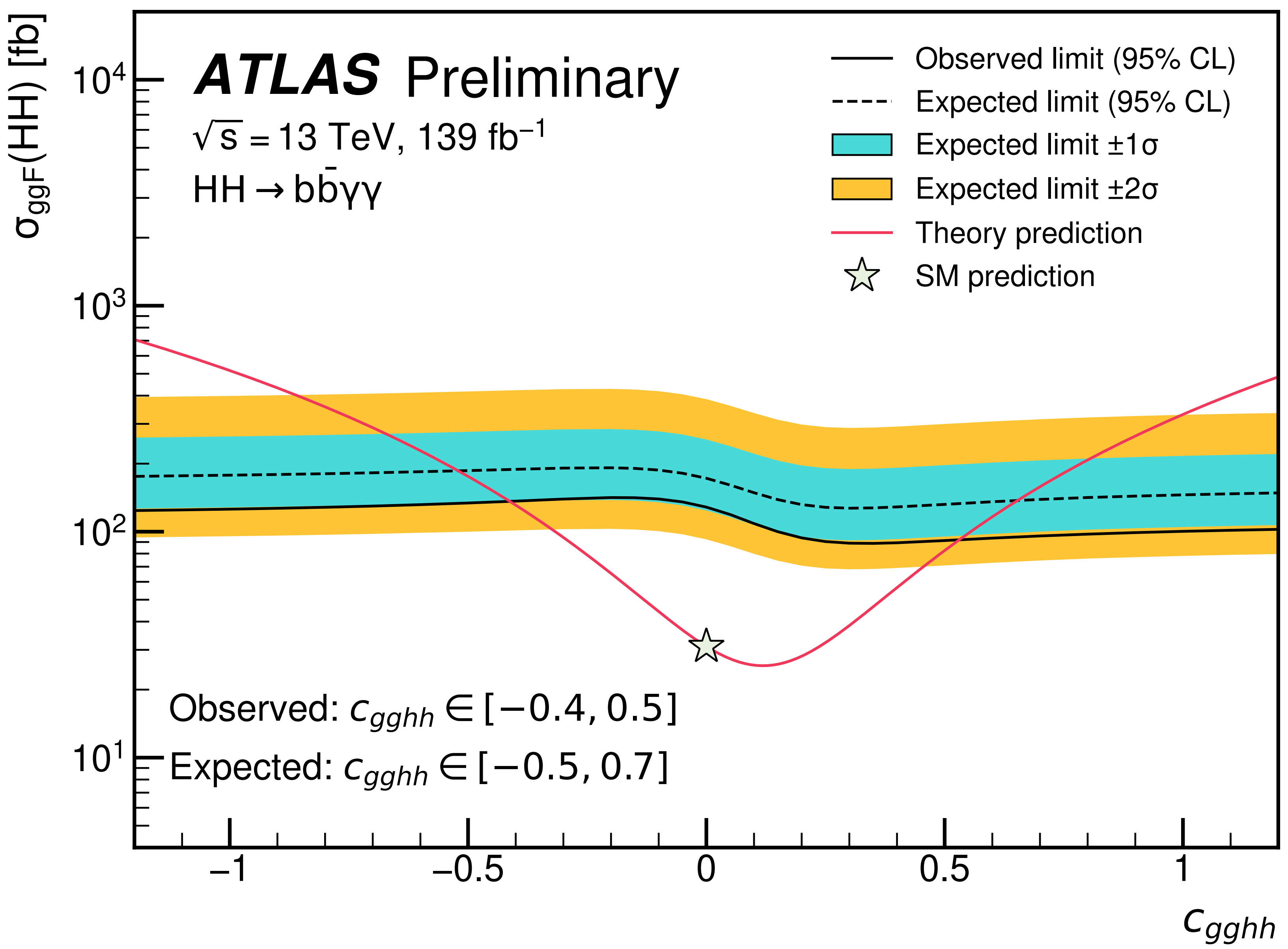

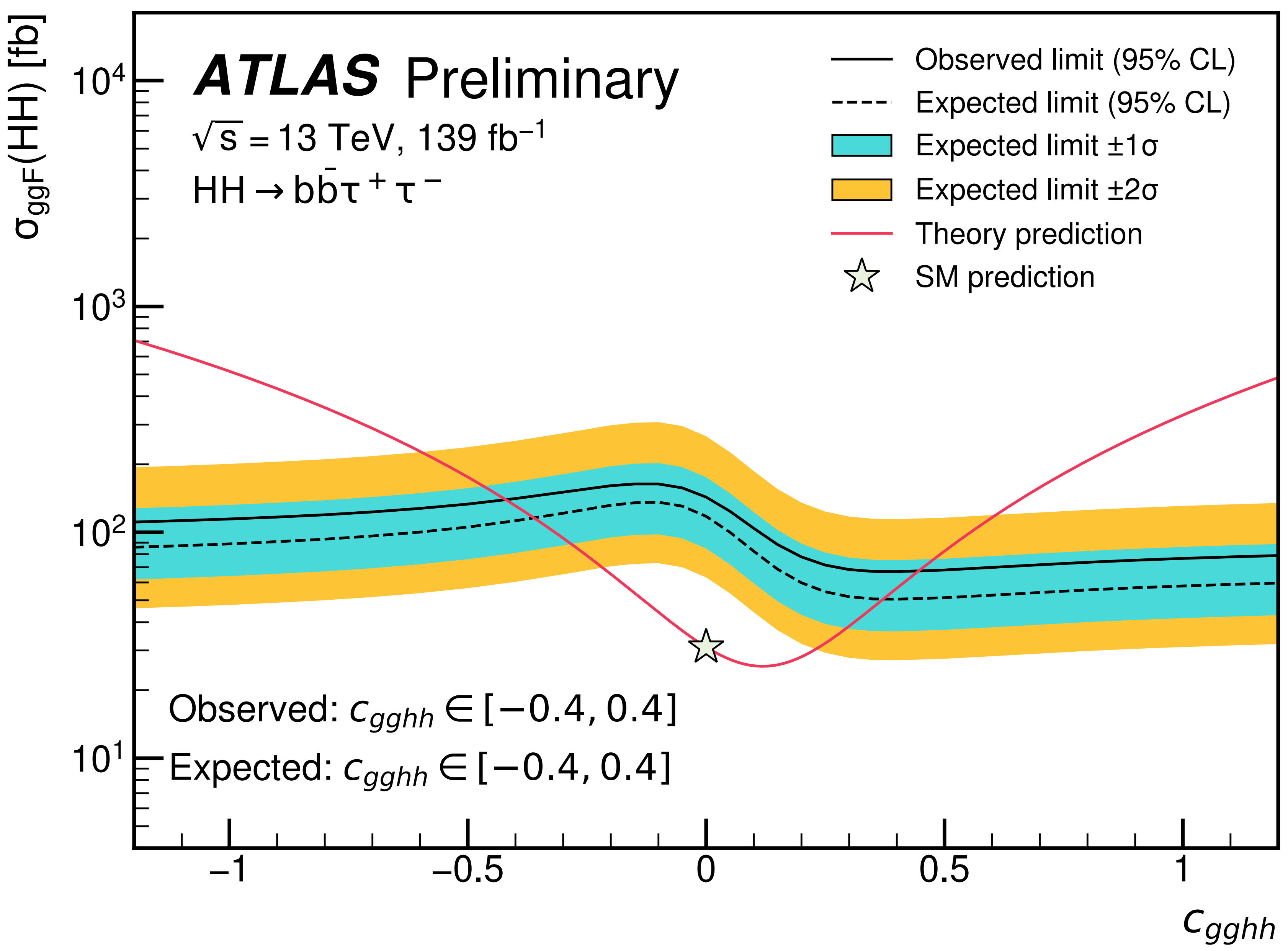

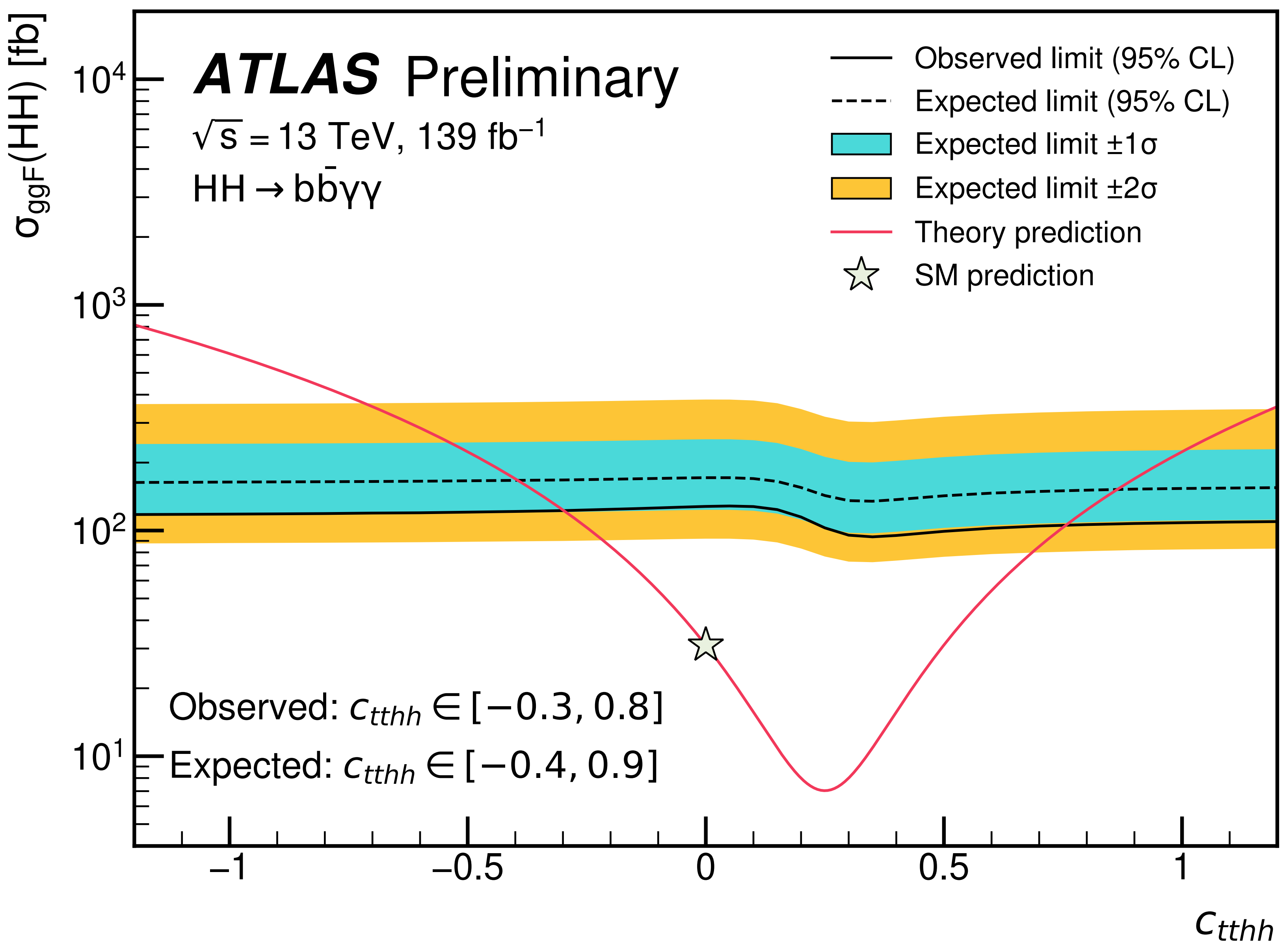

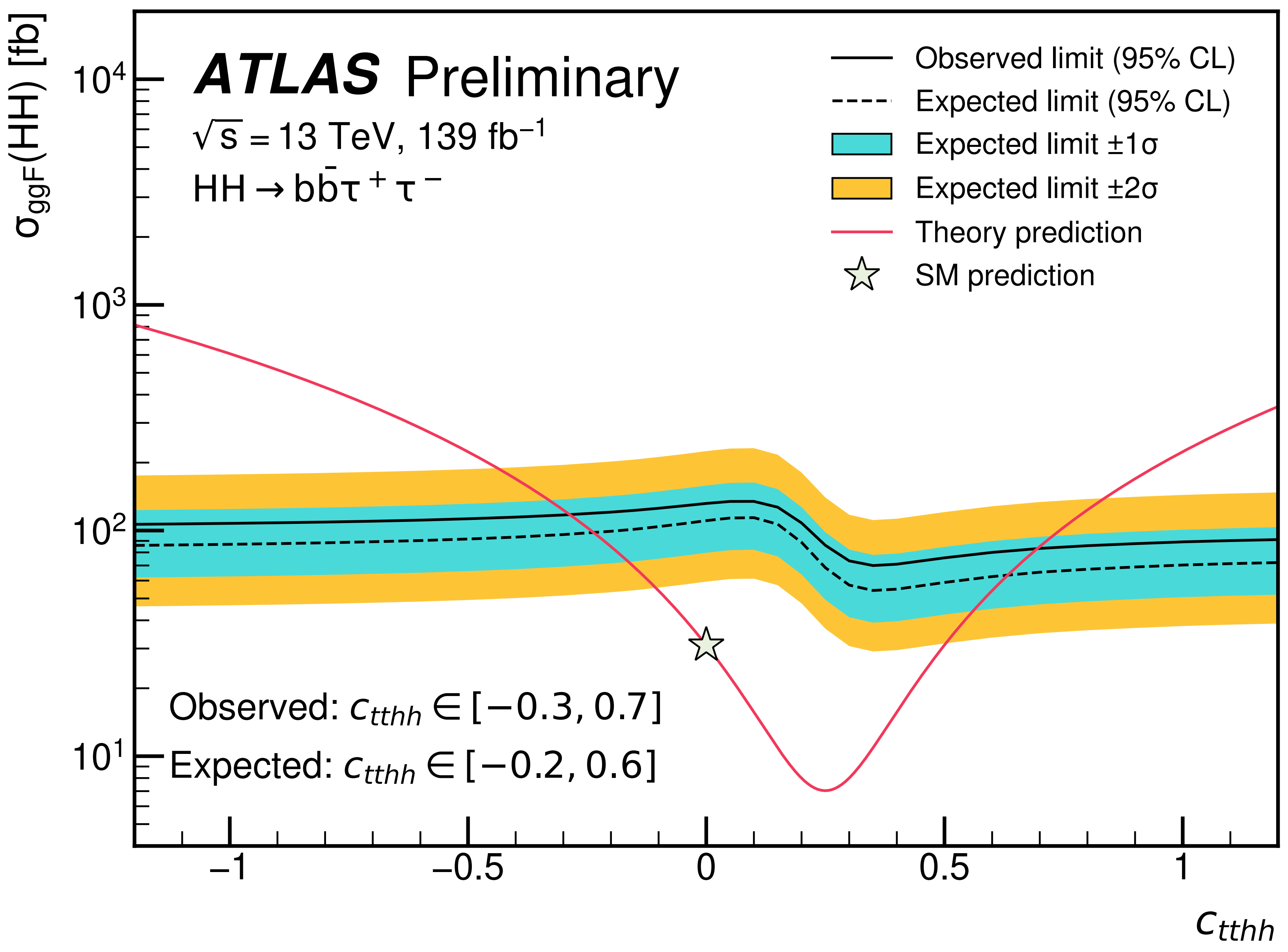

Effective Field Theory (EFT) interpretations

ATL-PHYS-PUB-2022-019

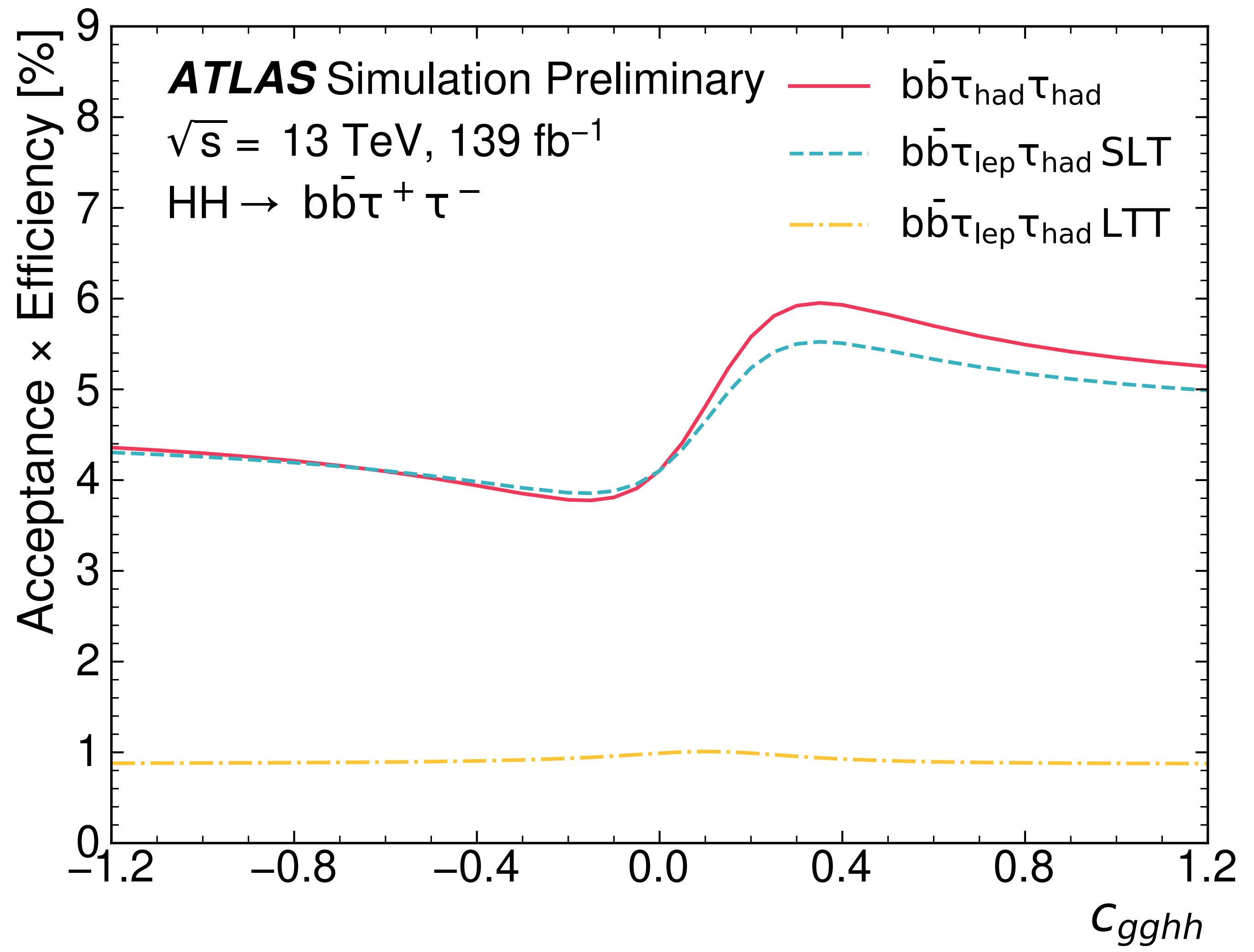

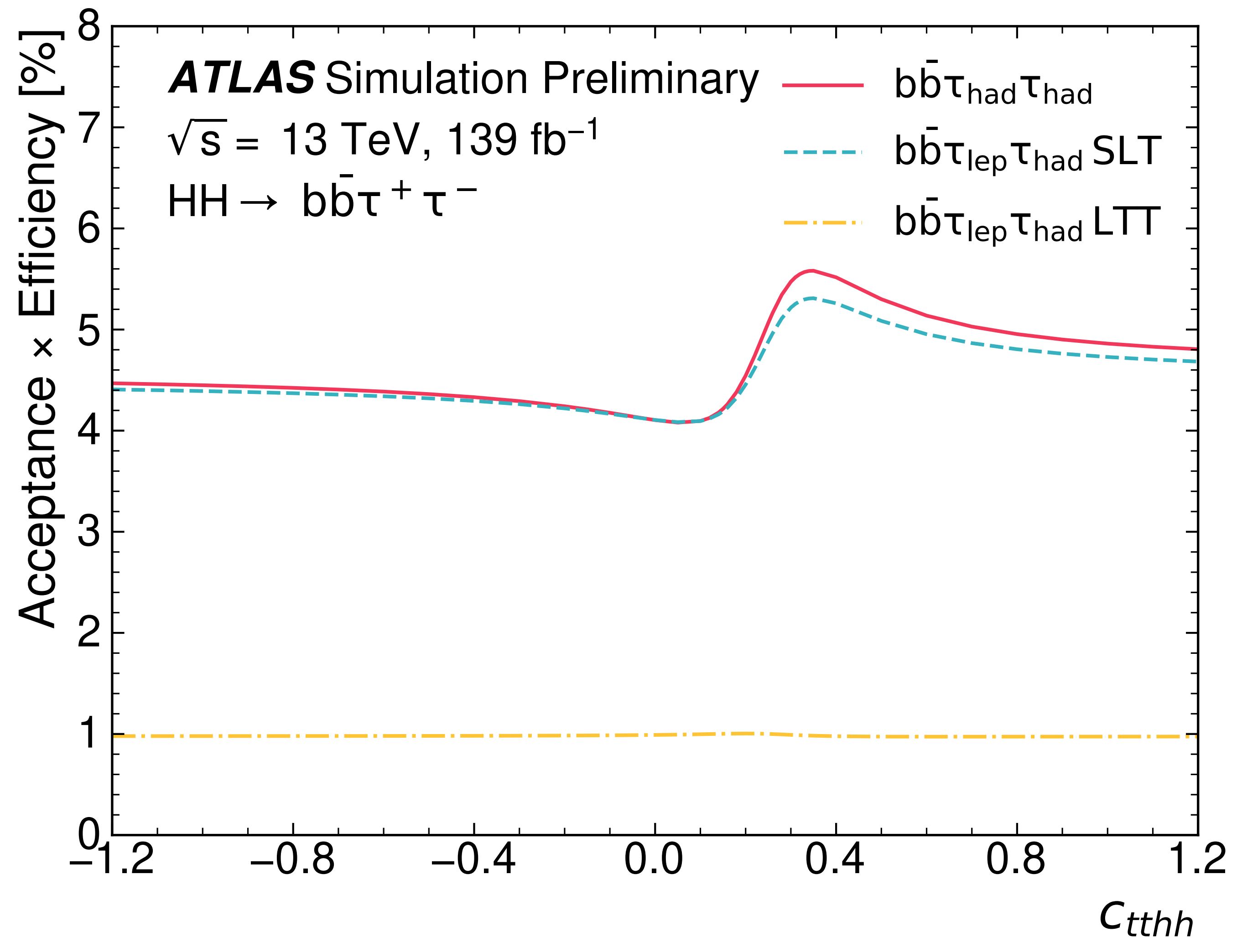

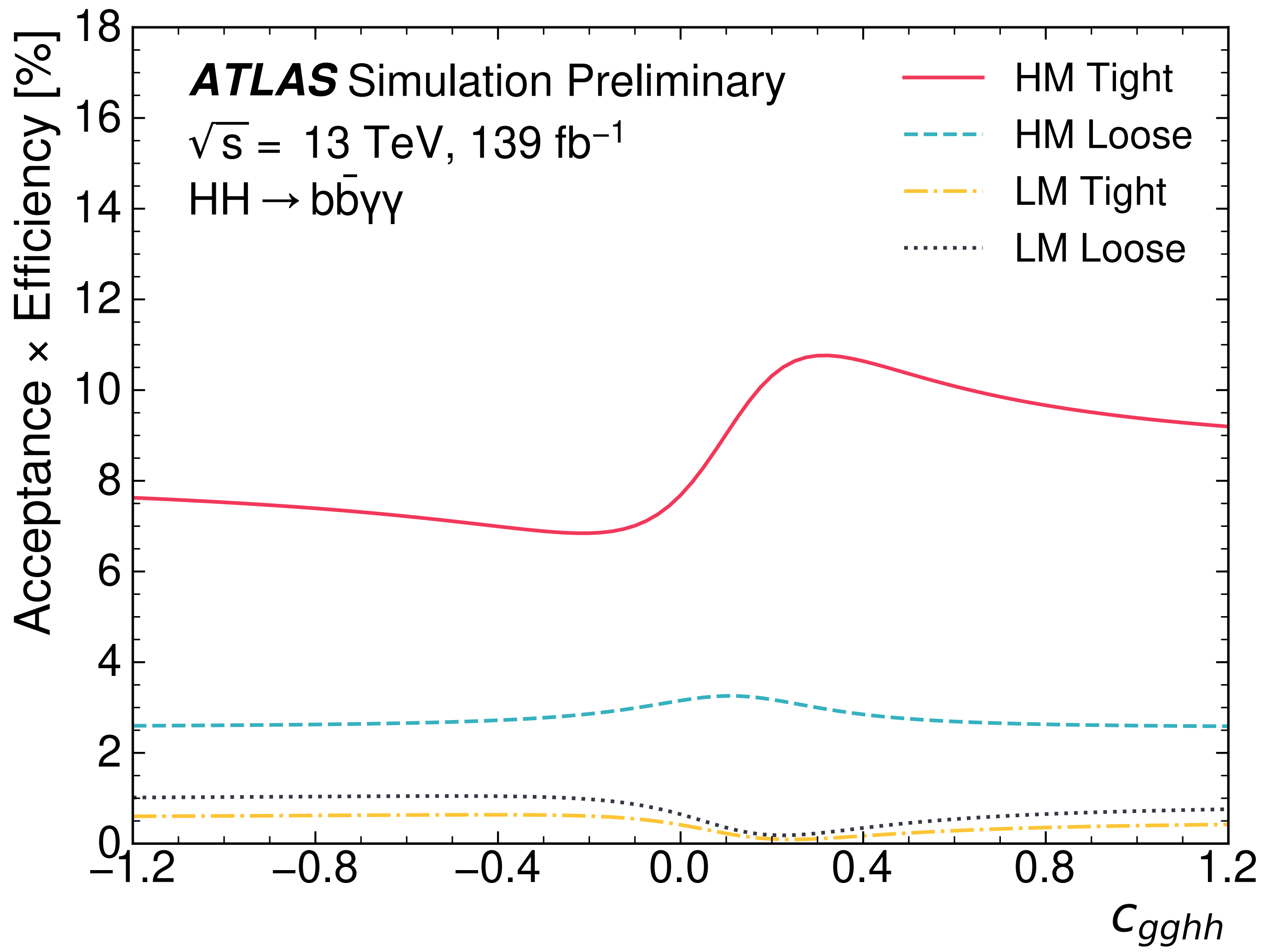

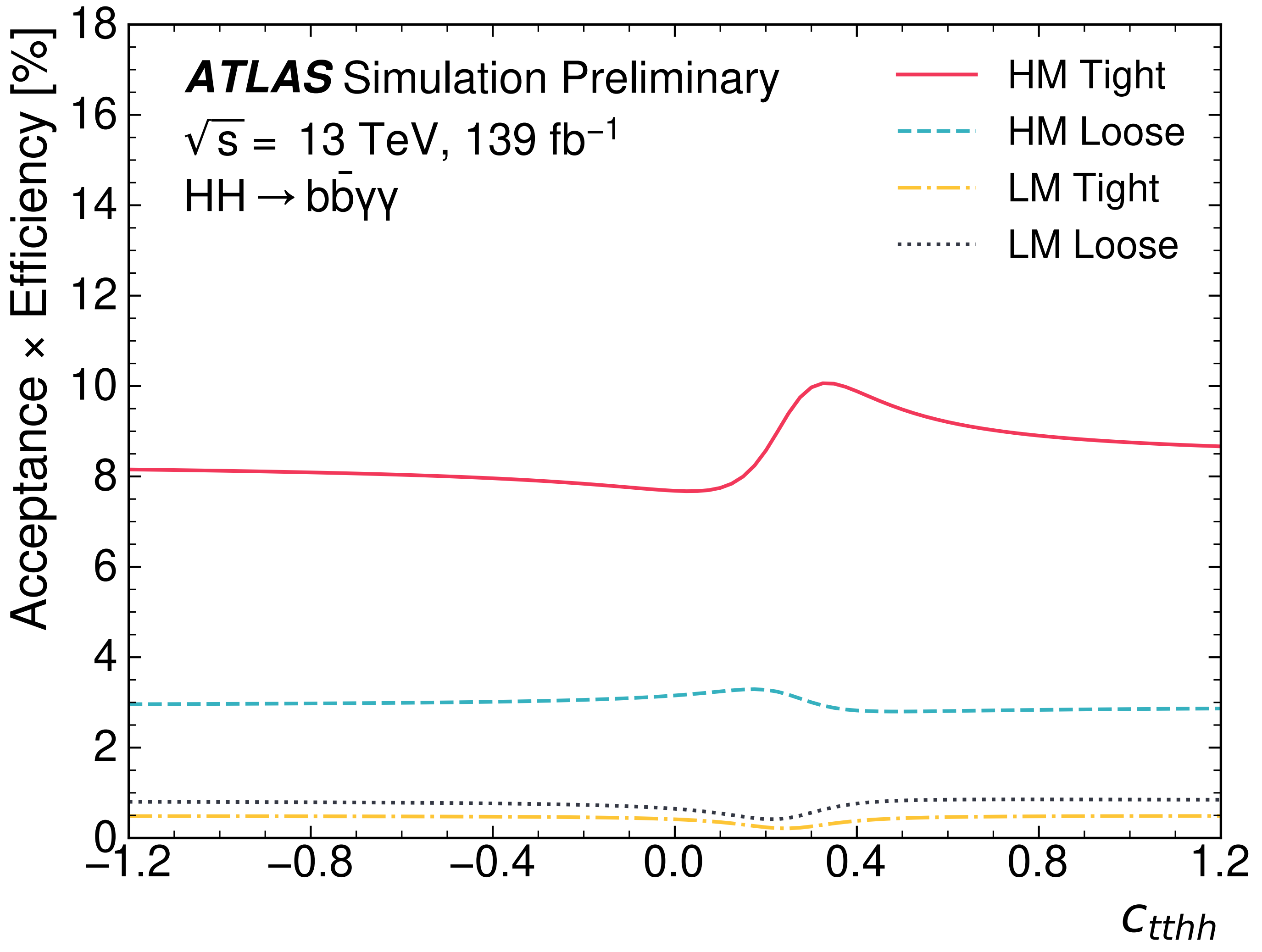

HL-LHC prospects: ATLAS detector phase-2 upgrade

To maximise physics outocome at the HL-LHC need of:

- Maintaining or improving object reconstruction efficiency and resolution
- Reduce fake rates even with more pile-up jets

ATLAS phase-2 upgrade:

- Upgrade of readout electronics
- Replace detectors with most recent technologies
- Extend angular coverage to forward region
- Upgrade of trigger and data acquisition systems to sustain higher rate

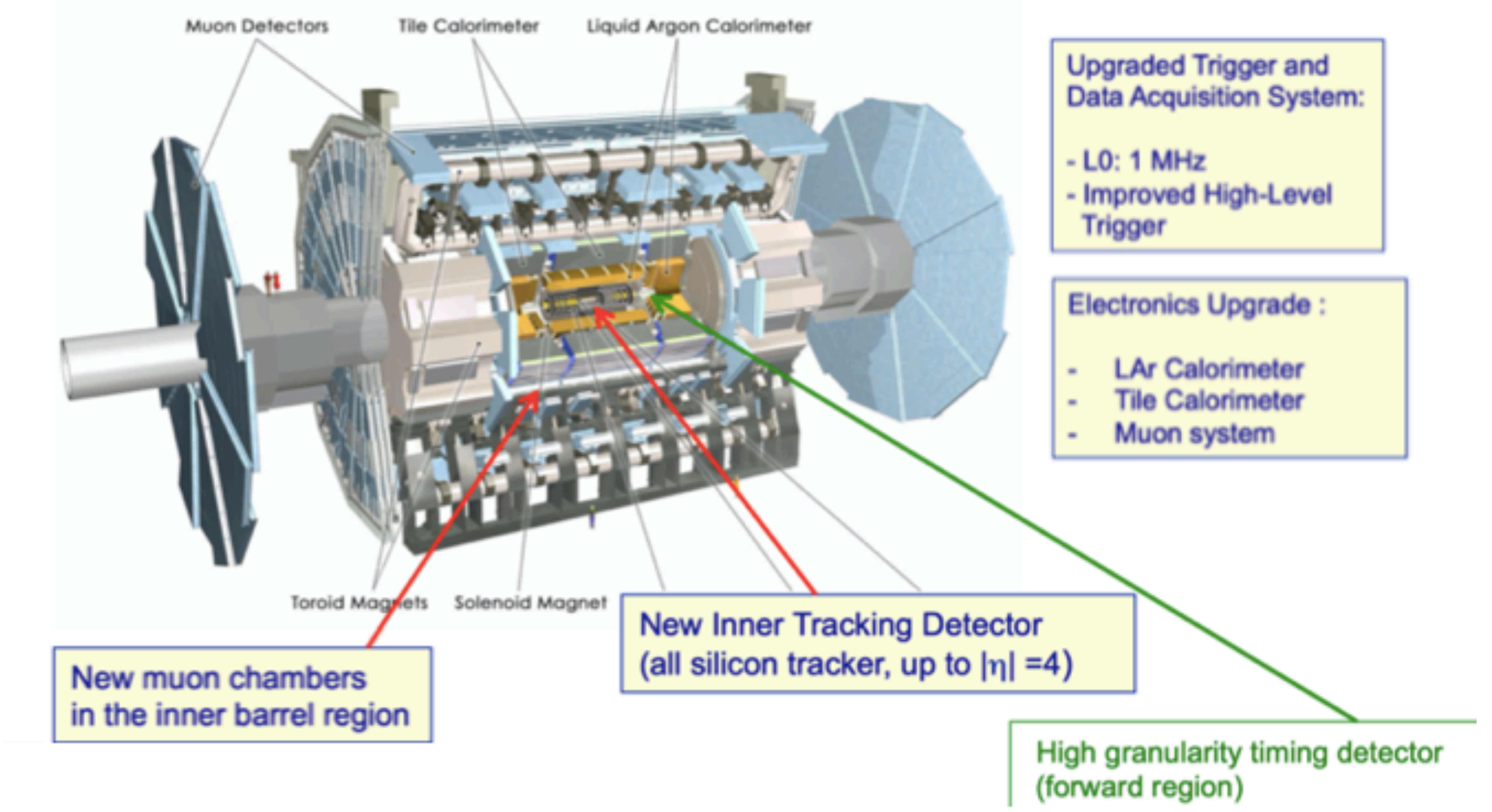

Prospects for di-Higgs searches at the HL-LHC

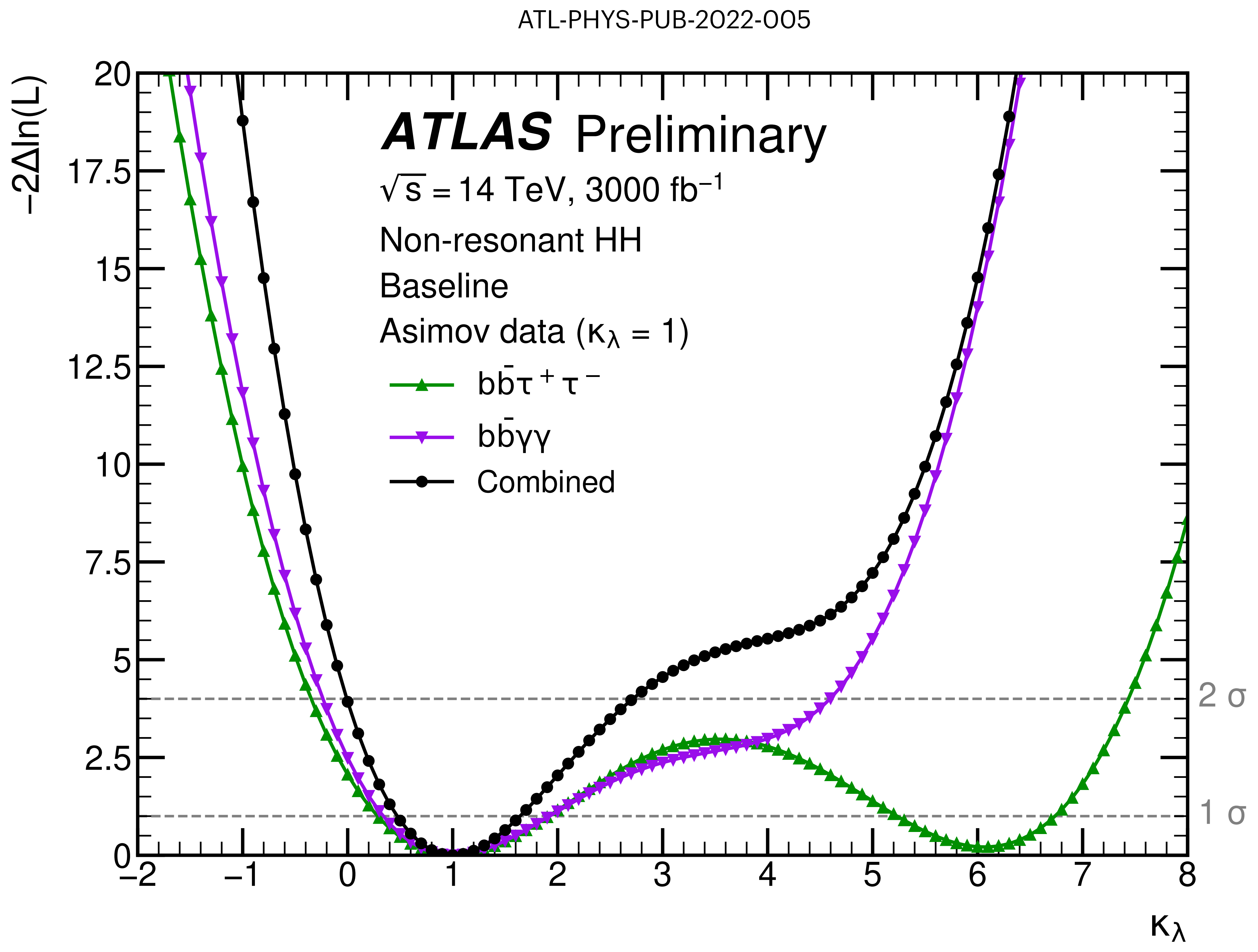

Uncertainty configuration	Likelihood scan 1σ CI for κ_λ: $b\bar{b}\gamma\gamma$	$b\bar{b}\tau^+\tau^-$	Combination
No syst. unc.	$[0.4, 1.8]$	$[0.5, 1.6]$	$[0.6, 1.5]$
Baseline	$[0.3, 1.9]$	$[0.3, 1.9] \cup [5.2, 6.7]$	$[0.5, 1.6]$
Theoretical unc. halved	$[-0.1, 4.3]$	$[0.0, 2.9] \cup [4.2, 7.1]$	$[0.2, 2.2]$
Run 2 syst. unc.	$[-0.1, 4.3]$	$[-0.2, 7.3]$	$[0.1, 2.5]$

Uncertainty configuration	Likelihood scan 2σ CI for κ_λ: $b\bar{b}\gamma\gamma$	$b\bar{b}\tau^+\tau^-$	Combination
No syst. unc.	$[-0.1, 4.6]$	$[0.1, 2.5] \cup [4.5, 6.5]$	$[0.3, 2.1]$
Baseline	$[-0.2, 4.6]$	$[-0.3, 7.4]$	$[0.0, 2.7]$
Theoretical unc. halved	$[-0.8, 5.7]$	$[-0.8, 8.0]$	$[-0.4, 5.6]$
Run 2 syst. unc.	$[-1.0, 5.8]$	$[-1.2, 8.3]$	$[-0.7, 5.7]$

- bbγγ and bbττ have comparable contribution to the κ_λ constraint on the negative side
- bbγγ dominates the κ_λ constraining power on the positive side

HL-LHC prospects

ATL-PHYS-PUB-2022-005

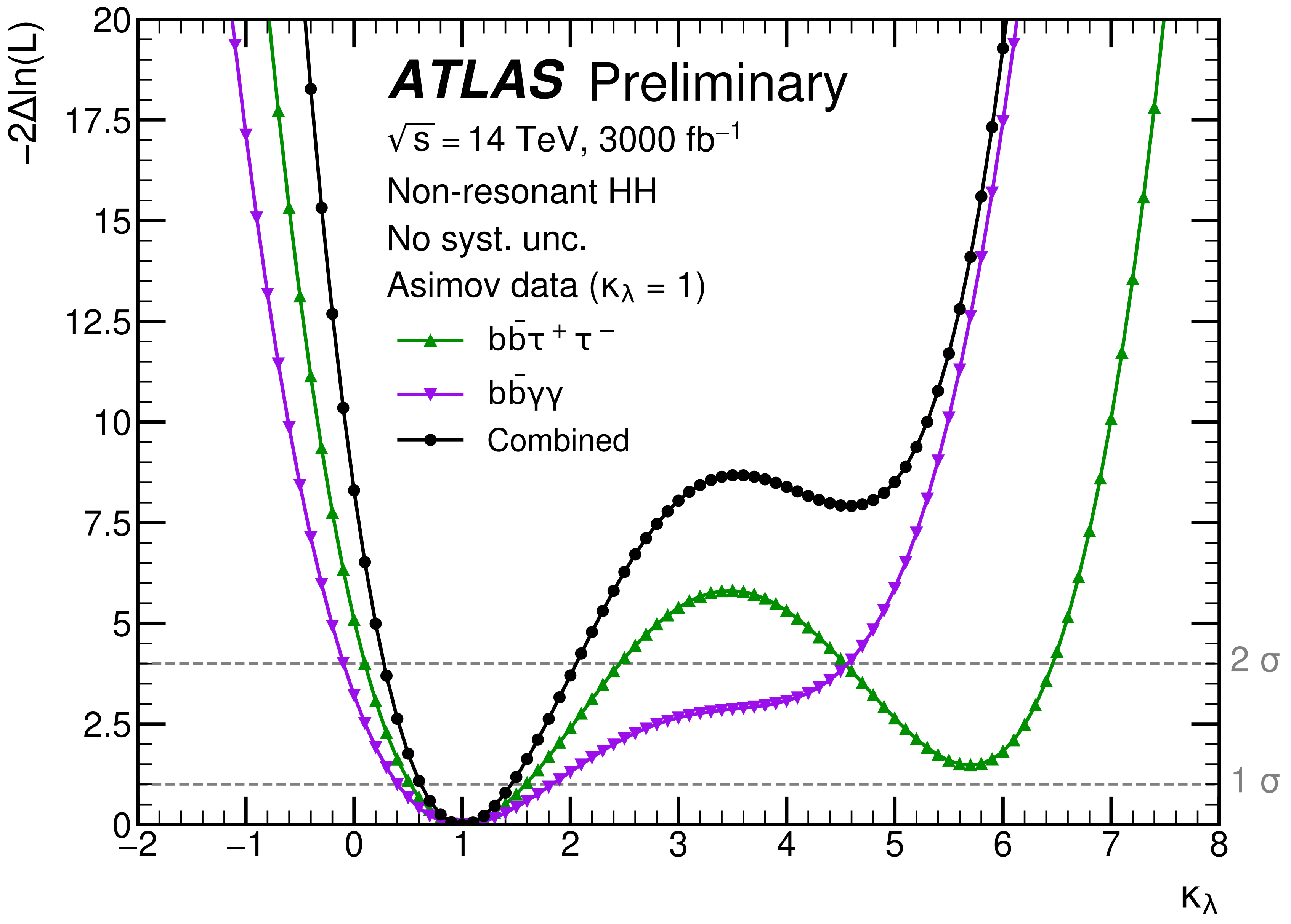

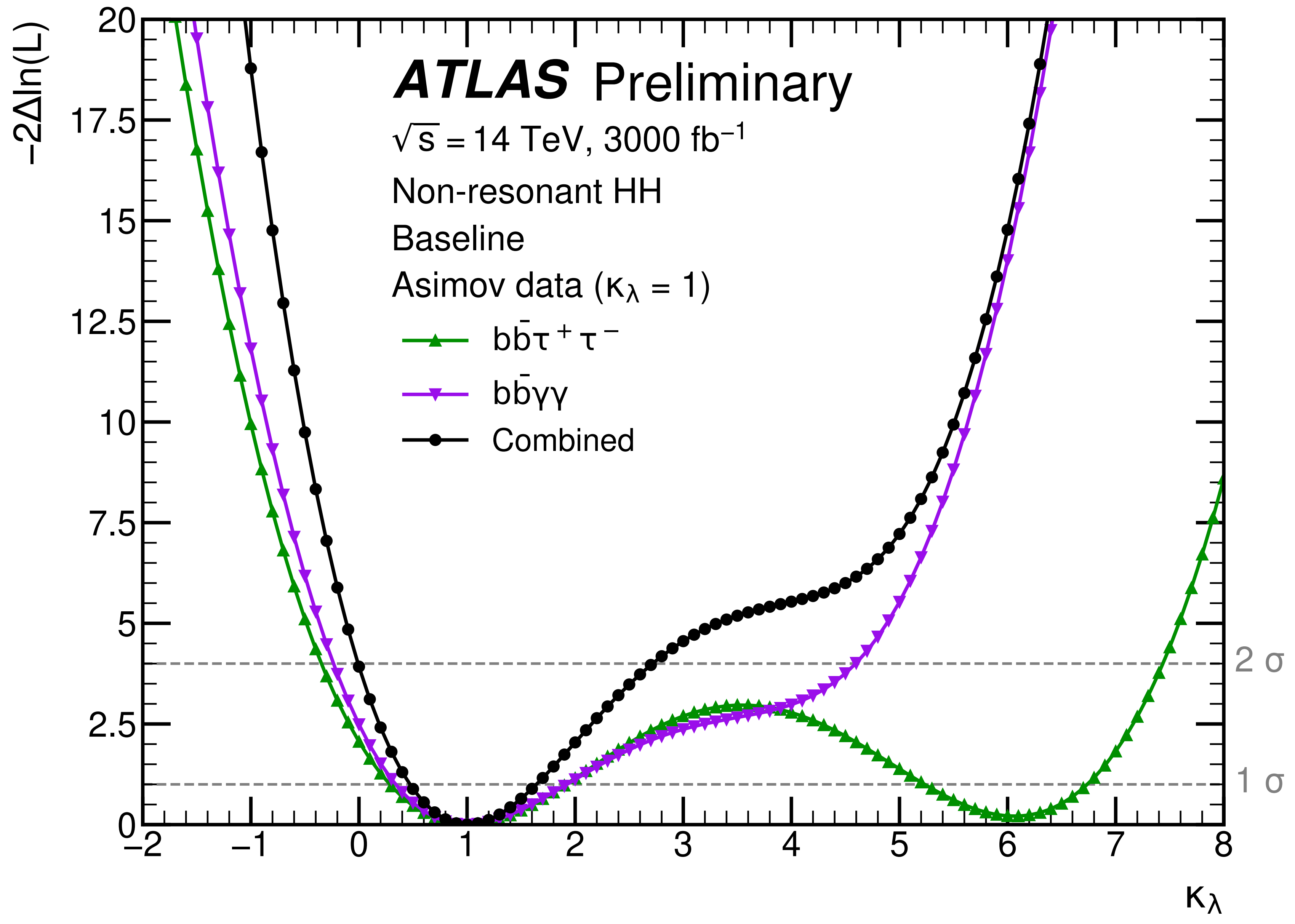

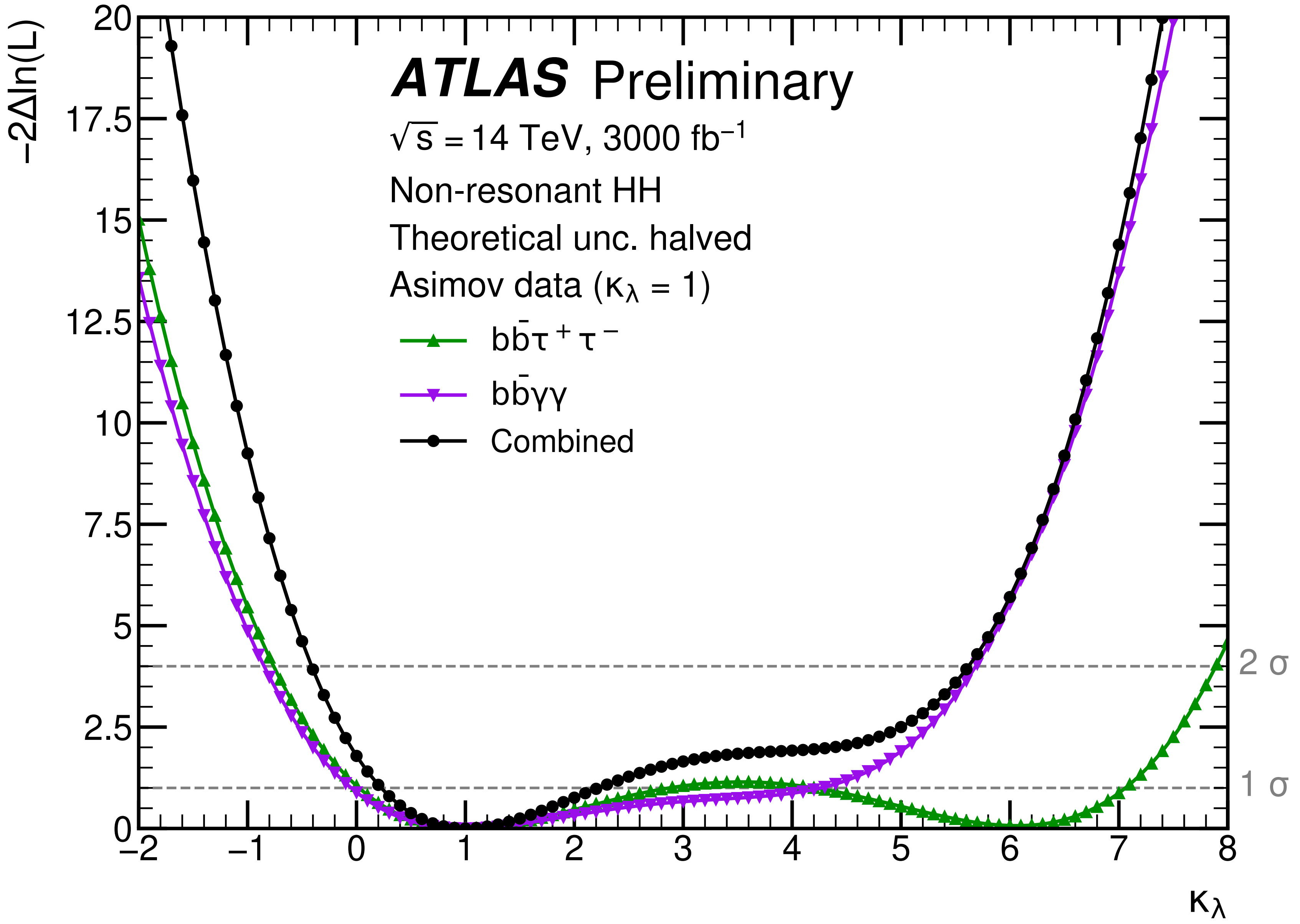

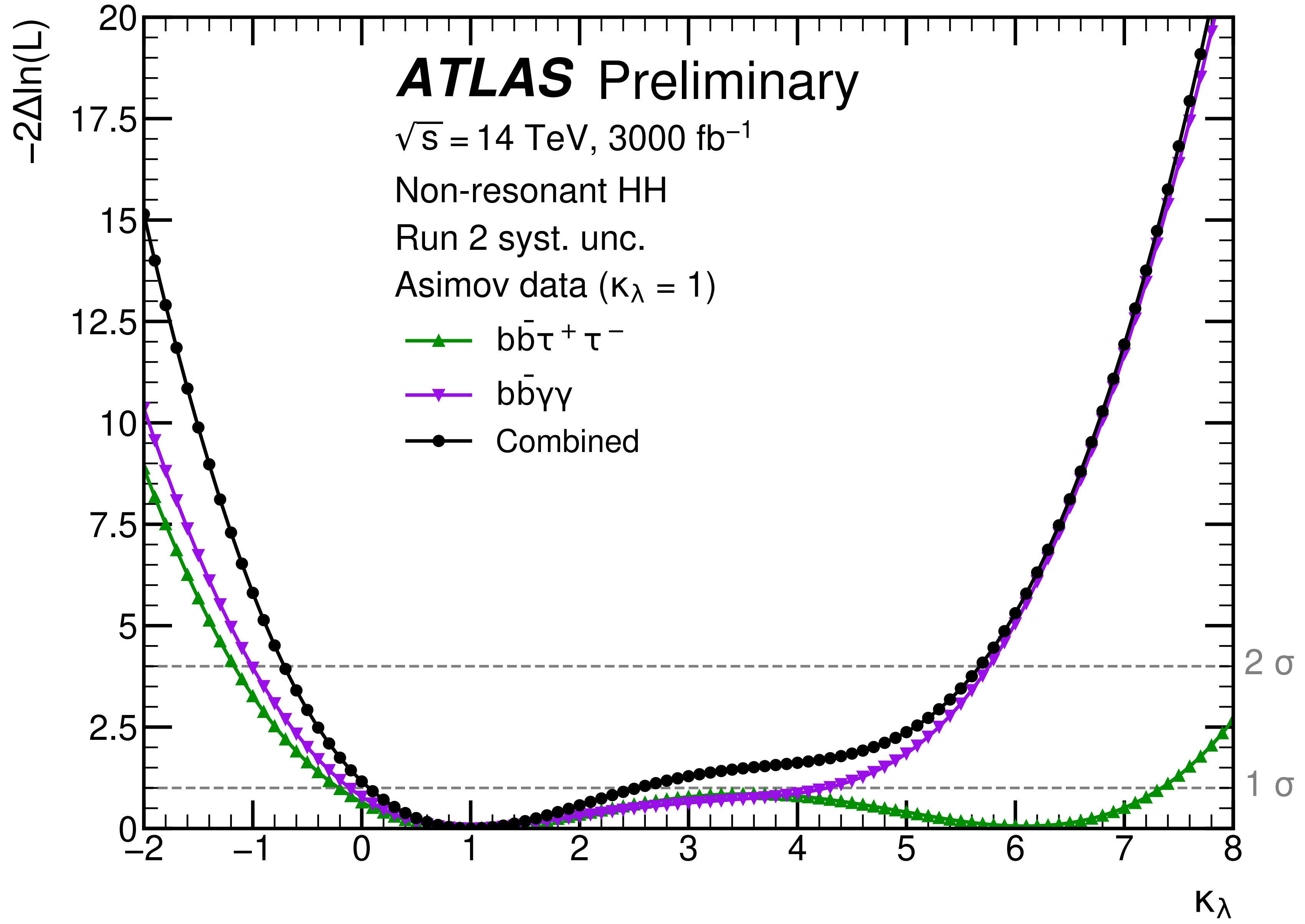

HL-LHC prospects

ATL-PHYS-PUB-2022-005

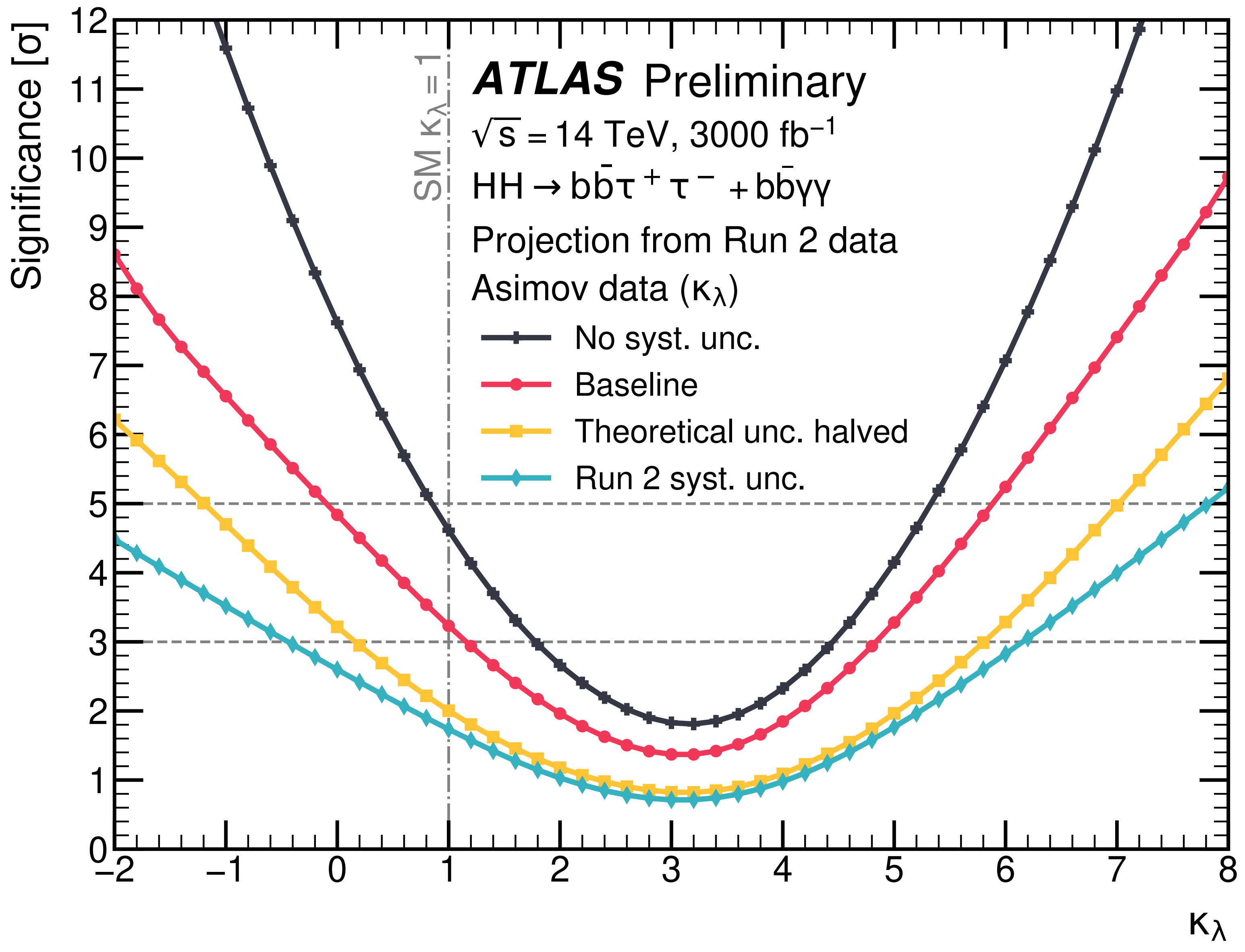

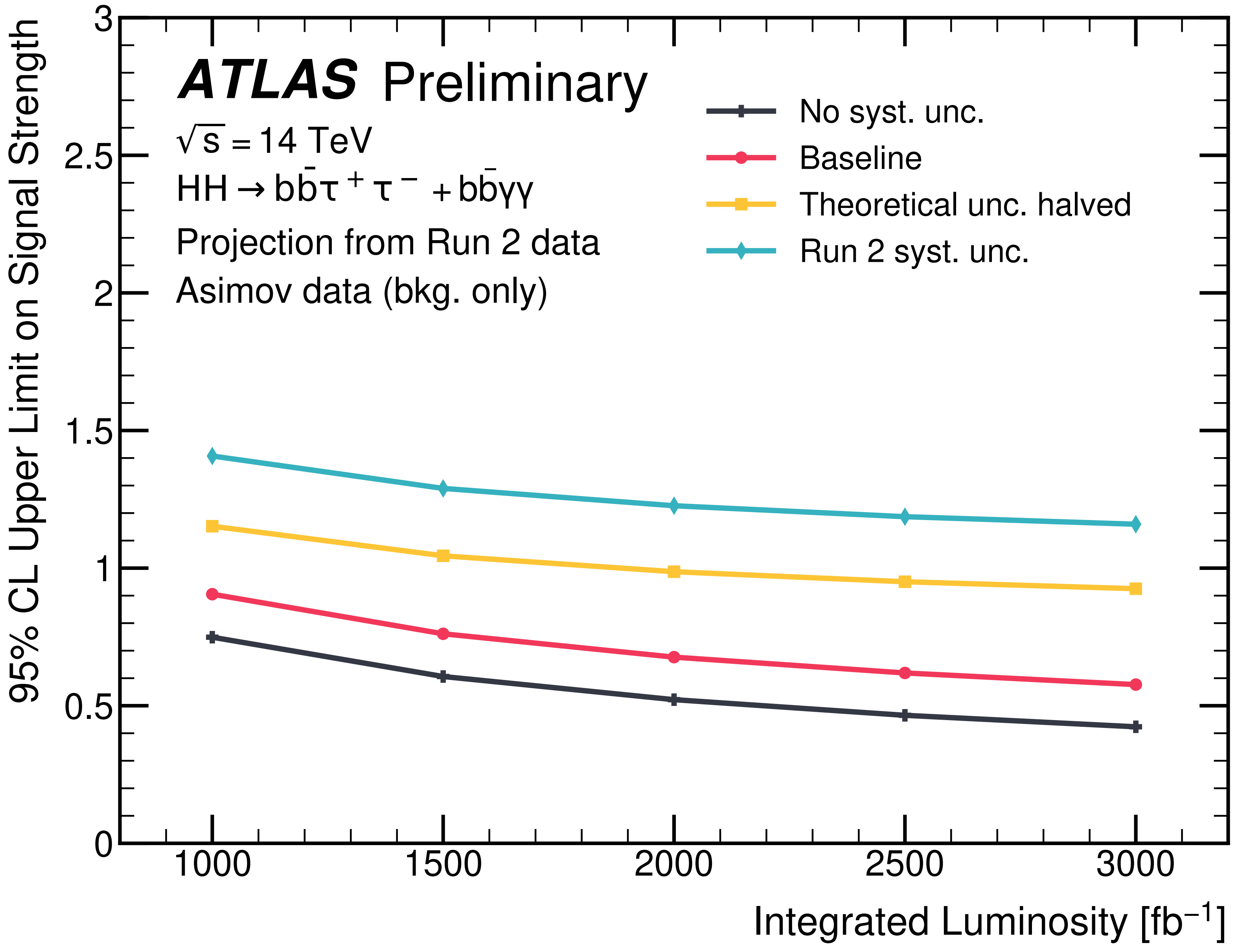

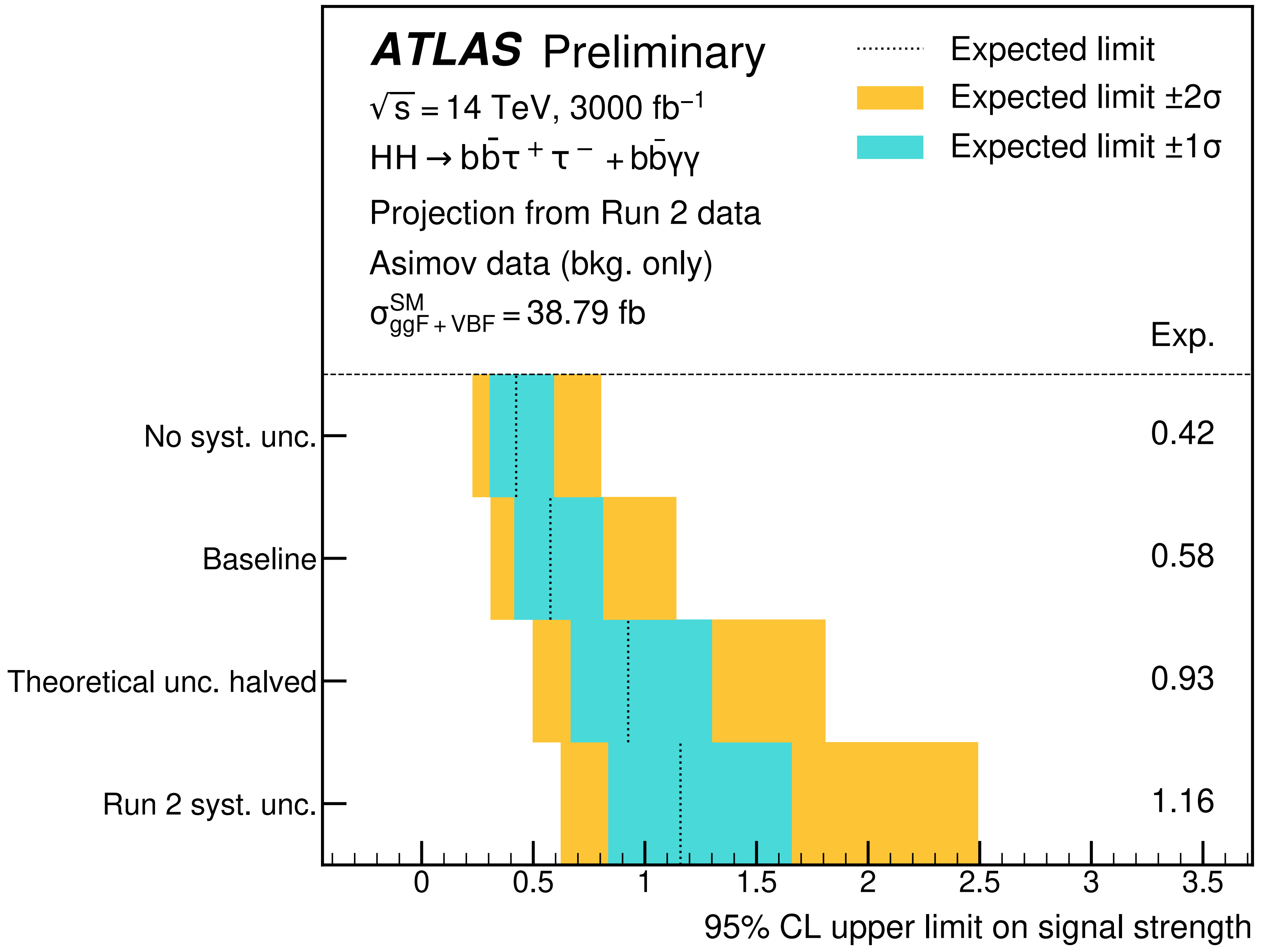

Future colliders

arXiv:1905.03764

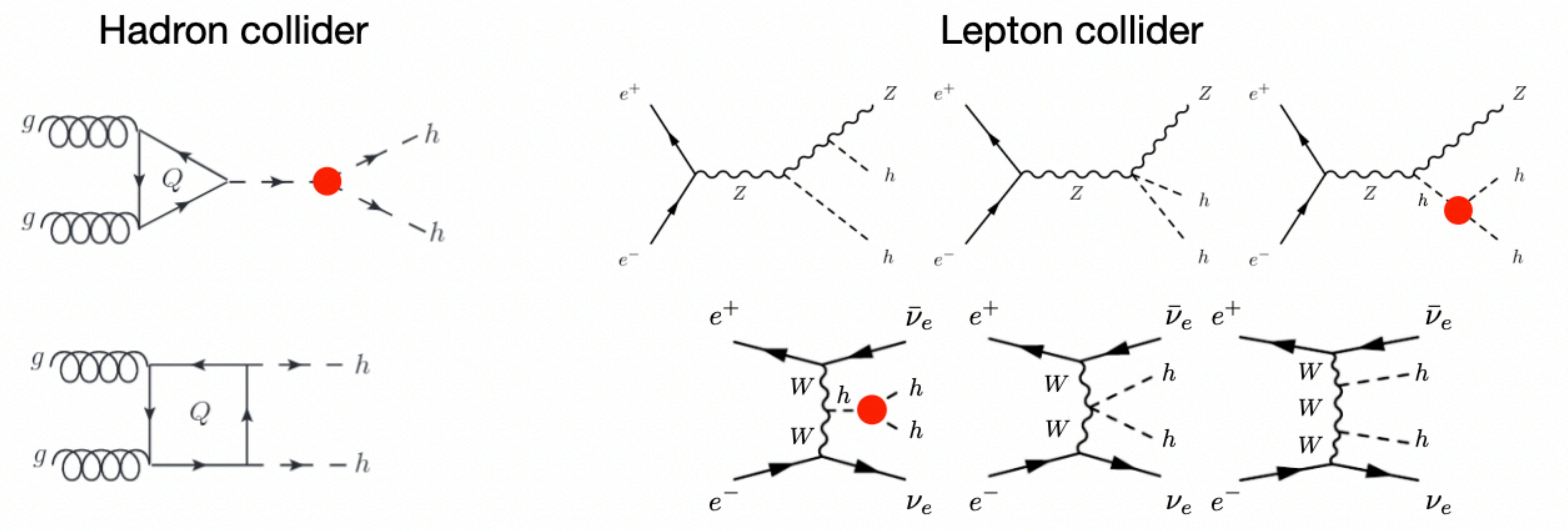

Expected uncertainty on κ_λ:

HL-LHC: 50%

↓

HE-LHC (27 TeV): 15%

FCC-ee (350 GeV): 20%

ee linear collider (ILC, 1 TeV): 10%

FCC-hh (100 TeV): 5%

Muon-collider (10 TeV): 5%

Resonant HH→bbbb with full Run 2 data

- Search for BSM resonant HH production: resonances with masses between 250 GeV and 3 TeV
- X→HH→bbbb
- Resolved and boosted categories

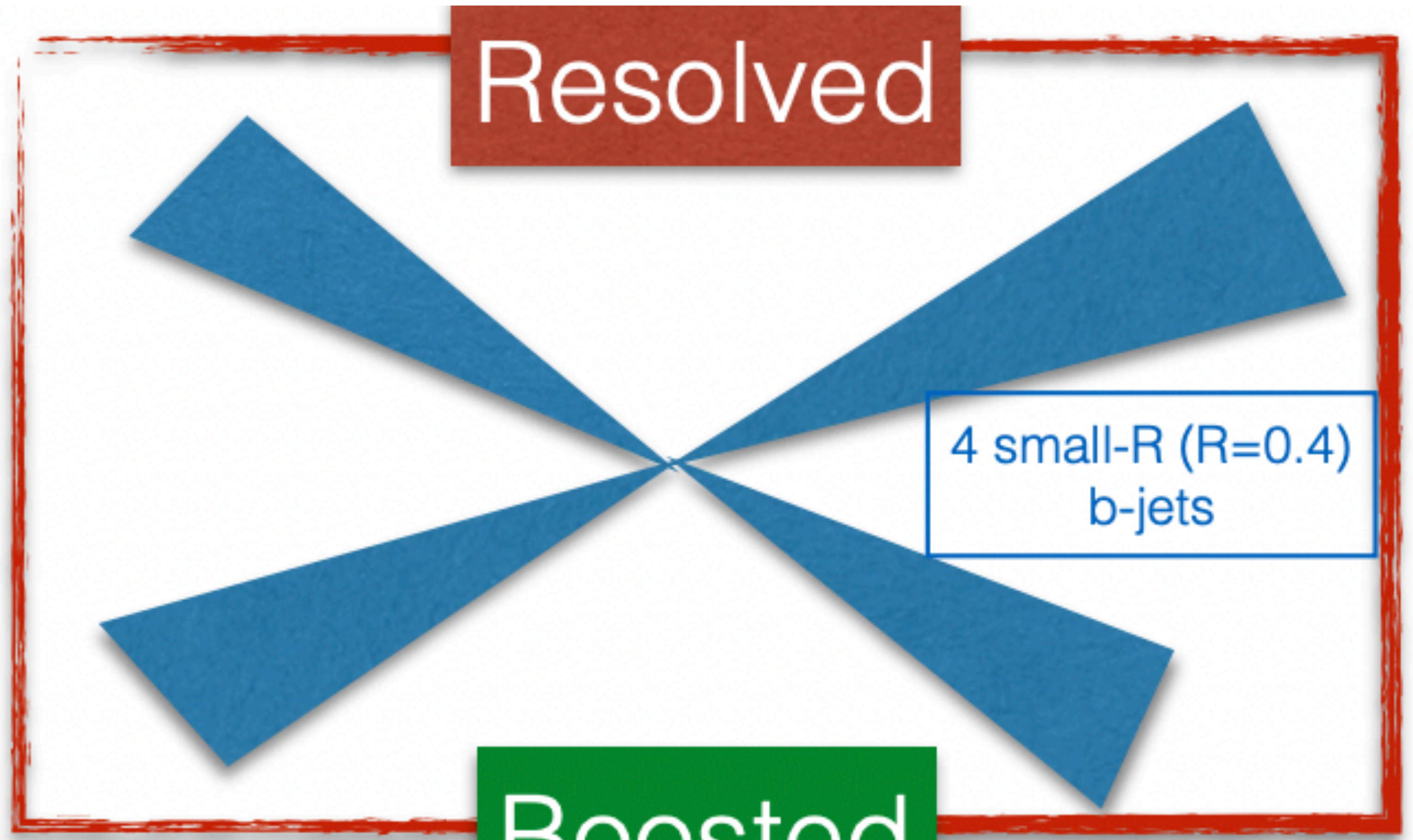

Resolved category:

- mX ∈ [250, 1500] GeV
- At least 4 b-tagged small-radius jets ($\Delta R = 0.4$)
- Boosted Decision Trees used to pair the 4 b-jets to form the 2 Higgs candidates
- Fully data-driven total background estimation (95% QCD multijet, 5% ttbar)

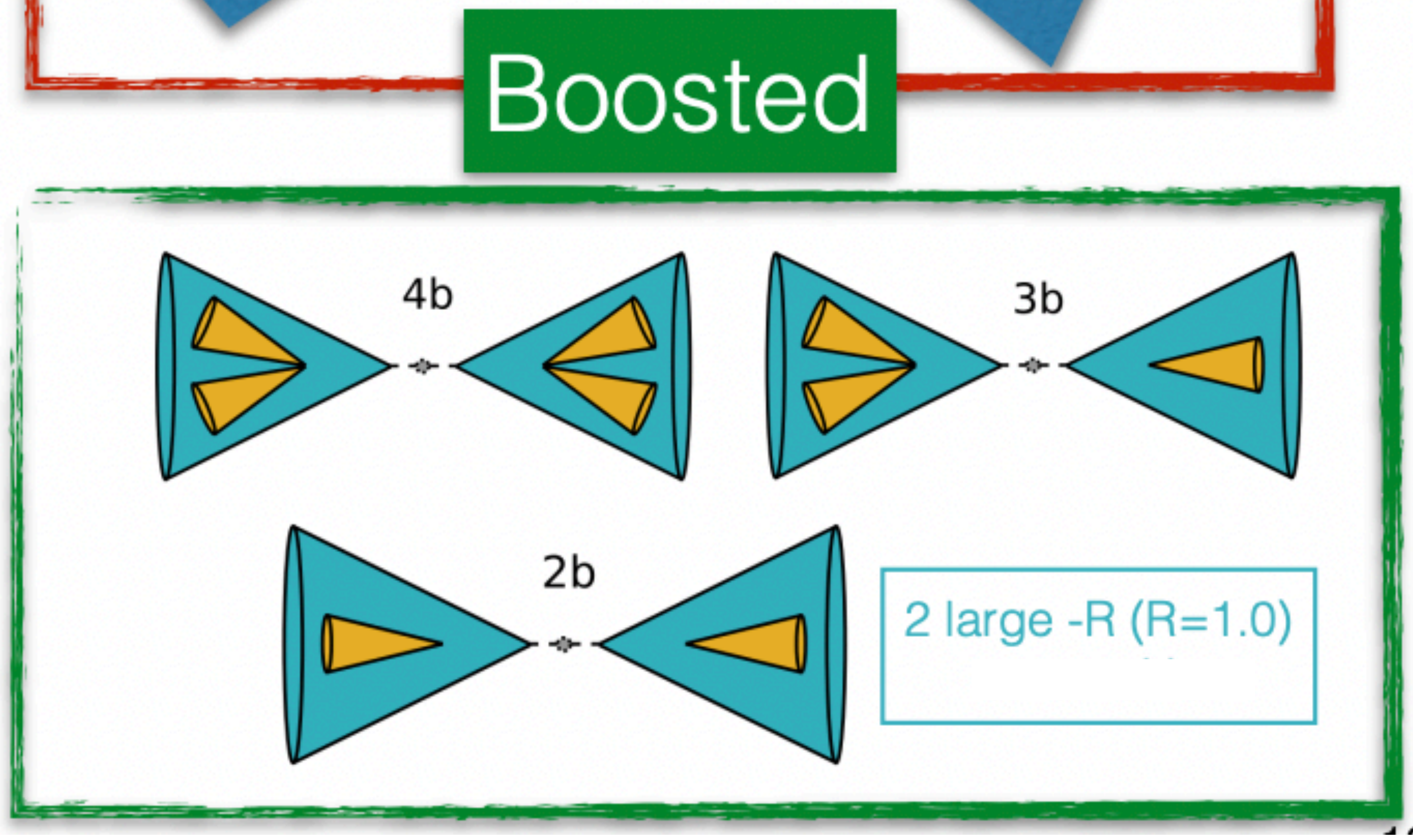

Boosted category:

- mX ∈ [900, 5000] GeV
- High mass resonance→boosted Higgs bosons→merged b-jets from the Higgs
- At least two large-radius jets ($\Delta R = 1.0$)
- 2b, 3b and 4b categories
- Fully data-driven QCD multi-jet background estimation (70%-90%)
- ttbar from Monte Carlo simulations (30-10%)

Resonant HH→bbbb with full Run 2 data

Signal regions defined by selections in the 2D m_{H1}-m_{H2} plane

m_{HH} used as final discriminant variable,
searching for a "bump" from the decay of a new BSM resonance

Phys. Rev. D 105, 092002

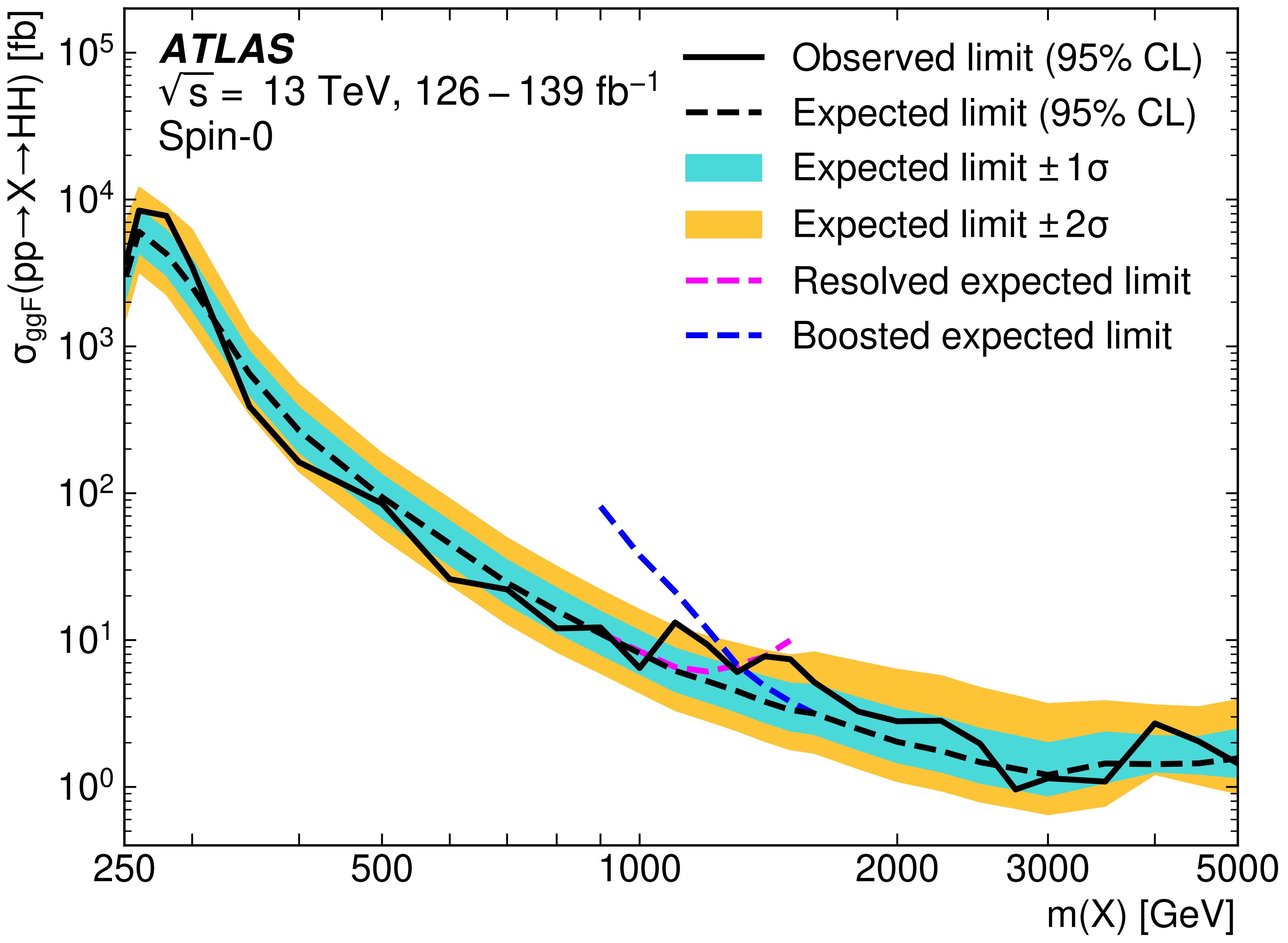

Small data excess at 1.1 TeV,
local (global) significance = 2.6σ (1.0 σ)

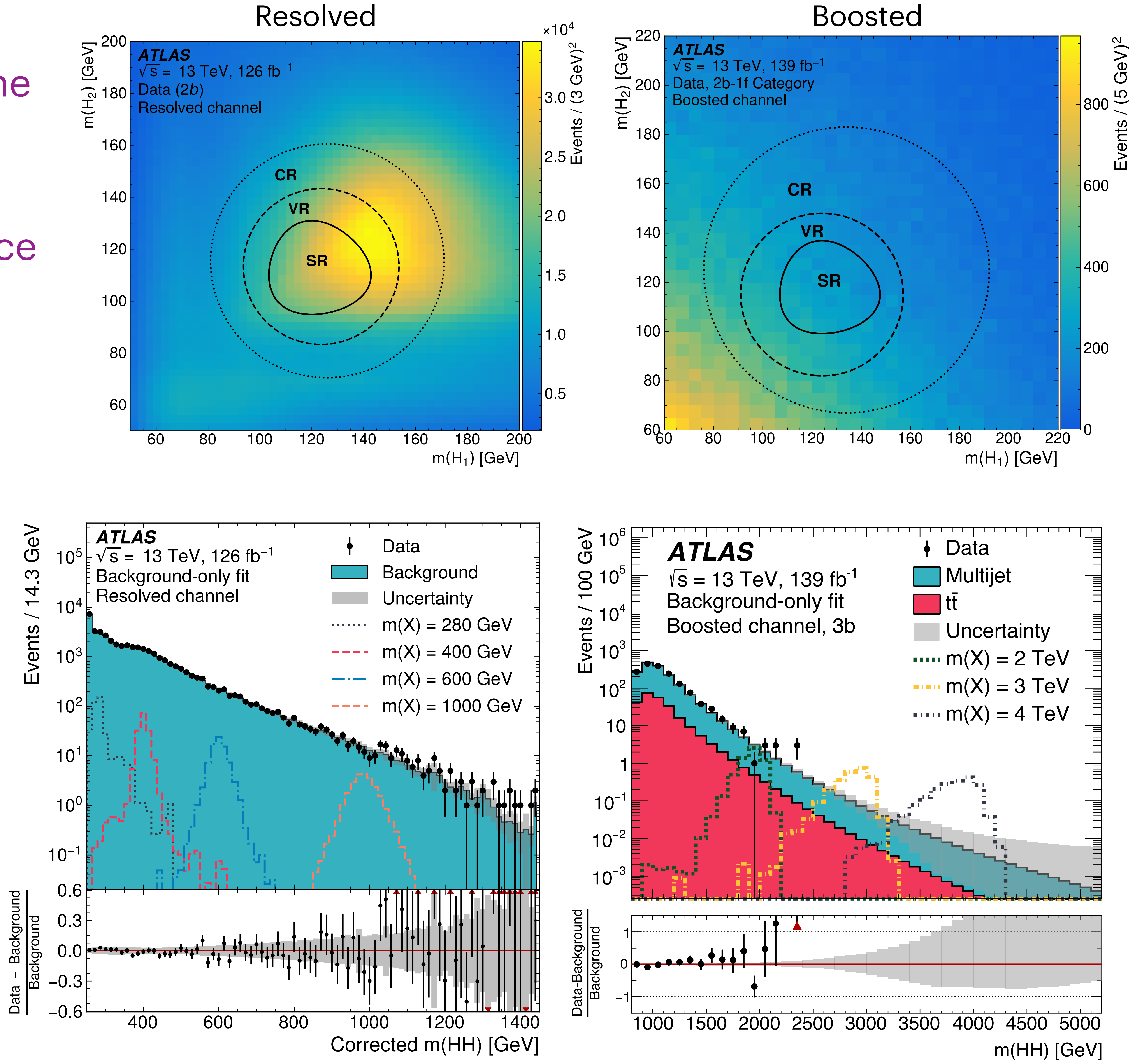

Resonant HH→bbbb with full Run 2 data

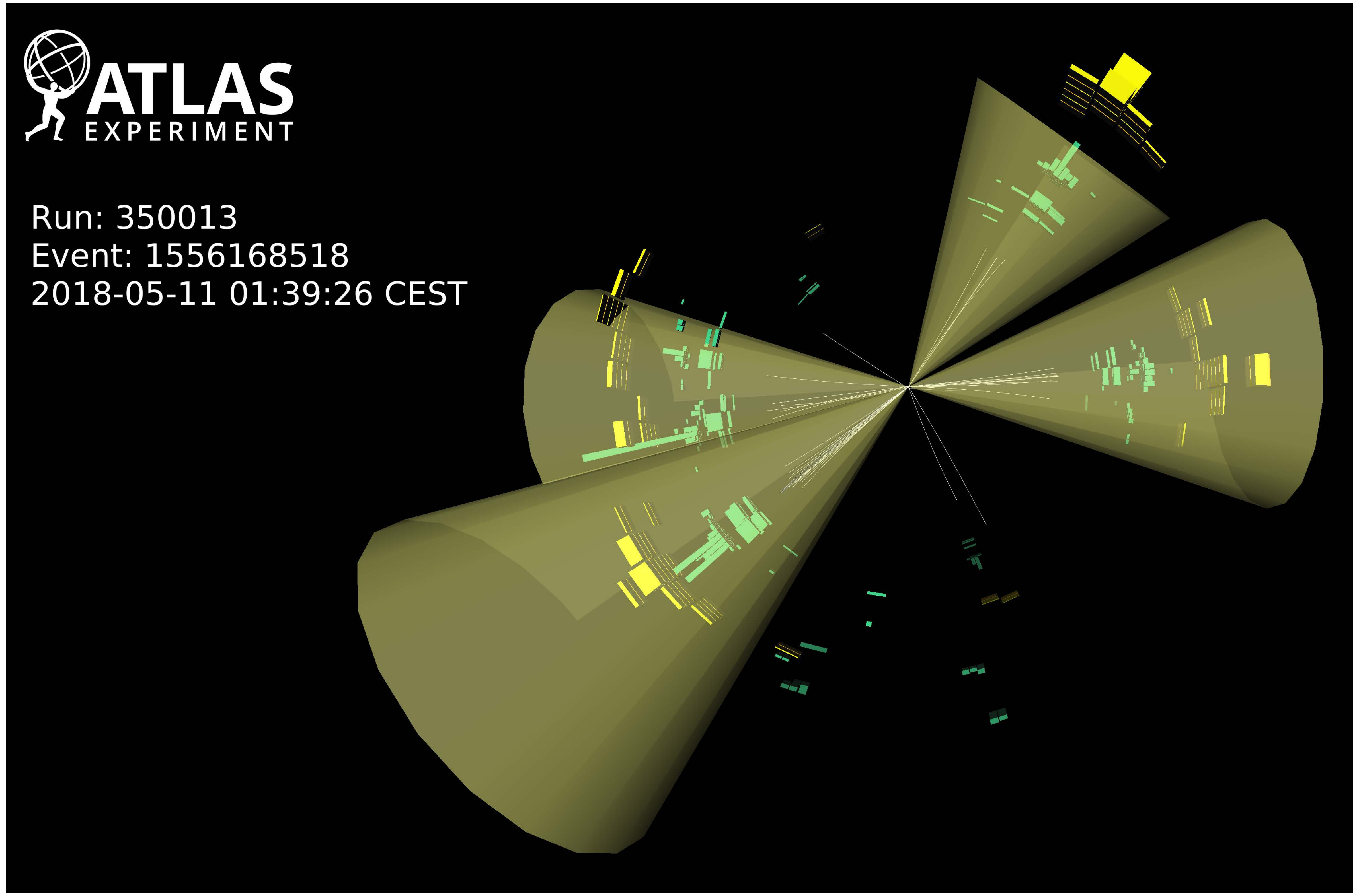

Data event passing the resolved signal region event selection

$m_{HH} = 629$ GeV, $m_{H1} = 111$ GeV and $m_{H2} = 116$ GeV

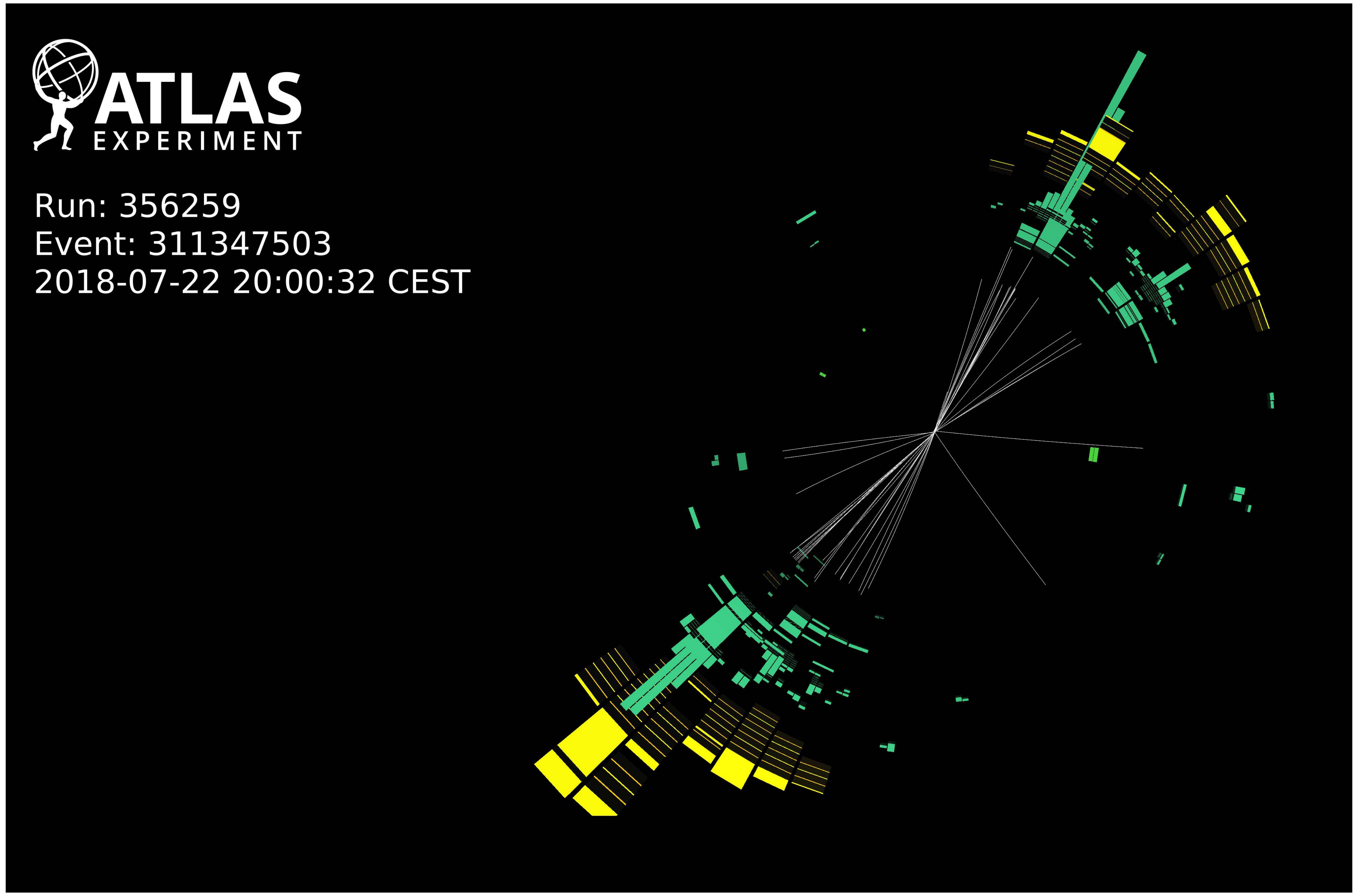

Data event passing the boosted 4b signal region event selection

$m_{HH} = 1023$ GeV, $m_{H1} = 127$ GeV and $m_{H2} = 123$ GeV

Resonant HH→bbττ with full Run 2 data

- Search for BSM resonant HH production: resonances with masses between 250 GeV and 1.6 TeV
- X→HH→bbττ
- Same 3 signal regions and background estimation as non-resonant search
- Parameterized Neural Network (PNN), with mass of the resonance as parameter, used to separate signals with different mass hypotheses from background
- PNN outputs used as final discriminants searching for an excess of events in the most signal-like bins of the PNNs

ATLAS-CONF-2021-030

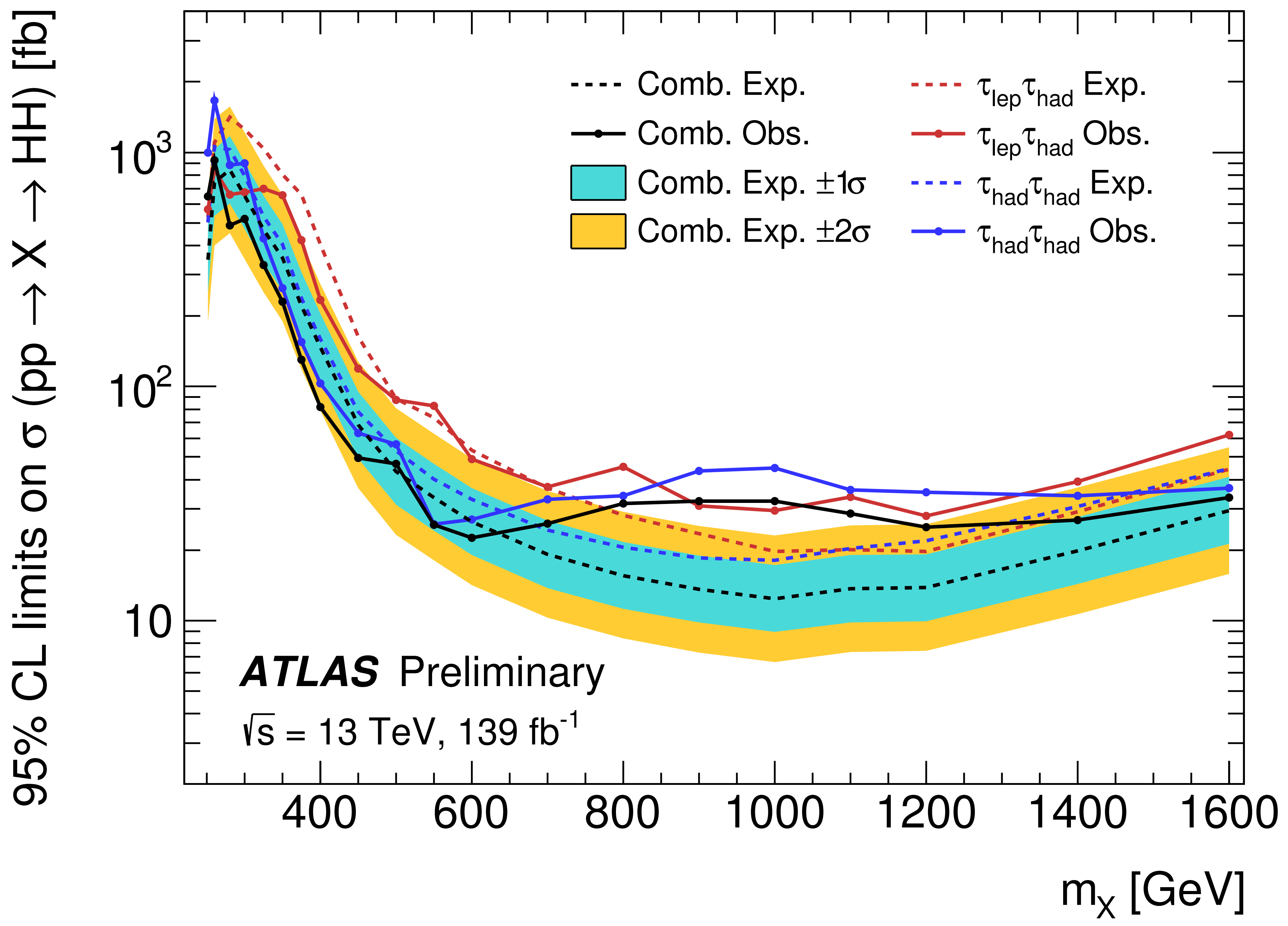

Small data excess between 800 GeV and 1.1 TeV, largest significance at 1 TeV, 3σ (2σ) local (global)

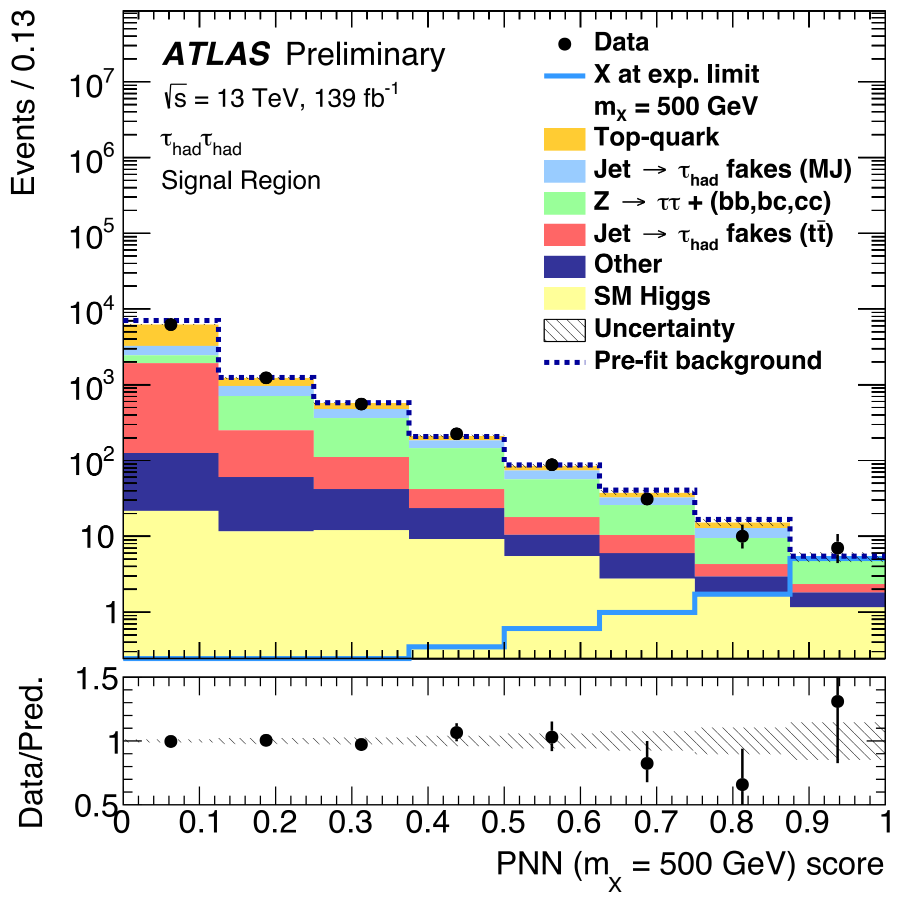

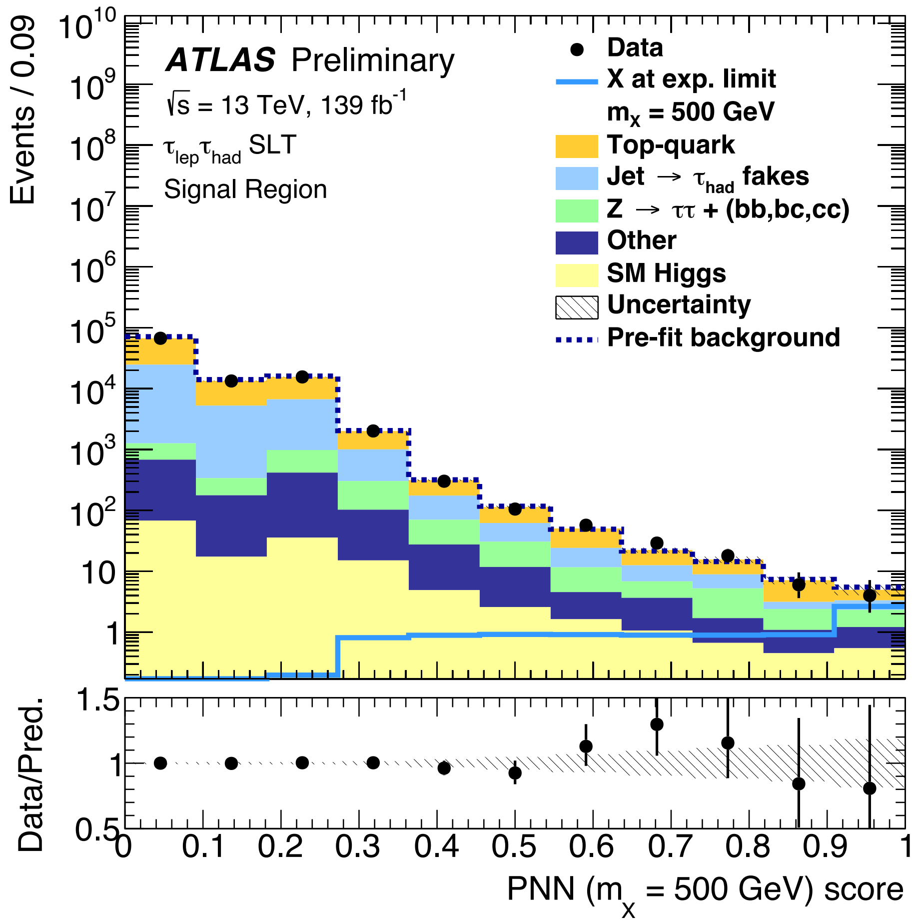

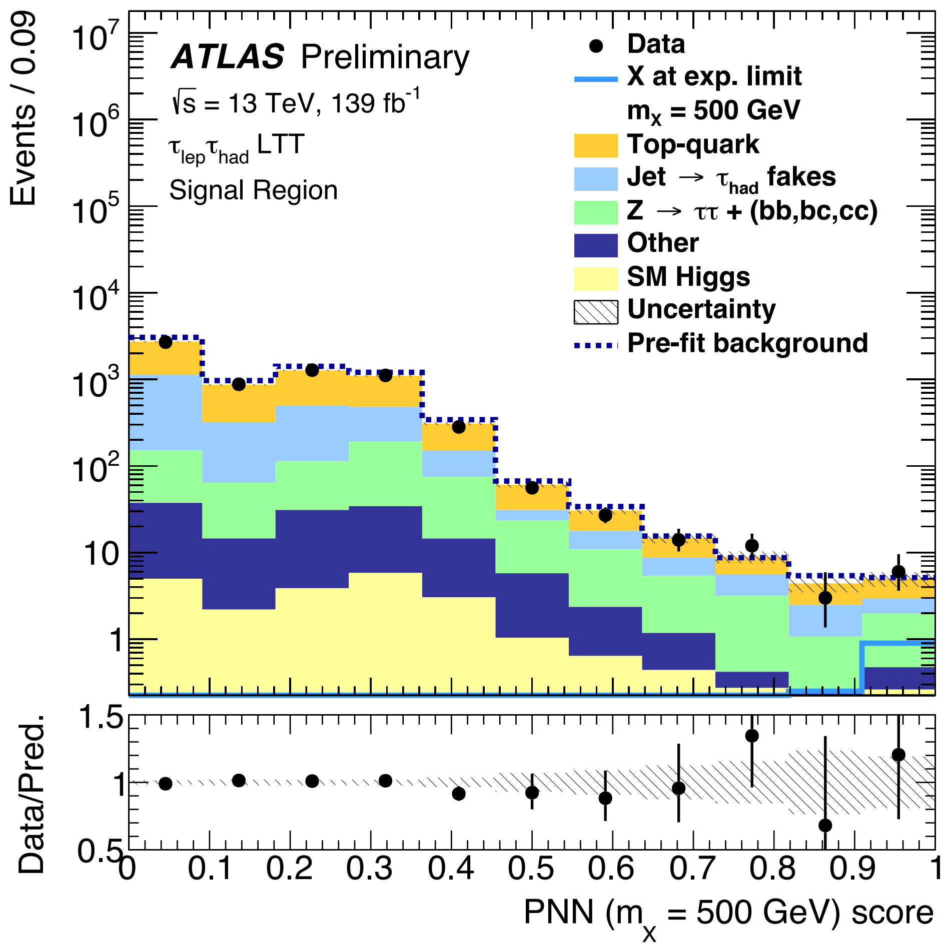

Resonant HH→bbγγ with full Run 2 data

- Search for BSM resonant HH production: resonances with masses between 250 GeV and 1 TeV
- X→HH→bbγγ
- Baseline event selection and background estimation same as in the non-resonant search

arXiv:2112.11876

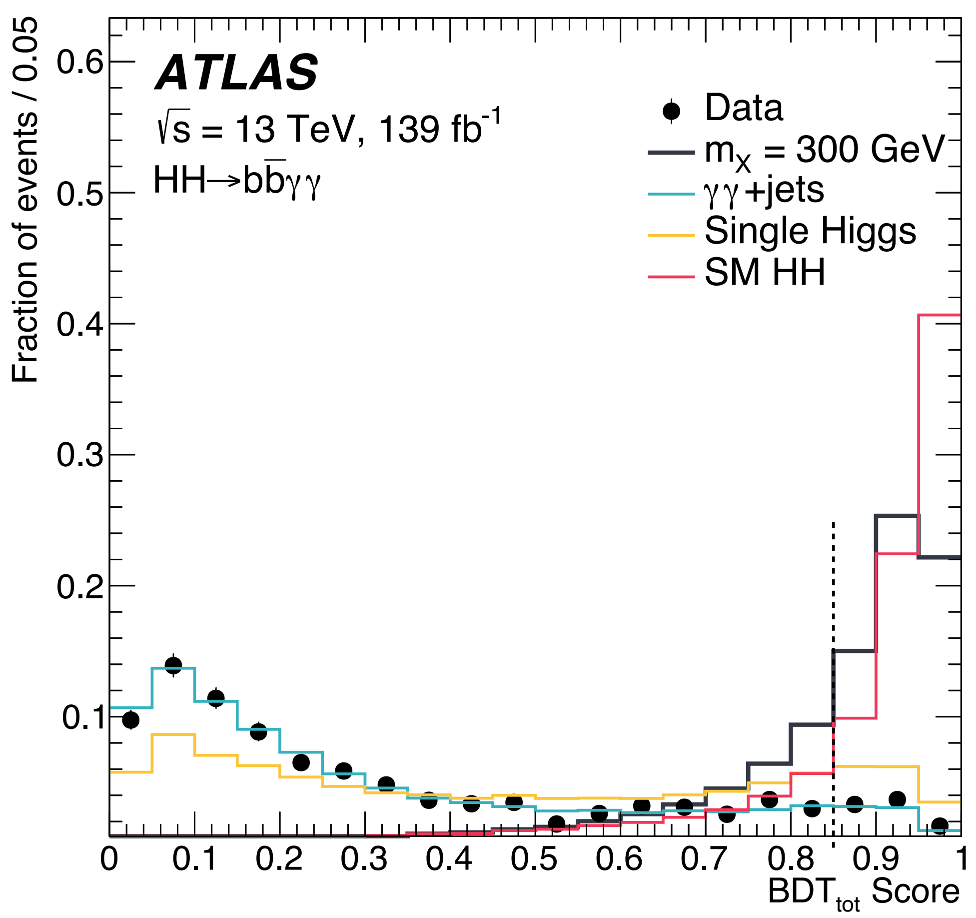

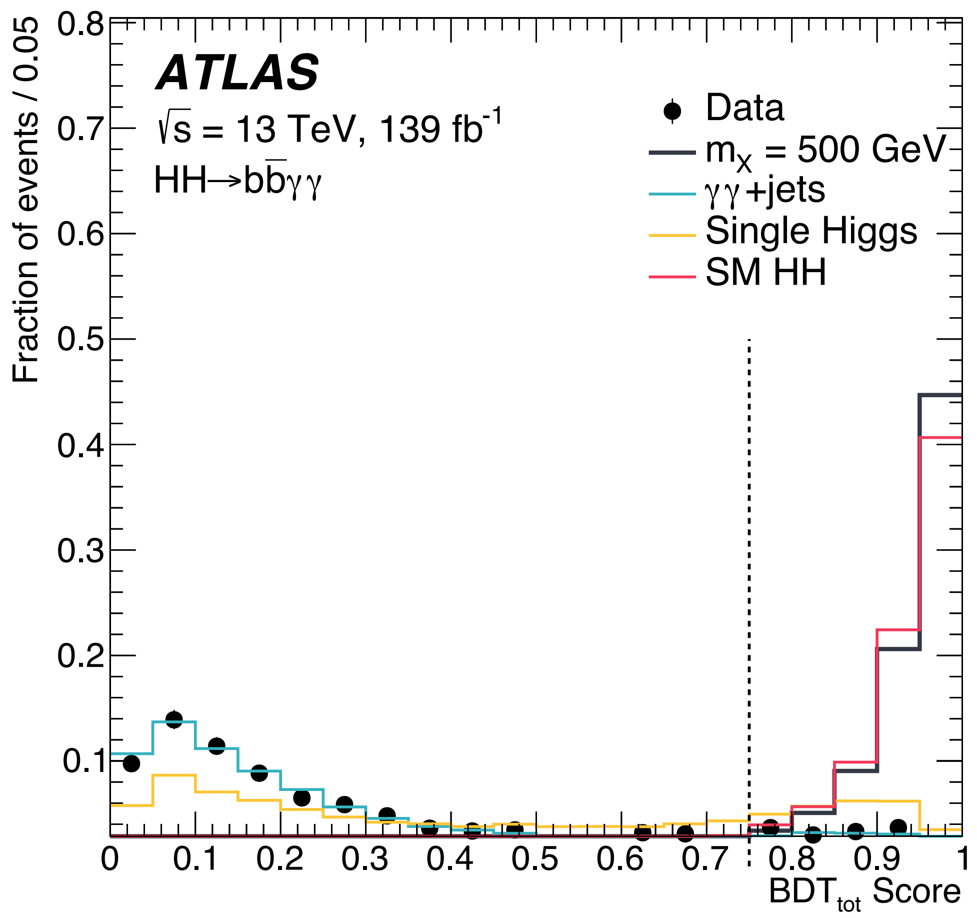

- Boosted Decision Trees used to discriminate signal and background
- Two BDTs trained one against γγ+jets and one against single-Higgs backgrounds and combined in one BDT_{tot} variable
- 1 signal region for each mass hypothesis defined by mass-dependent m_{HH} window selection and mass-dependent BDT cut

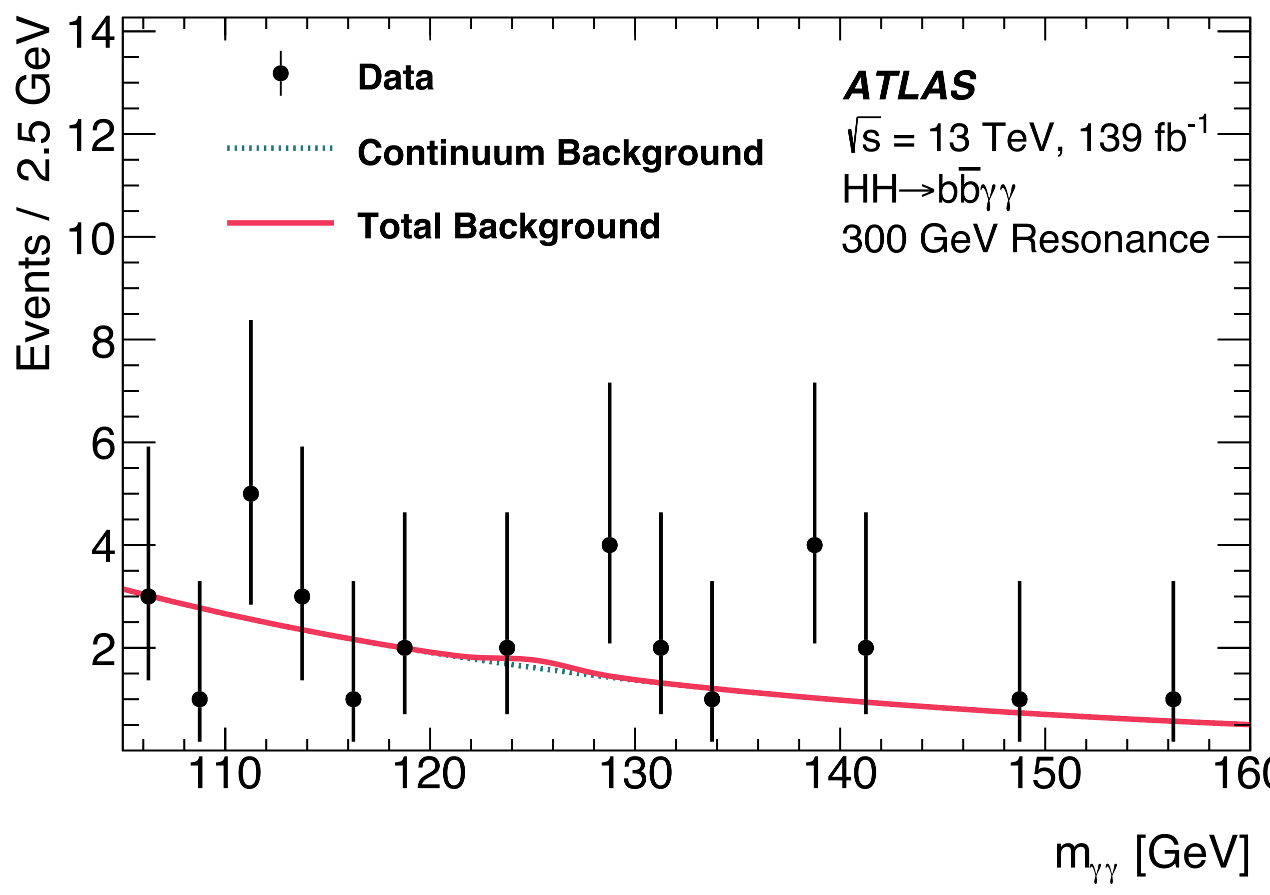

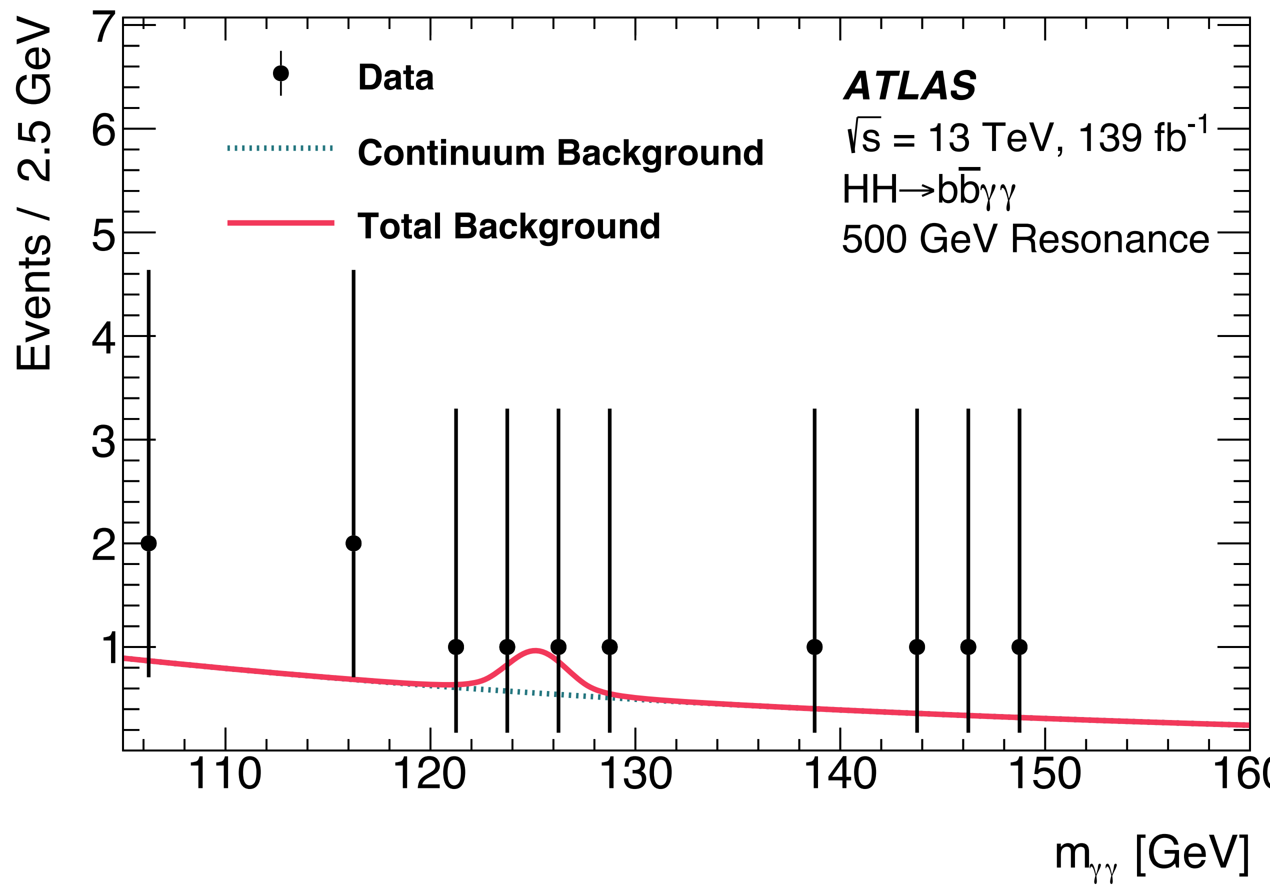

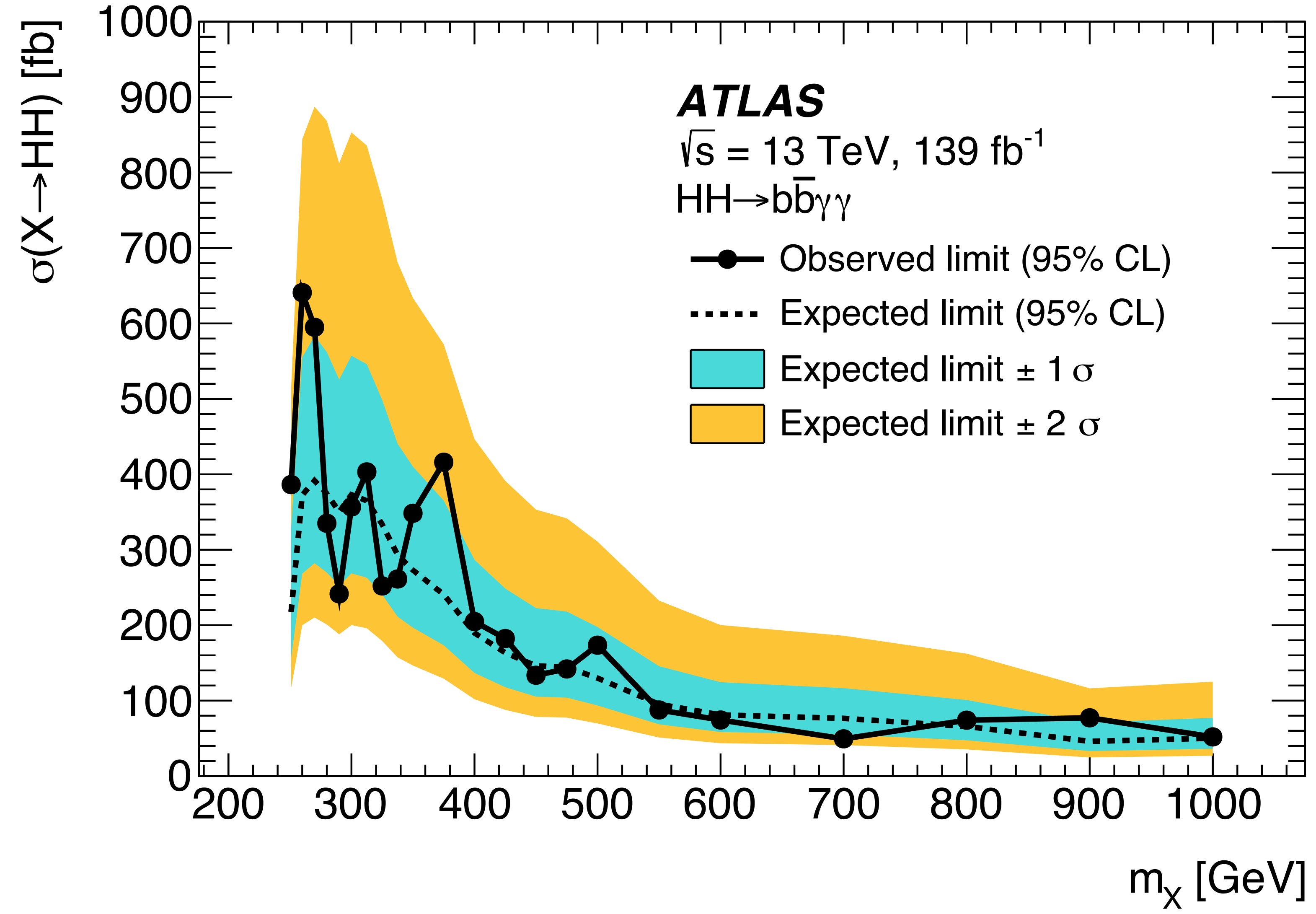

Resonant HH combination with full Run 2 data

Combination of HH analyses performed in 3 decay channels using full Run 2 LHC data corresponding to $139\ \mathrm{fb}^{-1}$:

- bbττ, bbγγ and bbbb channels for the searches for resonant HH production

ATLAS-CONF-2021-052

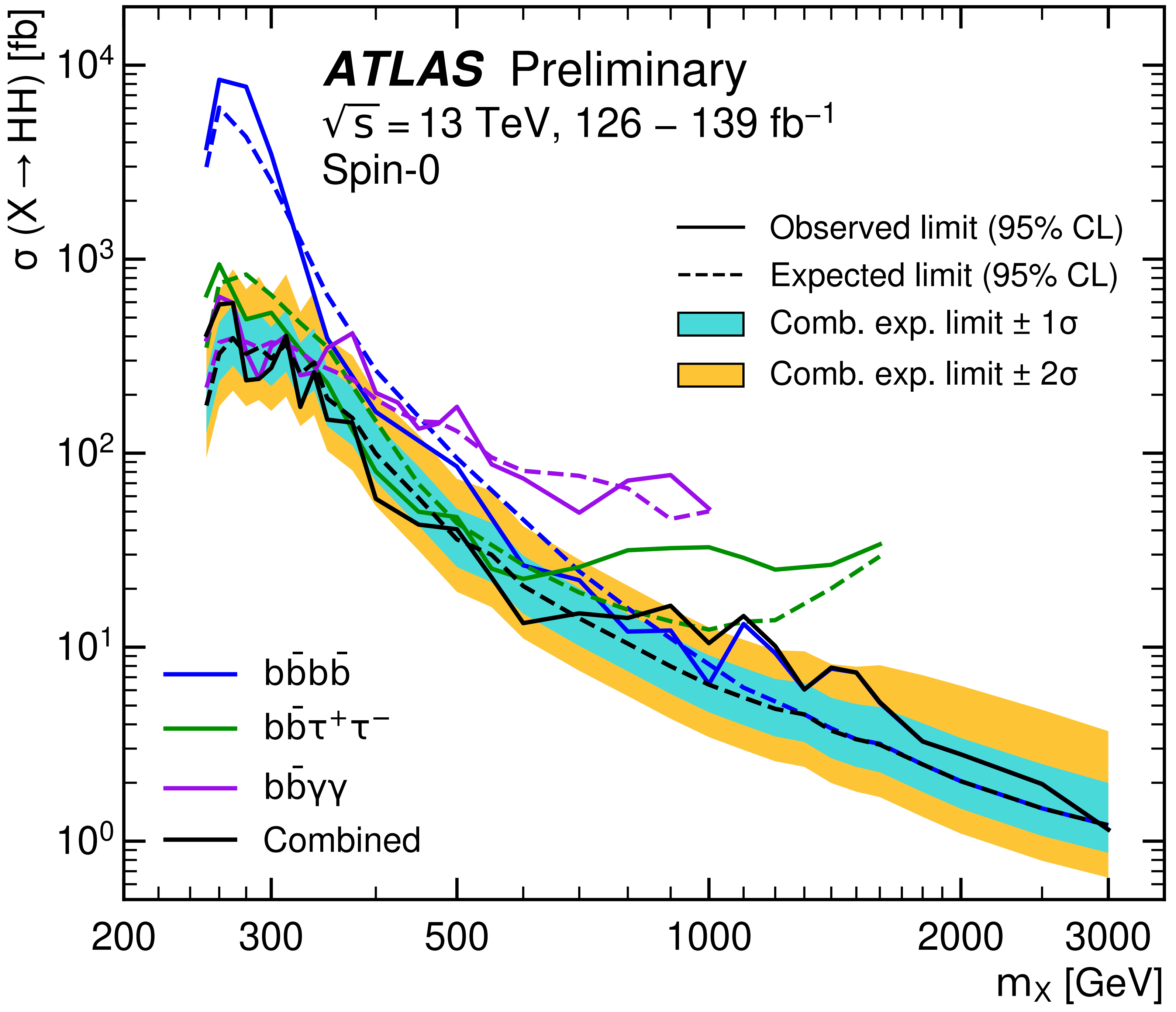

Small data excess at 1.1 TeV,
significance 3.2σ (2.1σ) local (global)

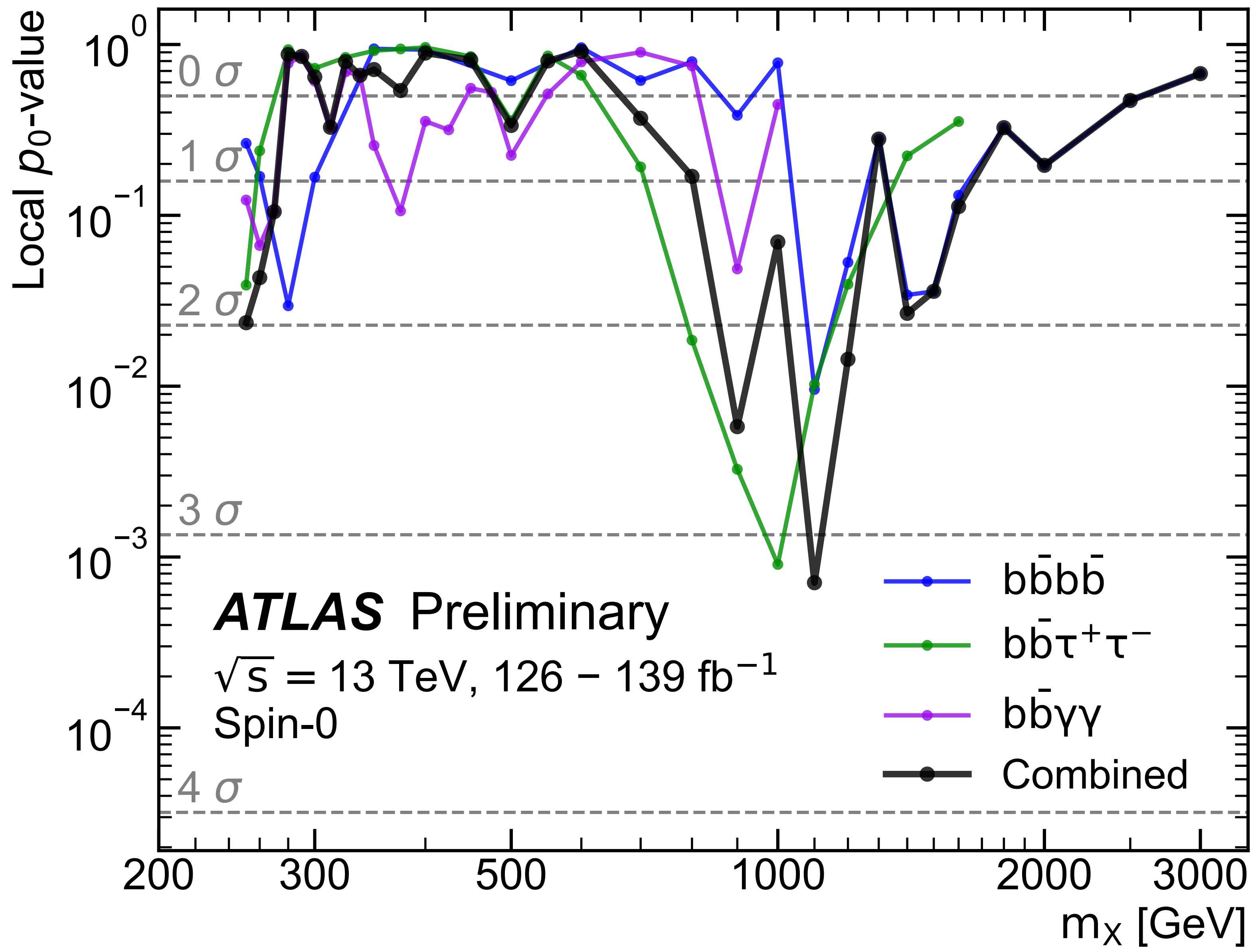

At 1.1 TeV: Local significance = 3.2σ and Global significance = 2.1σ

4b and bbττ measured signal strengths compatible with each other with a p-value of 33%

HH combination with partial Run 2 data

Combination of analyses performed in different decay channels using 2015+2016 data corresponding to $36\ \mathrm{fb}^{-1}$:

- 6 channels for upper limit on HH non-resonant and resonant cross section
- 3 most sensitive channels for extracting constraints on κ_λ

Phys. Lett. B 800 (2020) 135103

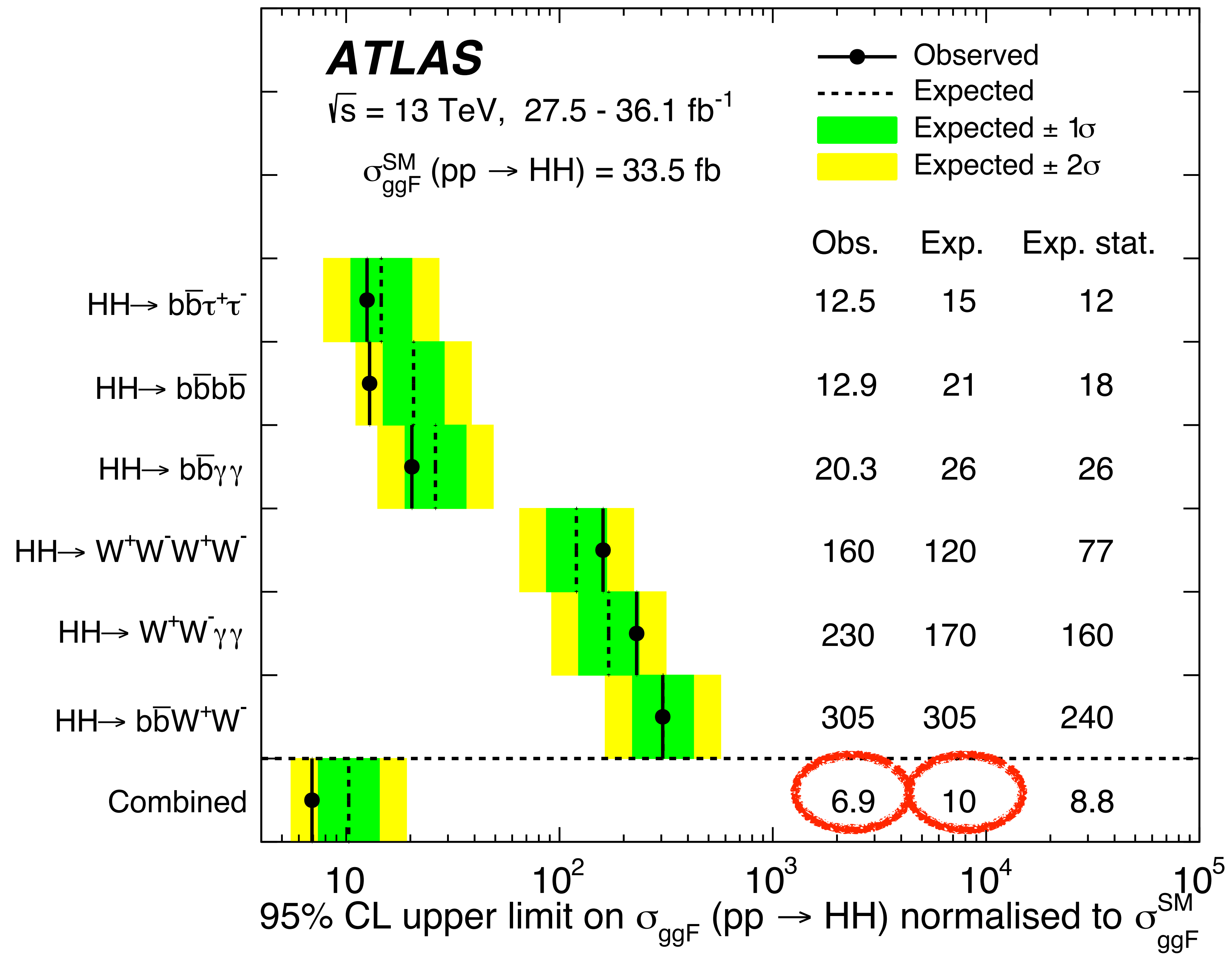

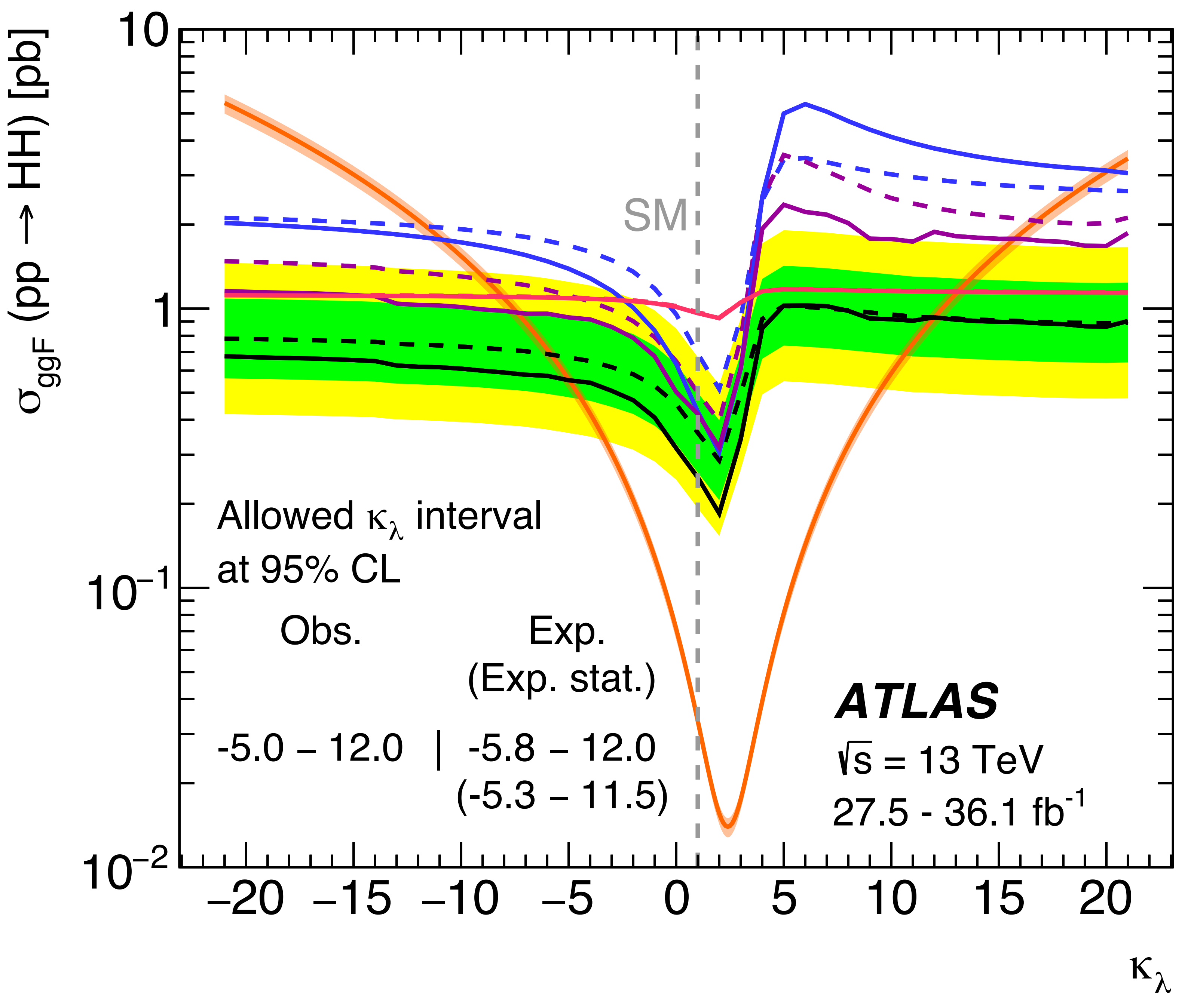

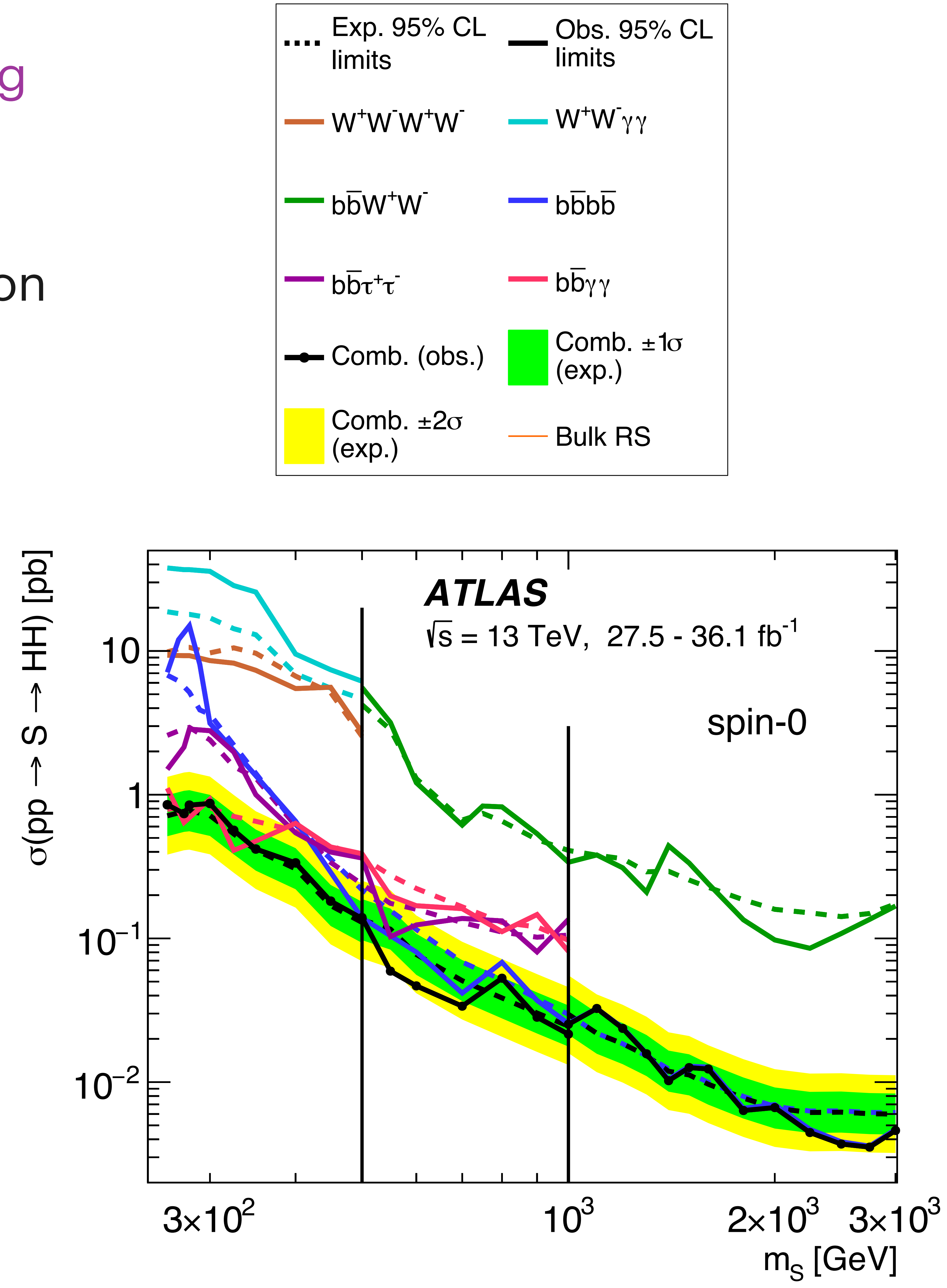

Best upper limit on HH production with early Run 2 dataset

HH HL-LHC prospects

Extrapolations from partial Run 2 analyses

ATL-PHYS-PUB-2018-053

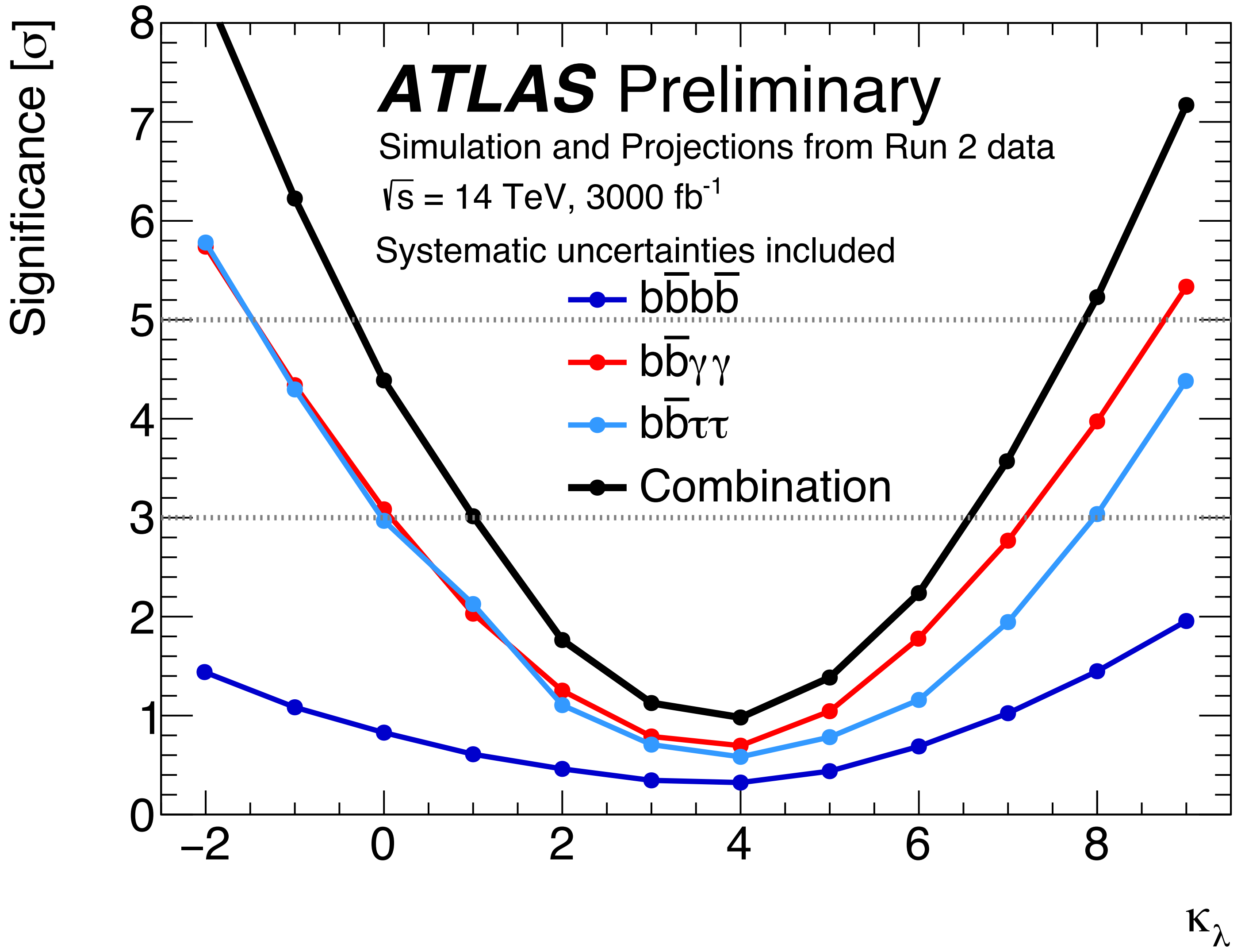

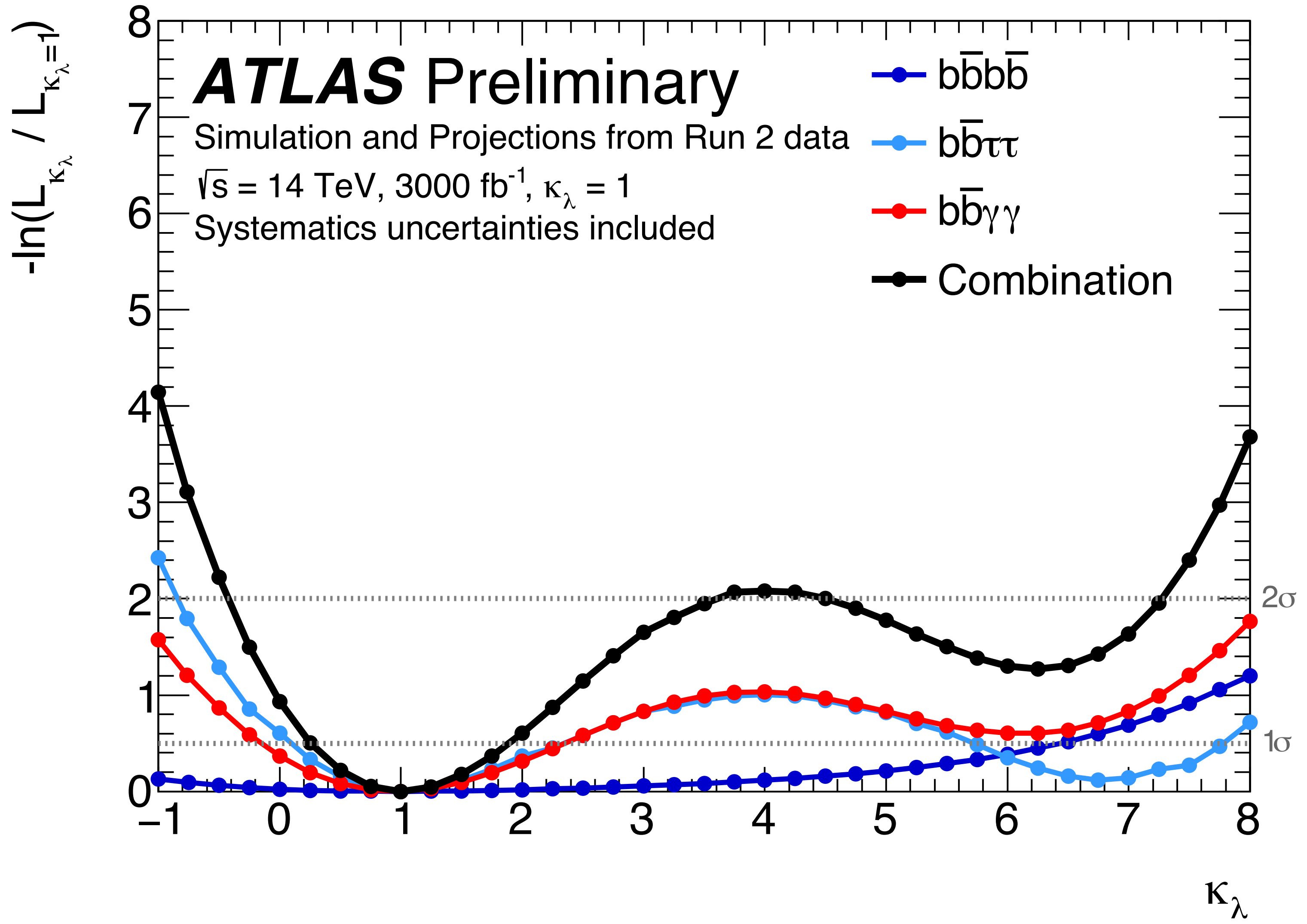

CERN-2019-007

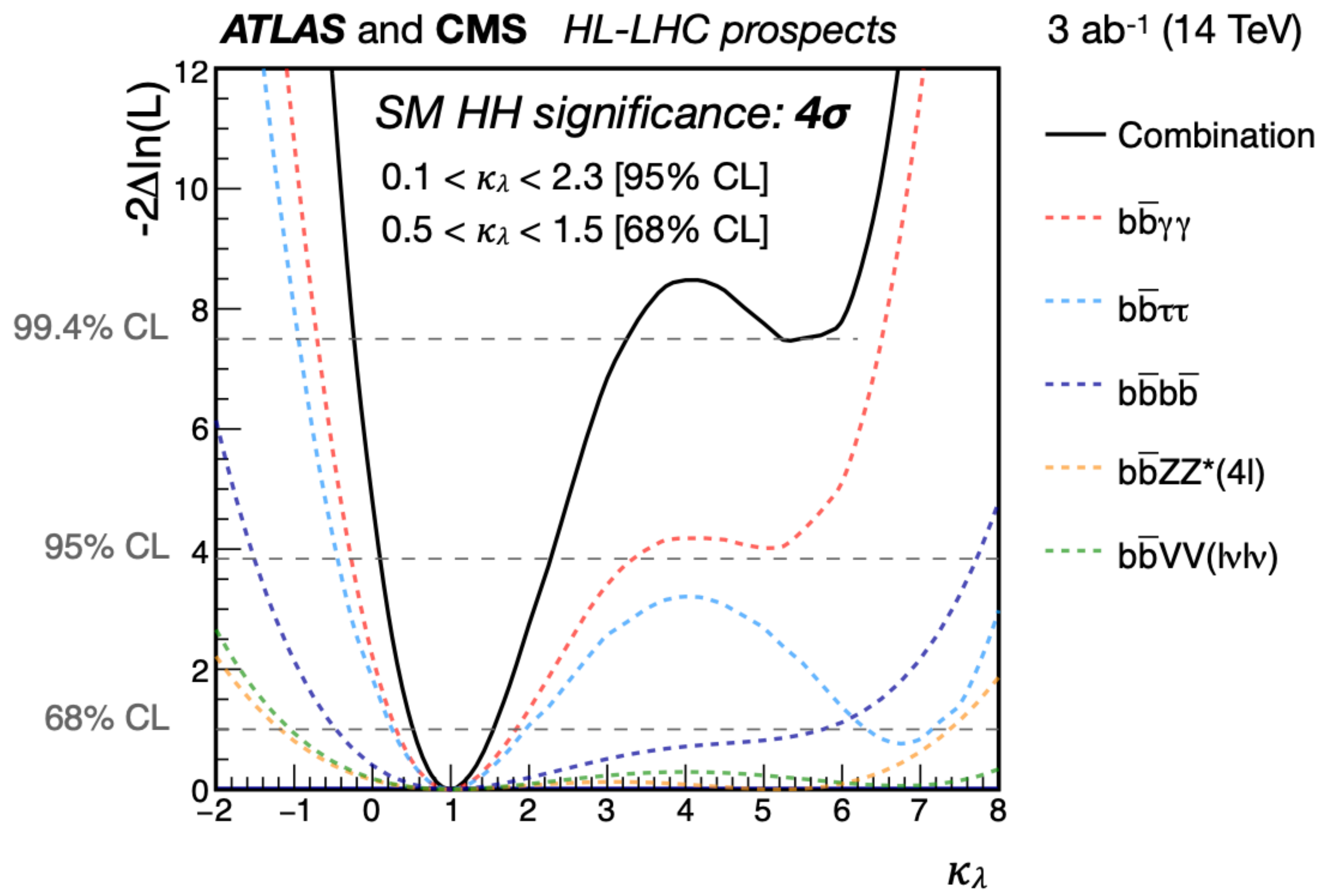

Channel	Statistical-only	Statistical + Systematic
$HH \to b\bar{b}b\bar{b}$	1.4	0.61
$HH \to b\bar{b}\tau^+\tau^-$	2.5	2.1
$HH \to b\bar{b}\gamma\gamma$	2.1	2.0
Combined	3.5	3.0

	Statistical-only		Statistical + Systematic	
	ATLAS	CMS	ATLAS	CMS
$HH \to b\bar{b}b\bar{b}$	1.4	1.2	0.61	0.95
$HH \to b\bar{b}\tau\tau$	2.5	1.6	2.1	1.4
$HH \to b\bar{b}\gamma\gamma$	2.1	1.8	2.0	1.8
$HH \to b\bar{b}VV(ll\nu\nu)$	-	0.59	-	0.56
$HH \to b\bar{b}ZZ(4l)$	-	0.37	-	0.37
combined	3.5	2.8	3.0	2.6
	Combined 4.5		Combined 4.0	

Scenario	1σ CI	2σ CI
Statistical uncertainties only	$0.4 \le \kappa_\lambda \le 1.7$	$-0.10 \le \kappa_\lambda \le 2.7 \cup 5.5 \le \kappa_\lambda \le 6.9$
Systematic uncertainties	$0.25 \le \kappa_\lambda \le 1.9$	$-0.4 \le \kappa_\lambda \le 7.3$

HH+H combination with partial Run 2 data

Single-Higgs production is also sensitive to κ_λ through NLO electroweak corrections:

- Higgs self-energy loop corrections
- Additional diagrams

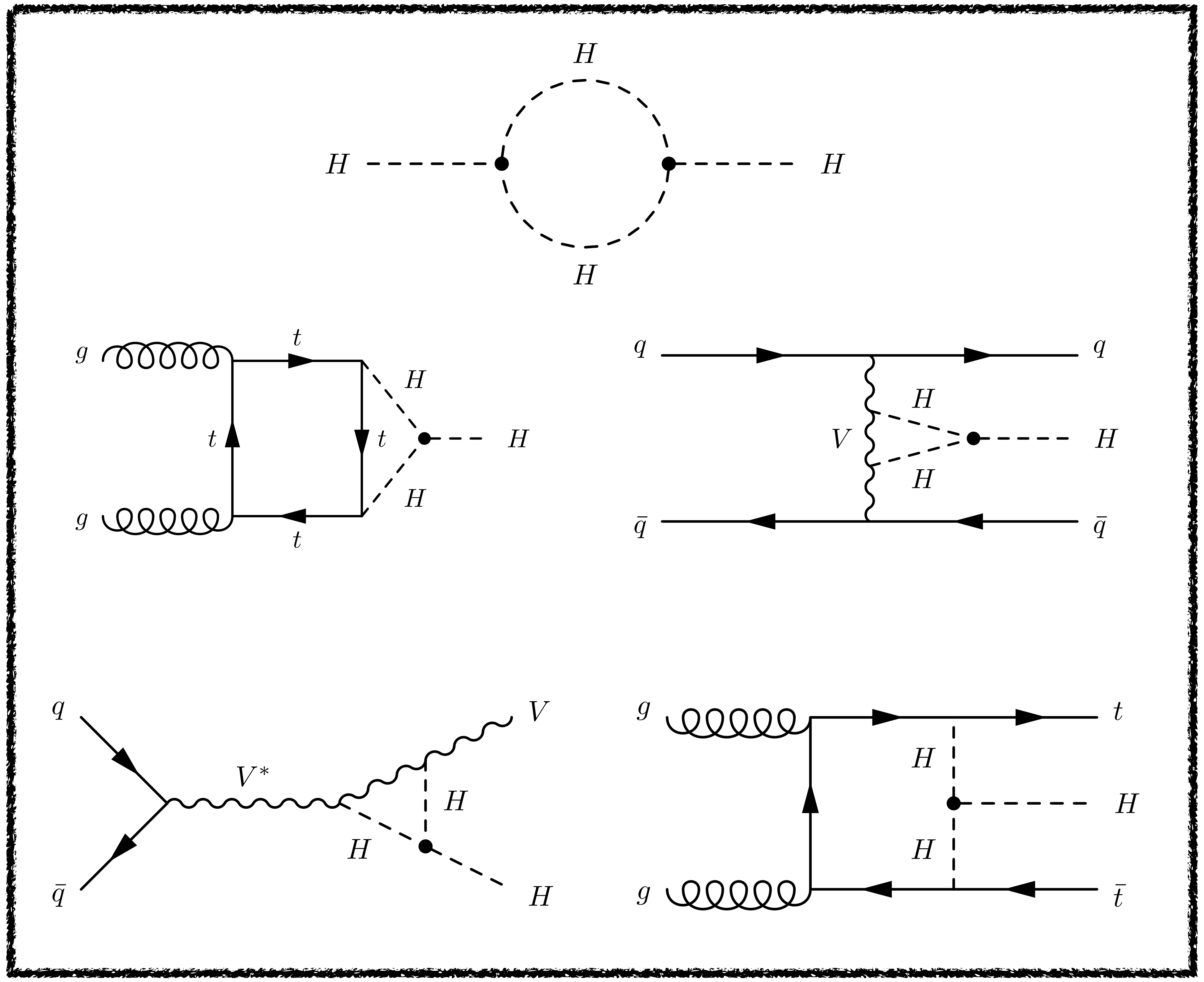

NLO electroweak corrections affect:

- Higgs production cross sections
- Higgs decay branching ratios
- Kinematics

ATL-PHYS-PUB-2019-009

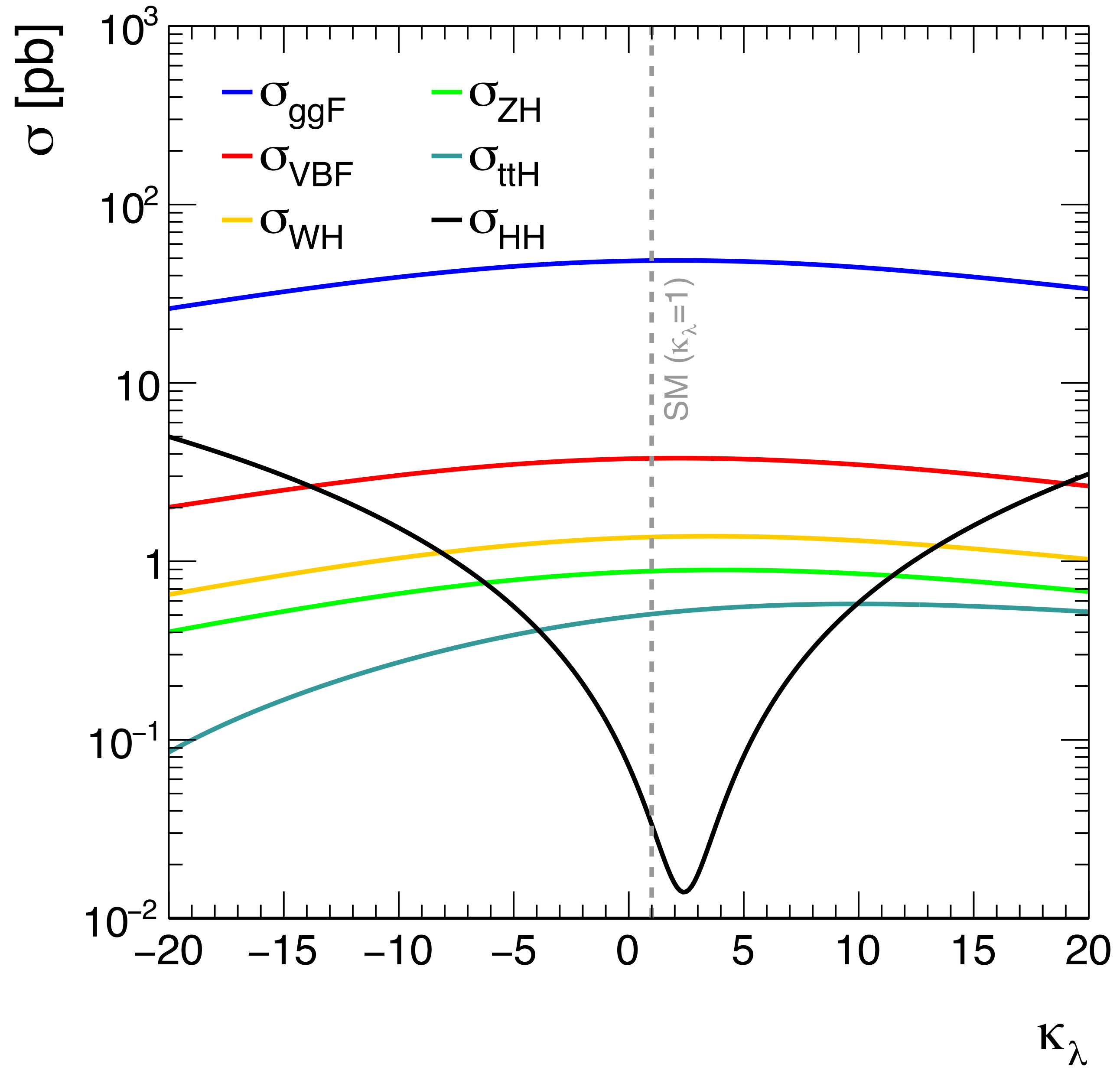

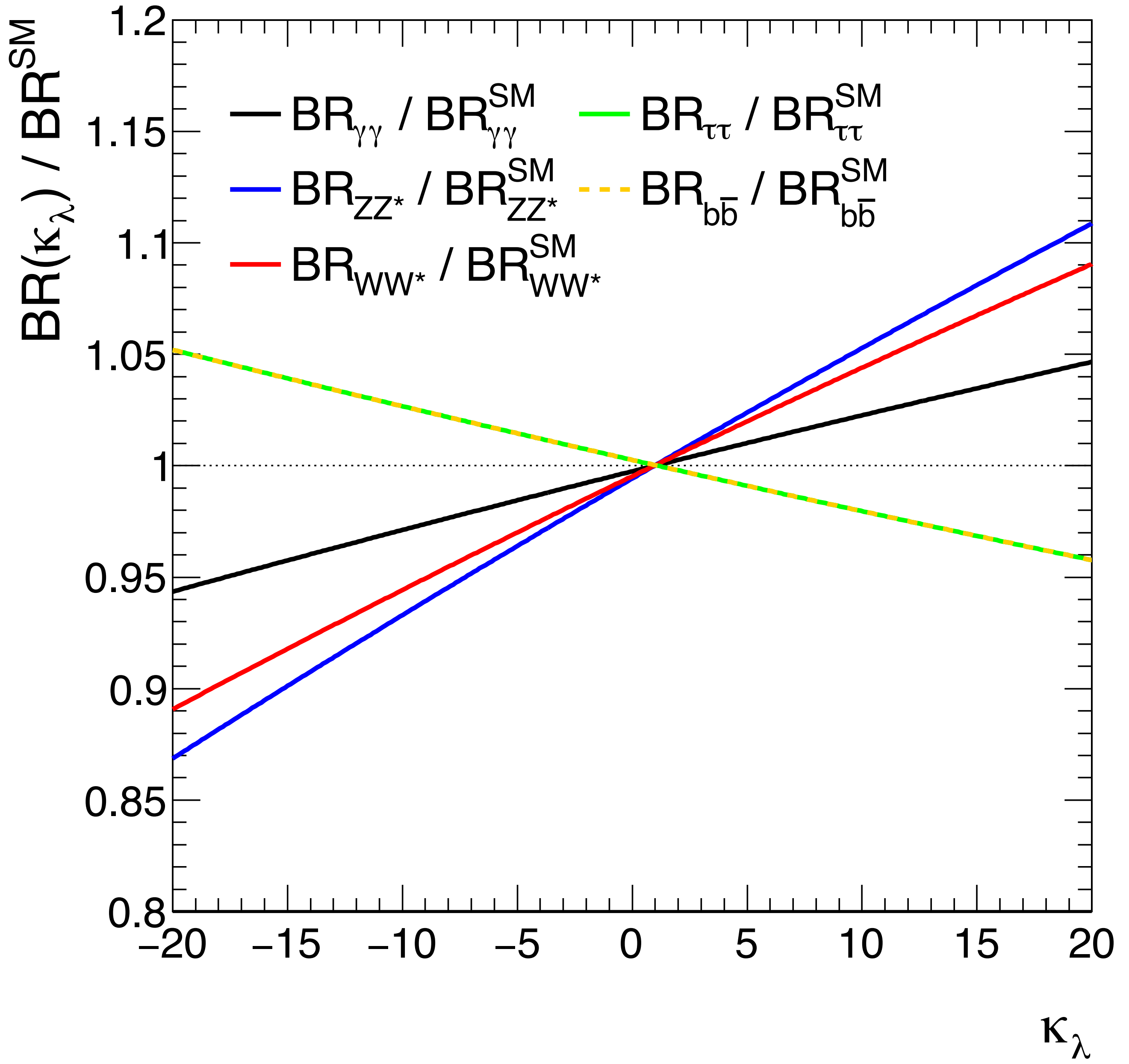

HH+H combination with partial Run 2 data

Combination of 3 most sensitive di-Higgs analyses
with single-Higgs analyses for improving constraints on κ_λ

- di-Higgs analyses with $36\ \mathrm{fb}^{-1}$ of data
- single-Higgs analyses with up to $80\ \mathrm{fb}^{-1}$ of data

ATLAS-CONF-2019-049

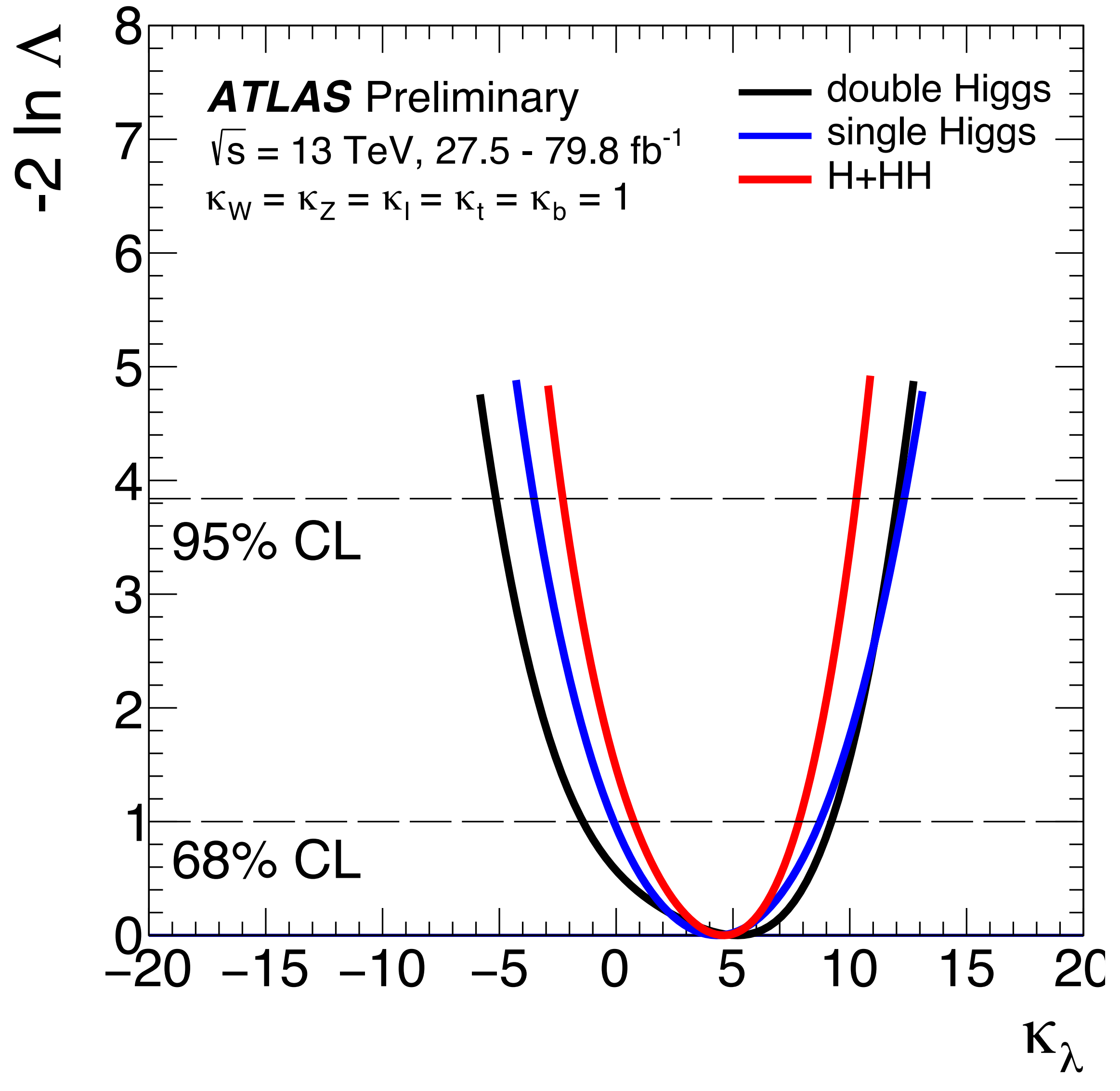

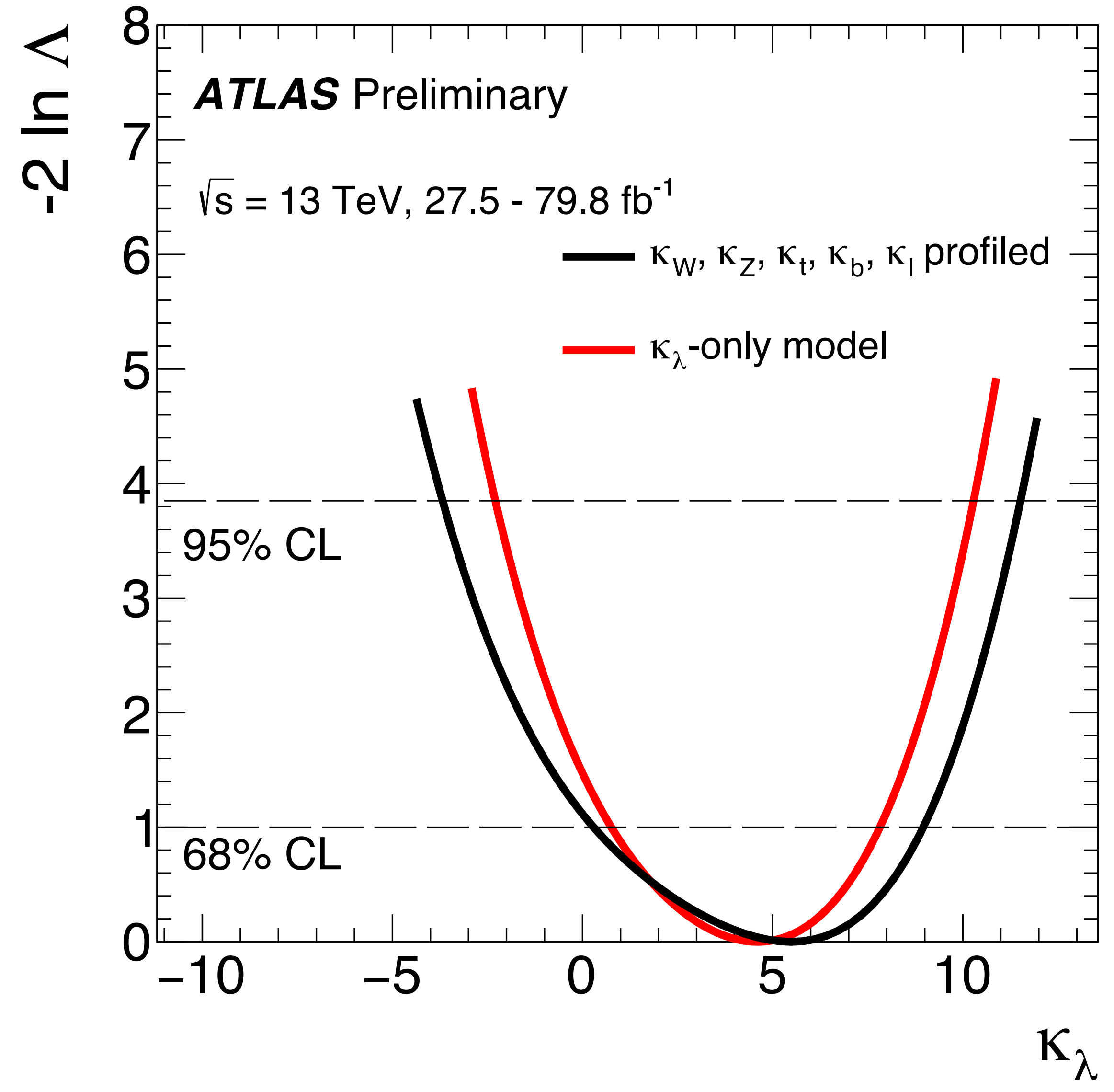

Analysis	Integrated luminosity (fb^{-1})
$H\to\gamma\gamma$ (excluding $t\bar{t}H, H\to\gamma\gamma$)	79.8
$H\to ZZ^*\to 4\ell$ (including $t\bar{t}H, H\to ZZ^*\to 4\ell$)	79.8
$H\to WW^*\to e\nu\mu\nu$	36.1
$H\to\tau^+\tau^-$	36.1
$VH, H\to b\bar{b}$	79.8
$t\bar{t}H, H\to b\bar{b}$	36.1
$t\bar{t}H, H\to$ multilepton	36.1
$HH\to b\bar{b}b\bar{b}$	27.5
$HH\to b\bar{b}\tau^+\tau^-$	36.1
$HH\to b\bar{b}\gamma\gamma$	36.1

Model	$\kappa_W{}^{+1\sigma}_{-1\sigma}$	$\kappa_Z{}^{+1\sigma}_{-1\sigma}$	$\kappa_t{}^{+1\sigma}_{-1\sigma}$	$\kappa_b{}^{+1\sigma}_{-1\sigma}$	$\kappa_\ell{}^{+1\sigma}_{-1\sigma}$	$\kappa_\lambda{}^{+1\sigma}_{-1\sigma}$	κ_λ [95% CL]	
κ_λ-only	1	1	1	1	1	$4.6^{+3.2}_{-3.8}$	[−2.3, 10.3]	obs.
						$1.0^{+7.3}_{-3.8}$	[−5.1, 11.2]	exp.
Generic	$1.03^{+0.08}_{-0.08}$	$1.10^{+0.09}_{-0.09}$	$1.00^{+0.12}_{-0.11}$	$1.03^{+0.20}_{-0.18}$	$1.06^{+0.16}_{-0.16}$	$5.5^{+3.5}_{-5.2}$	[−3.7, 11.5]	obs.
	$1.00^{+0.08}_{-0.08}$	$1.00^{+0.08}_{-0.08}$	$1.00^{+0.12}_{-0.12}$	$1.00^{+0.21}_{-0.19}$	$1.00^{+0.16}_{-0.15}$	$1.0^{+7.6}_{-4.5}$	[−6.2, 11.6]	exp.

Best constraints on κ_λ with partial Run 2 dataset

- Improvement in constraining κ_λ compared to HH-only combination: 12% on negative side and 3% on positive side (expected)
- Setting constraints on κ_λ in a more generic model with less assumptions on the other Higgs couplings

HH+H combination with partial Run 2 data

Exploiting variations of production cross sections and Higgs decay branching ratios, kinematic variations information also used in:

- HH, using BDT bins in bbττ and m_{HH} bins in bbbb, overall acceptance variations in bbγγ
- single-Higgs VH and VBF production modes, using STXS bins

Higgs production cross sections and decay BRs modified by parameters representing their ratio to the SM values as a function of κ_λ

For a given production process i the cross section modifier as a function of κ_λ can be written as:

$$\mu_i(\kappa_\lambda, \kappa_i) = \frac{\sigma^{\rm BSM}}{\sigma^{\rm SM}} = Z_H^{\rm BSM}(\kappa_\lambda)\left[\kappa_i^2 + \frac{(\kappa_\lambda - 1)C_1^i}{K_{\rm EW}^i}\right],$$

where $Z_H^{\rm BSM}(\kappa_\lambda)$ is defined as:

$$Z_H^{\rm BSM}(\kappa_\lambda) = \frac{1}{1-(\kappa_\lambda^2 - 1)\delta Z_H} \quad \text{with} \quad \delta Z_H = -1.536\times 10^{-3},$$

For a given decay channel f the BR modifier as a function of κ_λ can be written as:

$$\mu_f(\kappa_\lambda, \kappa_f) = \frac{\rm BR_f^{BSM}}{\rm BR_f^{SM}} = \frac{\kappa_f^2 + (\kappa_\lambda - 1)C_1^f}{\sum_j {\rm BR}_j^{\rm SM}\left[\kappa_j^2 + (\kappa_\lambda - 1)C_1^j\right]}.$$

- $\kappa_{EW}^i = \frac{\sigma_{NLO}^{SM,i}}{\sigma_{LO}^{SM,i}}$ accounts for the NLO EW corrections to the cross section for $\kappa_\lambda = 1$
- C_1^i is a process- and kinematic-dependent coefficient
- $\kappa_i = \frac{\sigma_{LO,i}^{BSM}}{\sigma_{LO}^{SM,i}}$ represent the modifiers to other Higgs boson couplings that can also be considered

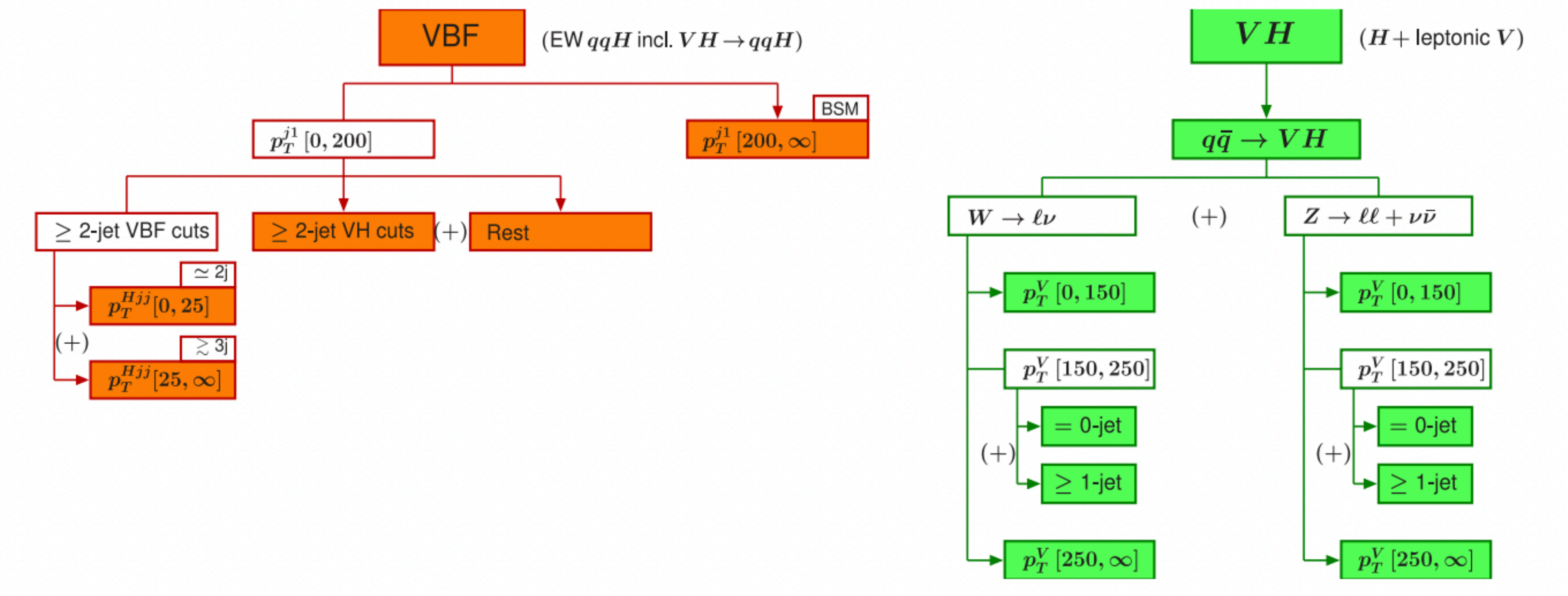

- ggF differential variation not included as theory predictions not available
- ttH differential information not included as experimental measurement in STXS bins not available

HH+H combination with partial Run 2 data

ATLAS-CONF-2019-049

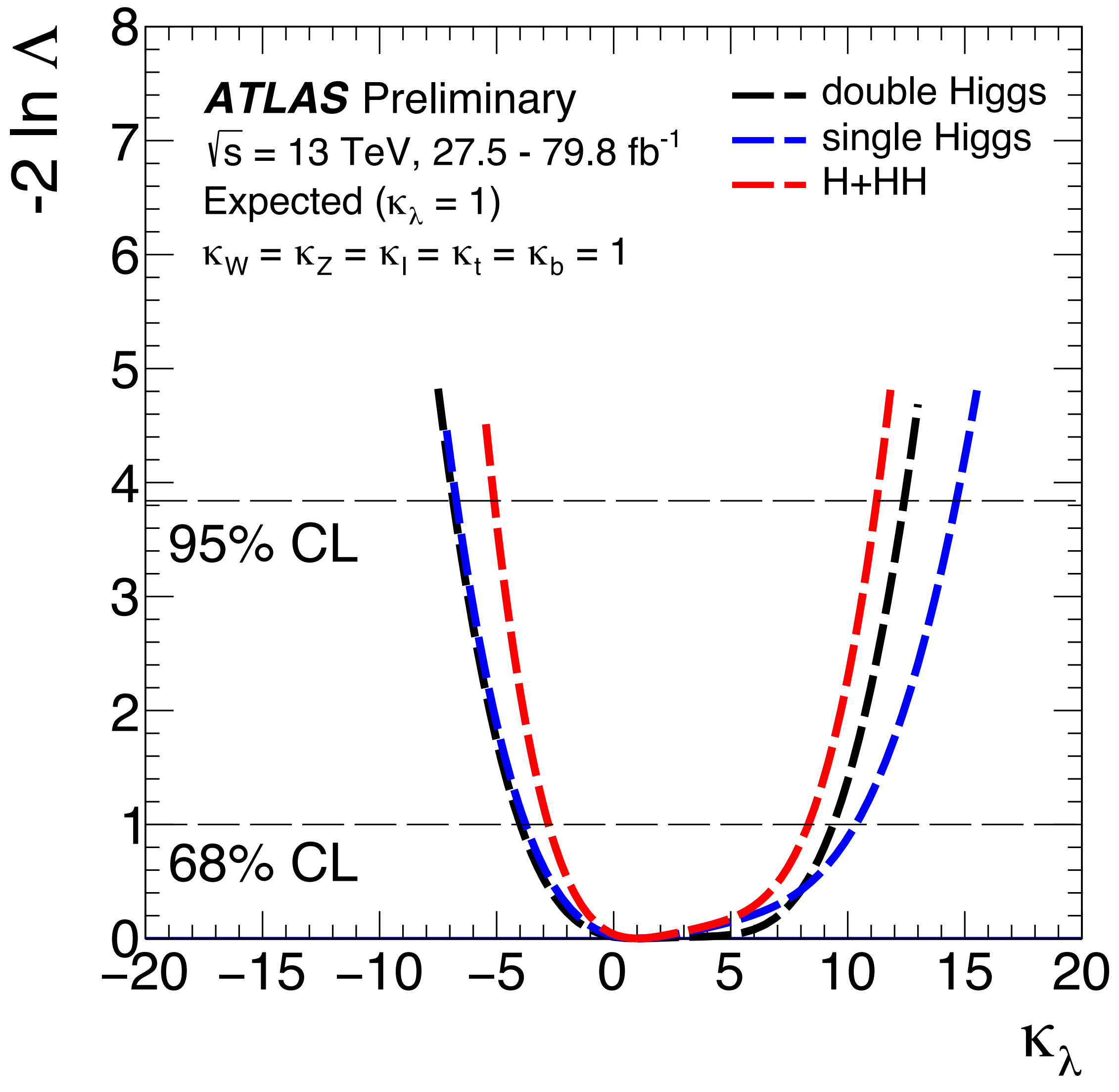

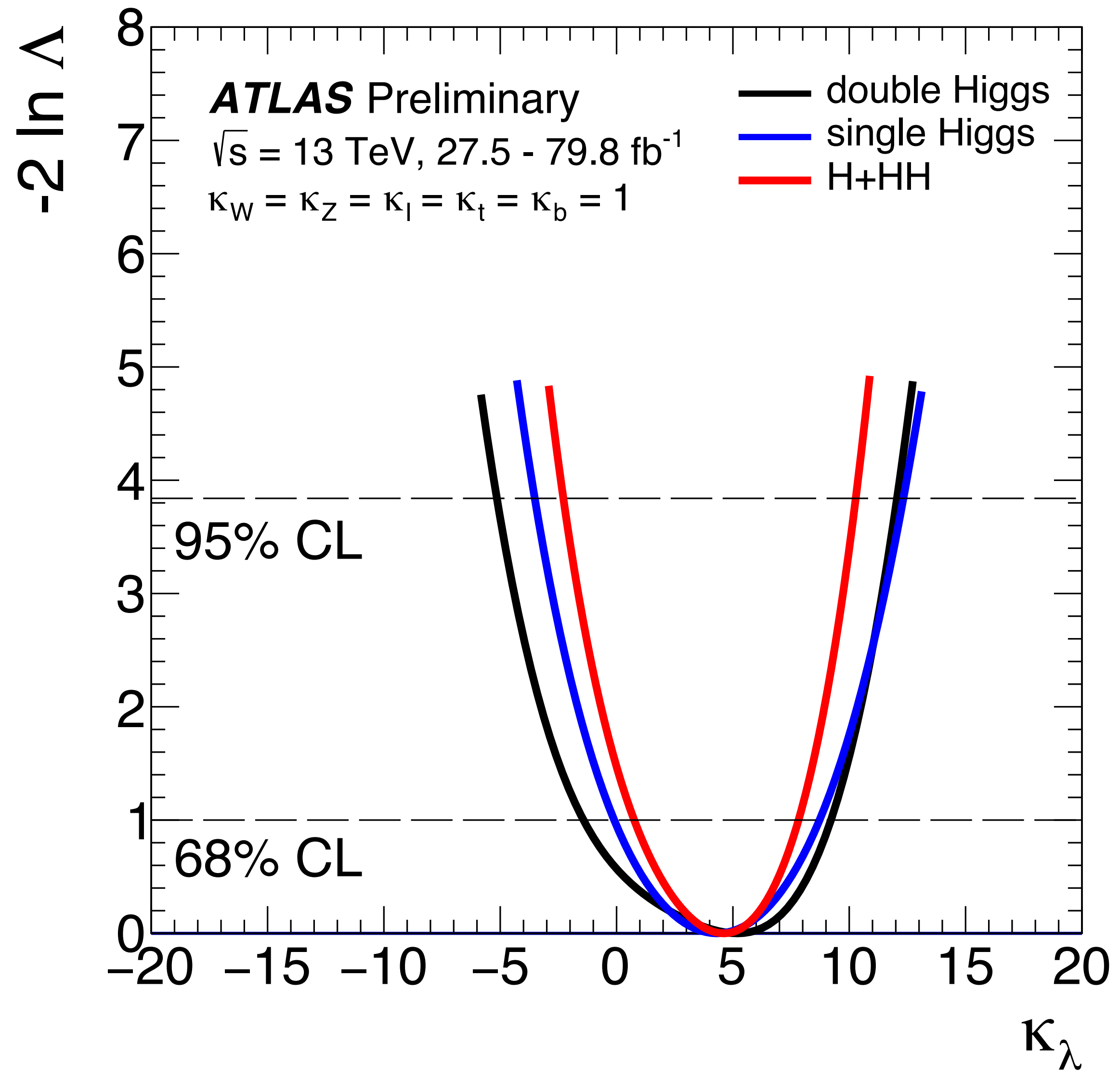

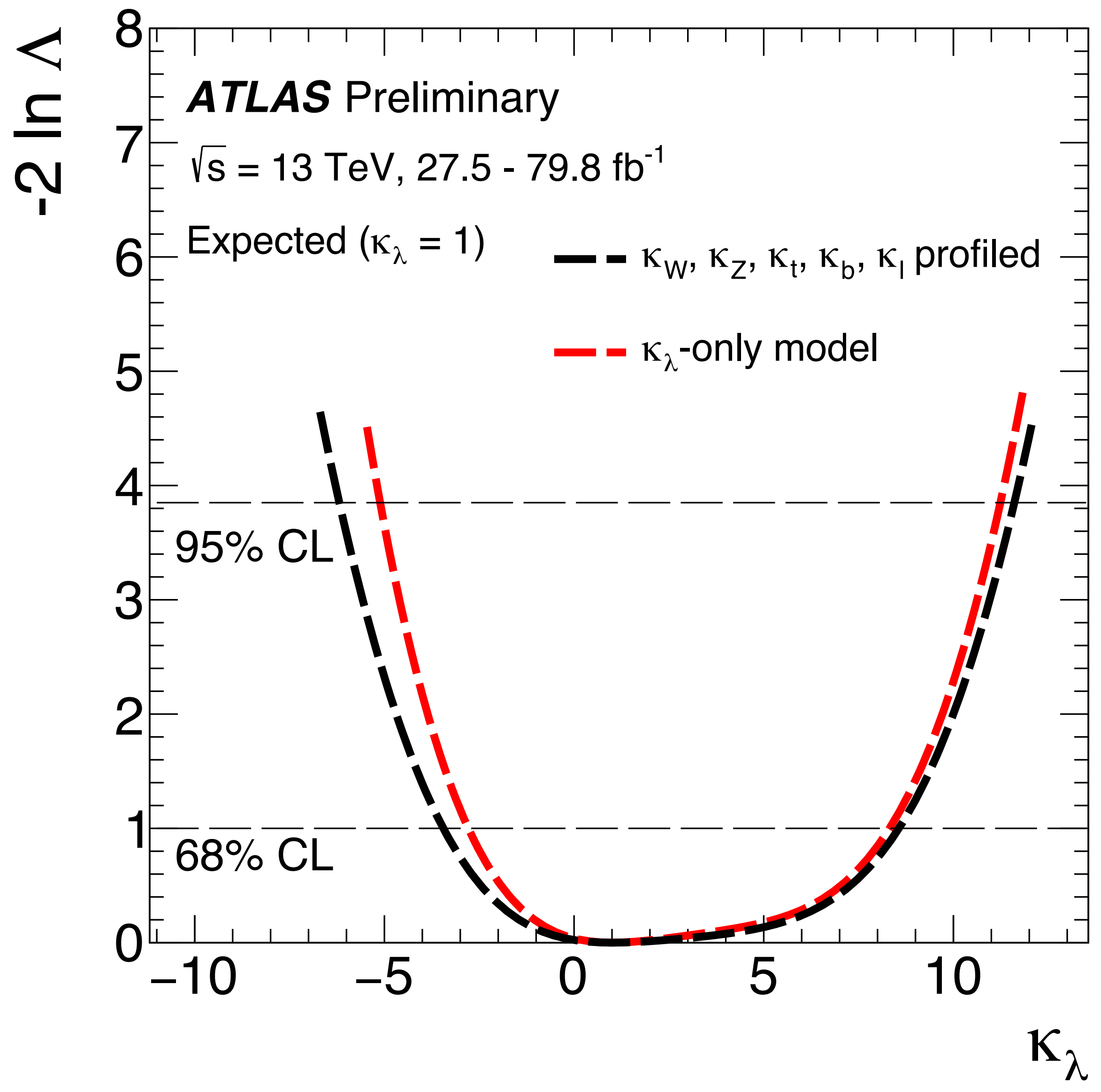

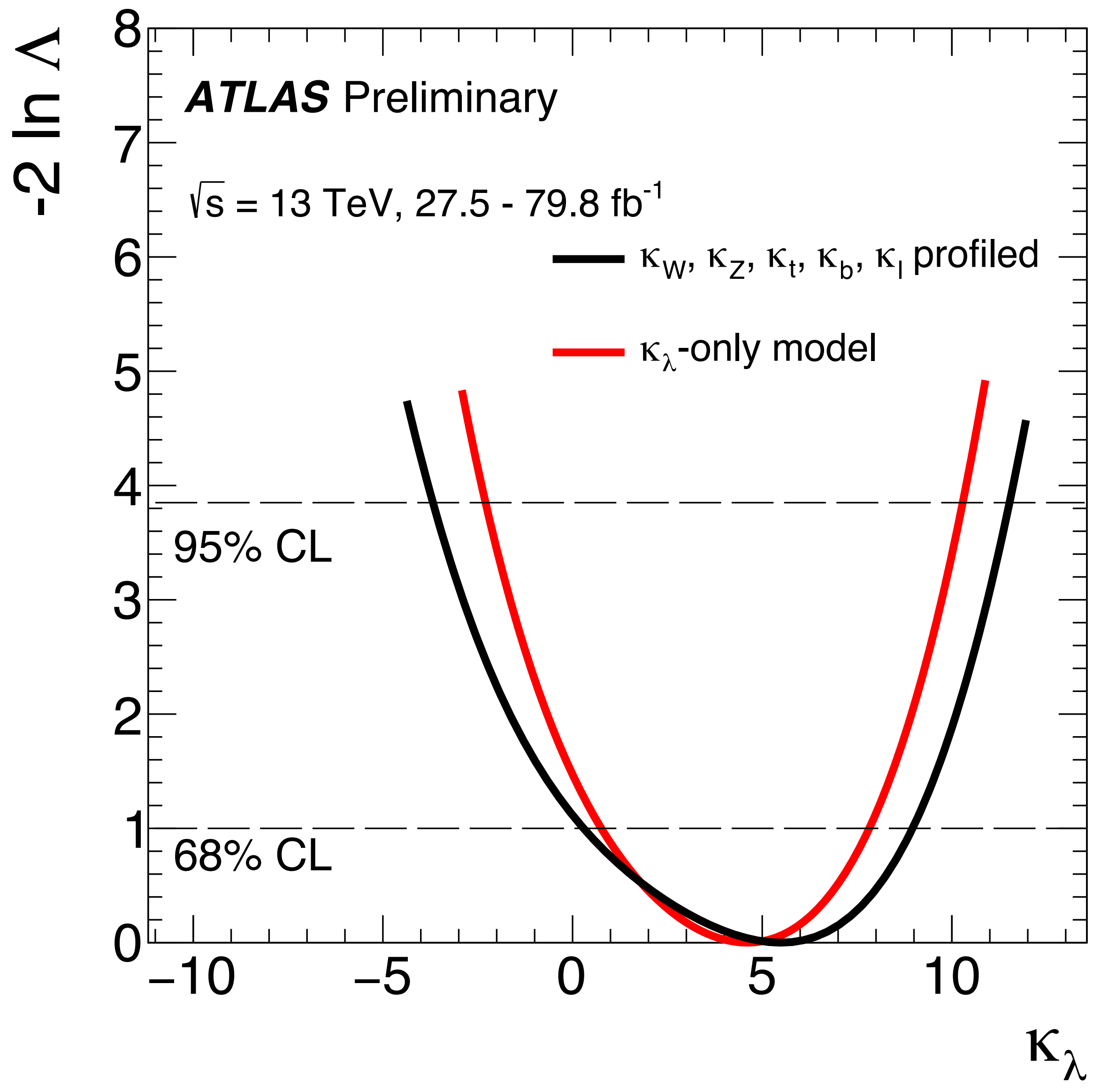

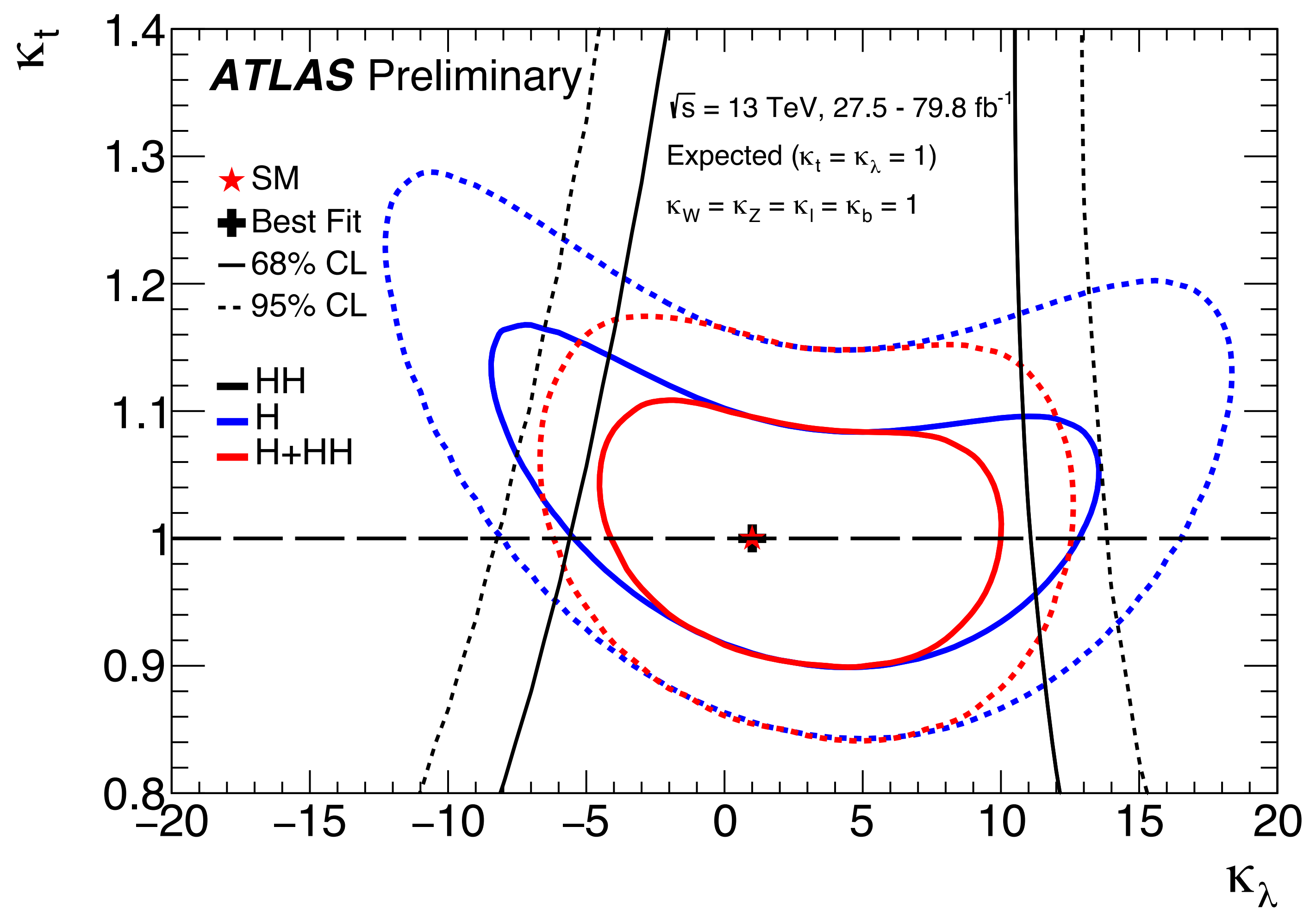

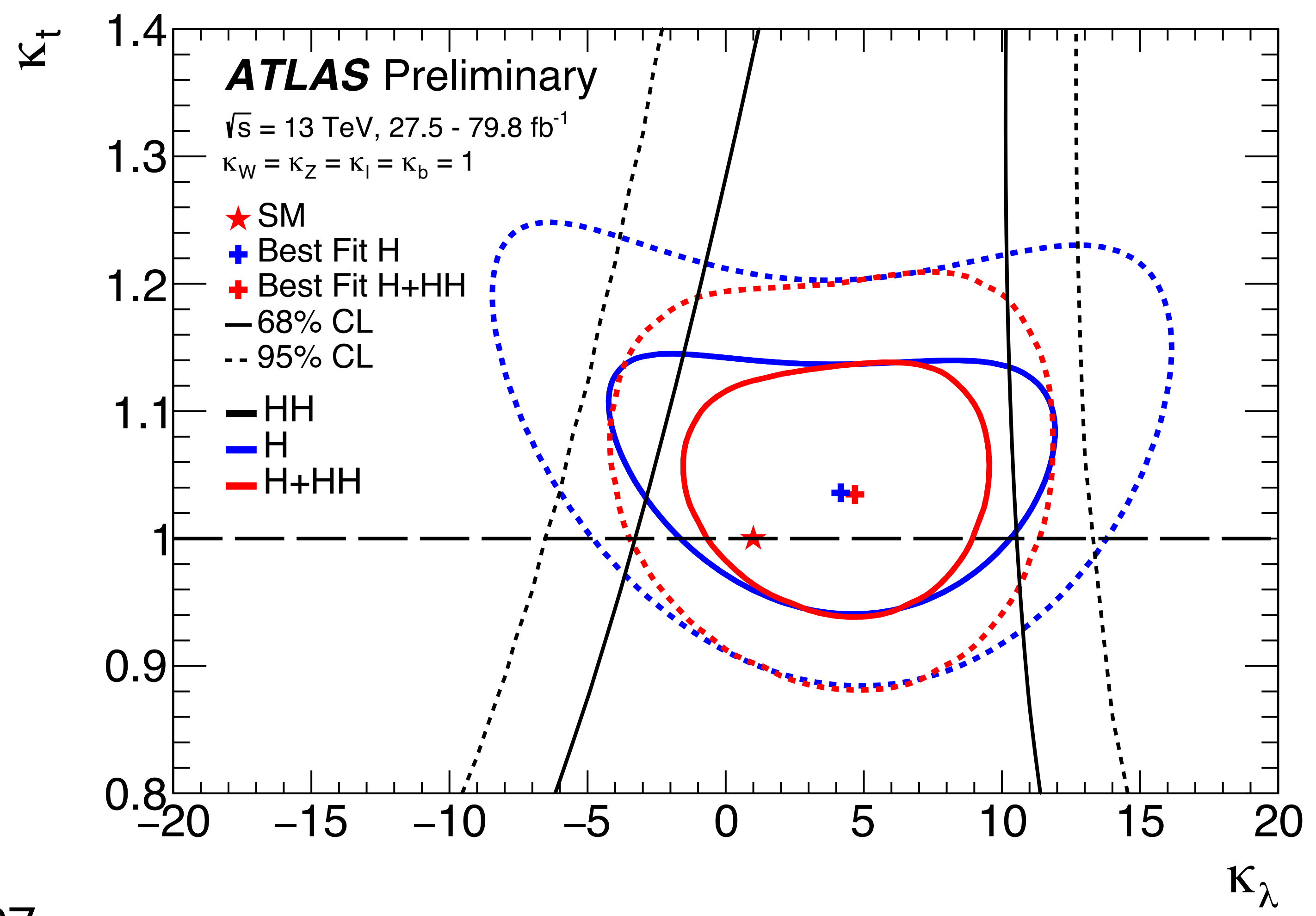

HH+H combination with partial Run 2 data

ATLAS-CONF-2019-049

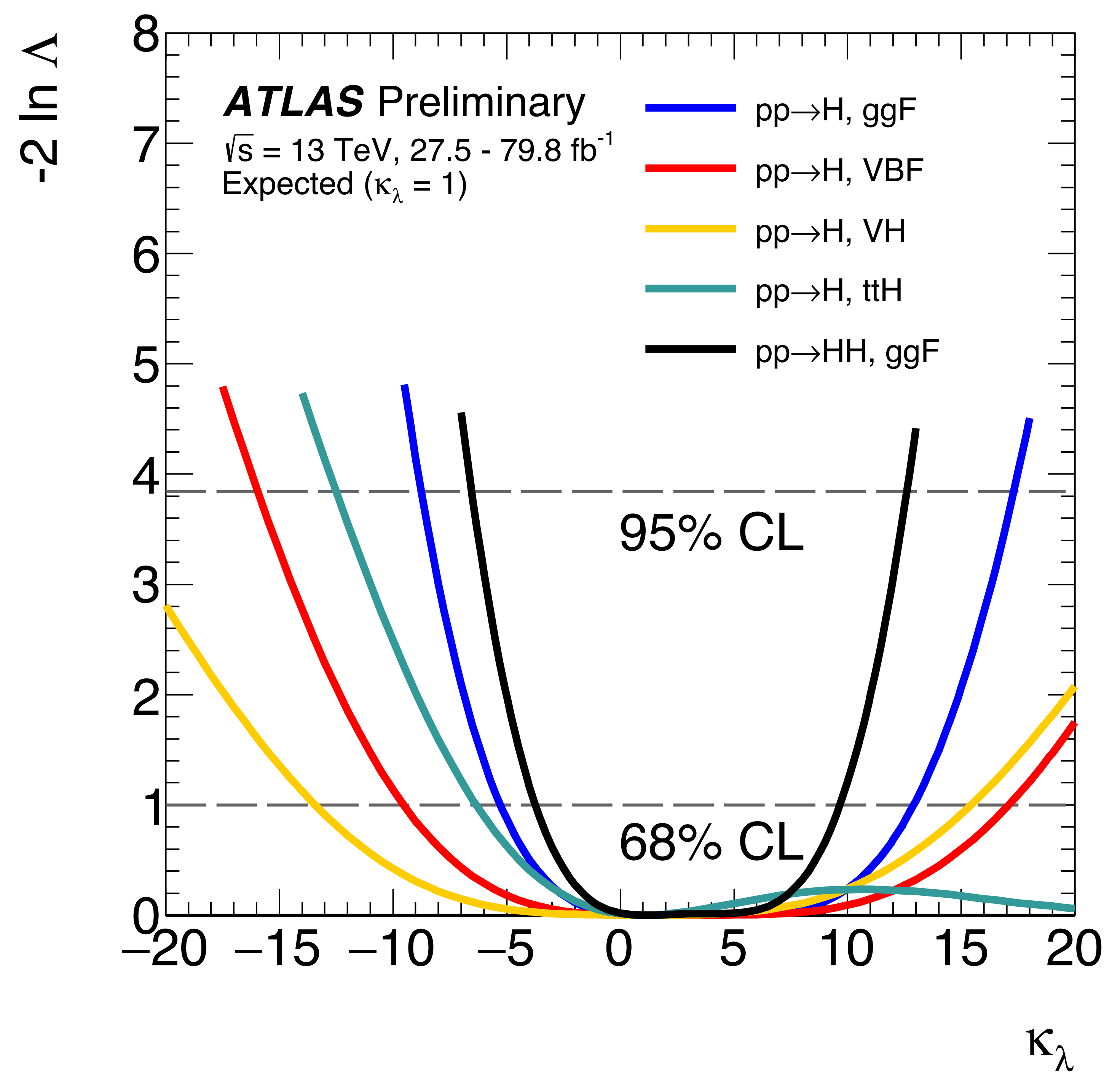

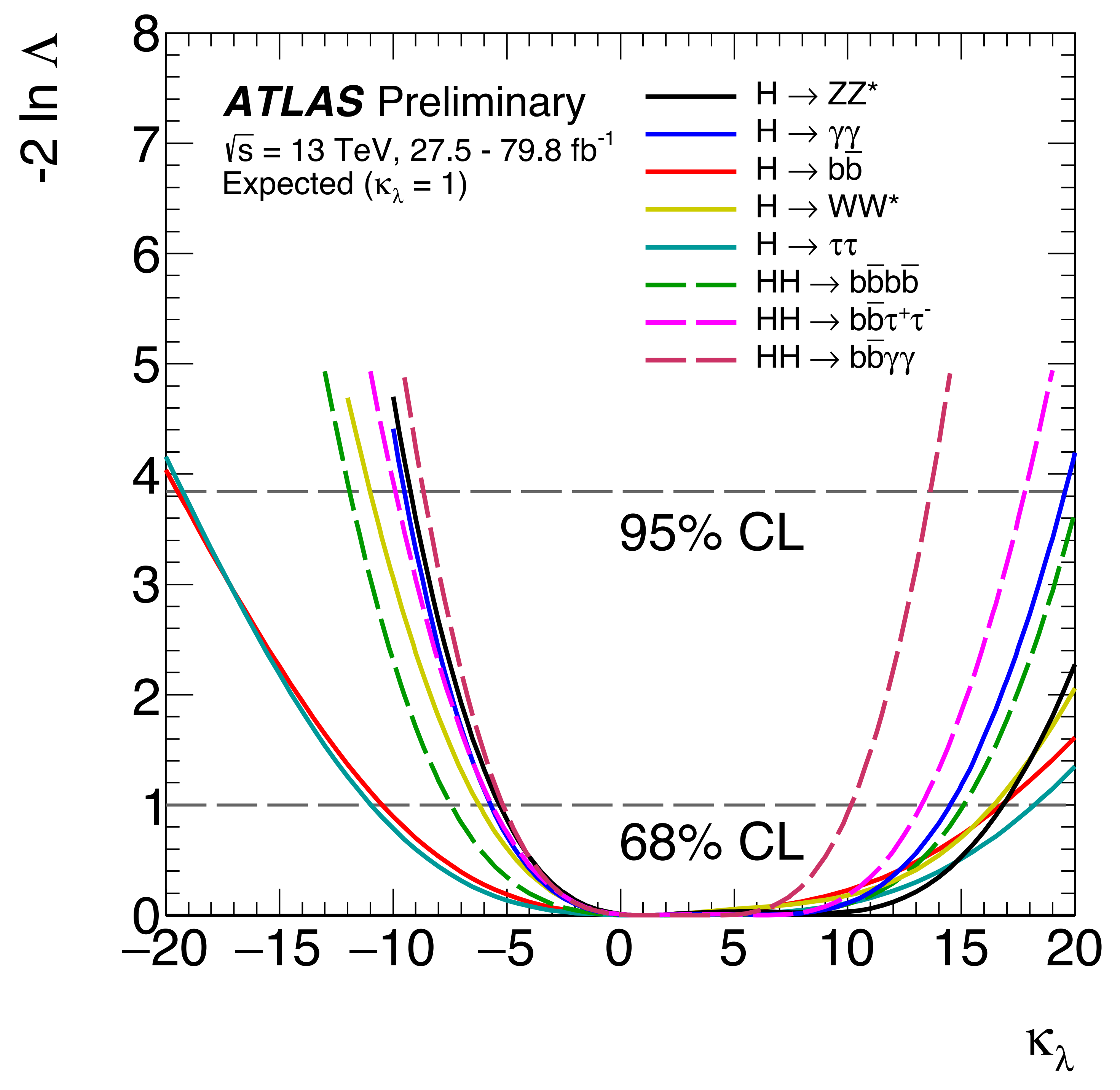

VBF HH→bbbb with full Run 2 data

- Search for non-resonant and resonant VBF HH production in the mass range 250 GeV - 1 TeV
- 4 central b-tagged small-radius jets (resolved topology)
- Jet pairing to form the Higgs candidates based on Higgs mass requirements
- 2 forward jets with large pseudo-rapidity separation and large invariant mass as VBF jets
- Multi-jet background data-driven from control regions (95% of total bkg)
- Signal region defined by selections in the 2D m_{H1}-m_{H2} plane

m_{HH} used as final discriminant variable in the signal region

JHEP 07 (2020) 108

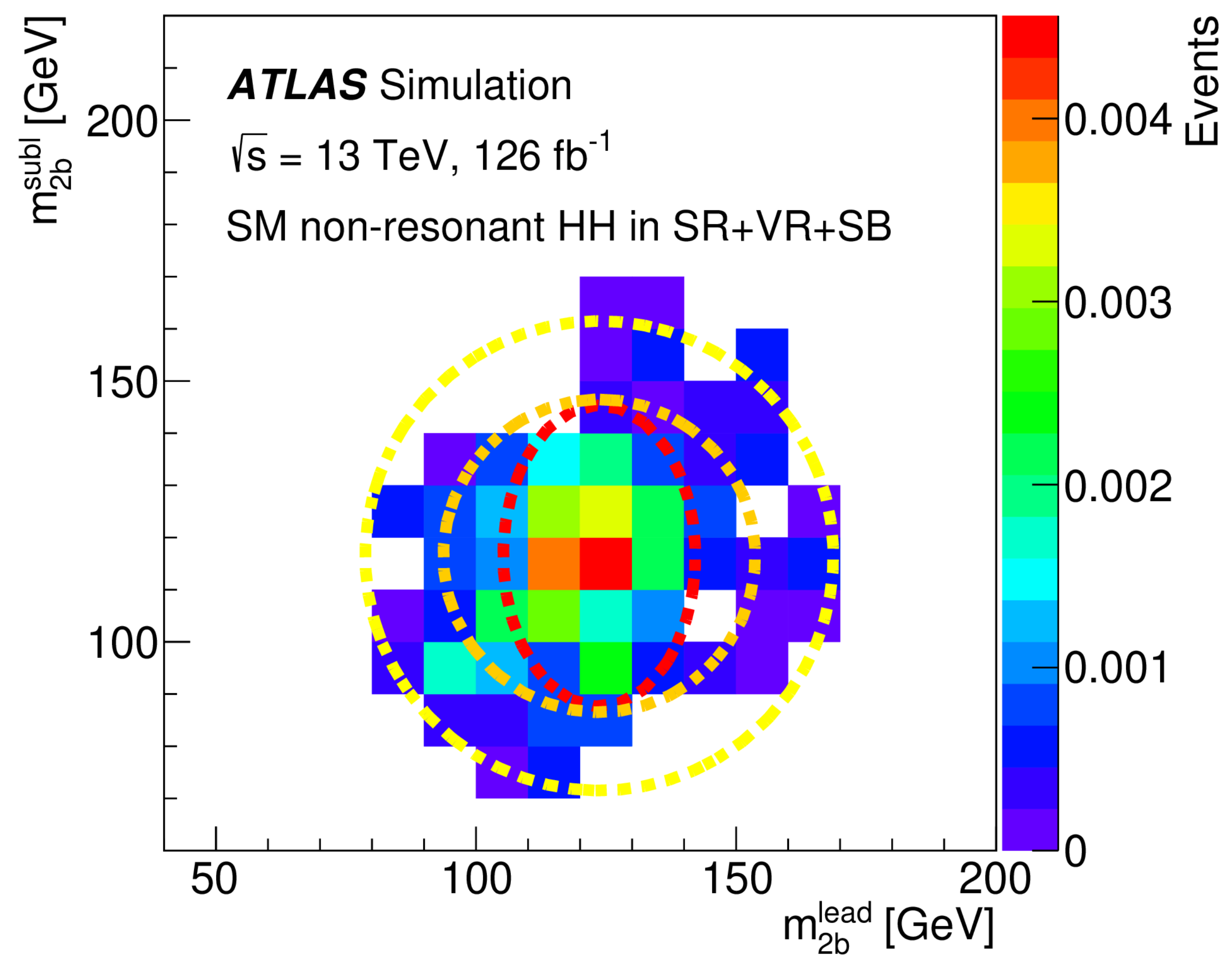

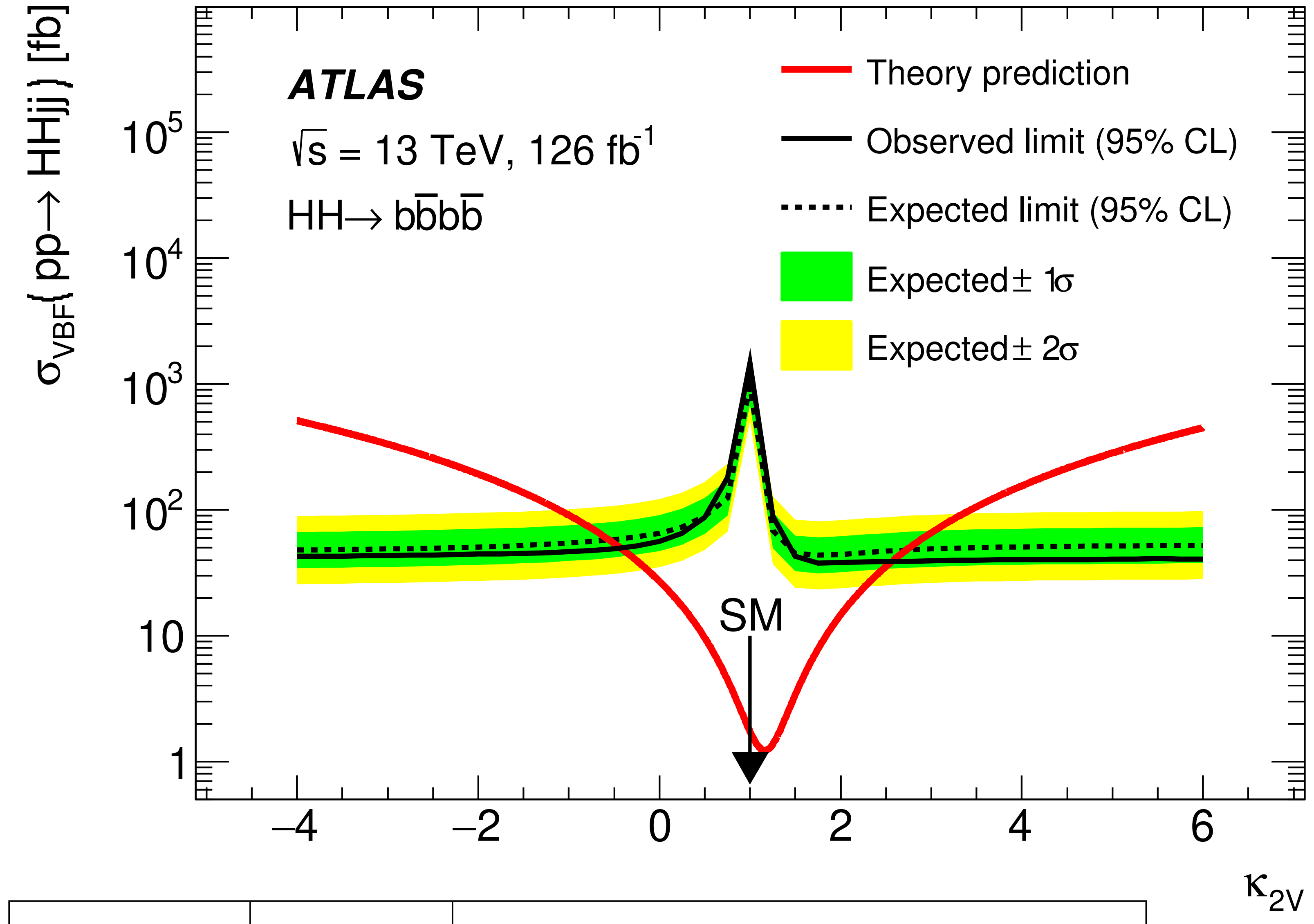

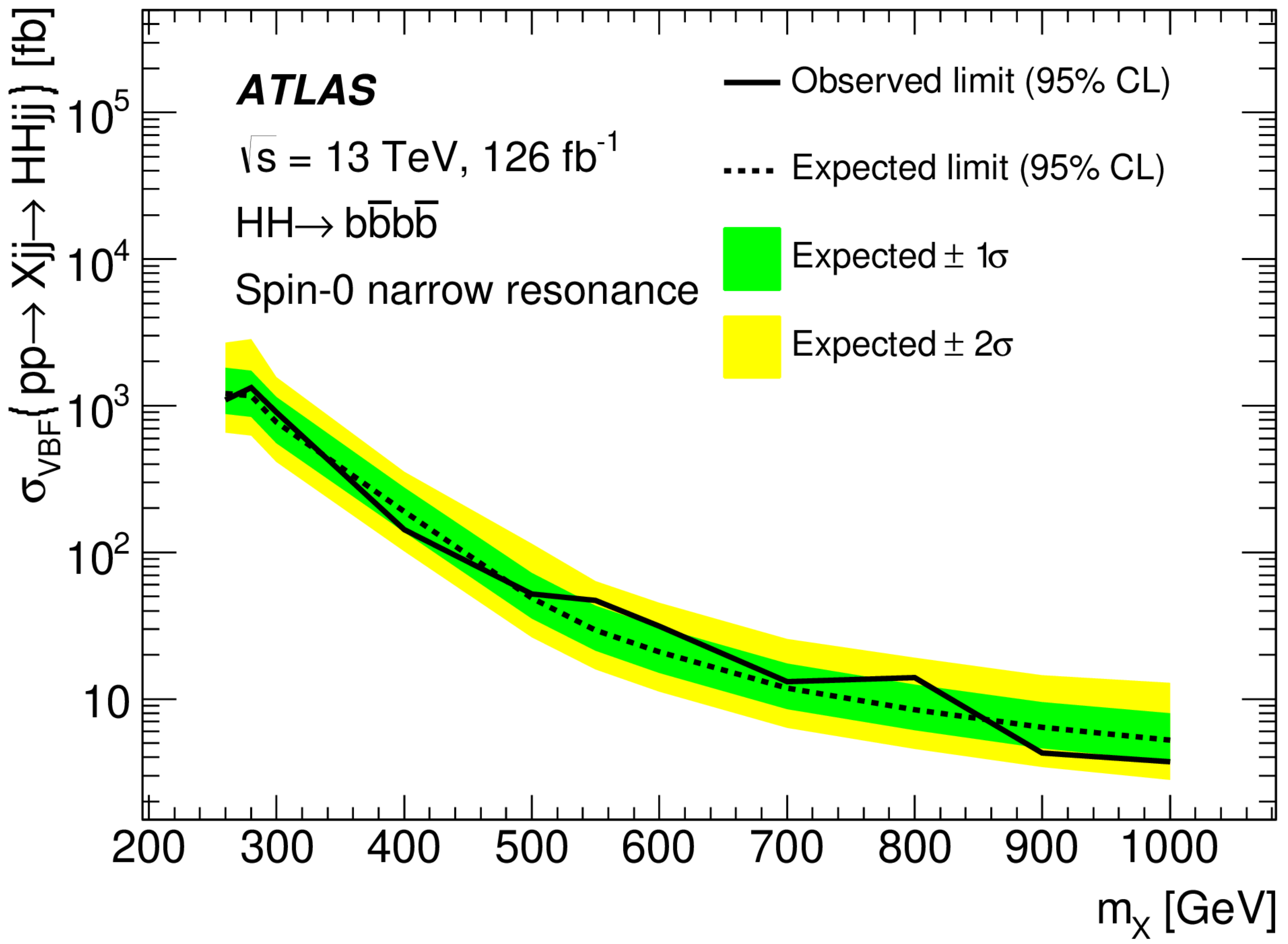

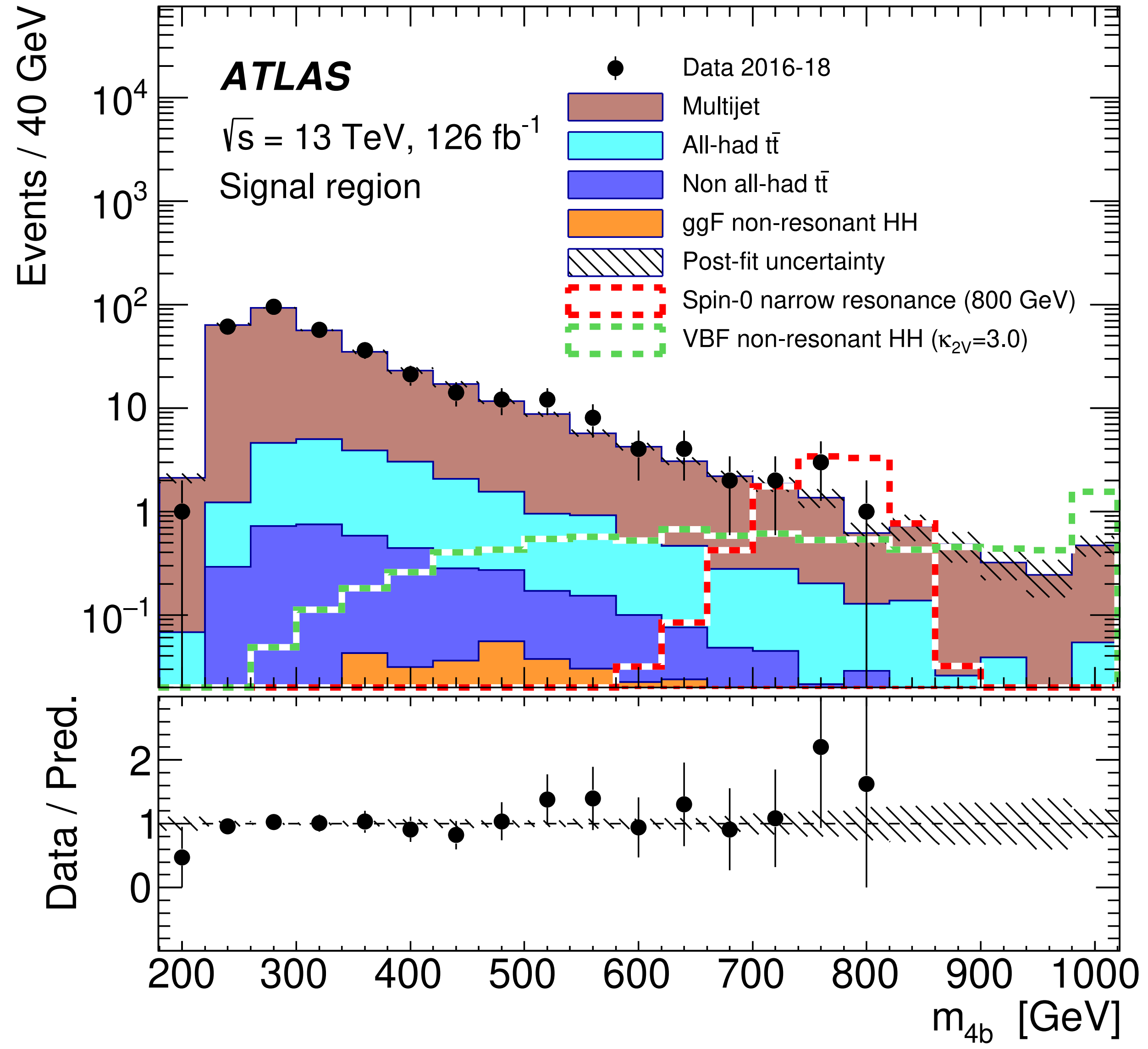

	Observed	-2σ	-1σ	Expected	$+1\sigma$	$+2\sigma$
σ_{VBF} [fb]	1450	500	660	920	1280	1720
$\sigma_{\mathrm{VBF}}/\sigma_{\mathrm{VBF}}^{\mathrm{SM}}$	840	290	390	540	750	1000

$-0.43 < \kappa_{2V} < 2.56$ at 95% CL

(expected $-0.55 < \kappa_{2V} < 2.72$)

Non-resonant HH→bbll with full Run 2 data

- Search for SM and BSM non-resonant HH production
- Only ggF HH production
- Looking for the HH decays with one H→bb and the other H→WW, ZZ,ττ in the 2 leptons final state
- At least two b-tagged jets and exactly two leptons (e/μ) with opposite charge
- 2 categories: same-flavour (SF) and different-flavour (DF) for the lepton pair
- Signal region defined by: $20 < m_{\ell\ell} < 60$ GeV, $110 < m_{bb} < 140$ GeV and a cut on a discriminant built from the output of a multi-class deep neural network (DNN) classifier ($d_{HH} > 5.45(5.55)$ for SR-SF (SR-DF))
- Event-counting analysis with a simultaneous fit of 2 signal regions: SF and DF

Phys. Lett. B 801 (2020) 135145

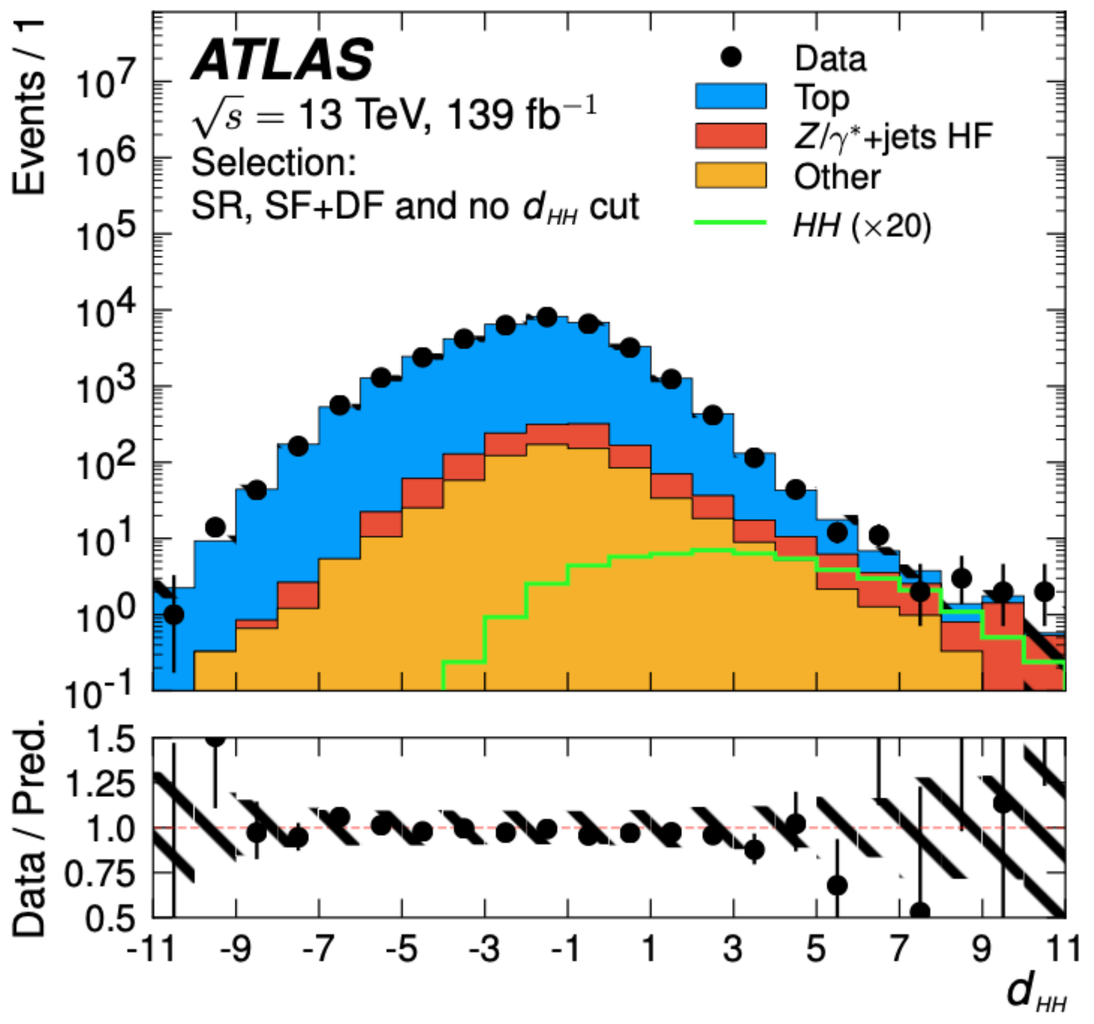

	-2σ	-1σ	**Expected**	$+1\sigma$	$+2\sigma$	**Observed**
$\sigma(gg \to HH)$ [pb]	0.5	0.6	0.9	1.3	1.9	1.2
$\sigma(gg \to HH)/\sigma^{SM}(gg \to HH)$	14	20	29	43	62	40

→ sensitivity not comparable to the other HH searches as upper limits are one order of magnitude higher (results not included in combinations)

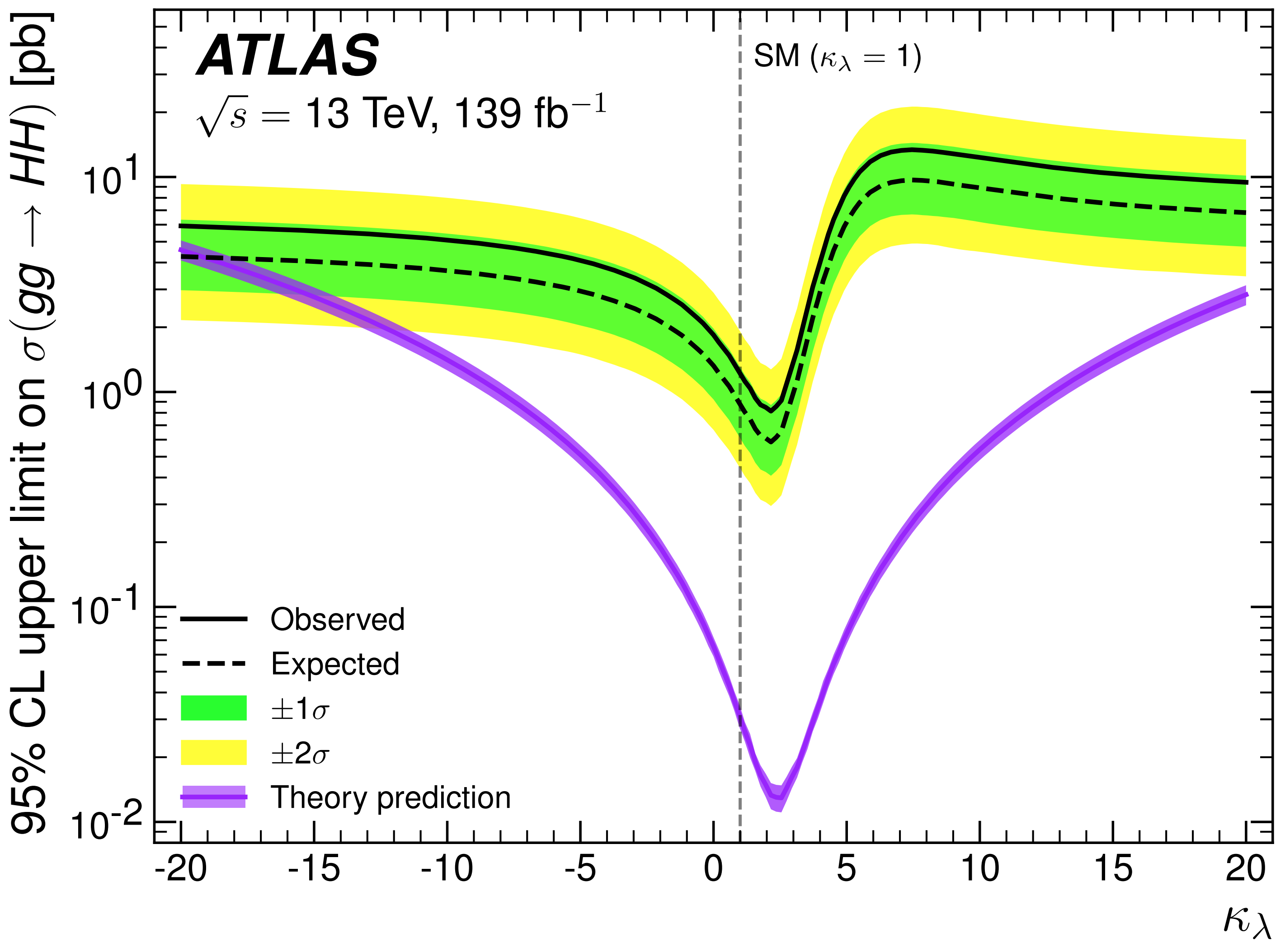

Resonant HH→bbττ boosted with full Run 2 data

- Search for resonant HH production in the mass range 1 - 3 TeV
- First use of boosted di-τ reconstruction and identification algorithm for the boosted H->ττ decay, based on a BDT applied on large-R jet ($R = 1.0$) with 2 sub-jets ($R = 0.2$)
- Boosted H→bb decay: large-R jet with 2 b-tags
- Mass-dependent m_{HH} cut to define signal region
- Counting experiment in the signal region

JHEP 11 (2020) 163

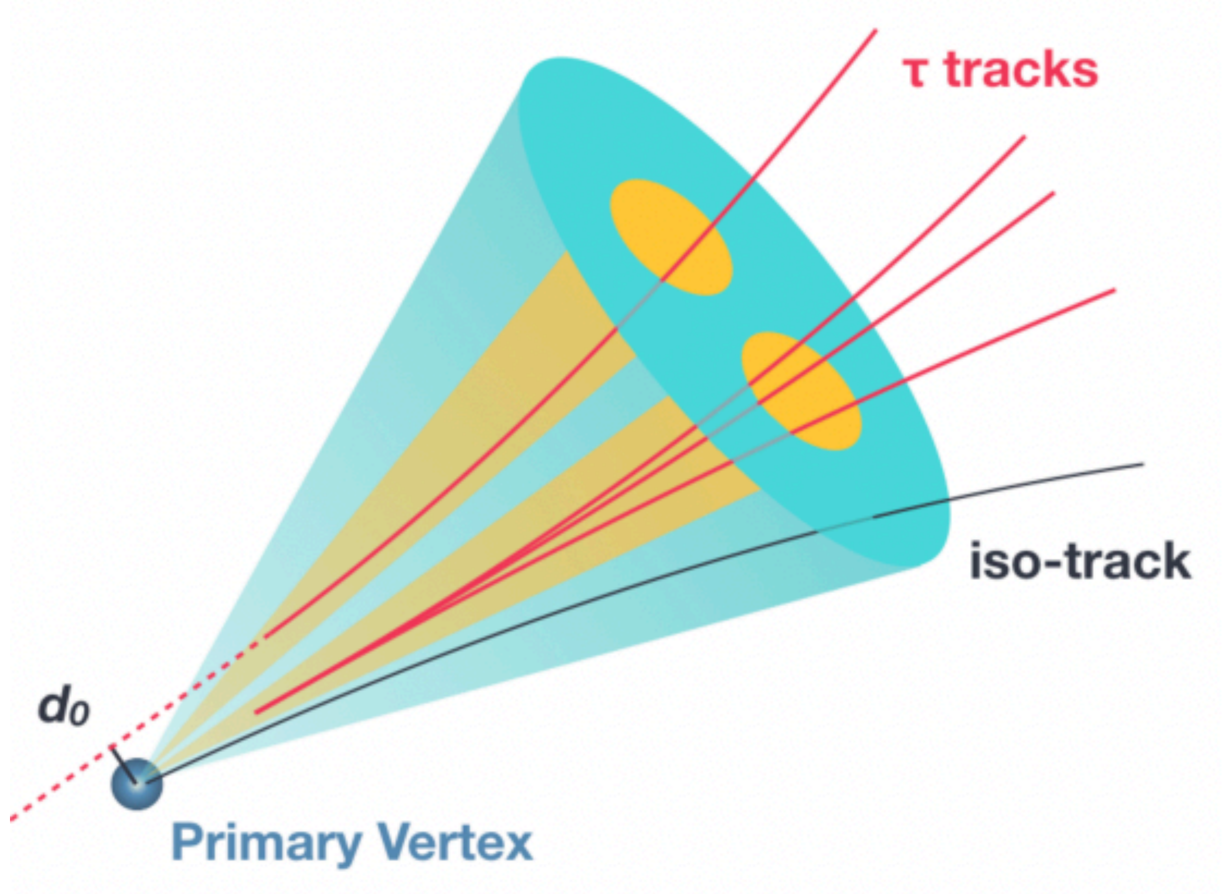

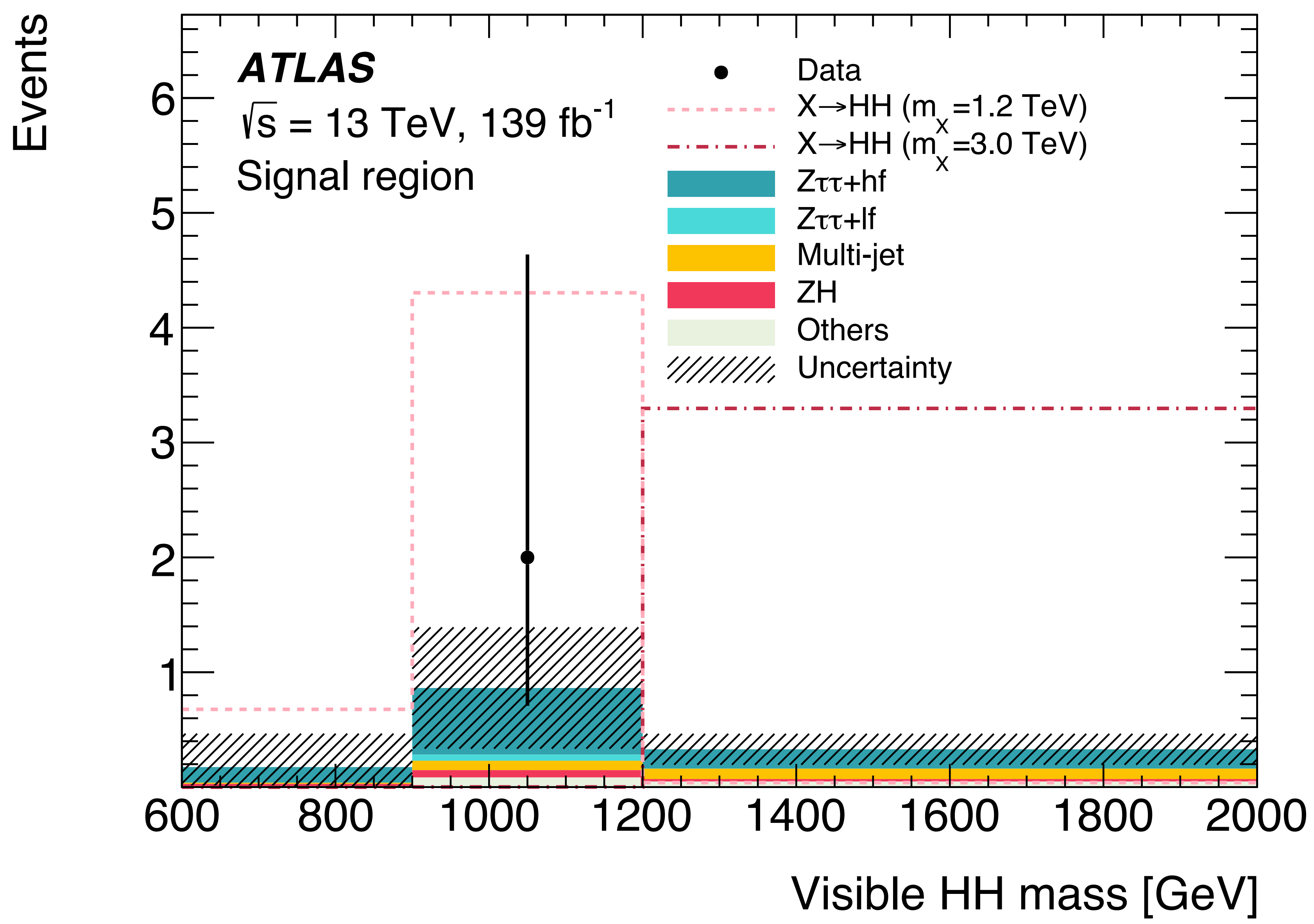

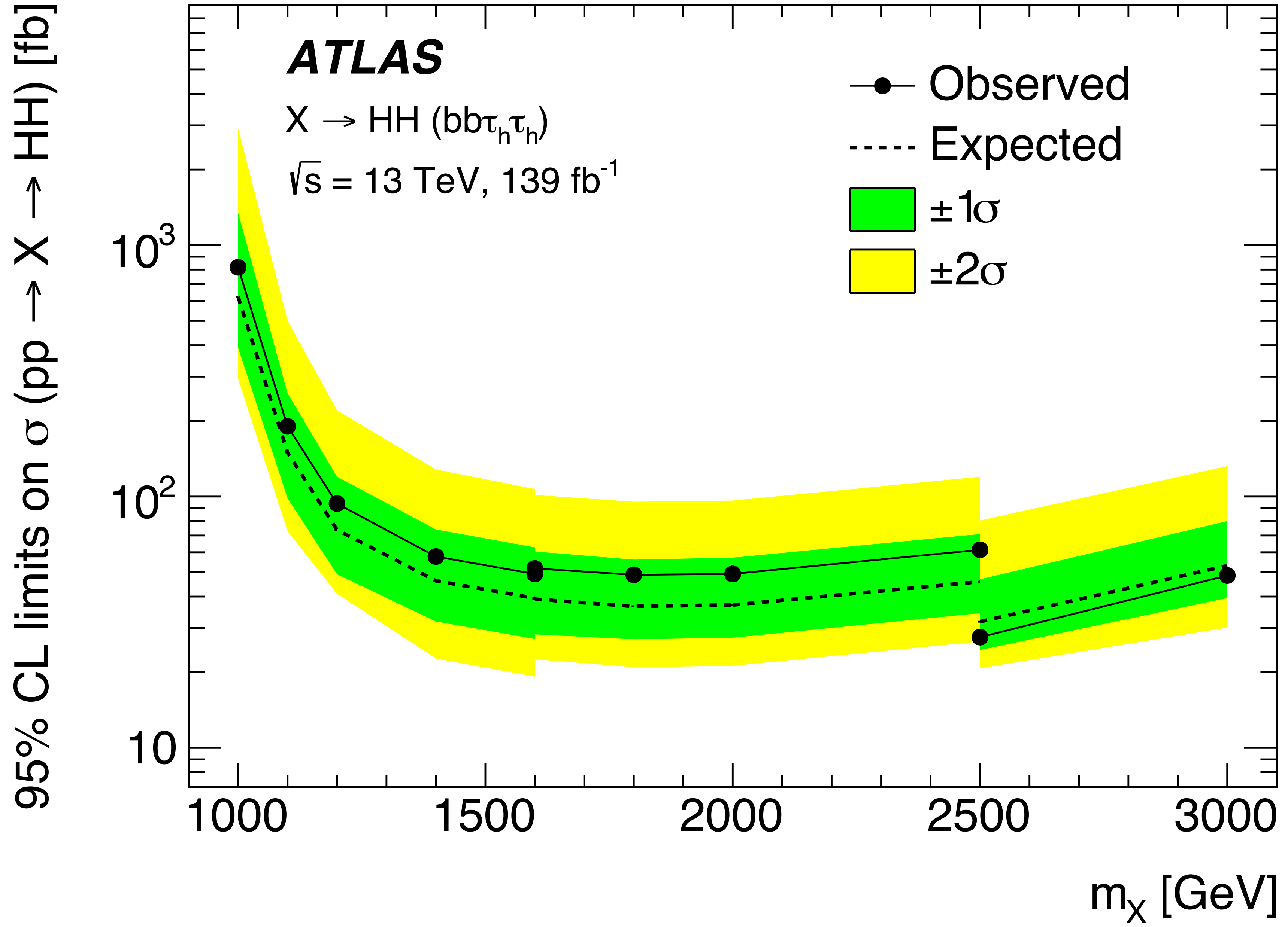

→ sensitivity not comparable to the high mass resonant search in the 4b channel as upper limits are one order of magnitude higher (results not included in combinations)

Resonant HH→bbbb full Run 2

Systematic uncertainties

Phys. Rev. D 105, 092002

Uncertainty category	Relative impact [%]			
	280 GeV	600 GeV	1600 GeV	4000 GeV
Background $m(HH)$ shape	12.5	8.7	1.1	1.0
Jet momentum/mass scale	0.6	0.1	1.2	1.7
Jet momentum/mass resolution	2.1	1.5	7.1	7.8
b-tagging calibration	0.7	0.4	2.1	7.0
Theory (signal)	0.6	0.6	1.4	1.2
Theory ($t\bar{t}$ background)	N/A	N/A	0.5	0.2
All systematic uncertainties	15.9	10.9	13.4	15.6

Resonant HH→bbbb full Run 2

Acceptance x efficiency

Phys. Rev. D 105, 092002

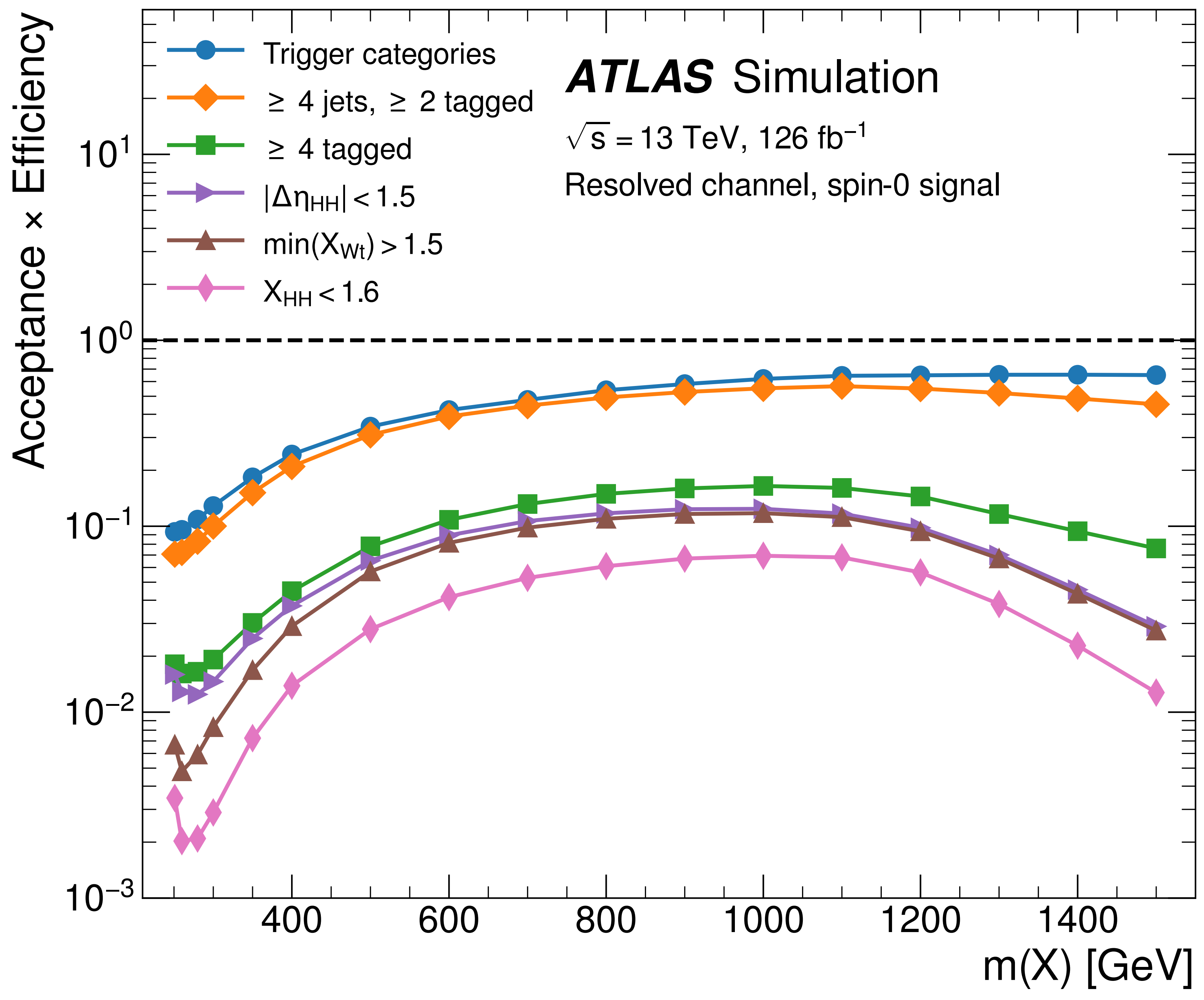

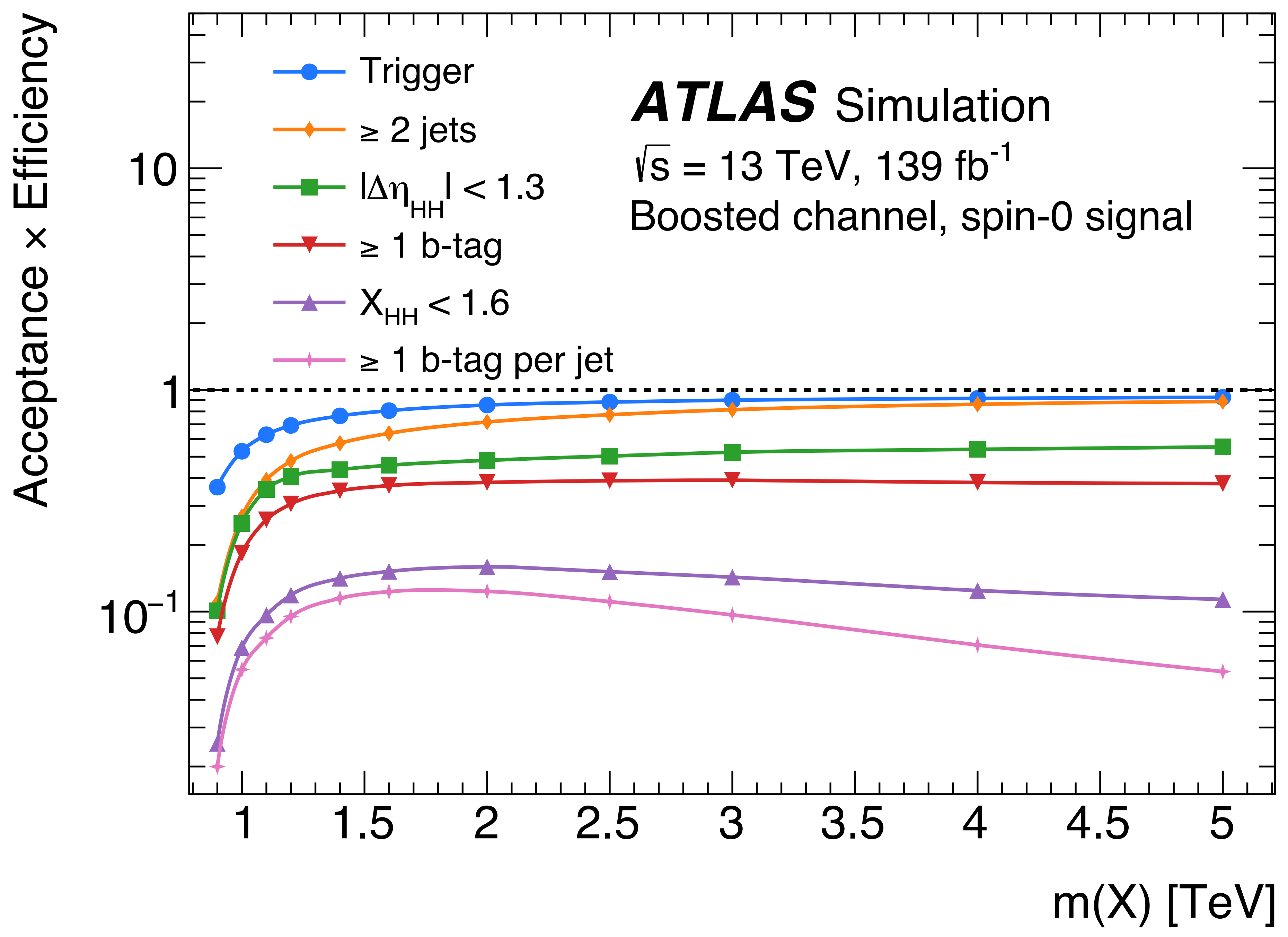

Non-resonant HH→bbbb full Run 2

Event selection

ATLAS-CONF-2022-035

	Data	ggF Signal		VBF Signal	
		SM	$\kappa_\lambda = 10$	**SM**	$\kappa_{2V} = 0$
Common preselection					
Preselection	5.70×10^8	526.6	7337.7	22.3	626.1
Trigger class	2.49×10^8	381.8	5279.1	16.1	405.2
ggF selection					
Fail VBF selection	2.46×10^8	376.6	5198.0	13.9	334.4
At least 4 b-tagged central jets	1.89×10^6	86.0	1001.7	1.9	65.2
$\lvert\Delta\eta_{HH}\rvert < 1.5$	1.03×10^6	71.9	850.6	0.9	46.4
$X_{Wt} > 1.5$	7.51×10^5	60.4	569.0	0.7	43.1
$X_{HH} < 1.6$ (ggF signal region)	1.62×10^4	29.1	182.7	0.2	23.0
VBF selection					
Pass VBF selection	3.30×10^6	5.2	81.1	2.2	70.7
At least 4 b-tagged central jets	2.71×10^4	1.1	15.3	0.7	27.6
$X_{Wt} > 1.5$	2.18×10^4	1.0	11.2	0.7	26.5
$X_{HH} < 1.6$	5.02×10^2	0.5	3.1	0.3	17.3
$m_{HH} > 400$ GeV (VBF signal region)	3.57×10^2	0.4	1.8	0.3	16.4

Non-resonant HH→bbbb full Run 2

Likelihood scans

ATLAS-CONF-2022-035

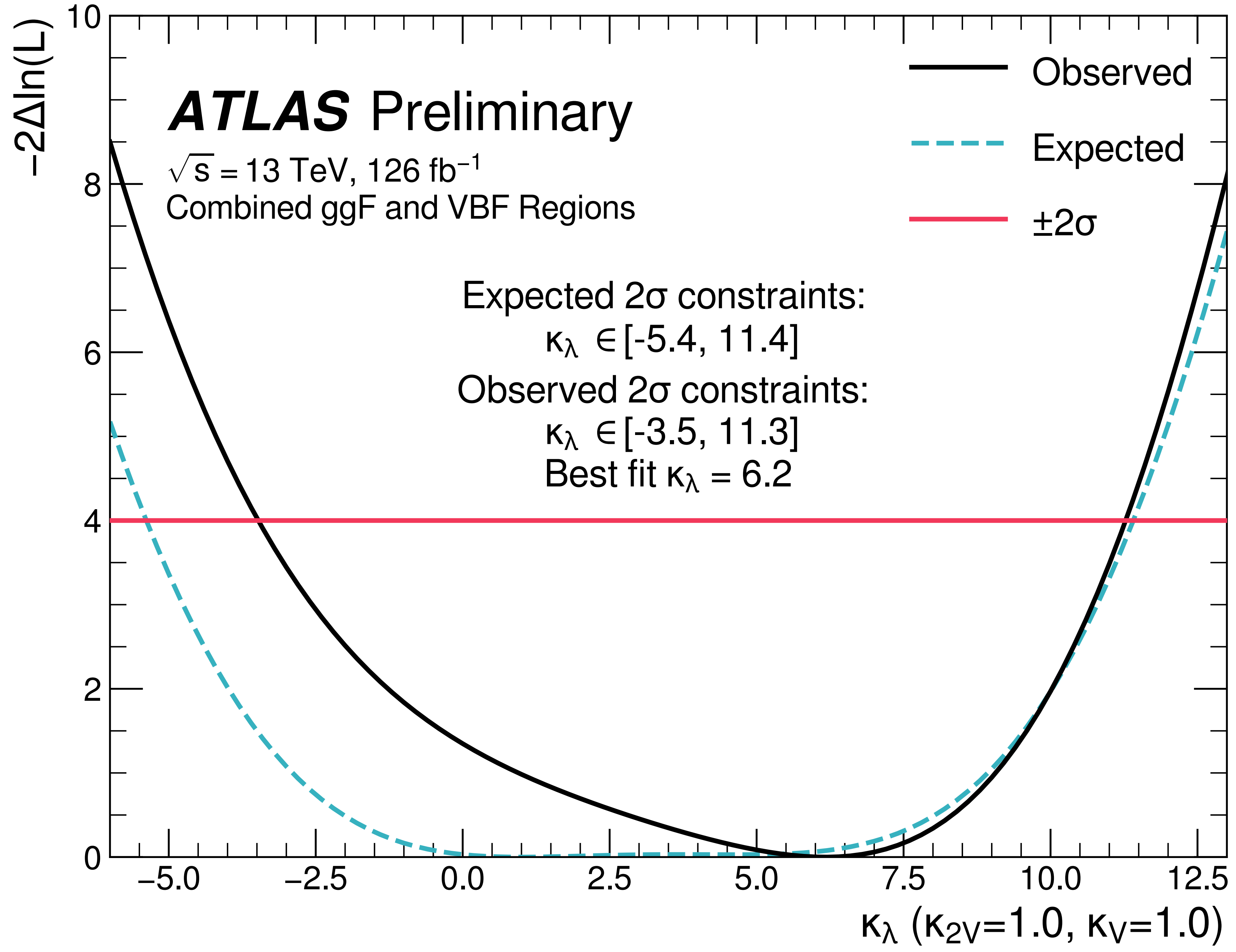

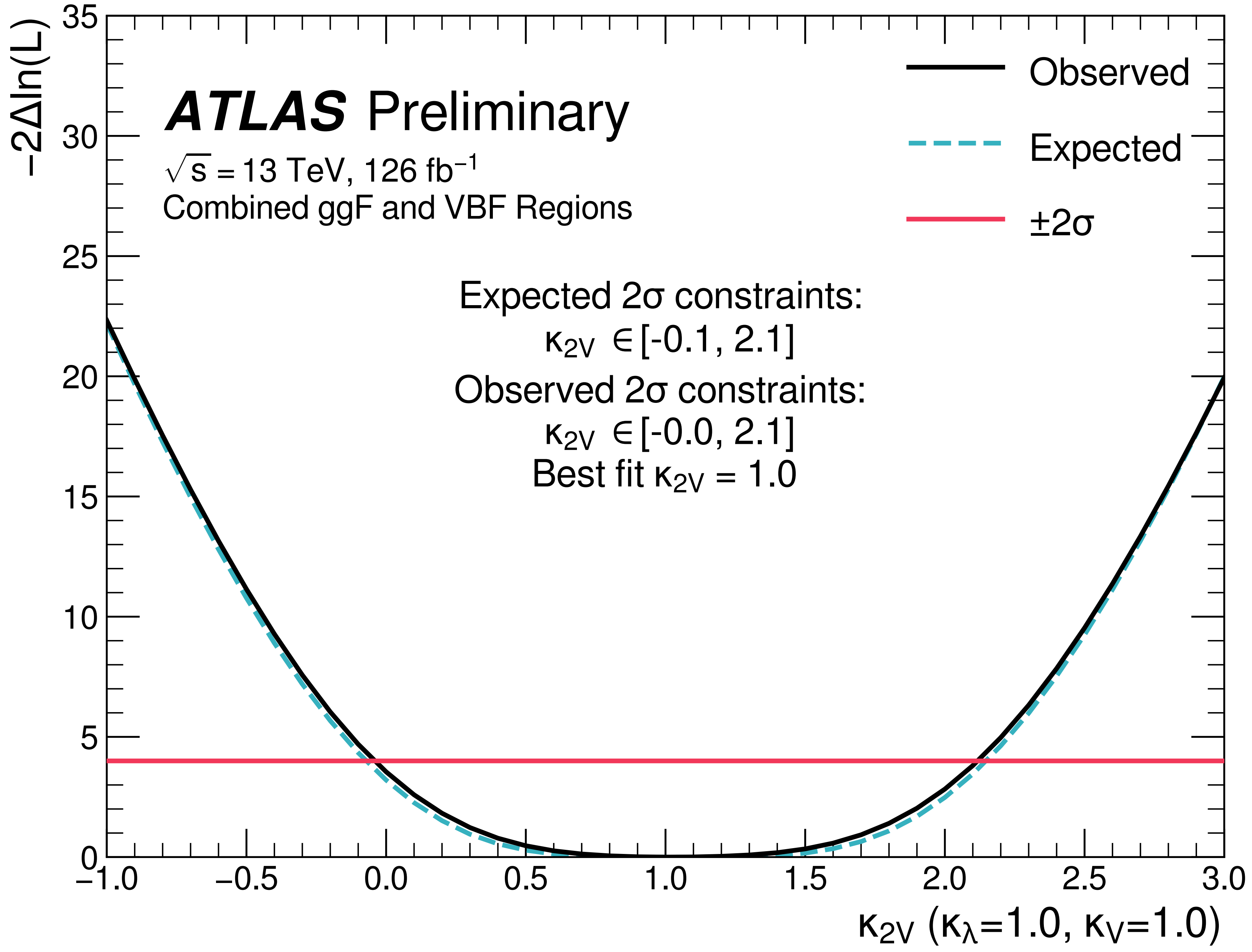

Non-resonant HH→bbbb full Run 2

NN input variables

ATLAS-CONF-2022-035

ggF	VBF
1. $\log(p_{\mathrm{T}})$ of the 2nd leading Higgs boson candidate jet 2. $\log(p_{\mathrm{T}})$ of the 4th leading Higgs boson candidate jet 3. $\log(\Delta R)$ between the closest two Higgs boson candidate jets 4. $\log(\Delta R)$ between the other two Higgs boson candidate jets 5. Average absolute η value of the Higgs boson candidate jets 6. $\log(p_{\mathrm{T}})$ of the di-Higgs system 7. ΔR between the two Higgs boson candidates 8. $\Delta\phi$ between jets in the leading Higgs boson candidate 9. $\Delta\phi$ between jets in the subleading Higgs boson candidate 10. $\log(X_{Wt})$ 11. Number of jets in the event 12. Trigger class index as one-hot encoder	1. Maximum di-jet mass out of the possible pairings of the four Higgs boson candidate jets 2. Minimum di-jet mass out of the possible pairings of the four Higgs boson candidate jets 3. Energy of the leading Higgs boson candidate 4. Energy of the subleading Higgs boson candidate 5. Second smallest ΔR between the jets in the leading Higgs boson candidate (out of the three possible pairings for the leading Higgs candidate) 6. Average absolute η value of Higgs boson candidate jets 7. $\log(X_{Wt})$ 8. Trigger class index as one-hot encoder 9. Year index as one-hot encoder (for years inclusive training)

HH→bbττ full Run 2

Acceptance x efficiency

ATLAS-CONF-2021-030

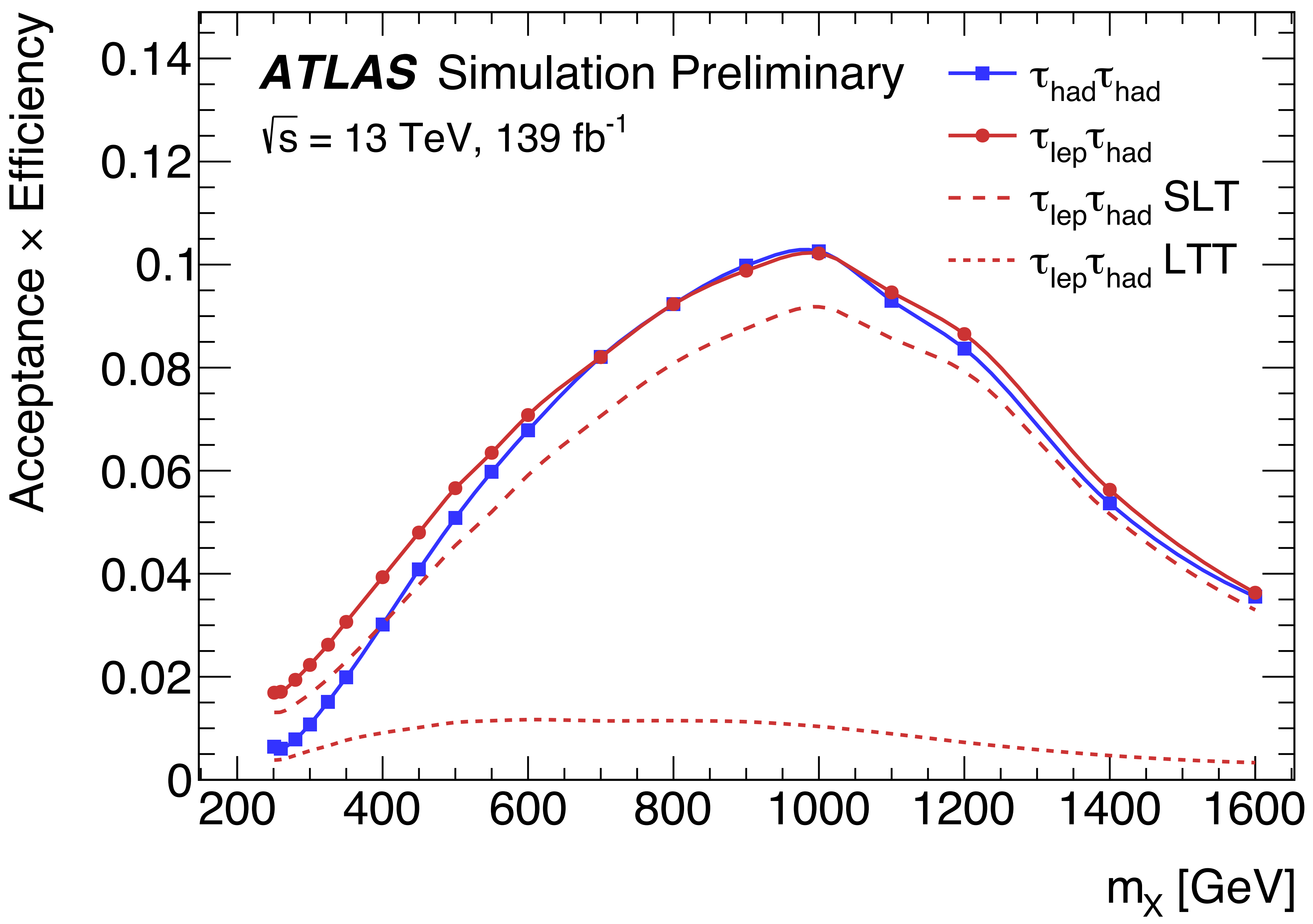

HH→bbττ full Run 2

MVA input variables

ATLAS-CONF-2021-030

Variable	$\tau_{\rm had}\tau_{\rm had}$	$\tau_{\rm lep}\tau_{\rm had}$ SLT	$\tau_{\rm lep}\tau_{\rm had}$ LTT
m_{HH}	✓	✓	✓
$m_{\tau\tau}^{\rm MMC}$	✓	✓	✓
m_{bb}	✓	✓	✓
$\Delta R(\tau,\tau)$	✓	✓	✓
$\Delta R(b,b)$	✓	✓	
$\Delta p_{\rm T}(\ell,\tau)$		✓	✓
Sub-leading b-tagged jet $p_{\rm T}$		✓	
$m_{\rm T}^{W}$		✓	
$E_{\rm T}^{\rm miss}$		✓	
$\mathbf{p}_{\rm T}^{\rm miss}$ ϕ centrality		✓	
$\Delta\phi(\tau\tau, bb)$		✓	
$\Delta\phi(\ell, \mathbf{p}_{\rm T}^{\rm miss})$			✓
$\Delta\phi(\ell\tau, \mathbf{p}_{\rm T}^{\rm miss})$			✓
$S_{\rm T}$			✓

HH→bbττ full Run 2

MVA input variables

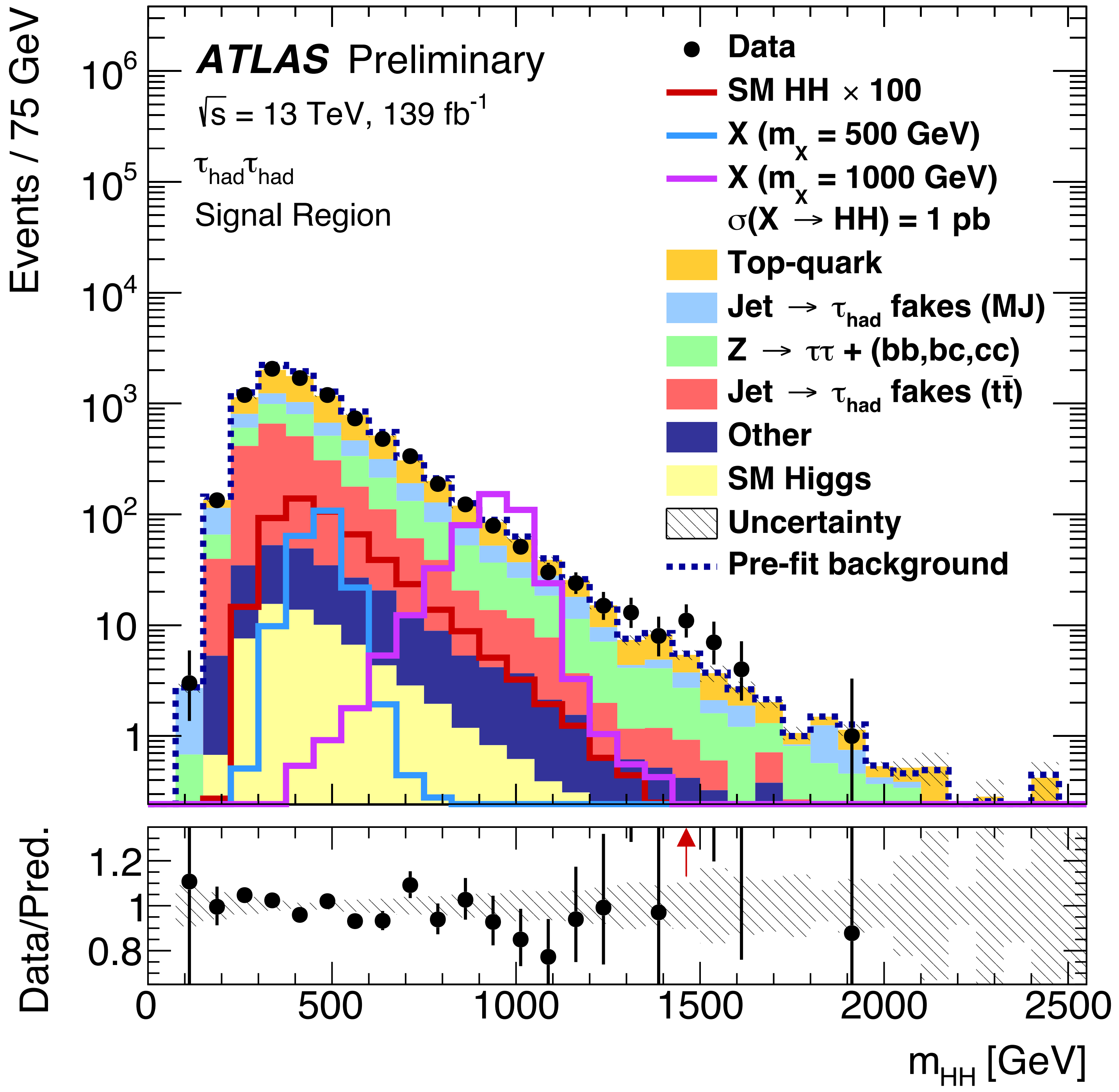

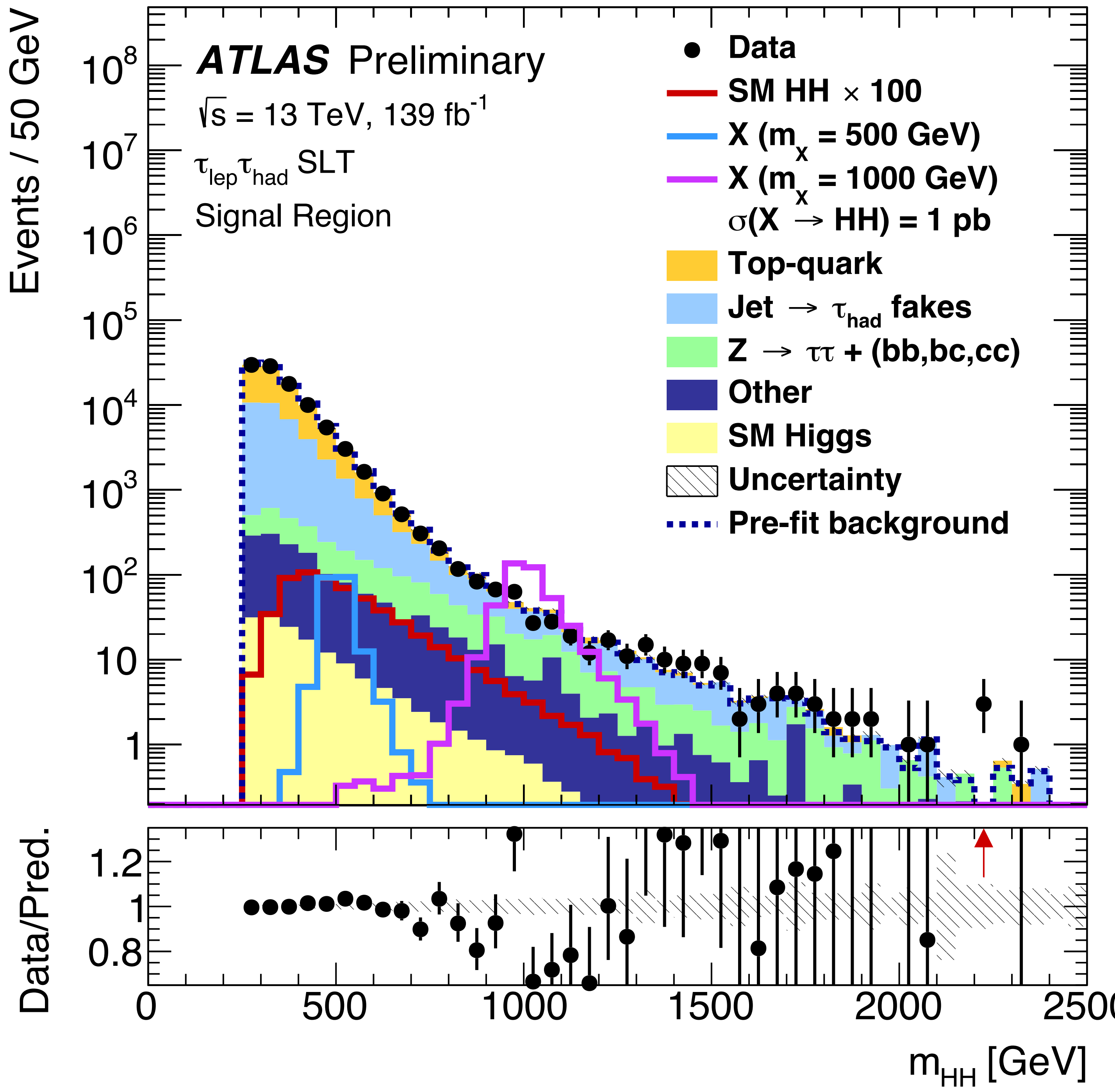

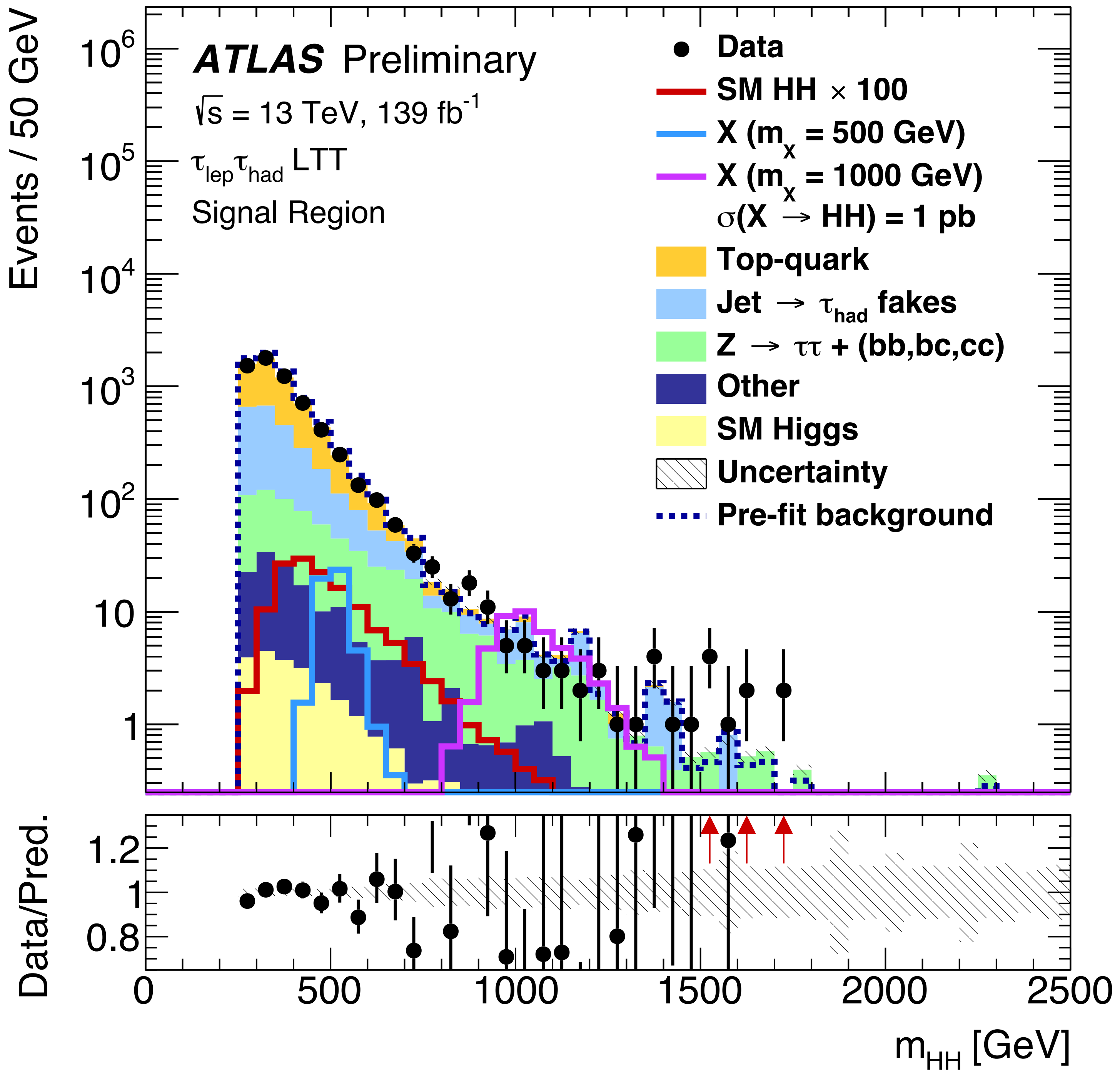

HH→bbττ full Run 2

MVA input variables

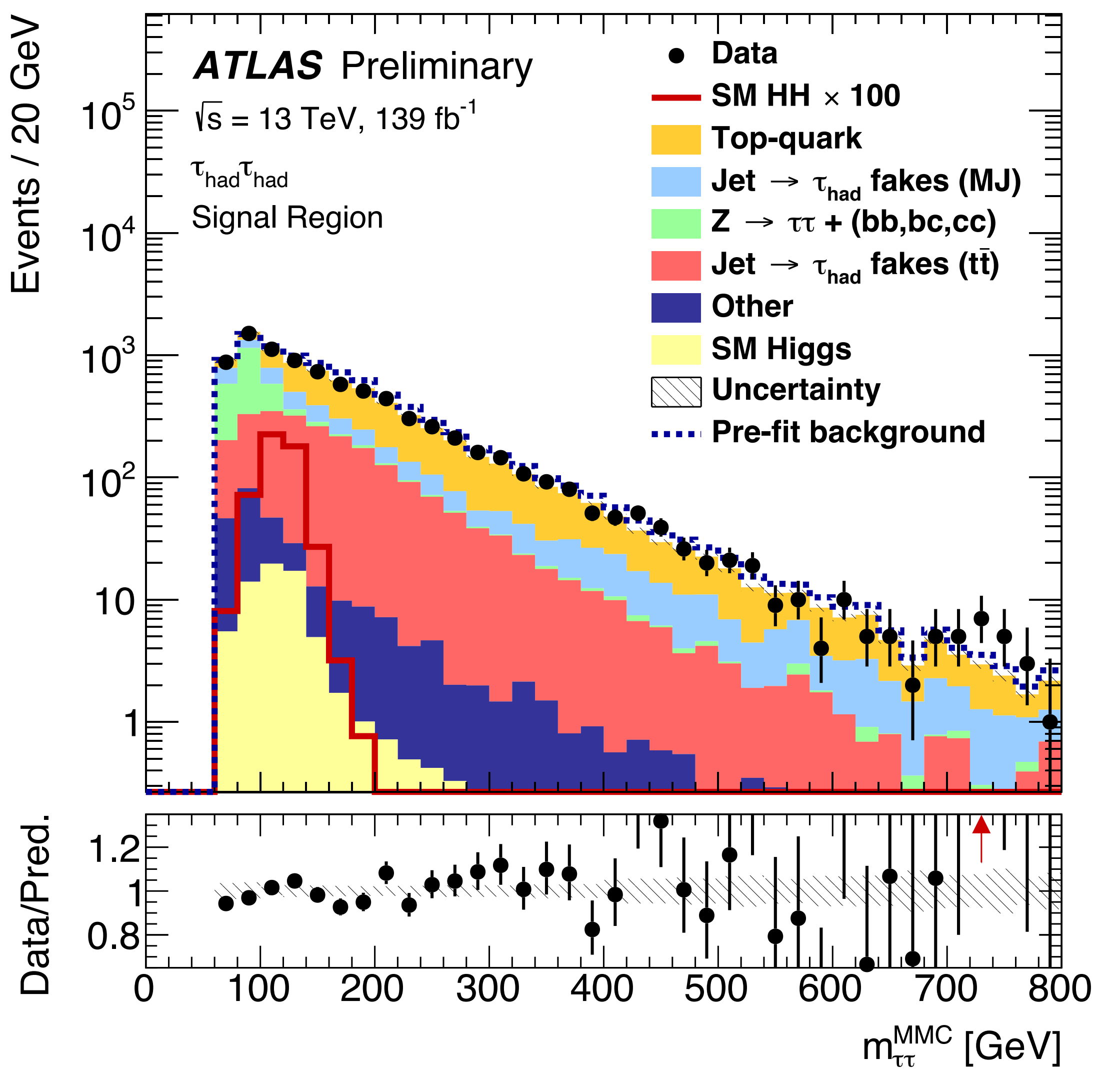

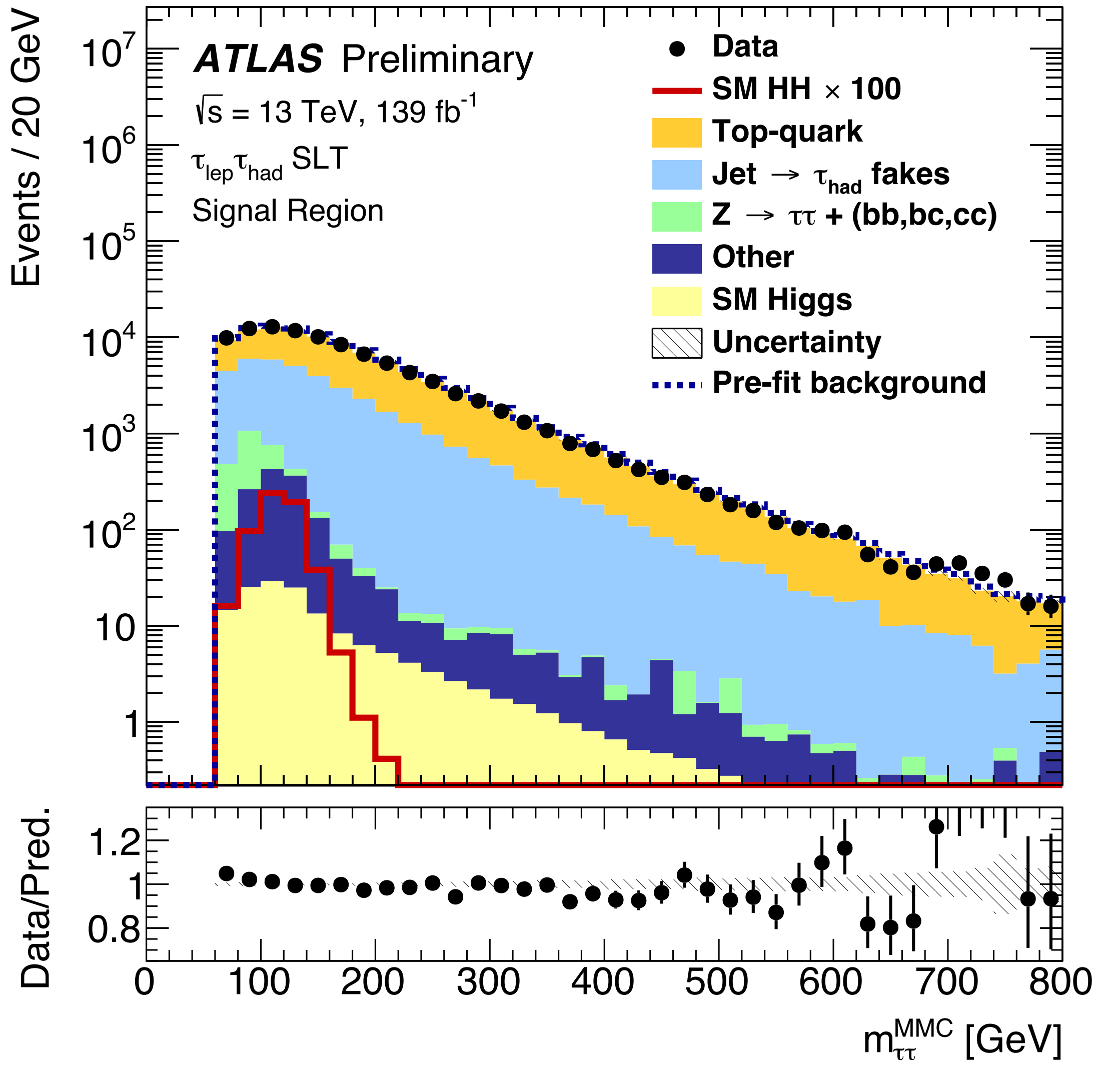

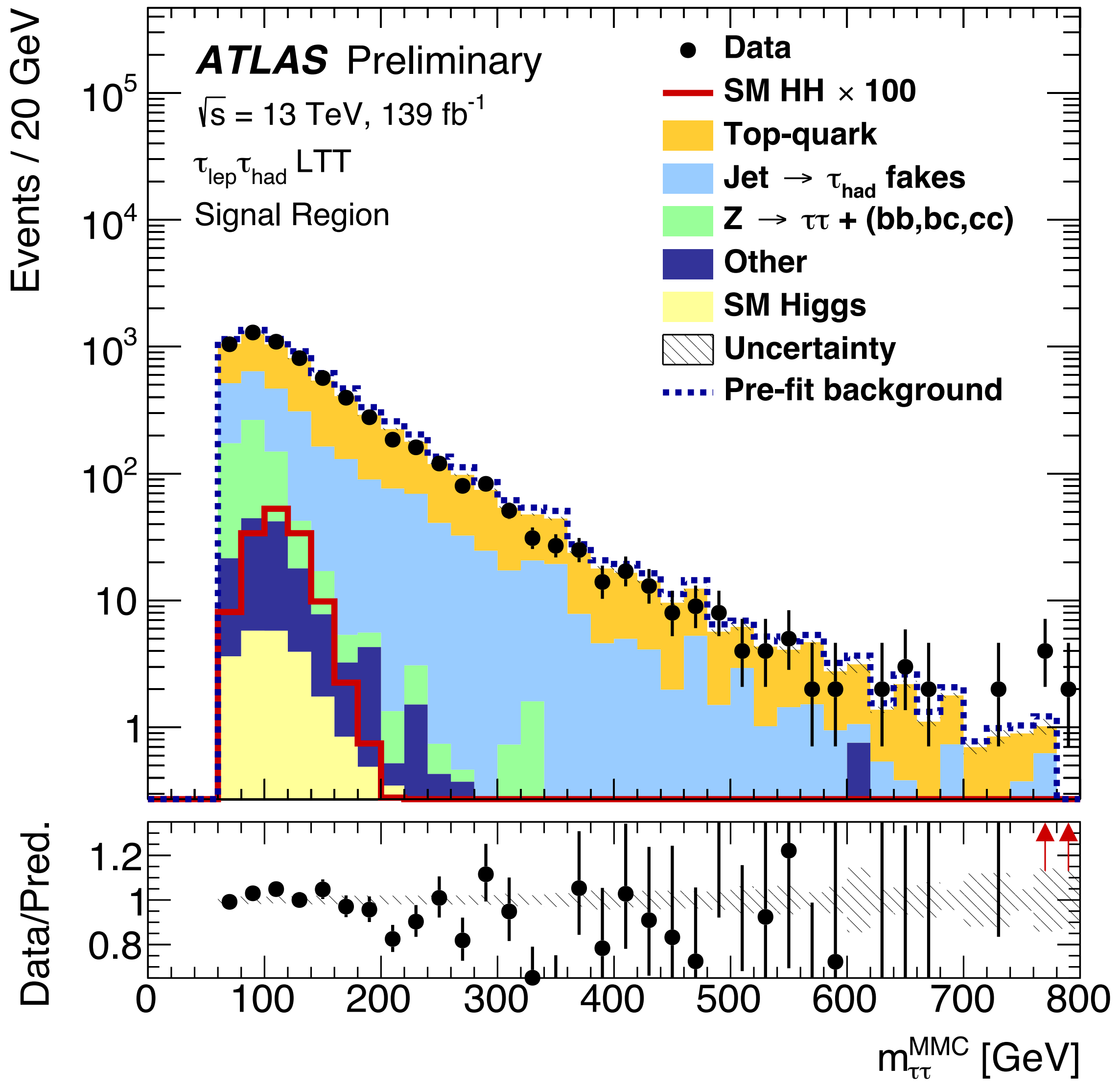

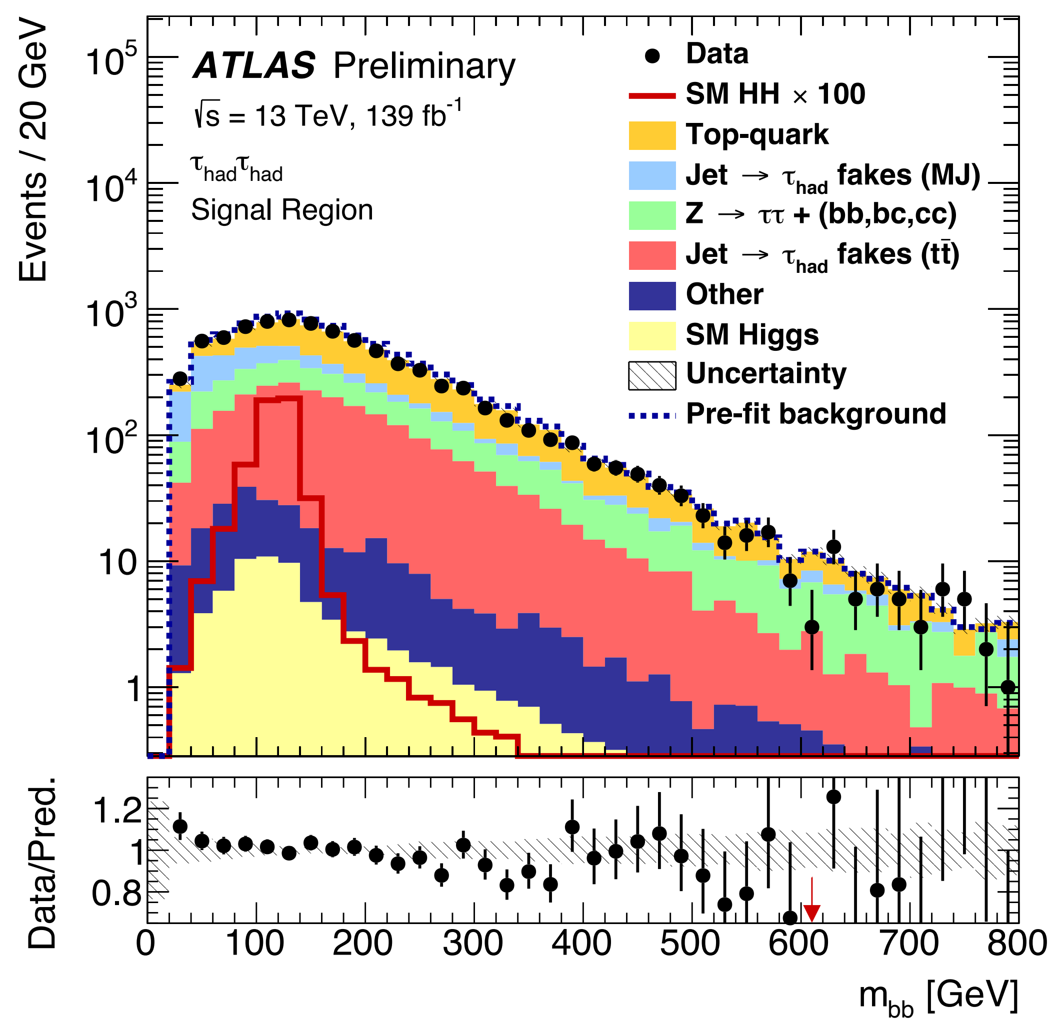

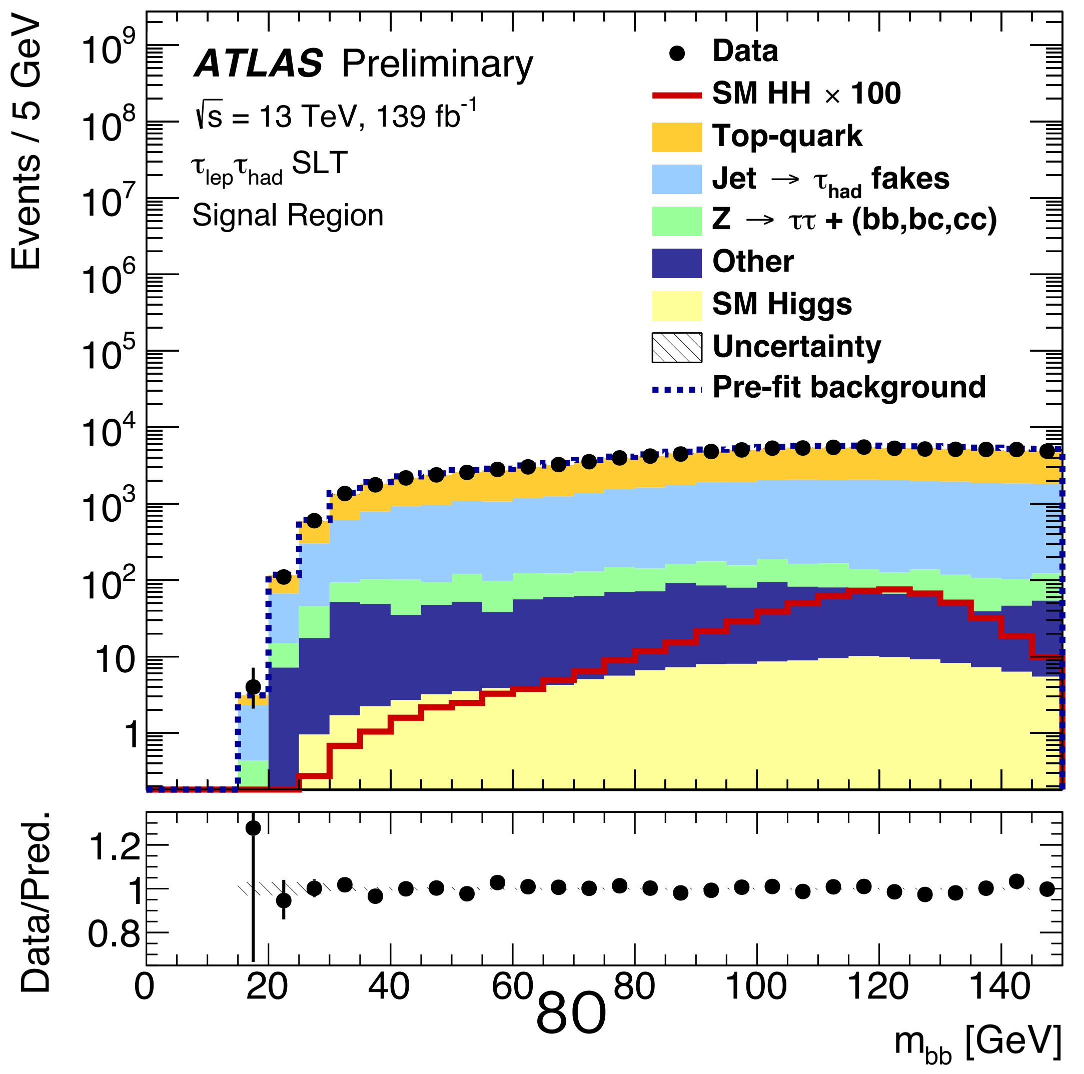

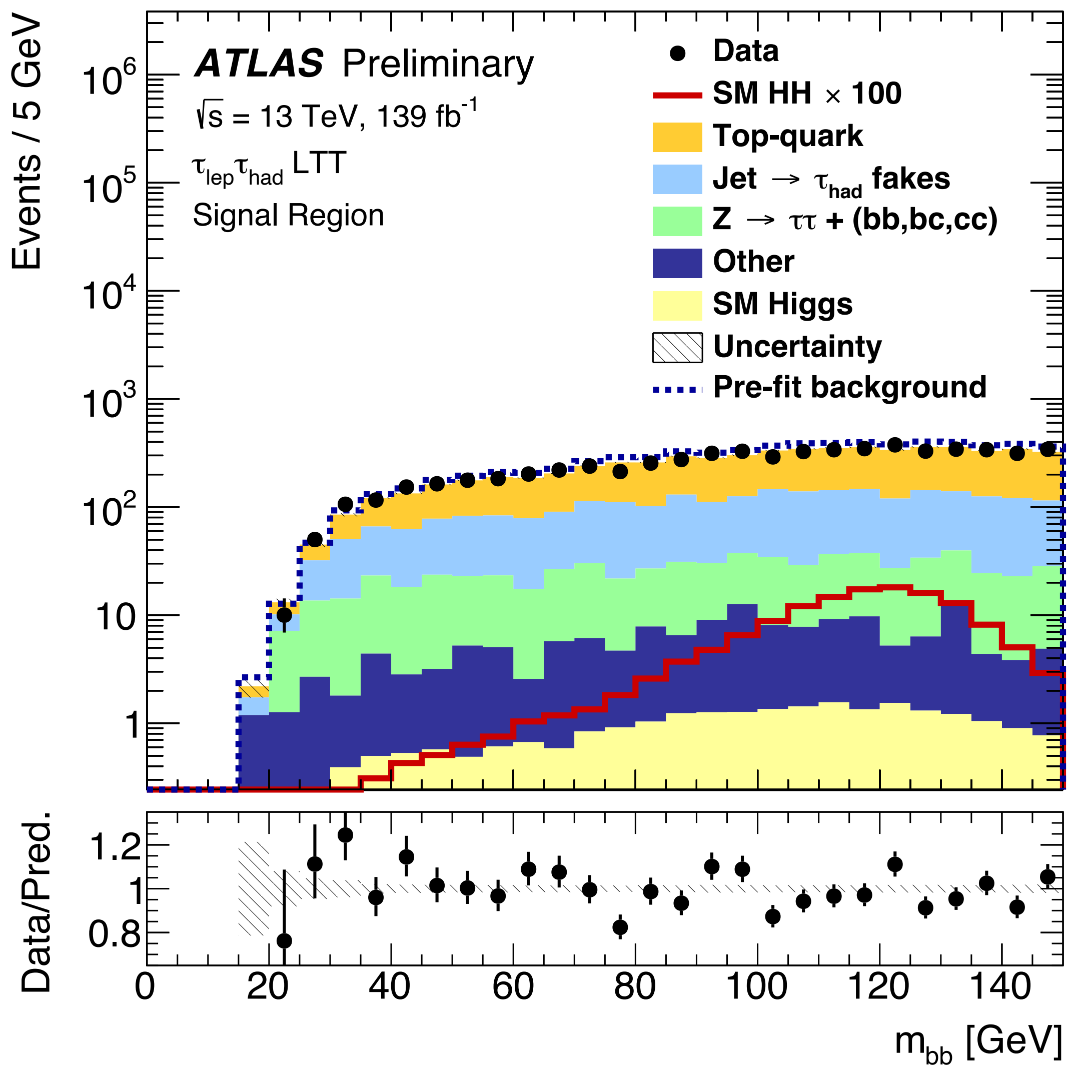

HH→bbττ full Run 2

MVA outputs

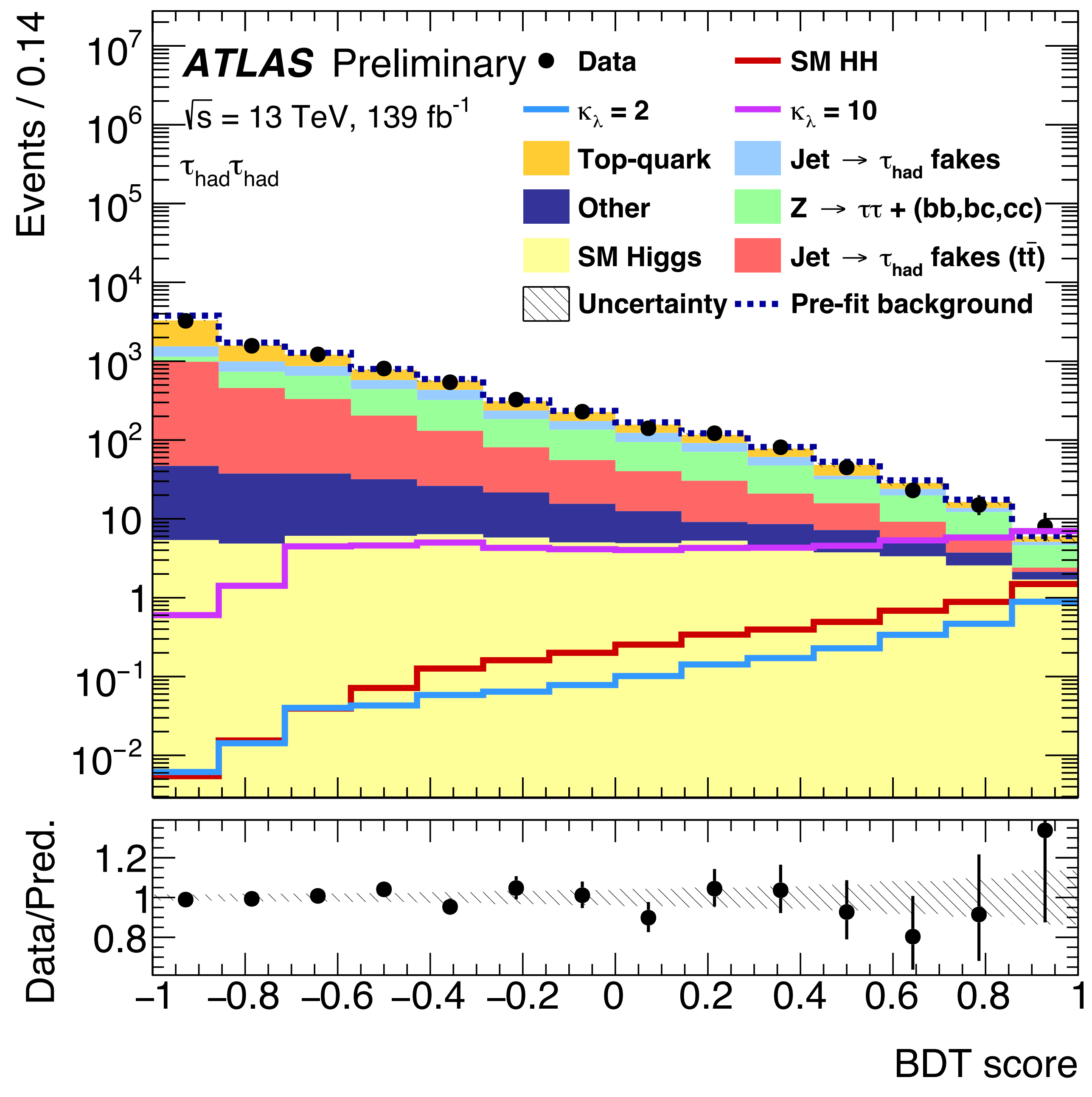

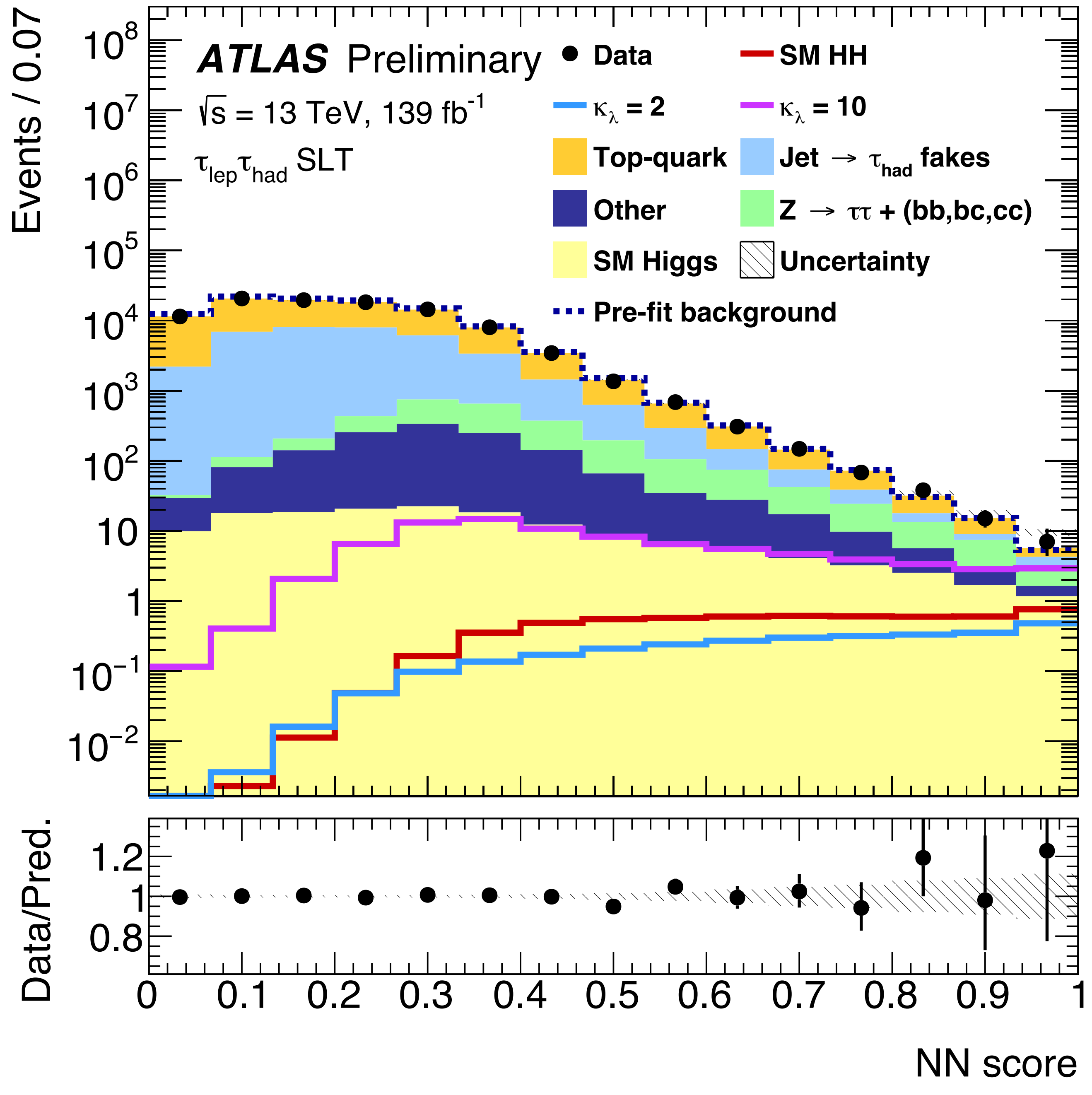

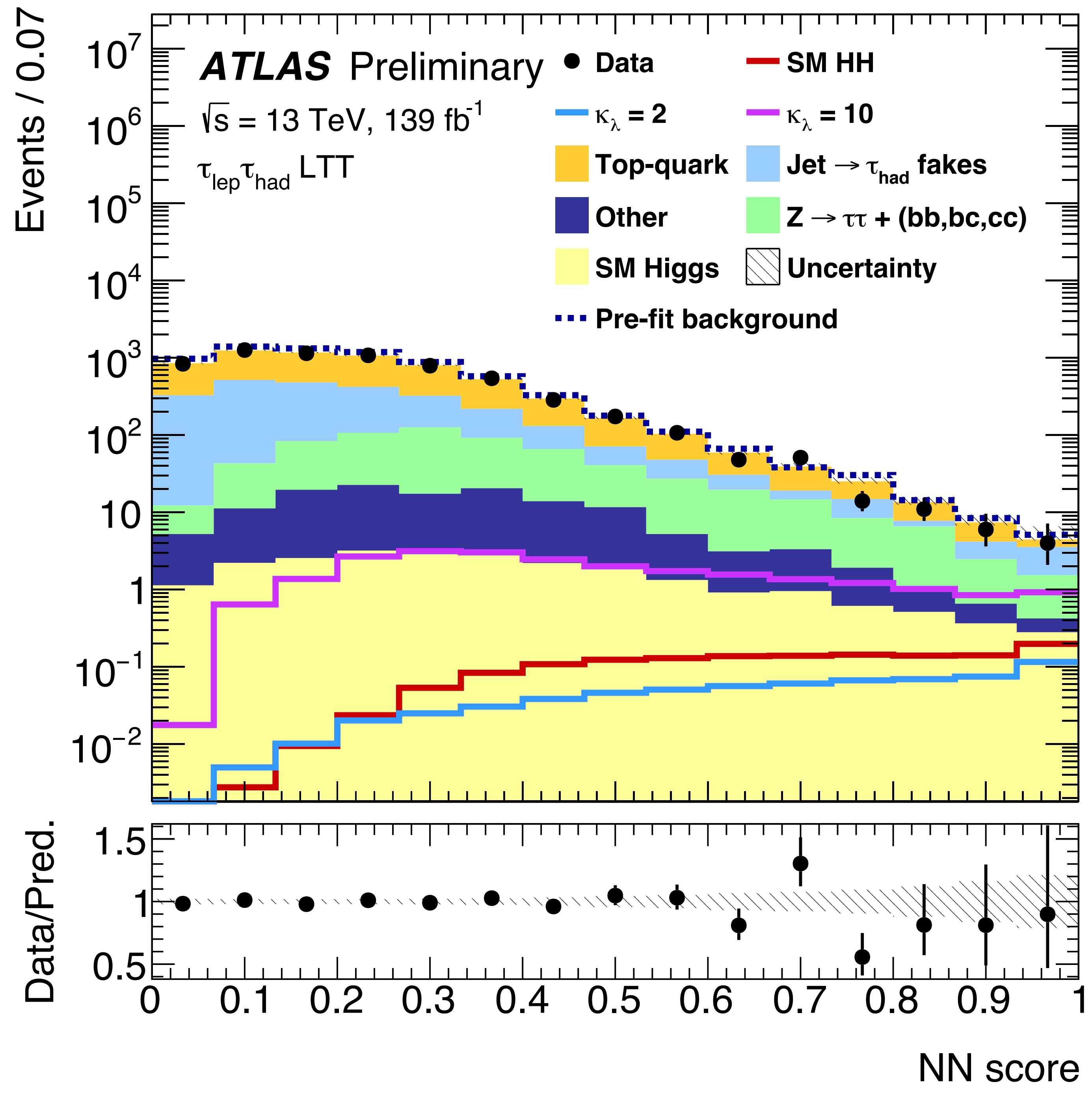

HH→bbττ full Run 2

MVA outputs

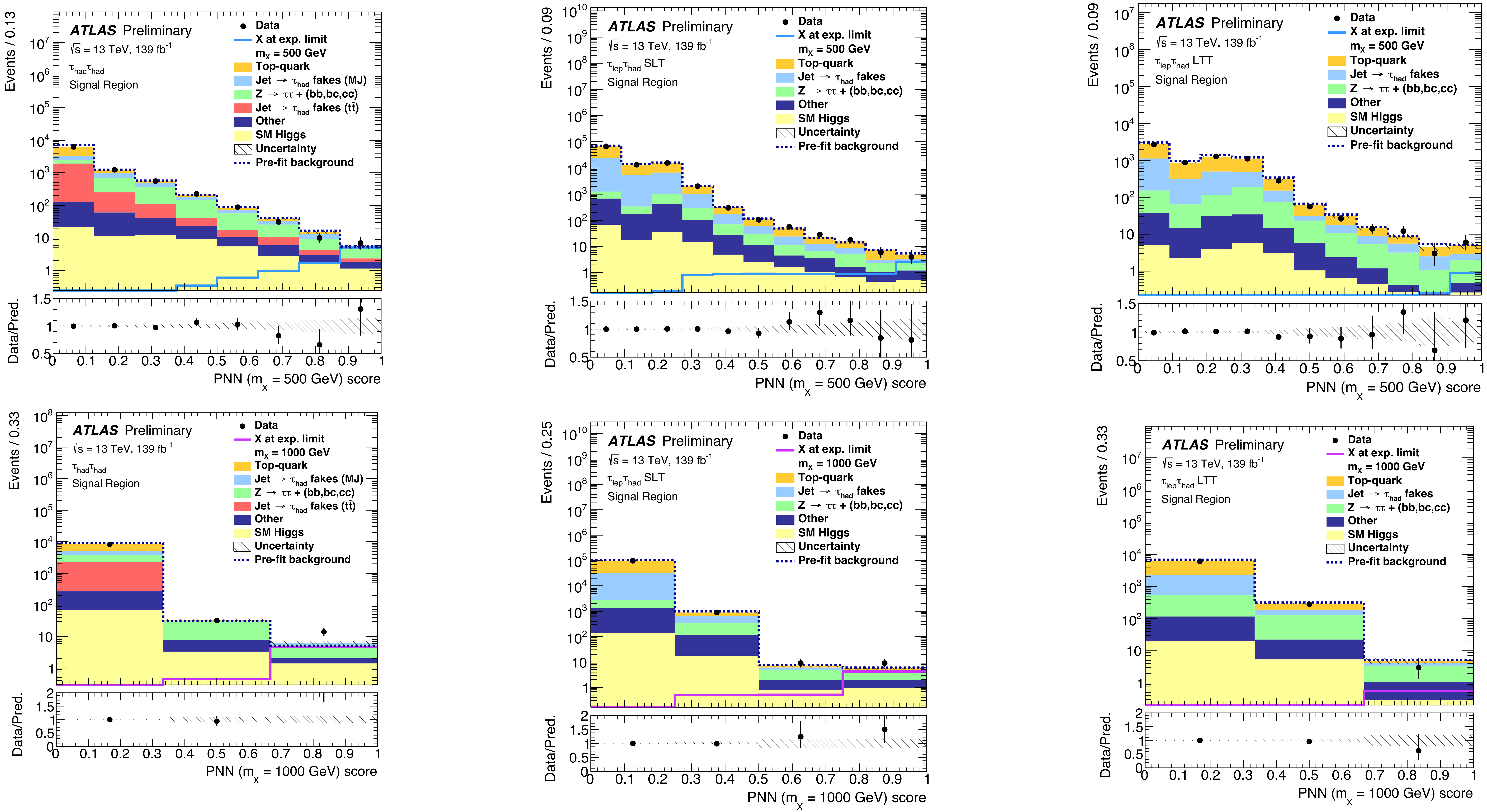

HH→bbττ full Run 2

Systematic uncertainties

ATLAS-CONF-2021-030

Uncertainty source	Non-resonant HH	Resonant $X \to HH$ 300 GeV	500 GeV	1000 GeV
Data statistical	81%	75%	89%	88%
Systematic	59%	66%	46%	48%
$t\bar{t}$ and $Z+\text{HF}$ normalisations	4%	15%	3%	3%
MC statistical	28%	44%	33%	18%
Experimental				
Jet and $E_{\text{T}}^{\text{miss}}$	7%	28%	5%	3%
b-jet tagging	3%	6%	3%	3%
$\tau_{\text{had-vis}}$	5%	13%	3%	7%
Electrons and muons	2%	3%	2%	1%
Luminosity and pileup	3%	2%	2%	5%
Theoretical and modelling				
Fake-$\tau_{\text{had-vis}}$	9%	22%	8%	7%
Top-quark	24%	17%	15%	8%
$Z(\to \tau\tau)+\text{HF}$	9%	17%	9%	15%
Single Higgs boson	29%	2%	15%	14%
Other backgrounds	3%	2%	5%	3%
Signal	5%	15%	13%	34%

HH→bbττ full Run 2

Fake-τ background data-driven estimation

ATLAS-CONF-2021-030

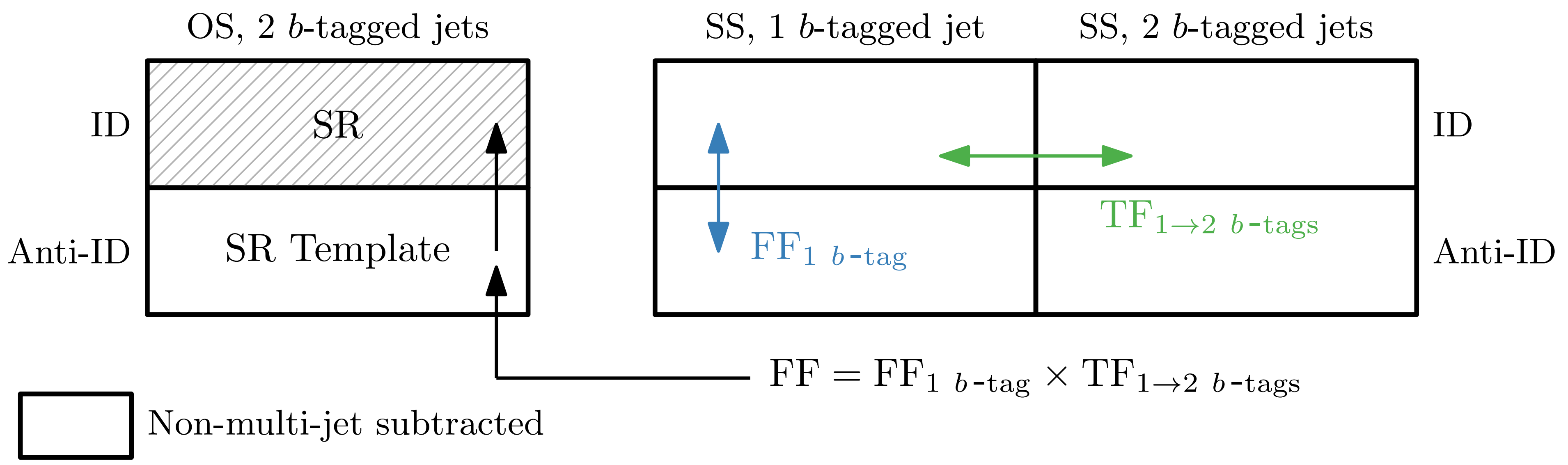

QCD multi-jet in HadHad:

- FFs derived as ID/Anti-ID in SS 1 b-tag
- Transfer factors from 1 b-tag to 2 b-tags in SS
- FFs x TFs applied to Anti-ID OS to derive SR template

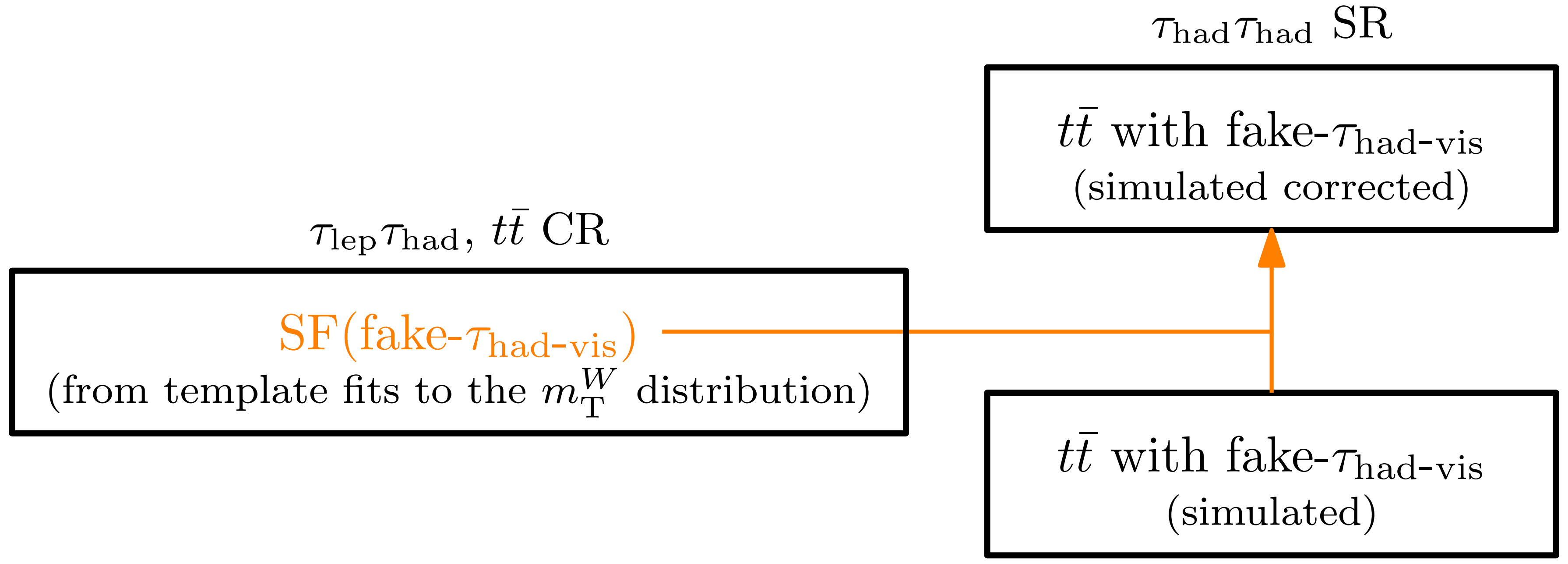

ttbar with fake-τ in HadHad:

- SFs derived in LepHad ttbar CR from template fits
- SFs applied to MC simulations in HadHad SR

to derive corrected template

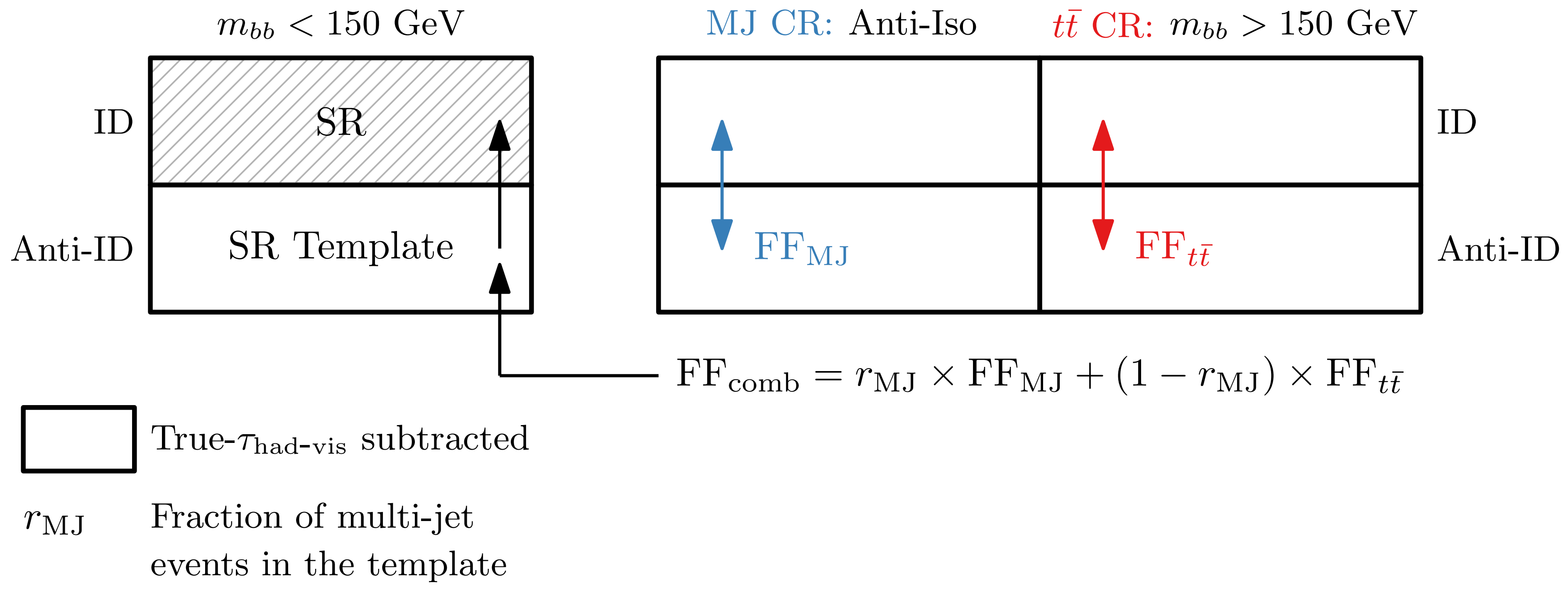

Bkg with fake-τ in LepHad:

- Combined FF method for fakes from ttbar and QCD multi-jet
- Separate FFs derived as ID/Anti-ID in dedicated MJ and ttbar CRs
- FFs combined and applied to the Anti-ID region to derive the SR template

HH→bbγγ full Run 2

BDT input variables

arXiv:2112.11876

Non-resonant

Variable	Definition
Photon-related kinematic variables	
$p_T/m_{\gamma\gamma}$	Transverse momentum of the two photons scaled by their invariant mass $m_{\gamma\gamma}$
η and ϕ	Pseudo-rapidity and azimuthal angle of the leading and sub-leading photon
Jet-related kinematic variables	
b-tag status	Highest fixed b-tag working point that the jet passes
p_T, η and ϕ	Transverse momentum, pseudo-rapidity and azimuthal angle of the two jets with the highest b-tagging score
$p_T^{b\bar{b}}$, $\eta_{b\bar{b}}$ and $\phi_{b\bar{b}}$	Transverse momentum, pseudo-rapidity and azimuthal angle of b-tagged jets system
$m_{b\bar{b}}$	Invariant mass built with the two jets with the highest b-tagging score
H_T	Scalar sum of the p_T of the jets in the event
Single topness	For the definition, see Eq. (1)
Missing transverse momentum-related variables	
E_T^{miss} and ϕ^{miss}	Missing transverse momentum and its azimuthal angle

Resonant

Variable	Definition
Photon-related kinematic variables	
$p_T^{\gamma\gamma}$, $y^{\gamma\gamma}$	Transverse momentum and rapidity of the di-photon system
$\Delta\phi_{\gamma\gamma}$ and $\Delta R_{\gamma\gamma}$	Azimuthal angular distance and ΔR between the two photons
Jet-related kinematic variables	
$m_{b\bar{b}}$, $p_T^{b\bar{b}}$ and $y_{b\bar{b}}$	Invariant mass, transverse momentum and rapidity of the b-tagged jets system
$\Delta\phi_{b\bar{b}}$ and $\Delta R_{b\bar{b}}$	Azimuthal angular distance and ΔR between the two b-tagged jets
N_{jets} and N_{b-jets}	Number of jets and number of b-tagged jets
H_T	Scalar sum of the p_T of the jets in the event
Photons and jets-related kinematic variables	
$m_{b\bar{b}\gamma\gamma}$	Invariant mass built with the di-photon and b-tagged jets system
$\Delta y_{\gamma\gamma,b\bar{b}}$, $\Delta\phi_{\gamma\gamma,b\bar{b}}$ and $\Delta R_{\gamma\gamma,b\bar{b}}$	Distance in rapidity, azimuthal angle and ΔR between the di-photon and the b-tagged jets system

HH→bbγγ full Run 2

BDT input variables

arXiv:2112.11876

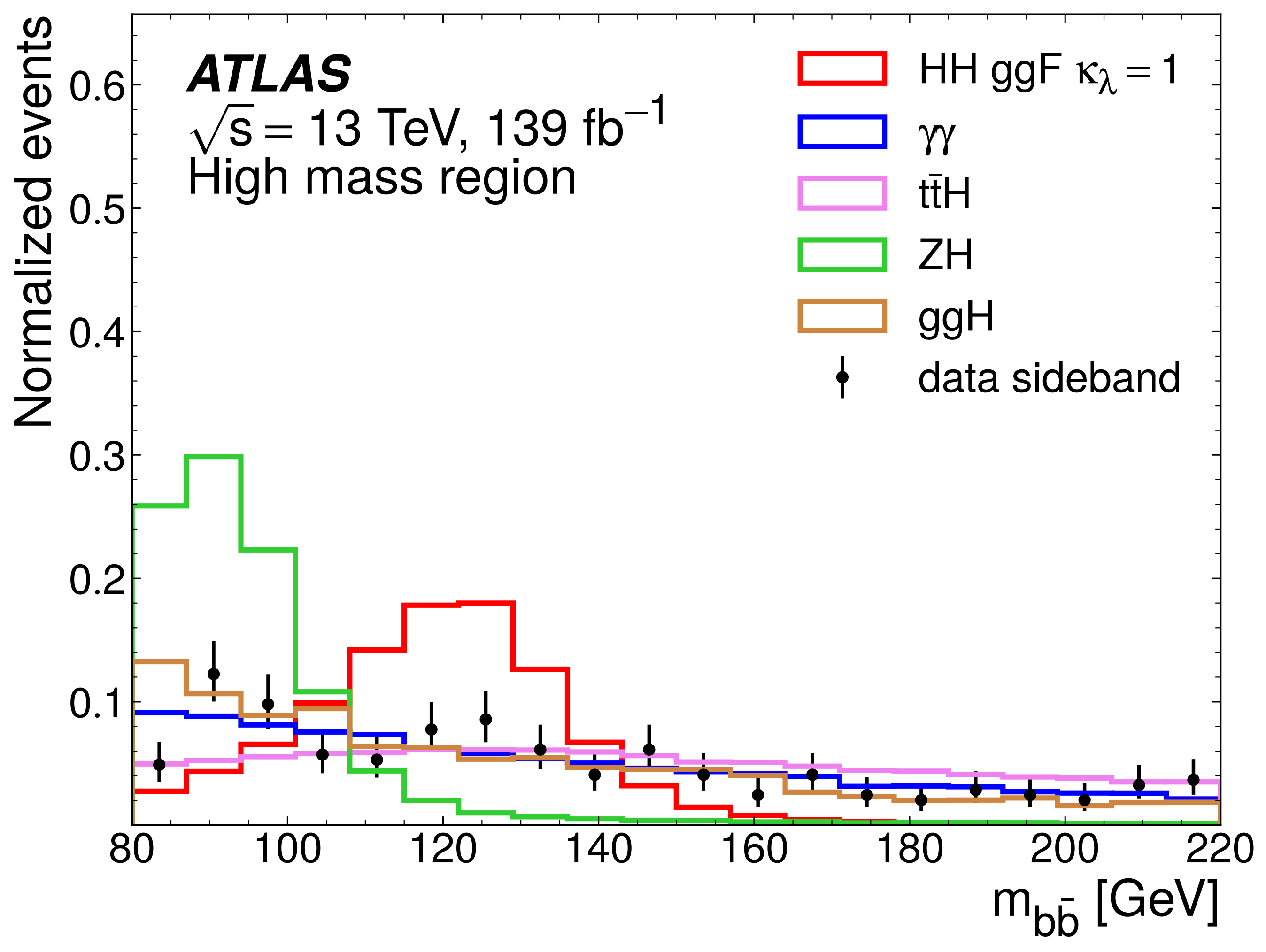

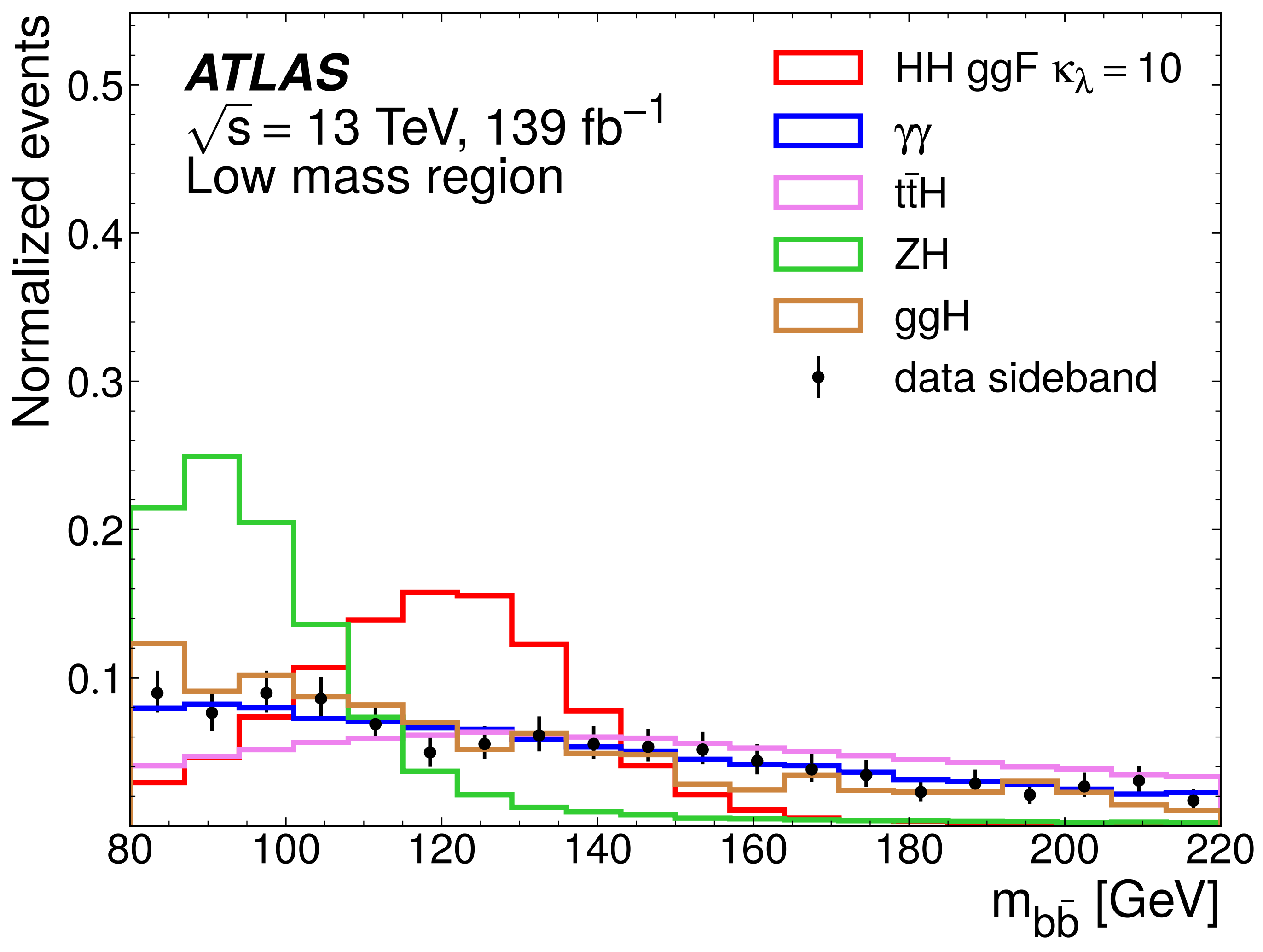

HH→bbγγ full Run 2

Event selection

arXiv:2112.11876

Cuts	Yields	Efficiency [%]
All events	12.11	100.00
Pass trigger	9.81	80.97
Has Primary Vertex	9.81	80.97
2 loose photons	7.07	58.42
$e-\gamma$ ambiguity	7.07	58.40
Trigger match	6.71	55.46
Photons tight ID cut	5.89	48.62
Photons isolation cut	5.22	43.13
rel. p_T cuts	4.70	38.78
$m_{\gamma\gamma} \in [105, 160]$ GeV	4.69	38.73
$N_{lep} = 0$	4.67	38.55
$N_j \geq 2$	3.94	32.53
N_j central <6	3.84	31.68
2 b-jets with 77% WP	1.62	13.37
Di-Higgs invariant mass >350 GeV	1.42	11.78
Di-Higgs invariant mass <350 GeV	0.19	1.58

HH→bbγγ full Run 2

Acceptance x efficiency

arXiv:2112.11876

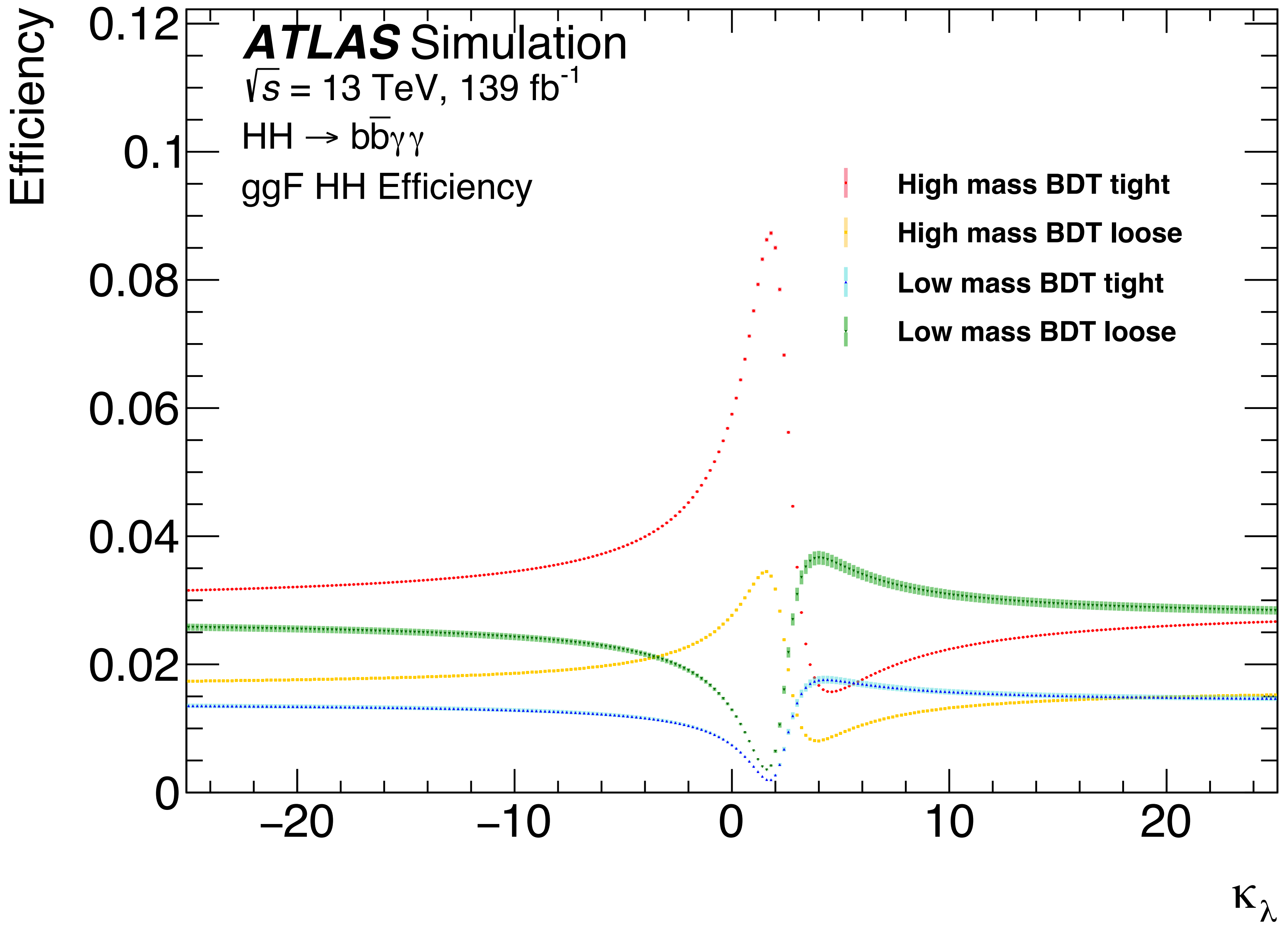

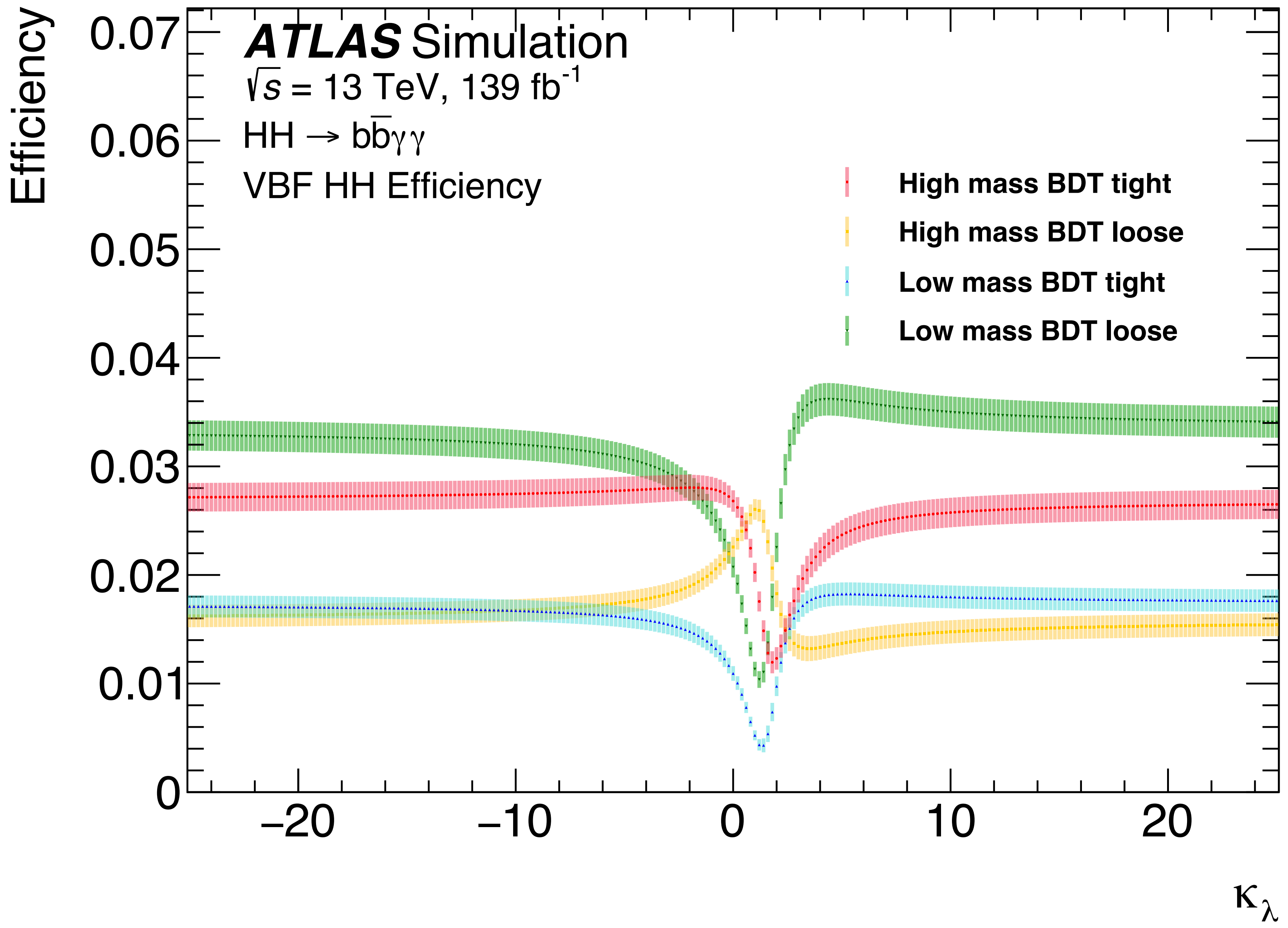

HH→bbγγ full Run 2

Likelihood scans

arXiv:2112.11876

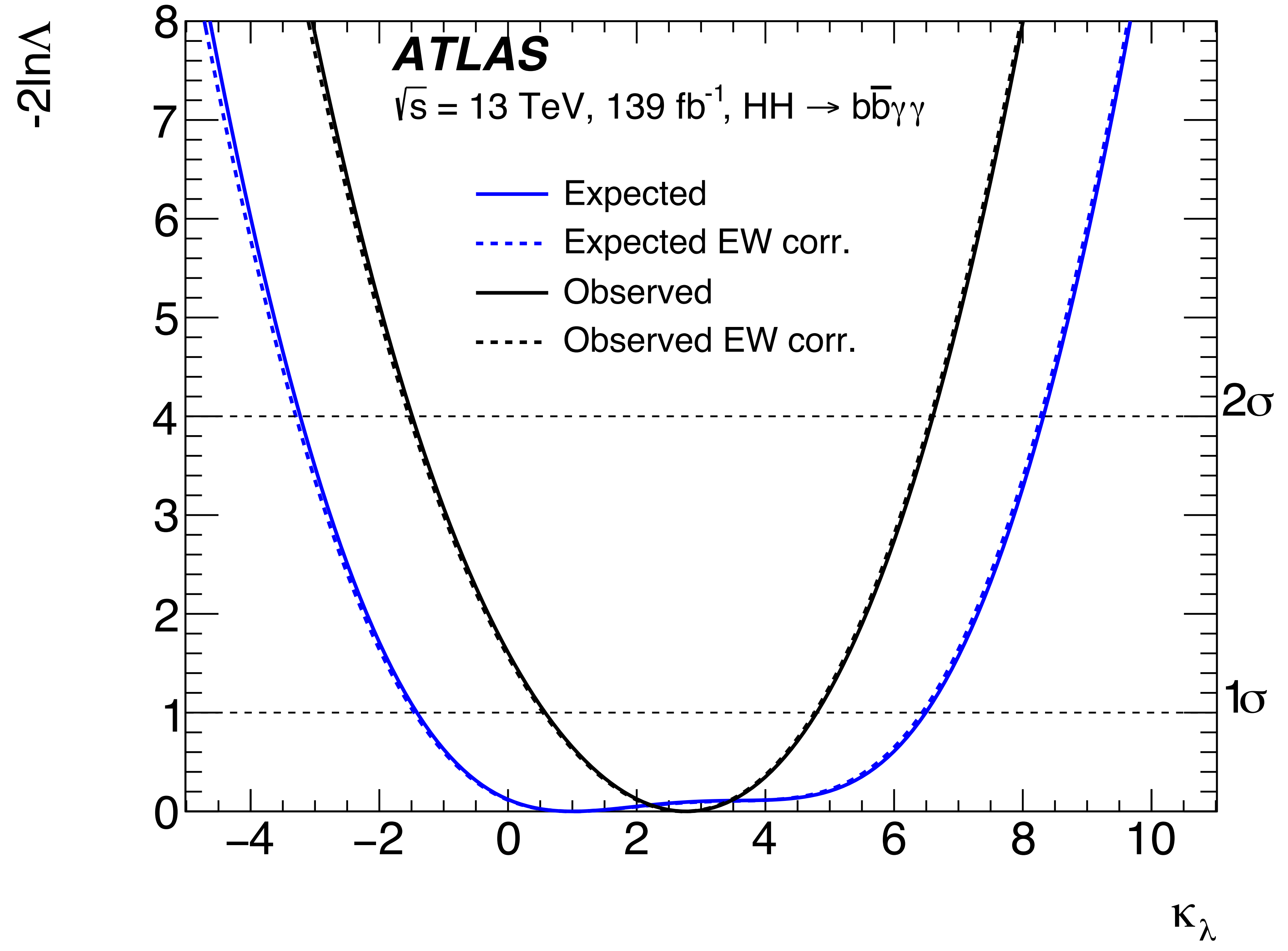

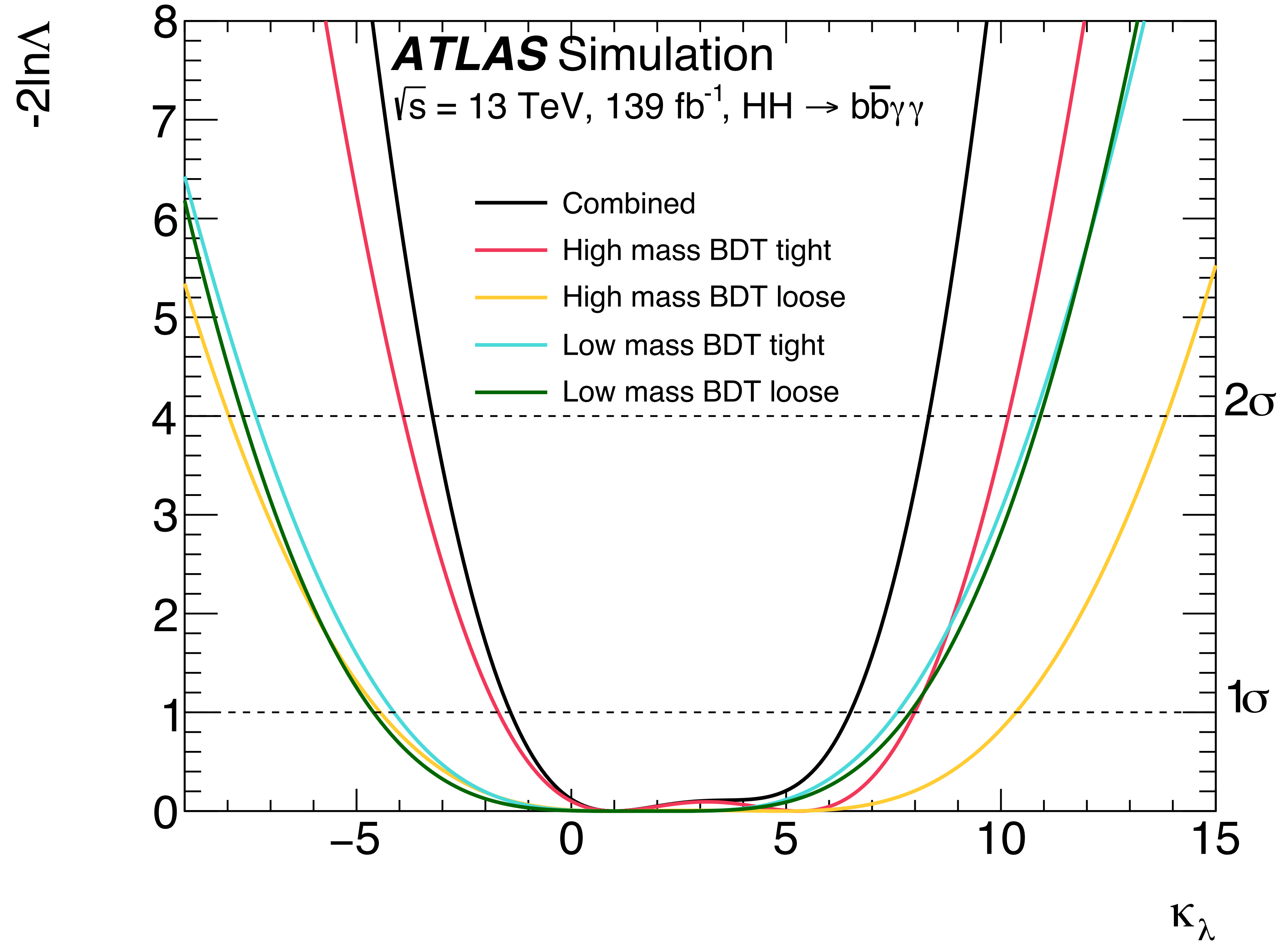

HH→bbγγ full Run 2

Systematic uncertainties

arXiv:2112.11876

		Relative impact of the systematic uncertainties [%]	
Source	Type	Nonresonant analysis HH	Resonant analysis $m_X = 300$ GeV
Experimental			
Photon energy resolution	Norm. + Shape	0.4	0.6
Jet energy scale and resolution	Normalization	< 0.2	0.3
Flavor tagging	Normalization	< 0.2	0.2
Theoretical			
Factorization and renormalization scale	Normalization	0.3	< 0.2
Parton showering model	Norm. + Shape	0.6	2.6
Heavy-flavor content	Normalization	0.3	< 0.2
$\mathcal{B}(H \to \gamma\gamma, b\bar{b})$	Normalization	0.2	< 0.2
Spurious signal	Normalization	3.0	3.3

HH→bbττ and HH→bbγγ full Run 2

Acceptance x efficiency

ATLAS-CONF-2021-052

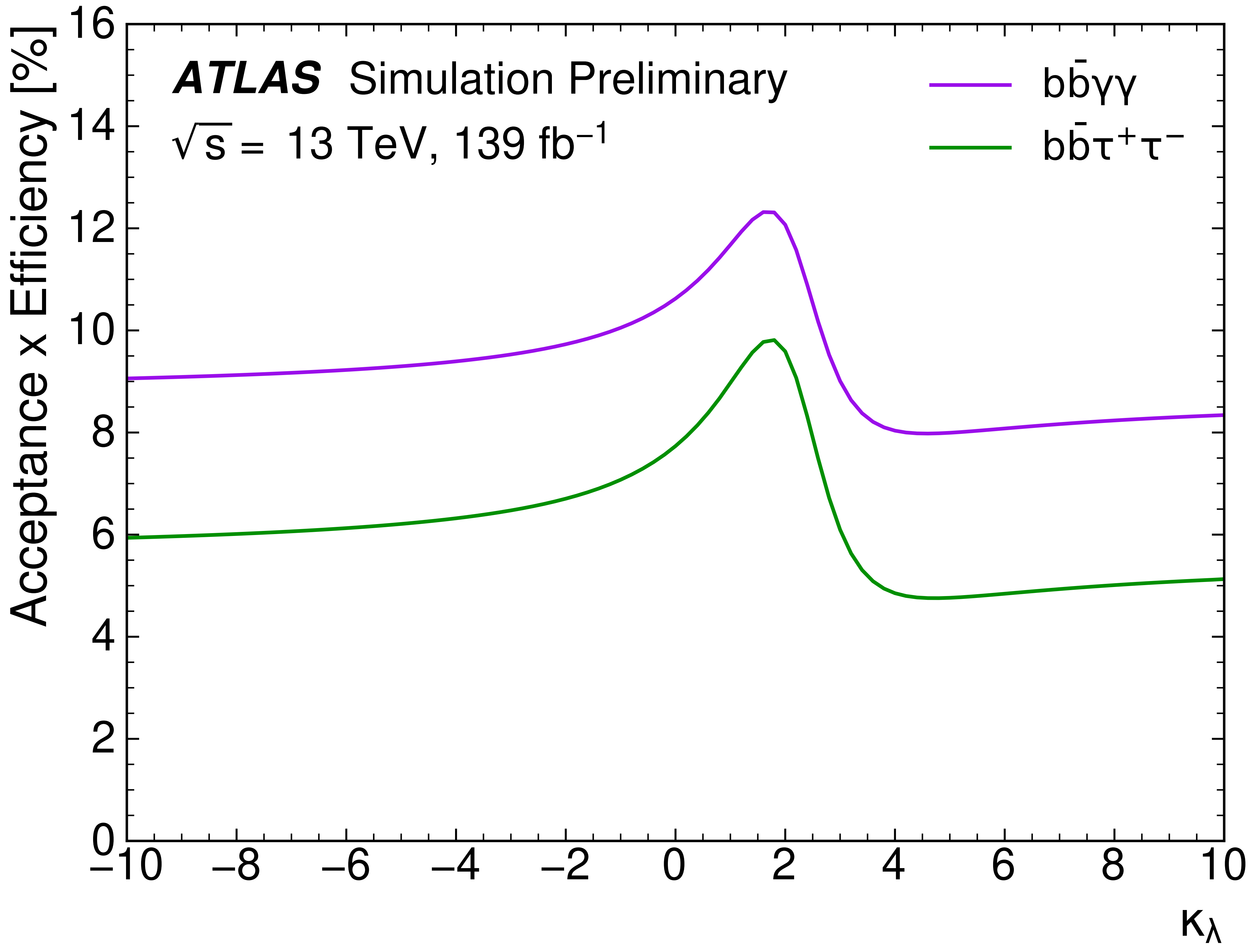

CMS HH full Run 2 results

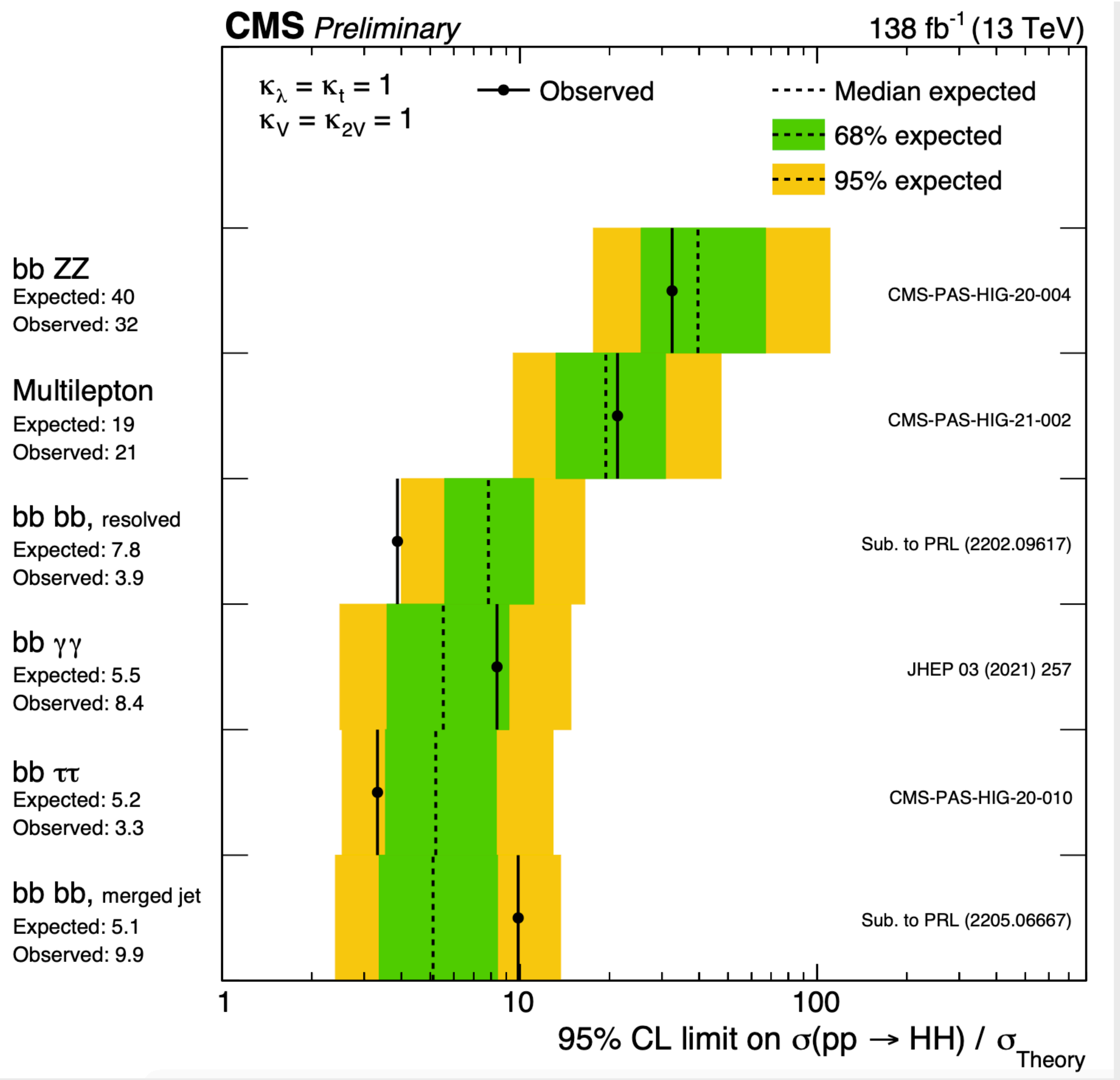

CMS HH full Run 2 results: bbbb resolved

arXiv:2202.09617

Obs.(exp.) upper limit on HH signal strength 3.9 (7.8)

Limit on HH XS vs k_λ

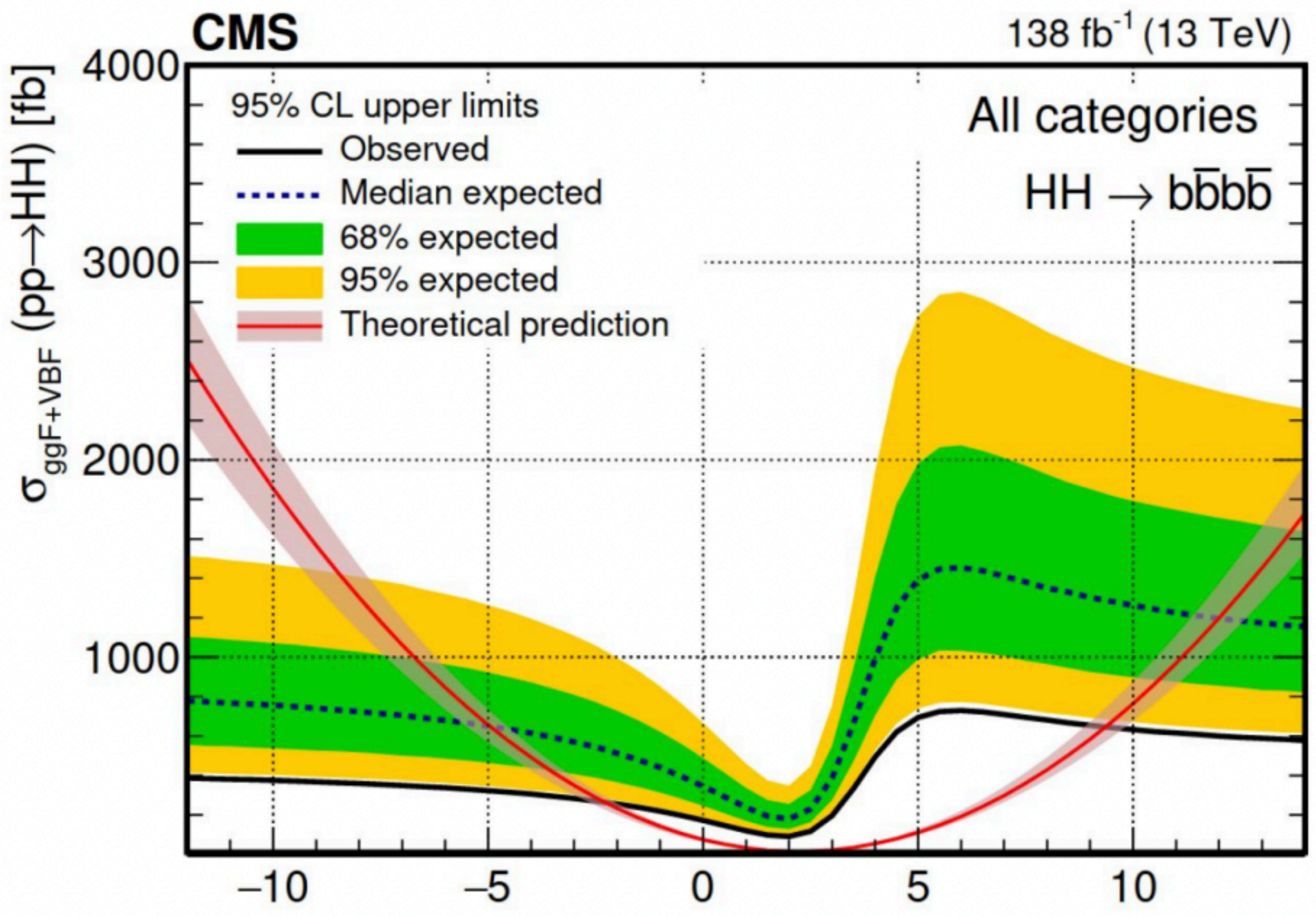

Obs. $k_\lambda \in$ [-2.3, 9.4]

Exp. $k_\lambda \in$ [-5.0, 12.0]

Limit on VBF HH XS vs k_{2V}

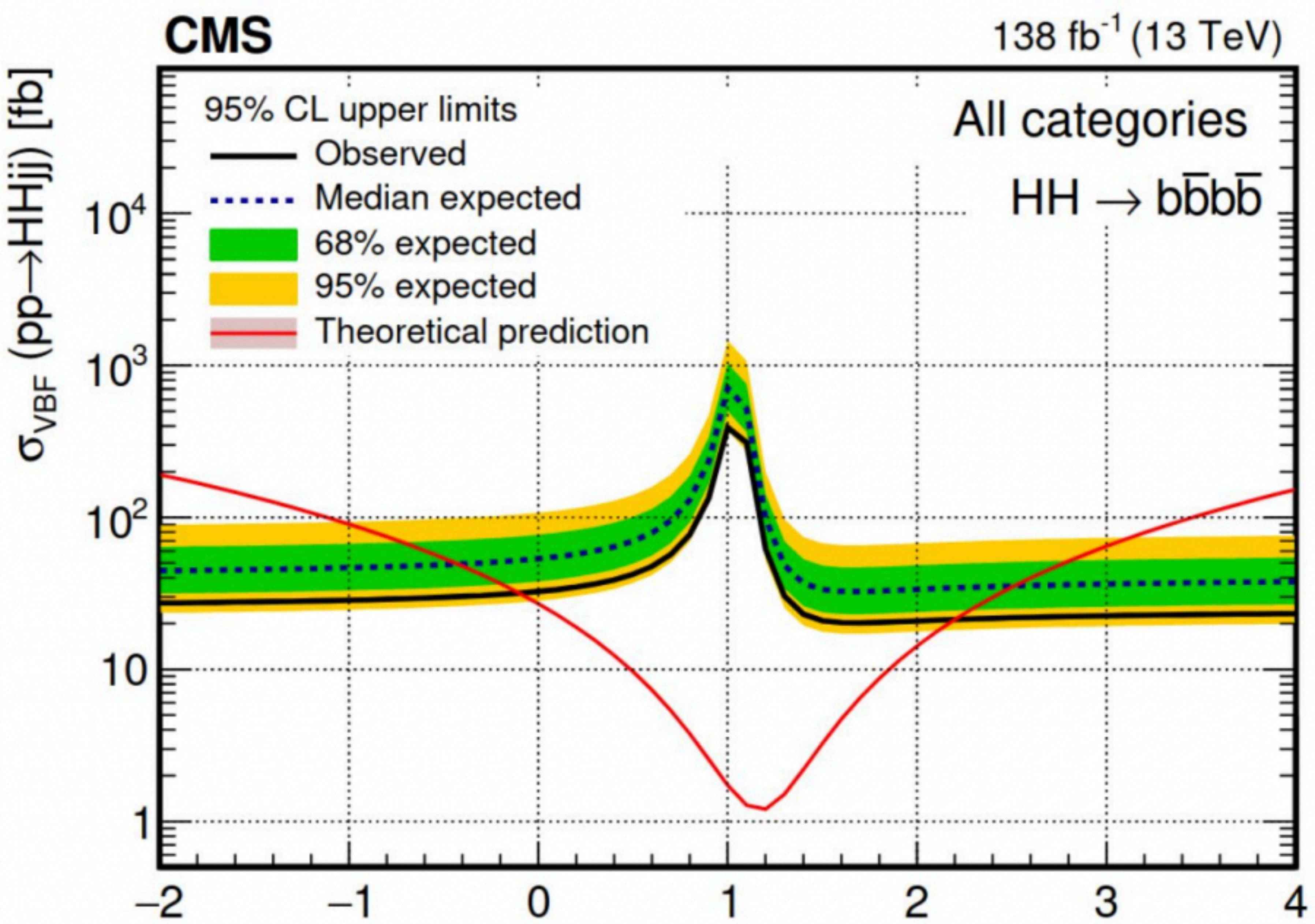

Obs. $k_{2V} \in$ [-0.1, 2.2]

Exp. $k_{2V} \in$ [-0.4, 2.5]

CMS HH full Run 2 results: bbbb boosted

CMS-PAS-B2G-22-003

Obs.(exp.) upper limit on HH signal strength 9.9 (5.1)

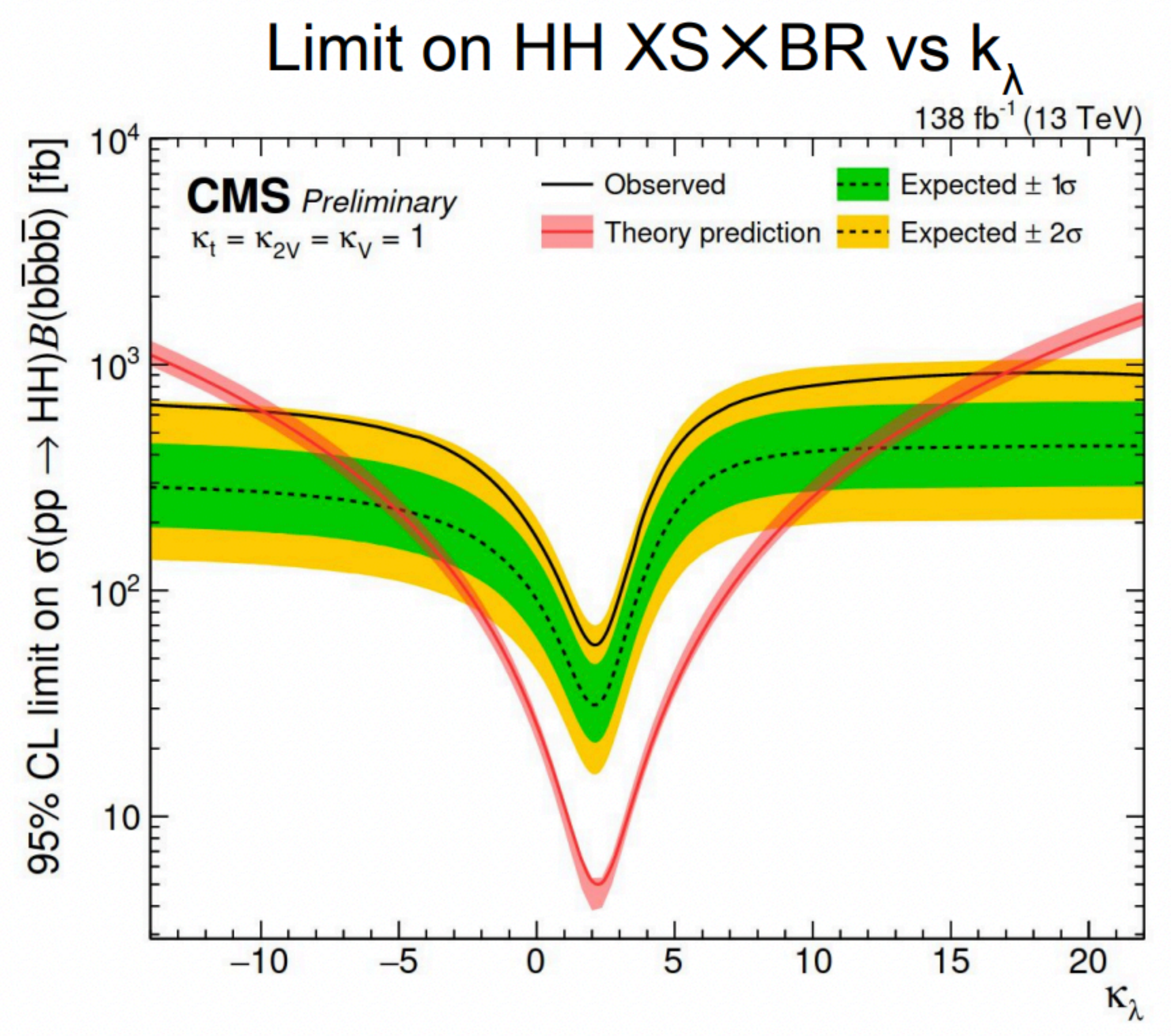

Obs. $k_\lambda \in [-9.9, 16.9]$

Exp. $k_\lambda \in [-5.1, 12.2]$

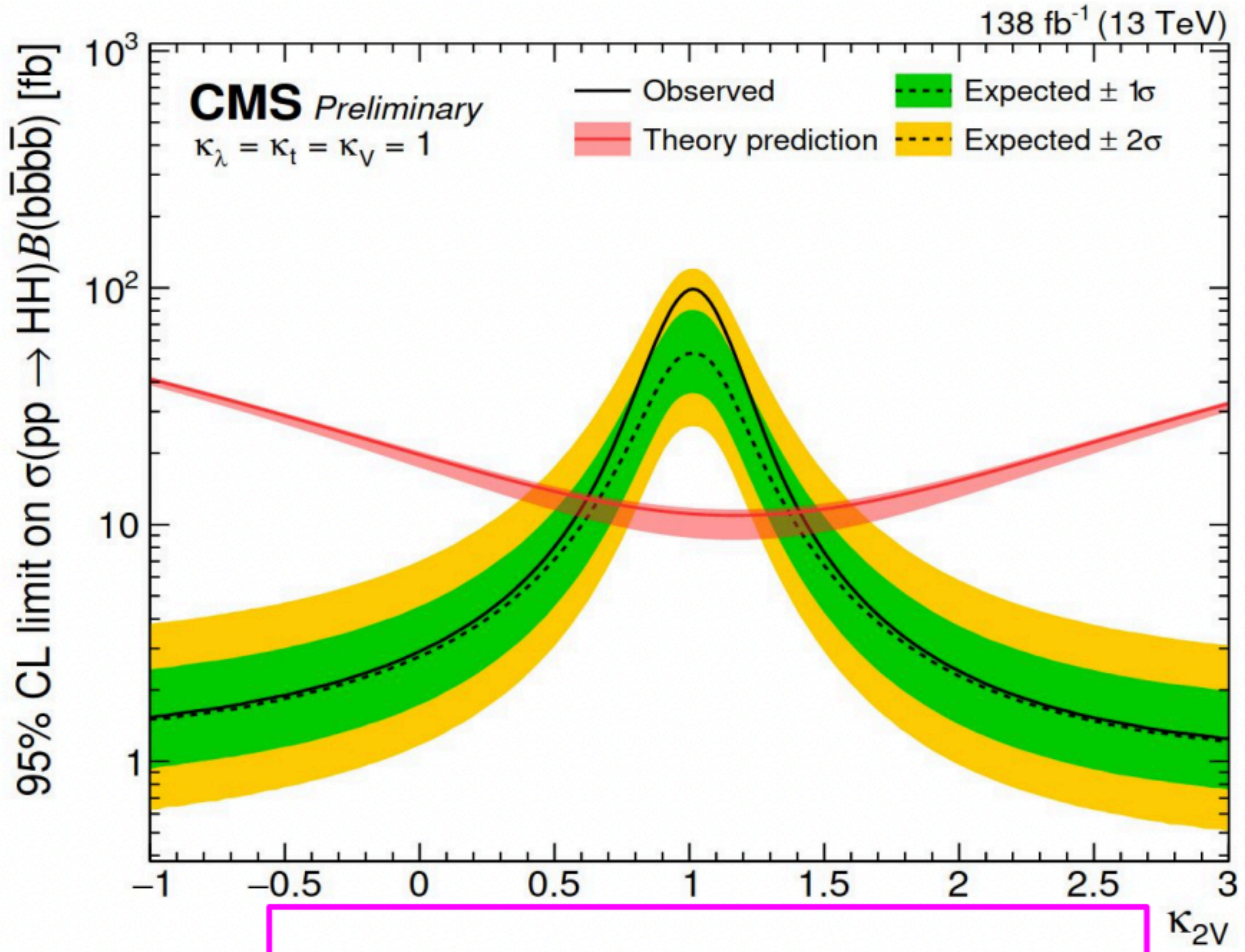

Obs. $k_{2V} \in [0.62, 1.41]$

Exp. $k_{2V} \in [0.66, 1.37]$

Most stringent constraints on κ_{2V} to date

CMS HH full Run 2 results: bbττ

CMS PAS HIG-20-010

Obs.(exp.) upper limit on HH signal strength 3.33 (5.22)

Upper limit on HH XS×BR vs k_λ

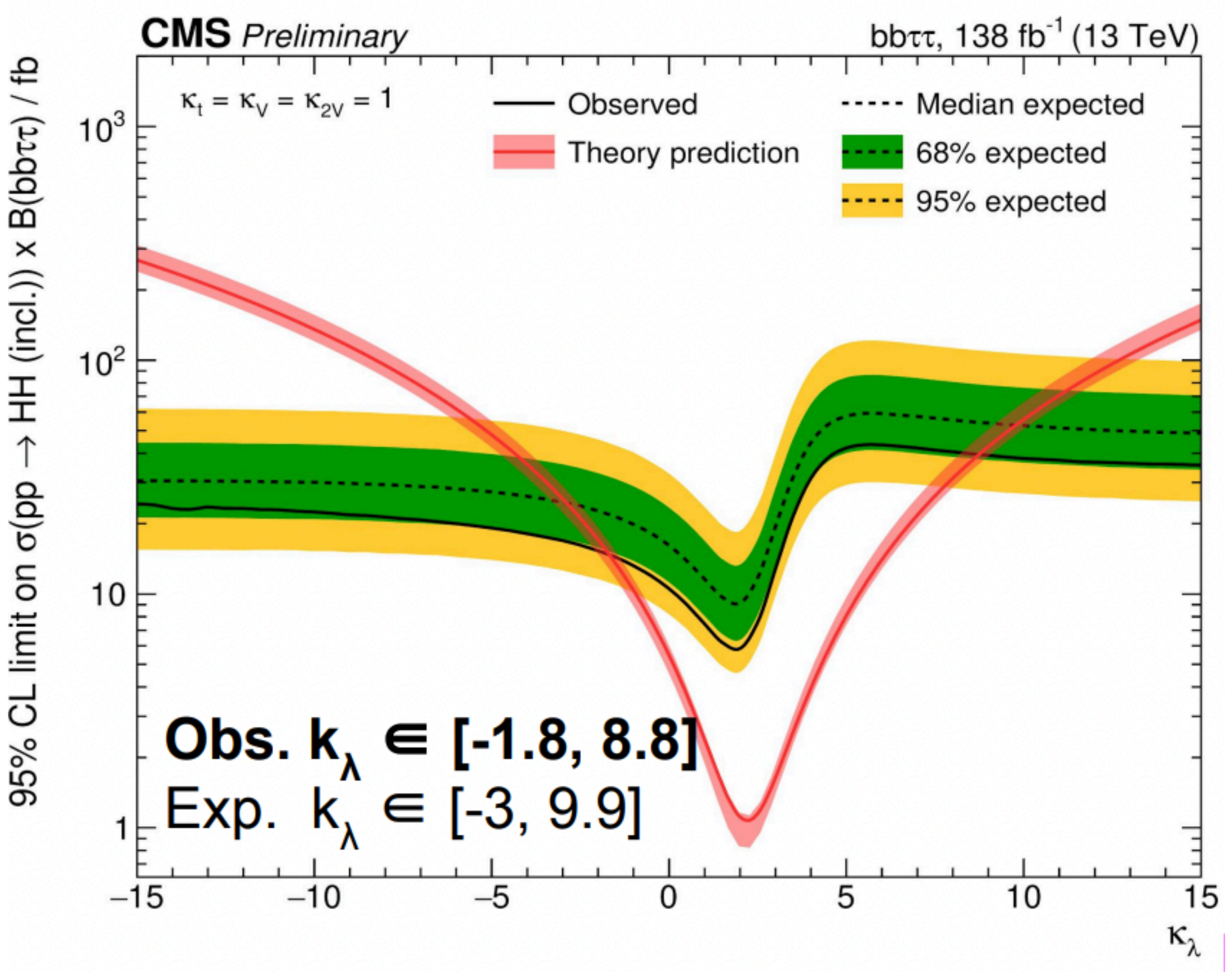

Upper limit on VBF HH XS x BR vs κ_{2V}

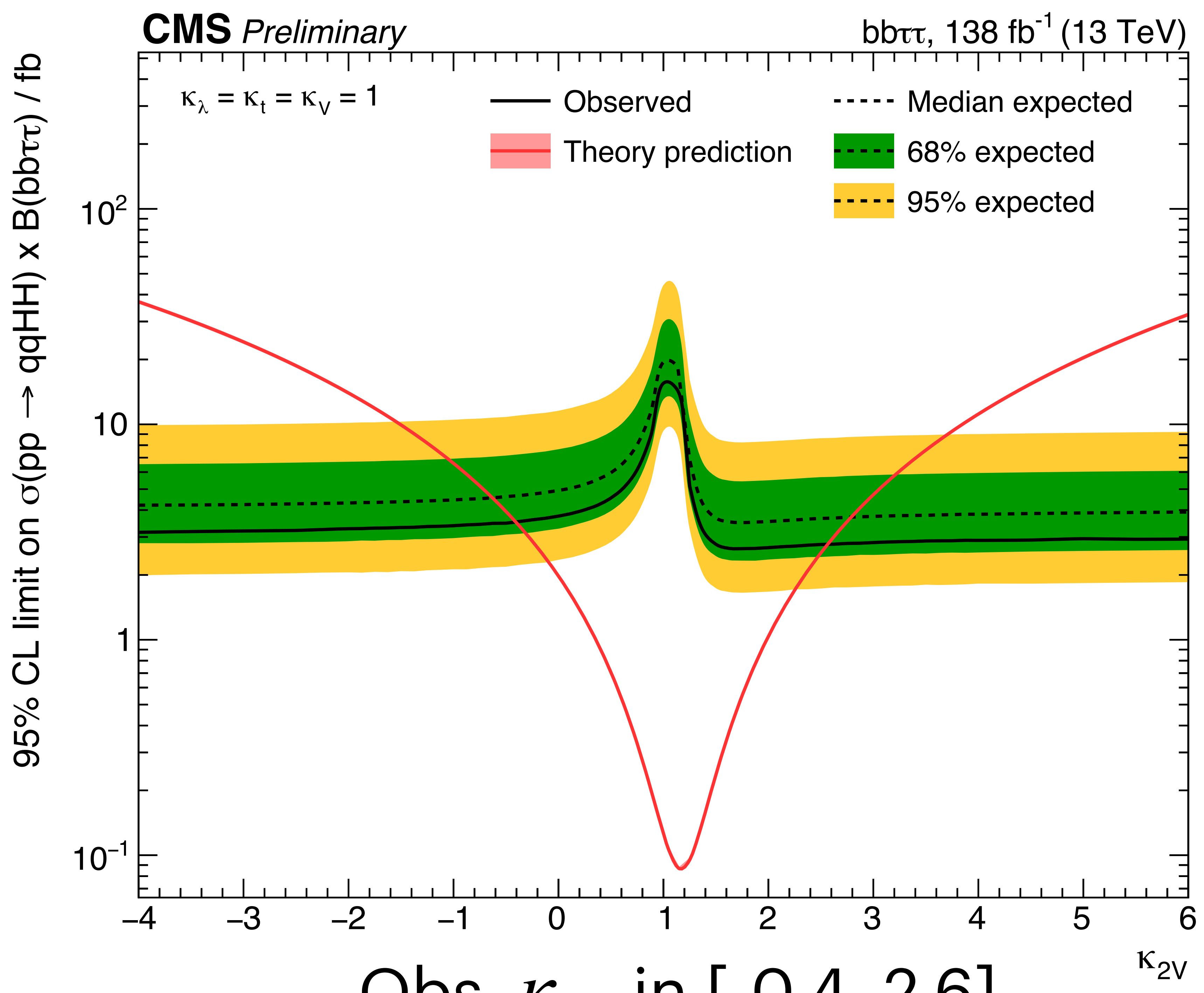

Obs. κ_{2V} in [-0.4, 2.6]

Exp. κ_{2V} in [-0.6, 2.8]

CMS HH full Run 2 results: bbγγ

JHEP03(2021)257

Obs.(exp.) upper limit on HH signal strength 7.7 (5.2)

Limit on HH XS×BR vs k_λ

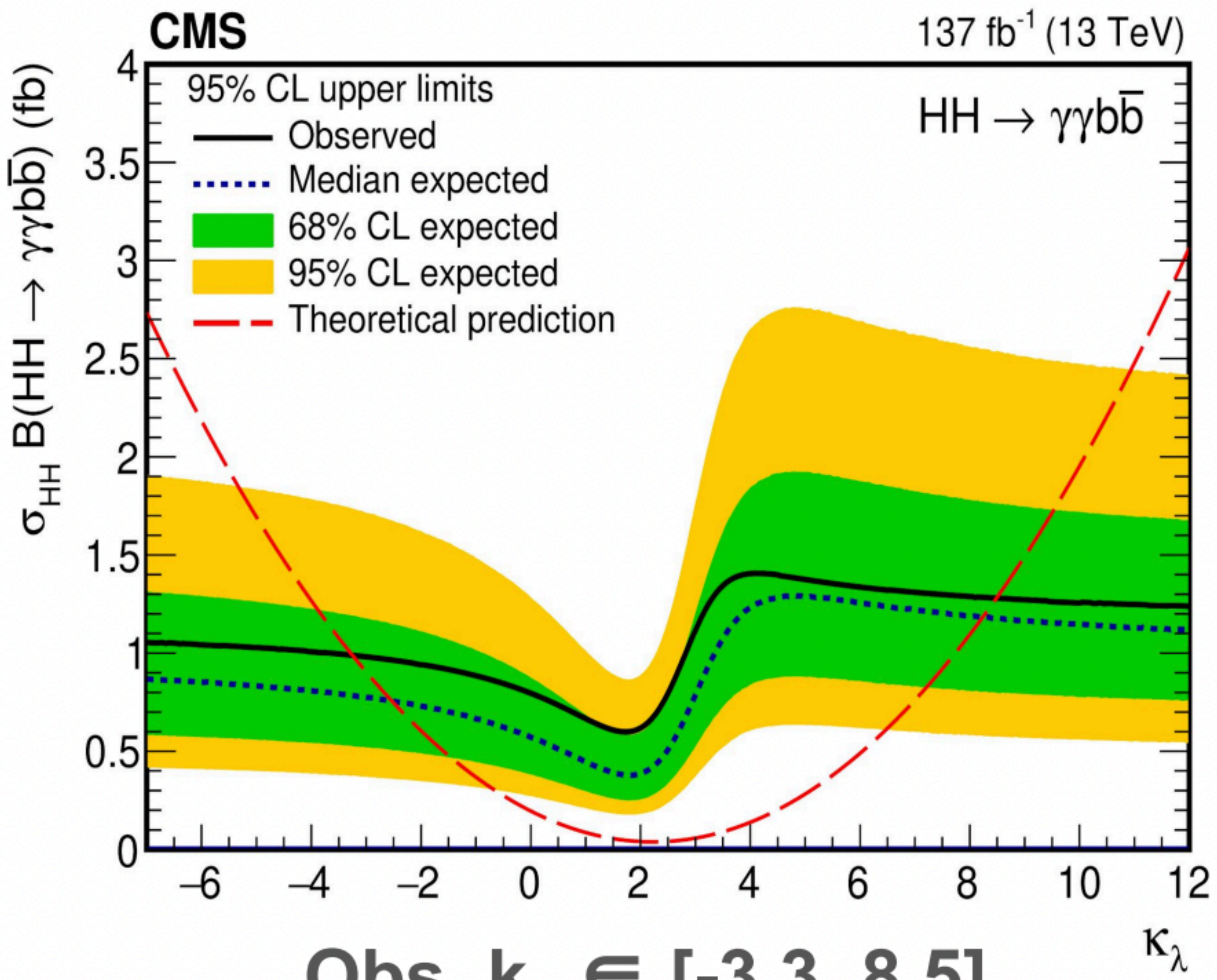

Obs. $k_\lambda \in$ [-3.3, 8.5]
Exp. $k_\lambda \in$ [-2.5, 8.2]

Limit on VBF HH XS×BR vs k_{2V}

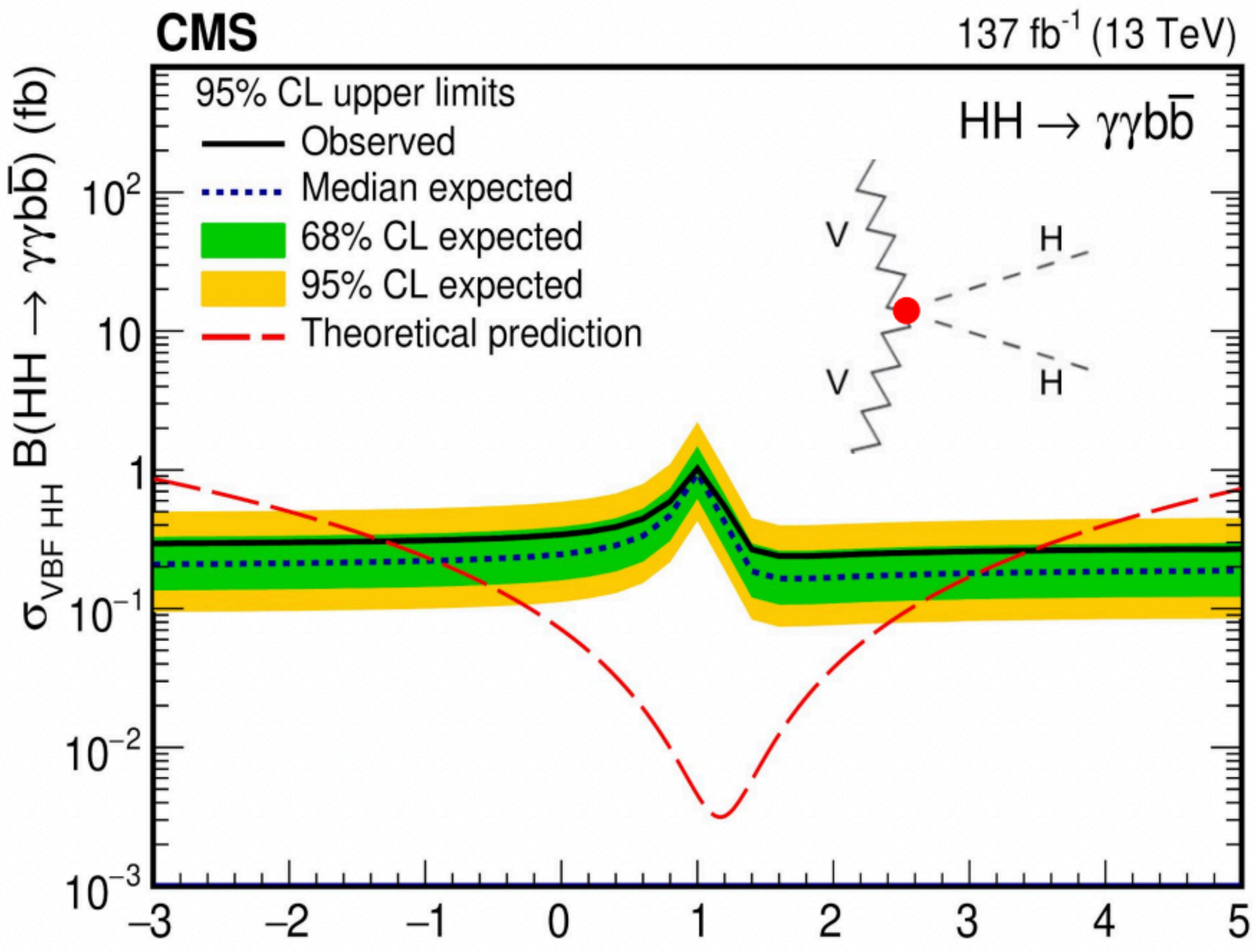

Obs. $k_{2V} \in$ [-1.3, 3.5]
Exp. $k_{2V} \in$ [-0.9, 3.0]

Summary of ATLAS and CMS HH full Run 2 results